

Open Research Online

The Open University's repository of research publications
and other research outputs

Factors regulating transitions among life cycle phases in the marine pennate diatom *Pseudo-nitzschia multistriata*

Thesis

How to cite:

Scalco, Eleonora (2013). Factors regulating transitions among life cycle phases in the marine pennate diatom *Pseudo-nitzschia multistriata*. PhD thesis The Open University.

For guidance on citations see [FAQs](#).

© 2012 The Author



<https://creativecommons.org/licenses/by-nc-nd/4.0/>

Version: Version of Record

Link(s) to article on publisher's website:

<http://dx.doi.org/doi:10.21954/ou.ro.0000d593>

Copyright and Moral Rights for the articles on this site are retained by the individual authors and/or other copyright owners. For more information on Open Research Online's data [policy](#) on reuse of materials please consult the policies page.

oro.open.ac.uk

Eleonora Scalco

MASTER DEGREE IN MARINE BIOLOGY, UNIVERSITY OF PADOVA, ITALY

Factors regulating transitions among life cycle
phases in the marine pennate diatom

Pseudo-nitzschia multistriata

Doctor of Philosophy

The Open University, London, UK



Stazione Zoologica Anton Dohrn, Napoli, Italy



September 2012

DATE OF SUBMISSION: 28 SEPTEMBER 2012

DATE OF AWARD: 2 JANUARY 2013

THE DISC THAT SHOULD
ACOMPANY THIS THESIS IS
MISSING FROM THE
ORIGINAL THESIS

IMAGING SERVICES NORTH

Boston Spa, Wetherby
West Yorkshire, LS23 7BQ
www.bl.uk

**MISSING PAGE/PAGES
HAVE NO CONTENT**

Director of studies: Dr Marina Montresor (SZN Napoli, Italy)

External supervisor: Prof. Dr David G. Mann (Royal Botanic Garden Edinburgh, UK)

Examination panel: Prof. Dr David H. Jewson (University of Ulster, N. Ireland, UK)

Dr Maria I. Ferrante (SZN Napoli, Italy)

Alle Mie 'Due' Famiglie

*A quella Vicentina , che mi ha cresciuto amandomi, sostenendomi
e credendo sempre in me*

*A quella Napoletana che mi ha accolto a braccia aperte
facendomi sentire a casa*

Table of contents

Thesis abstract	11
Acknowledgments	13
List of figures	15
List of tables	25
 Chapter one: General introduction	 27
1.1 Diatoms: a short overview	29
1.2 The life cycle of diatoms: what do we know from laboratory studies?	33
1.2.1 <i>Vegetative division</i>	33
1.2.2 <i>The sexual phase</i>	37
1.2.2.1 <i>The sexual phase: centric diatoms</i>	38
1.2.2.2 <i>The sexual phase: pennate diatoms</i>	41
1.2.3 <i>Vegetative cell enlargement and asexual auxosporulation</i>	44
1.2.4 <i>The resting phase</i>	45
1.3 Factors influencing the sexual phase of diatoms life cycle	47
1.3.1 <i>Endogenous factors</i>	47
1.3.2 <i>Exogenous factors</i>	49
1.4 The sexual cycle of diatoms: what do we know from the observation of natural populations?	53
1.4.1 <i>Resting stages in sediments</i>	55
1.5 The genus <i>Pseudo-nitzschia</i>	57
1.5.1 <i>The life cycle of Pseudo-nitzschia species and the factors that induce sexual reproduction</i>	63
1.6 <i>Pseudo-nitzschia multistriata</i>	66
1.7 Aims of the thesis	67
 Chapter two: The life cycle of <i>Pseudo-nitzschia multistriata</i> : investigation in confocal and time lapse microscopy	 71
2.1 Introduction	73
2.2 Material and Methods	75
2.2.1 <i>Cultures</i>	75

2.2.2	<i>Observations in time-lapse microscopy</i>	82
2.2.3	<i>Observations in confocal microscopy</i>	83
2.2.4	<i>Size of initial cells</i>	87
2.2.5	<i>Mating experiments</i>	88
2.3	Results	90
2.3.1	<i>The life cycle of P. multistriata in time lapse-microscopy</i>	90
2.3.1.1	<i>Gametogenesis and conjugation</i>	90
2.3.1.2	<i>Anomalies during gametogenesis</i>	95
2.3.1.3	<i>Auxospore development and formation of the initial cell</i>	96
2.3.1.4	<i>Bacteria</i>	98
2.3.2	<i>The life cycle of P. multistriata in confocal microscopy</i>	98
2.3.2.1	<i>Vegetative cells and mitotic division</i>	99
2.3.2.2	<i>Gametogenesis</i>	102
2.3.2.3	<i>Gamete conjugation, auxospore development and formation of initial cell</i>	105
2.3.2.4	<i>Atypical stages during sexual reproduction</i>	109
2.3.3	<i>The size of initial cells</i>	111
2.3.4	<i>Mating experiments</i>	112
2.4	Discussion	116
2.4.1	<i>Vegetative division</i>	116
2.4.2	<i>Gametogenesis and gamete conjugation</i>	117
2.4.3	<i>The auxospore</i>	120
2.4.4	<i>The initial cells</i>	120
2.4.5	<i>Abnormal stages</i>	121
2.4.6	<i>The size of initial cells</i>	121
2.4.7	<i>Factors modulating the success of sexual reproduction</i>	123
2.4.8	<i>Mating experiments</i>	126

Chapter three: Parental cell density and growth phase as factors influencing the occurrence and success of sexual reproduction in *Pseudo-nitzschia multistriata*: 133

3.1	Introduction	135
3.2	Material and Methods	138
3.2.1	<i>Culture isolation and maintenance</i>	138
3.2.2	<i>Calculation of growth rate</i>	138
3.2.3	<i>Growth rates of parental cultures in different culture vessels</i>	139

3.2.4	<i>Sexual reproduction in crosses carried out with parental strains at different cell densities and growth phase (Experiment #1)</i>	140
3.2.5	<i>Sexual reproduction in crosses carried out with parental strains from different growth phases, but diluted at the same cell concentration (Experiment #2)</i>	143
3.3	Results	145
3.3.1	<i>Growth rates in different culture vessels</i>	145
3.3.2	<i>Sexual reproduction in crosses carried out with parental strains at different cell density and growth phase (Experiment #1)</i>	146
3.3.3	<i>Sexual reproduction in crosses carried out with parental strains from different growth phases, but diluted at the same cell concentration (Experiment#2)</i>	156
3.4	Discussion	167
3.4.1	<i>Sexual reproduction and growth phase of parental strains</i>	167
3.4.2	<i>The timing and cell density threshold for sex</i>	169
3.4.3	<i>Sex and growth</i>	171
3.4.4	<i>The success of sexual reproduction</i>	172

Chapter four: Is there a chemical cue that induces gametogenesis in *Pseudo-nitzschia multistriata*? 175

4.1	Introduction	177
4.2	Material and Methods	180
4.2.1	<i>Culture isolation and maintenance</i>	180
4.2.2	<i>Effect of sexual reproduction on the growth rate of parental strains (Experiment #1)</i>	181
4.2.3	<i>Test for the presence of a chemical cue inducing gametogenesis (Experiment #2)</i>	182
4.2.4	<i>Test for the presence of oxidative stress during meiosis/gametogenesis (Experiment#3)</i>	190
4.3	Results	192
4.3.1	<i>Effect of sexual reproduction on the growth of parental strains (Experiment #1)</i>	192
4.3.2	<i>Test for the presence of a chemical cue inducing gametogenesis (Experiment #2)</i>	198

4.3.3	<i>Test for the presence of oxidative stress during meiosis/gametogenesis (Experiment#3)</i>	209
4.4	Discussion	210
4.4.1	<i>A diffusible compound promotes gametogenesis</i>	210
4.4.2	<i>Cell density of vegetative cells during sexual reproduction</i>	214
Chapter five: Timing and success of sexual reproduction under 'mixed' and 'still' conditions		217
5.1	Introduction	219
5.2	Material and methods	222
5.2.1	<i>Culture isolation and maintenance</i>	222
5.2.2	<i>Calculation of growth rate</i>	222
5.2.3	<i>'Mixed' and 'calm' conditions</i>	223
5.3	Results	226
5.3.1	<i>Growth dynamics of the individual parental strains on RW and SH</i>	226
5.3.2	<i>Growth dynamics and sexual reproduction of the co-cultures of the two parental strains on RW and SH</i>	229
5.3.3	<i>The dead cells</i>	234
5.4	Discussion	236
5.4.1	<i>The dynamics in the cultures as related to nutrient concentration</i>	236
5.4.2	<i>Sexual reproduction in mixed and still conditions</i>	238
5.4.3	<i>Dead cells</i>	240
Chapter six: General conclusions and future perspectives		243
Appendix I <i>Fragilariopsis kerguelensis</i>		251
Appendix II Glossary of the terminology used in studies on diatom life cycles		261
References		265

Abstract

The marine pennate diatom *Pseudo-nitzschia multistriata* has a heterothallic life cycle and the two mating types ('+' and '-') need to be in contact to allow sexual reproduction to occur. In this thesis, results are presented of an investigation using confocal and time lapse microscopy aimed at describing the different stages of the life cycle of this species. Results are also presented of various experiments aimed at defining the endogenous and exogenous factors that induce sexual reproduction. Parental strains need to reach a certain cell density before undergoing sexual reproduction and an inverse correlation was observed between the inoculum size and the time required for the induction of sexual reproduction. This suggests that sexual reproduction is a density-dependent event, regulated by a chemical mediator. Support for this latter hypothesis was provided by experiments on single parental strains which underwent gametogenesis and formation of gametes when exposed to culture medium conditioned by the growth of the opposite mating type. Other support was provided by the fact that sexual reproduction was considerably reduced in cultures incubated in mixed conditions versus still ones. In the latter experimental setting, cells could settle to the bottom, therefore increasing their density and facilitating the onset of the sexual phase. Evidence was also obtained to support the hypothesis that chemical compounds produced during sexual reproduction might reduce the growth of parental strains. The results obtained in the project have provided novel insights into the mechanisms that regulate the life cycle of this planktonic diatom, showing that the transition from vegetative to sexual phase is regulated by chemical mediators. This information represents an experimental background that will allow future studies, aimed at the characterization of the chemical signalling molecules and/or at molecular investigation, to characterize the genes involved in the different life phases.

Acknowledgments

My first thanks goes to the Stazione Zoologica Anton Dohrn for the financial support for my PhD fellowship, without which this project would not have been possible.

Thanks to Marina Montresor, my Director of Studies, for giving me the opportunity to have this experience, for teaching, helping, supporting me during these three years and to whom I owe a great debt of gratitude. Sincere thanks to David G. Mann, my external supervisor, for the intense and fruitful meetings, his many questions that helped me to consider in a critical way my research, and his great suggestions.

Thanks to all the staff and colleagues at the Institute and especially to: Giovanna Benvenuto for sharing with me her knowledge and her time during the analysis at the confocal and time lapse microscopy; Monia Russo for training and helping with the RNA extractions; Krzysztof Stec who prepared and performed the experiment with the rotating wheel with me; Daniele Iudicone who provided much good advice and with whom I have planned and discussed the results of the rotating wheel experiment. Thanks also to Cristina Tortora and Christophe Brunet for the support for the statistical analysis and to Francesca Margiotta and Augusto Passarelli for the analysis of nutrients. Thanks to Christophe Brunet, Wiebe Kooistra, Francesca Margiotta, Diana Sarno, Raffaele Siano and Adriana Zingone for the scientific discussion and friendly support. Thanks to Martina Ciardi and Fabio DeVita who helped in some experiments during their bachelor degree thesis. Many thanks to Alessandro Manfredonia, Carmen Minucci and Gandi Forlani for their technical support and ... for the jokes that cheered up the difficult moments. To Laura Escalera for helping with the editing of

the figures and for reading and ‘pruning’ the mistakes from my thesis together with Luciana Barra and Sandra Fernandes.

Thanks to Deepak Nanjappa, a friend and a colleague, who has shared with me the PhD thesis’ time: I’m glad to have passed these three years with you on my side desk!

I also want to thank all the people that I met during this period: my sincere thanks for sharing with me your free time! Especially to Alessandra, Angela, Anna, Cristina F., Cristina T., Davide, Deepak, Francesca, Gaia, Giovanna, Isabella, Krzysztof, Lara, Laura, Luciana, M. Luisa, M. Grazia, Martina, Philip, Sandra, Serena E., Serena F., Swaraj and Vasco for the ‘aperitivo’ time, the stories and jokes and many other things!

Un speciale ringraziamento va a Roberto, Carmela e Giulia che sono sempre la mia roccia e il mio faro. Agli zii ad Alessia, Claudia, Elisa, Federica, Ilenia, Sonia, Cinzia, i Roberti, Denis, Ombra e Tiziano per avermi sempre ‘aspettato’ quando tornavo a casa.

Ad Anna, Isabella, Luciana, Giovanna e Maria che mi hanno preso per mano quando sono arrivata e non mi hanno più lasciato, a Francesca, Laura e Serena che che si sono aggregate lungo il mio cammino. Ad Antonio che non mi ha fatto pesare la mia ‘modalità tesi’ ma anzi mi ha sempre incoraggiato. Avete fatto di Napoli la mia seconda casa.

Grazie

List of Figures

- Figure 1.1.** Schematic overview of the structure of a pennate diatom (from Falciatore and Bowler 2002). 29
- Figure 1.2.** Phylogenetic tree of diatoms based on SSU rDNA (modified from Kooistra *et al.* 2007). 31
- Figure 1.3.** Cell size reduction of diatom cells due to mitotic divisions. 36
- Figure 1.4.** Scheme of the life cycle of a centric diatom. a) vegetative phase (black arrows), b) sexual phase (orange arrows). (Modified from Round *et al.* 1990). 39
- Figure 1.5.** Scheme of the life cycle of a *Pseudo-nitzschia* species (pennate diatom). 41
- Figure 1.6.** Light and electron micrographs of *Pseudo-nitzschia multistriata*. (panels 1, 3-9: TEM; panel 2: LM).
 Panel 1. *P. multistriata* valve in valvar view. Panel 2. A chain of cells in girdle view; note the undulate shape.
 Panel 3. Central part of the valve; striae (S), interstriae (I), raphe interspaces (RI) and fibulae (F) are arrowed.
 Panel 4. Central part of the valve with raphe and proximal mantle; note the different pattern of the striae of the proximal mantle. Panels 5, 6. Opposite ends of the same valve. Note the difference in the structure of the terminal striae. Panel 7. Cingulum with first band (=valvocopula) (I), second band (II) with a single row of poroids in the perforated part, and a third (III) non-areolated band. Panel 8. A similar cingulum with the second band showing a double row of poroids (arrowed). Panel 9. Terminal part of a first cingular band (=valvocopula). Scale bars represent: panels 1, 10 μm ; panel 2, 20 μm ; panels 3-6, 9, 1 μm ; panels 7, 8, 0 \pm 5 μm (from Orsini *et al.* 2002). 58
- Figure 2.1.** Schematic drawings of the confocal laser scanning microscope. The laser emits the light; the rotating scanning mirrors direct light; the pinhole, a single small aperture, permits the passage of the light; the filter selects the wavelengths required for the excitation of the specific fluorochrome and the detector for the signal detects the specific wavelengths emitted by the stained/epifluorescent sample. 84
- Figure 2.2.** Time lapse bright field (BF) micrograph frames selected from a movie serie_053d that show the contact between opposite mating type cells. (a-c) One '+' (small) cell and one (a), two (b) or five (c) '-' cells (big) close to each other. (d) Pair of '+' and a '-' gametangia. Note that the time in hours (h), from the beginning of the experiment, is indicated on each sequence. Scale bar = 25 μm . 91
- Figure 2.3.** Time lapse BF micrograph frames selection from a movie serie_053a; gametogenesis and conjugation. (a) Pairing of '+' (left) and '-' (right) gametangia. (b-c) Cytoplasm rearrangement inside of each gametangium. (d-e) Cytokinesis within the '+' (white arrow) and (f) the '-' (black arrow) gametangia. (f-g) Cytoplasm contraction, within the small '+' and (h-k) big '-' gametangia, from the tips of the frustule to the

central area before the formation of '+' (*j*) and '-' (*l*) rounded gametes respectively. (*l-m*) Movement of one '+' gamete (white arrowhead) towards the '-' one (*n-p*) previous the conjugation. Note that the time in hours (h), from the beginning of the experiment, is indicated on each sequence. Scale bar = 25 μ m. 93

Figure 2.4. Selection of BF micrograph frames from a movie Series_015; gamete conjugation. (*a*) A zygote – the slightly larger spherical body (arrow) – and a '-' gamete (upper part) are joined on the right side of the '-' gametangium whereas the '+' gamete is attached to the left side of the '+' gametangium. (*b-d*) The '+' gamete moved toward the '-' one (*e-f*) prior the conjugation. Note that the time in hours (h), from the beginning of the experiment, is indicated on each sequence. Scale bar = 25 μ m. 94

Figure 2.5. Selection of BF micrograph frames from a movie serie_053c; gametogenesis and gamete destruction by bacteria. (*a*) Paired gametangia of opposite mating types. (*b*) Cytokinesis in the '+' gametangium (arrowhead), followed by (*c-d*) the contraction and formation of the two '+' gametes. Rearrangement (*b-d*) and contraction (*e-f*) of the cytoplasm in the '-' gametangium with the formation of a single large spherical body (anomalous gamete) (*g*). The '+' gametes were attacked by bacteria (*h-j*). Two dark small bodies remained after the gamete destruction (arrows) (*k-l*). Note that the time in hours (h), from the beginning of the experiment, is indicated on each sequence. Scale bar = 25 μ m. 95

Figure 2.6. Selection of BF micrograph frames from a movie serie_087; auxospore formation. (*a*) Two auxospores attached to an empty '-' gametangium as generally produced in this species. (*b*) One auxospore starts to elongate while in the other a small spherical body (arrow) is extruded. (*c-h*) The elongation and the expansion of the normal auxospore are illustrated; the four chloroplasts were also visible (arrowheads) (*g-h*). The small spherical body of the other auxospore expand and (*c-e*) but was destroyed by bacteria. Note that the time in hours (h), from the beginning of the experiment, is indicated on each sequence. Scale bar = 25 μ m. 97

Figure 2.7. Selection of BF micrograph frames from a movie serie_03. Initial cell formation. The detachment of the auxospore cytoplasm from the perizonium membrane (arrow) (*a*) and the production of the first valve of the initial cell (*b*) are shown. Note that the time in hours (h), from the beginning of the experiment, is indicated on each sequence. Scale bar = 25 μ m. 97

Figure 2.8. Confocal laser scanning (CLS) micrographs of two vegetative cells that are different in size (small strain Sy373 '+' and large strain Sy800 '-'). The SYBR Green I (green) stained nuclei were visible in the central part of the cell. Scale bar = 25 μ m. 100

Figure 2.9. Phase contrast (PC) micrograph of a small '+' vegetative cell (strain Sy373) with a constriction in its central part. Scale bar = 25 μ m. 100

Figure 2.10. PC (a) and epifluorescence (b) micrographs of '-' vegetative cells in a chain (strain Sy800) in valve view. Nuclei (green), stained with SYBR Green I, were visible in the centre of the cells with the chloroplasts (red) at both sides. Note that the first two cells were under mitotic division. Scale bar = 25 µm. 100

Figure 2.11. CLS micrograph of two vegetative cells different in size (small strain Sy373 '+' and large strain Sy800 '-'). The nuclei, stained with SYBR Green I (green), were visible in the central part of the cell. The large cell was undergoing mitotic division. Scale bar = 25 µm. 101

Figure 2.12. CLS micrographs of recently divided vegetative cells (strain Sy800 '-'). Nuclei, stained with SYBR Green I (green), were perpendicular to the length of the cells (a-b) chloroplasts (red) were placed on each side of the nucleus (b). Scale bar = 25 µm. 102

Figure 2.13. CLS micrographs of two paired gametangia (small '+' strain Sy373; and large '-' strain Sy800). The SYBR Green I stained nuclei (green) were visible in the central portion of the cell; note that the nucleus of the smaller cell (left) has started to undergo the first meiotic division (a, b); two chloroplasts (red) were visible inside each cell (b). Scale bar = 25 µm. 104

Figure 2.14. Confocal Z-stack projection onto CLSM micrographs of different pairing gametangia showing asynchronous gametogenesis (small '+' strain Sy793 and large '-' strain Sy799); nuclei were stained with SYBR Green I (green). (a-b) The small gametangium in Meiosis I with a nucleus inside each protoplast. (a-d) The nucleus of the large gametangium has lost the rounded shape and was starting Meiosis I. (c-f) The small gametangium was in Meiosis II where the 4 nuclei - 2 inside each protoplasm – and the segregation of the cytoplasm (arrow) were visible. The small gametangium was at the end of Meiosis I with 1 (c-d) or 2 (e-f) nuclei inside each protoplasm. (g-h) Both gametangia are in Meiosis II; two nuclei are present in the gametangium on the right, while only one nucleus with a possible pycnotic one (arrowhead) was present on the other cell. Note that the segregated cytoplasm is marked with an arrow. Scale bar = 25 µm. 104

Figure 2.15. Confocal Z-stack projection onto CLSM micrographs of gametes at different sexual stages within a small '+' gametangium (strain Sy379), their nuclei were stained with SYBR Green I (green). (a) Bi- and uni-nucleate elongated gametes and (b) rounded uni-nucleate gametes. Scale bar = 25 µm. 105

Figure 2.16. CLSM micrographs of a binucleated zygote. Both nuclei, SYBR Green I (green) stained (a-b) and, the red auto-fluorescence of the chlorophyll, were visible (b). Scale bar = 10 µm. 107

Figure 2.17. PC micrograph of an auxospore attached to the empty '-' gametangium; its four chloroplasts were visible. Scale bar = 25 µm. 107

- Figure 2.18.** Confocal Z-stack projection onto CLSM micrographs of auxospores. Stained nuclei, with SYBR Green I (green) and the red auto-fluorescence of chlorophyll were visible (*a-b*). The round globule on the left auxospore is a free gamete. Scale bar = 25 μm . 107
- Figure 2.19.** CLSM micrographs of the initial cell formation. (*a*) Binucleated auxospore, stained with SYBR Green I (green), at the end of the expansion, and (*b*) a complete initial cell inside the perizonium with its nucleus at the centre. Scale bar = 25 μm . 108
- Figure 2.20.** CLSM micrograph of the first mitotic division undertaken in an initial cell inside the perizonium membrane. Two chloroplasts (red) and one nucleus, stained with DAPI (blue), were visible inside each daughter cell. Scale bar = 25 μm . 108
- Figure 2.21.** Confocal Z-stack projection onto CLSM micrographs of two zygotes with three nuclei (stained with SYBR Green I) each; a polar body is visible in the lower part of the gametangium. Scale bar = 25 μm . 110
- Figure 2.22.** PC (*a*) and epifluorescence (*b*) micrographs of an auxospore in which four nuclei, stained with SYBR Green I (green), and 8 chloroplasts (red) were visible. Scale bar = 25 μm . 110
- Figure 2.23.** Box plot distribution of the initial cells size produced under different parental strains (*x* axis) crosses as listed in Table 2.5. 112
- Figure 3.1.** Schematic drawings of the experimental set up of Experiment #1 (*a*) and #2 (*b*). See the text for explanation. 142
- Figure 3.2.** The different life stages that were enumerated in the experiments: (*a*) vegetative cells, (*b*) gametes or zygotes, (*c*) auxospores, (*d*) initial cells and (*e*) large F1 generation cells. Bright field (*a*, *b* and *e*) and differential interference contrast (DIC; *c* and *e*) micrographs; scale bars = 20 μm . 142
- Figure 3.3.** Growth curve of Sy373 '+' (blue) and Sy379 '-' (pink) parental strains grown in flasks (*a*) and in culture plates (*b*). Each point represents the average value of duplicate counts; maximum and minimum values are represented with vertical bars. 146
- Figure 3.4.** Growth curve of Sy373 '+' (blue) and Sy379 '-' (pink) parental strains grown in flasks at 110 $\mu\text{mol photons m}^{-2}\text{s}^{-1}$. Each point represents the average value of duplicate counts; maximum and minimum values are reported by the vertical bars (Experiment #1). 148
- Figure 3.5.** Growth curve of Sy373 '+' (blue) and Sy379 '-' (pink) parental strains grown in flasks at 60 $\mu\text{mol photons m}^{-2}\text{s}^{-1}$. Each point represents the average value of duplicate counts; maximum and minimum values are reported by the vertical bars. 148

Figure 3.6. Variation of cell concentration (cells·ml⁻¹, on the left panels) and average percentage values (on the right panels) of parental strains (black squares), sexual stages (gametes, zygotes, auxospores and initial cells: orange circles) and large F1 cells (light-blue circles) with time in Experiment #1 at 60 μmol photons m⁻²s⁻¹. Note the different scales on the y axes.

151

Figure 3.7. Variation of cell concentration (cells·ml⁻¹, on the left panels) and average percentage values (on the right panels) of parental strains (black squares), sexual stages (gametes, zygotes, auxospores and initial cells: orange circles) and large F1 cells (light-blue circles) with time in Experiment #1 at 110 μmol photons m⁻²s⁻¹. Note the different scales on the y axes.

153

Figure 3.8. Time of appearance of the first sexual stages (gametes) as related to the inoculum size (cells·ml⁻¹ of the two parental strains). The points represent the different replicate for each cross, from T0 to T8, in Experiment #1 at low (a) and high (b) irradiances, respectively.

154

Figure 3.9. Time course of cell concentration for parental strain Sy373 '+' (blue), Sy379 '-' (pink), the total number of cells (parental vegetative cells, sexual stages, large F1 cells) in crosses carried out at T0 (green triangles) and T2 (red triangles) in Experiment #1. Panel (a) illustrates the results obtained at 60 and panel (b) at 110 μmol photons m⁻²s⁻¹. Each co-culture was plotted at the time from which parental cells were sampled and mixed. Each point for the parental strains (squares) represents the average value of duplicate counts with maximum and minimum, each point for the crosses (triangles) represents the average of triplicate counts with standard deviation.

155

Figure 3.10. Growth curve of Sy373 '+' (blue) and Sy379 '-' (pink) parental strains grown in flasks at and 110 μmol photons m⁻²s⁻¹. Each point represents the average value of duplicate counts; maximum and minimum values are reported by the vertical bars (Experiment #2).

157

Figure 3.11. Variation of cell concentration (cells·ml⁻¹, on the left panels) and percentage values (on the right panels) of parental strains (black rectangles), sexual stages (gametes, zygotes, auxospores and initial cells: orange circles) and large F1 cells (light-blue circles) with time in Experiment #2 at 60 μmol photons m⁻²s⁻¹. Note the different scales on the y axes.

160

Figure 3.12. Variation of cell concentration (cells·ml⁻¹, on the left panels) and percentage values (on the right panels) of parental strains (black squares), sexual stages (gametes, zygotes, auxospores and initial cells: orange circles) and large F1 cells (light-blue circles) with time in Experiment #2 at 110 μmol photons m⁻²s⁻¹. Note the different scales on the y axes.

162

Figure 3.13. Day at which the formation of the first sexual stages (gametes) was observed plotted on the respective inoculum size (cells·ml⁻¹) of the two parental strains. The points represent the different triplicates for each cross, from T0 to T8, carried out in Experiment #2 at low (a) and high (b) irradiances. 163

Figure 3.14. Time course of cell concentration for parental strain Sy373 '+' (blue), Sy379 '-' (pink), the total number of cells (parental vegetative cells, sexual stages, large F1 cells) in crosses carried out at T0 (green triangles) and T2 (red triangles) in Experiment #2. Panel (a) illustrates the results obtained at 60 and panel (b) at 110 $\mu\text{mol photons m}^{-2}\text{s}^{-1}$. Each point for the parental strains (squares) represents the average value of duplicate counts with maximum and minimum, each point for the crosses (triangles) represents the average of triplicate counts with standard deviation. 163

Figure 3.15. Time course of cell concentration for parental strain Sy373 '+' (blue), Sy379 '-' (pink), the total number of cells (parental vegetative cells, sexual stages, large F1 cells) in crosses carried out at T4 (grey triangles) and T6 (light-green triangles) in Experiment #2. Panel (a) illustrates the results obtained at 60 and panel (b) at 110 $\mu\text{mol photons m}^{-2}\text{s}^{-1}$. Each point for the parental strains (squares) represents the average value of duplicate counts with maximum and minimum, each point for the crosses (triangles) represents the average of triplicate counts with standard deviation. 164

Figure 3.16. The cell density of parental cells on the first day in which sexual stages were detected in the crosses carried out at different times in Experiment #2; black circles: low irradiance, grey circles: high irradiance. 164

Figure 4.1. Schematic drawings illustrating the experimental setup for Experiment#2a.1. See the text for explanation. 185

Figure 4.2. Schematic drawings illustrating the experimental setup for Experiment#2a.2 and #2a.3. See the text for explanation. 187

Figures 4.3. Pictures and drawings showing the position of the nuclei in the different life stages. 188

Figure 4.4. Experiment#1. Growth curve of '+' (blue) and '-' (pink) parental strains grown in single culture. a) Small parental strains Sy373 '+' and Sy379 '-', b) large parental strains Sy668 '+' and Sy800 '-', c) small parental strains Sy793 '+' and Sy776 '-', d) large parental strains Sy710 '+' and Sy686 '-'. (a) and (b) first experiment, (c) and (d) second experiment. Each point represents the average values of duplicate counts; maximum and minimum values are reported by vertical bars. 193

Figure 4.5. Experiment#1. Growth curve of '+' (blue) and '-' (pink) parental strains grown together with the same mating type. (a) Co-cultures of small (Sy373 circle) and large (Sy668 square) '+' strains; (b) co-cultures of large (Sy800 square) and small (Sy379 circle) '-' strains; (c) co-cultures of small (Sy793 circle) and large (Sy710

square) '+' strains; (d) co-cultures of small (Sy776 circle) and large (Sy686 square) '-' strains. (a) and (b) first experiment, (c) and (d) second experiment. Each point represents the average values of duplicate counts; maximum and minimum are reported by vertical bars.

195

Figure 4.6. Experiment#1a. Cell concentration of parental strains and sexual stages obtained when co-culturing strains of opposite mating type with different cell size. Panel (a) Sy373 S '+' x Sy800 L '-'; panel (b) Sy668 L '+' x Sy379 S '-'. On the left axis, parental cell concentration (cells·ml⁻¹; blue square for '+' and pink square for '-'); on the right axis concentration of sexual stages ml⁻¹ (yellow circles for gametes and zygotes; green circles for auxospores; violet circles for initial cells; light blue circles for large F1 cells. To allow the visualization of the different symbols of the sexual stages, they were plotted slightly apart.

197

Figure 4.7. Experiment#1b. Cell concentration of parental strains and sexual stages obtained when co-culturing strains of opposite mating type with different cell size. Panel (a) Sy793 S '+' x Sy686 L '-'; panel (b) Sy710 L '+' x Sy776 S '-'. On the left axis, parental cell concentration (cells·ml⁻¹; blue square for '+' and pink square for '-'); on the right axis concentration of sexual stages ml⁻¹ (yellow circles for gametes and zygotes; green circles for auxospores; violet circles for initial cells; light blue circles for large F1 cells). To allow the visualization of the different symbols of the sexual stages, they were plotted slightly apart.

197

Figure 4.8. Experiment#2a. Production of gametes in strains incubated in the medium conditioned by the opposite mating type. (a) The '+' Sy373 S strain grown in '-' Sy800 L conditioned medium; (b) the '-' Sy800 L strain grown in '+' Sy373 S conditioned medium. On the left y axis cell concentration (cell·ml⁻¹) of parental, strains (blue squares '+'; pink squares Sy800 L '-'), on the right y axis concentration of sexual stages (sexual stages ml⁻¹): blue stars '+' meiotic cells with segregated cytoplasm (MSC), pink stars '-' meiotic cells with segregated cytoplasm, blue circles '+' round gametes and pink circles '-' round gametes. The black and white bars below the x axis indicate the Light:Dark cycle.

199

Figure 4.9. Experiment#2a. Production of gametes in strains incubated in the sex-conditioned medium. (a) The '+' Sy373 S grown in sex-conditioned medium; (b) the '-' Sy800 L strain grown in sex-conditioned medium. On the left y axis cell concentration (cells·ml⁻¹) of parental strains: blue squares Sy373 S '+', pink squares Sy800 L '-'; on the right y axis concentration of sexual stages (sexual stages ml⁻¹): blue stars: '+' meiotic cells with segregated cytoplasm (MSC), pink stars '-' meiotic cells with segregated cytoplasm (MSC), blue circles '+' round gametes and pink circles '-' round gametes. The black and white bars below the x axis indicate the Light:Dark cycle.

200

Figure 4.10. Experiment#2a. (a) Production of gametes in the '+' Sy793S strain incubated in the medium conditioned by the opposite mating type '-' Sy686 L and in (b) the medium conditioned by its own growth. On the left y axis, cell concentration (cells·ml⁻¹) of the parental strains (blue squares); on the right y axis, concentration of sexual stages (sexual stages ml⁻¹): blue stars, '+' meiotic cells with segregated cytoplasm (MSC); blue circles, '+' round gametes. The black and white bars below the x axis indicate the Light:Dark cycle. 202

Figure 4.11. Experiment#2a. (a) Production of gametes in the '-' Sy686 L strain incubated in the medium conditioned by the opposite mating type '+' Sy793S and in (b) the medium conditioned by its own growth. On the left y axis, cell concentration (cells·ml⁻¹) of the parental strains (pink squares); on the right y axis, concentration of sexual stages (sexual stages ml⁻¹): pink stars, '+' meiotic cells with segregated cytoplasm (MSC); pink circles, '+' round gametes. The black and white bars below the x axis indicate the Light:Dark cycle. 203

Figure 4.12. Experiment#2a.1. Control cross of the two parental strains (blue squares '+' Sy373 S, pink squares '-' Sy800 L). On the left y axis cell concentration of parental strains (cells·ml⁻¹); on the right y axis concentration of the different sexual stages: blue stars, '+' meiotic cells with segregated cytoplasm (MSC); pink stars, '-' MCS cells; light green circles, round gametes; yellow circles, zygotes; green circles, auxospores. The black and white bars below the x axis indicate the Light:Dark cycle. 205

Figure 4.13. Experiment#2a.2. Control cross of the two parental strains (blue squares '+' Sy793 S, pink squares '-' Sy686 L). On the left y axis cell concentration of parental strains (cells·ml⁻¹); on the right y axis concentration of the different sexual stages: blue stars, '+' meiotic cells with segregated cytoplasm (MSC); pink stars, '-' MCS cells; light green circles, round gametes; yellow circles, zygotes; green circles, auxospores; violet circles initial cells. The black and white bars below the x axis indicate the Light:Dark cycle. 205

Figure 4.14. Experiment#2a. Control cross of the two parental strains (blue squares '+' Sy793S, pink squares '-' Sy799 L). On the left y axis cell concentration of parental strains (cells·ml⁻¹); on the right y axis concentration of the different sexual stages: red hearths, paired gametangia; blue stars, '+' meiotic cells with segregated cytoplasm (MSC); pink stars, '-' MCS cells; light green circles, round gametes; yellow circles, zygotes; green circles, auxospores; violet circles, initial cells. The black and white bars below the x axis indicate the Light:Dark cycle. 206

Figure 4.15. Experiment#2b. Concentration of the vegetative cells and the sexual stages of the two parental strains separated by the insert membrane: '-' Sy799 L (pink squares) above the insert and '+' Sy793S (blue squares) below the insert. On the left y axis, cell concentration (cells·ml⁻¹) of parental strains; on the right y axis,

concentration of sexual stages (sexual stages ml^{-1}): blue stars, '+' meiotic cells with segregated cytoplasm (MSC); pink stars: '-' MSC cells, blue circles round '+' gametes and pink circles '-' round gametes. 207

Figure 4.16. Experiment#2b. Concentration of the vegetative cells and the sexual stages of the two parental strains separated by the insert membrane: '+' Sy793S (blue squares) above the insert and '-' Sy799 L (pink squares) below the insert. On the left y axis, cell concentration ($\text{cells}\cdot\text{ml}^{-1}$) of parental strains; on the right y axis, concentration of sexual stages (sexual stages ml^{-1}): blue stars, '+' meiotic cells with segregated cytoplasm (MSC); pink stars: '-' MSC cells, blue circles round '+' gametes and pink circles '-' round gametes. 208

Figure 4.17. Micrographs of the two monoclonal cultures '+' Sy793 (a), '-' Sy686 (b, e), and the cross undergoing sexual reproduction (c and d) treated with the stain DHR123 that binds to reactive oxygen species (ROS) after 10' (a), 40' (b) and 48h (c, e) after the inoculum. Epifluorescence micrographs (a, b, c, e), bright field micrographs (d); scale bar = 25 μm . 209

Figure 5.1. Schematic drawings of the experimental set-up. Two kinds of flasks were placed both on the rotating wheel and on a shelf and sampled in the same days: 20 flasks with monoclonal cultures (blue for '+' and pink for '-'), and 18 flasks with co-cultures/crosses of the two mating types (blue and pink). The circle with 'N' indicates the time at which the nutrient analyses were carried out. 225

Figure 5.2. Cell concentration of the two parental strains in monoclonal culture and concentration of nutrients on the rotating wheel (RW); '+' strain (blue square, panel a) and '-' strain (pink square, panel b). On the left axis, cell concentration ($\text{cells}\cdot\text{ml}^{-1}$); on the two right axes, nutrient concentration with different scales ($\mu\text{mol}\cdot\text{l}^{-1}$; yellow circles nitrate, brown circles silicates, green circles orthophosphates). 227

Figure 5.3. Cell concentration of the two parental strains in monoclonal culture and concentration of nutrients on the shelf (SH); '+' strain (blue square, panel a) and '-' strain (pink square, panel b). On the left axis, cell concentration ($\text{cells}\cdot\text{ml}^{-1}$); on the two right axes, nutrient concentration with different scales ($\mu\text{mol}\cdot\text{l}^{-1}$; yellow circles nitrate, brown circles silicates, green circles orthophosphates). 228

Figure 5.4. Cell concentration of the two parental strains in co-culture and concentration of nutrients on the rotating wheel (RW, panel a) and shelf (SH, panel b). On the left axis, concentration ($\text{cells}\cdot\text{ml}^{-1}$, grey squares) of the total number of cells: parental strains + sexual stages + large F1 Cells generation, where each point represents the average value of triplicates counts and st.dev. is represented with vertical bars. On the right axis, nutrient concentration ($\mu\text{mol}\cdot\text{l}^{-1}$; yellow circles nitrate, brown circles silicates, green circles orthophosphates). 230

Figure 5.5. Cell concentration ($\text{cell}\cdot\text{ml}^{-1}$) of the two parental strains (blue square for '+' and pink square for '-'), sexual stages (orange circles for zygotes+auxospores+initial cells) and large F1 Cells generation (light blue 23

circles) cells in co-cultures on the rotating wheel (RW, panel a) and shelf (SH, panel b). Each point represents the average value of triplicates counts; st.dev. is represented with vertical bars. 232

Figure 5.6. Cell concentration (cell·ml⁻¹) of the two parental strains (blue square for '+' and pink square for '-'), sexual stages (light yellow circles: gametes; green circles: auxospores and violet circles: initial cells) in co-cultures on the rotating wheel (RW, panel a) and shelf (SH, panel b). Each point represents the average value of triplicates counts; st.dev. is represented with vertical bars. 233

Figure 5.7. Cell concentration (cells·ml⁻¹) of live (square) and dead (cross) cells of parental strains in monoclonal cultures on the rotating wheel (RW; in panel a '+' and in panel b '-') and shelf (SH, in panel c '+' and in panel d '-'). 234

Figure 5.8. Cell concentration (cells·ml⁻¹) of live (square) and dead (cross) cells of parental strains in co-cultures on the rotating wheel (RW; in panel a '+' and in panel b '-') and shelf (SH, in panel c '+' and in panel d '-'). Each point represents the average value of triplicates counts; st.dev. are represented with vertical bars. 235

Figure 5.9. Cell concentration (cells·ml⁻¹) of live (square) and dead (cross) cells of large F1 generation cells in co-cultures on the rotating wheel (RW, panel a) and shelf (SH, panel b). Each point represents the average value of triplicates counts; st.dev. are represented with vertical bars. 235

Figure A1. Percentage distribution of single cells (blue), cells in chains (green) and sexual stages (gametes + zygotes; red) in the monoclonal parental strains (L2-d6 and L9-c3) and in the cross between them (cross). 258

Figure A2. Phase contrast (*b-c,e,g,i,k,m*) and epifluorescence (*a,d,f,h,l,n*) micrographs of *Fragilariopsis kerguelensis* life stages. Vegetative cells in chain; DAPI-stained nuclei in blue (*a*); gametangium is approaching Meiosis I, the enlarged nucleus is arrowed (*b*). Meiosis I has taken place, meiosis II is completed in the left protoplasm and is in progress in the right protoplasm (the same subject *c* phase contrast, *d* epifluorescence). Gametangium after completion of meiosis II, the separation of the protoplasm is arrowed (the same subject *e* phase contrast *f* epifluorescence). A bi-nucleated rounded gamete inside a valve (the same subject: *g* phase contrast, *h* epifluorescence). Zygote with 4 nuclei (the same subject: *i* phase contrast, *j* epifluorescence). Auxospore with two nuclei (the same subject: *k* phase contrast, *l* epifluorescence). Formation of the initial cell, only one nucleus is visible, the first valve has been deposited (same subject: *m* phase contrast, *n* epifluorescence). Scale bars = 10 µm. 259

Figure A3. Scanning Electron Microscopy (SEM) micrographs of *F. kerguelensis* auxospore. Fully expanded auxospore (*a*); detail of the auxospore cap, note the rounded thin scales (*b,c*). Scale bars: *a*, 10 µm; *b,c*, 1 µm. 260

List of Tables

Table 1.1. List of *Pseudo-nitzschia* species described up to now with information on their toxicity. Species present in the Mediterranean Sea are marked with ‘*’ and species for which information on the life cycle is available are marked with ‘§’. Yes/no was used when toxicity was detected only in some of the strains tested.

61

Table 2.1. Strains of *Pseudo-nitzschia multistriata* used for the experiments to assess the mating type. For each strain are reported: the strain code, the isolation date, the LTER-MC sample code, the average length of the apical axis at the time when the cultures were established, and, when available, the average cell size at the time when the crosses were carried out (in parenthesis); an asterisk (*) marks the strains isolated in 2009 that were crossed with only one member of the reference couple; n.a. = data not available.

76

Table 2.2. Parental strains used during the confocal analysis. For each strain are indicated: the mating type (‘+’, male; ‘-’, female) and the average cell size (\pm st. dev.) at the time when crosses were made.

84

Table 2.3. Combination of excitation laser (Ex. laser), percentage of laser intensity (%) and filter of acquisition (Filter Ac.) used for each dye for observations in confocal microscopy. The absorbance (Abs.) and emission (Em) wavelength range for the different fluorochromes is also indicated.

86

Table 2.4. Parental strains used to test the size of the initial cells. For each strain are indicated: the strain code, the mating type (‘+’, ‘-’) and the average apical axis length (\pm st. dev.) at the moment in which crosses were carried out.

87

Table 2.5. Size of initial cells produced by parental strains of different cell size (S=small, M=medium, L=large size). For each parental strain, the mating type (‘+’, ‘-’) and the average size (μ m) at the moment in which crosses were carried out are reported; the average size of initial cells (μ m) is reported together with st. dev., 20 initial cells were measured for each cross.

111

Table 2.6. Attribution of the mating type (‘+’ and ‘-’ strains; ‘+?’ and ‘-?’ for when it uncertain whether male or female strains; n.a. = not assigned); an asterisk (*) marks the strains isolated in 2009 that were crossed with only one member of the reference couple to the strains tested in the different years (See Table 2.1 for the details on isolation dates and cell size).

113

Table 2.7. Synthesis of the assignment of mating type to strains of *P. multistriata* isolated over three consecutive years. For each year, the total number of tested strains (N) are reported, as well as the number and percentage of

‘+’ and ‘-’ mating type, of mating type assigned with uncertainty ‘+’?, ‘-’?, and of the non-assigned mating types (NA).

115

Table 2.8. Attribution of the microsatellite populations (pop1, pop2, pop3 and hybrid; n.a. = data not available) and the mating type (‘+’ and ‘-’ strains; n.a. = not assigned) to the strains tested in the different years (See Table 2.1 for the details on isolation dates and cell size).

128

Table 2.9. For each year, it is reported the number of successful crosses between strains belonging to the 3 populations (pop1, pop2 and pop3) and for the ‘hybrid’ strains.

131

Table 3.1. Strains of *Pseudo-nitzschia multistriata* used for the experiments illustrated in this chapter. For each strain are reported: the strain code and the mating type, the isolation date, the LTER-MC sample code, the average length of the apical axis at the moment in which the cultures were established (I), and the average length (\pm standard deviation) of the apical axis at the moment in which the experiments were carried out (II).

138

Table 3.2. Maximum cell density (cells·ml⁻¹) and maximum growth rate (divisions·day⁻¹) of the two parental strains grown in different vessels.

146

Table 4.1. Strains of *Pseudo-nitzschia multistriata* used for the experiments reported in Chapter 4. For each experiment, details are given of the strain code, the isolation date, the average length of the apical axis at the moment in which the culture was established (I), and the average length of the apical axis at the time when the experiments were carried out (II). The superscripts ^(a) and ^(b) denote the strains used in the first and second crosses, respectively, in Experiment#1.

180

Table 4.2. Strains of *Pseudo-nitzschia multistriata* used in Experiment#2a. The mating type (‘+’ male mating type; ‘-’ female mating type), the size of the cells (S = small; L = large), the cell concentration (cells·ml⁻¹) at the time in which cultures were filtered to obtain the conditioned medium, the strain inoculated in the conditioned medium.

188

Table 4.3. Maximum growth rate (divisions·day⁻¹) and maximum cell concentration (cells· ml⁻¹) of the eight strains grown in mono-culture (A), in co-cultures with same mating type (B), and in co-culture with the opposite mating type (C). The superscript ^(a) and ^(b) mark the strains used in the first and second crosses, respectively, in Experiment#1.

194

Table 5.1. Strains of *Pseudo-nitzschia multistriata* used for the experiments illustrated in this chapter. For each strain are reported: the strain code and the mating type, the isolation date, the LTER-MC sample code, the average length of the apical axis at the moment in which the cultures were established (I), and the average length (\pm standard deviation) of the apical axis at the moment in which the experiments were carried out (II).

223

Chapter 1

General introduction

1.1 Diatoms: a short overview

The word ‘diatom’ derives from the Greek ‘dia’ that means ‘two’ and ‘tomos’ that means ‘parts’. The etymology of the word perfectly illustrates the distinguishing character of these microalgae: they are surrounded by a mineral theca, the frustule, made of polymerized silicic acid that consists of two, slightly unequal parts that fit together like the lid on a box. These two parts are called ‘epi-theca’ and ‘hypo-theca’, and each of them consists of a valve and a series of cingular bands (Fig. 1.1). The size of diatom cells spans from a few micrometers, as in the very small picoplanktonic species, e.g. *Minutocellus*, to hundreds of micrometers, as in the largest species of the genera *Rhizosolenia* or *Thalassiothrix*. Several species can form more or less long colonies in which the single cells are joined together by mucous material (e.g. *Pseudo-nitzschia*, *Fragilariopsis*), by siliceous extrusions (e.g. *Chaetoceros*) or by chitin filaments (e.g. *Thalassiosira*).

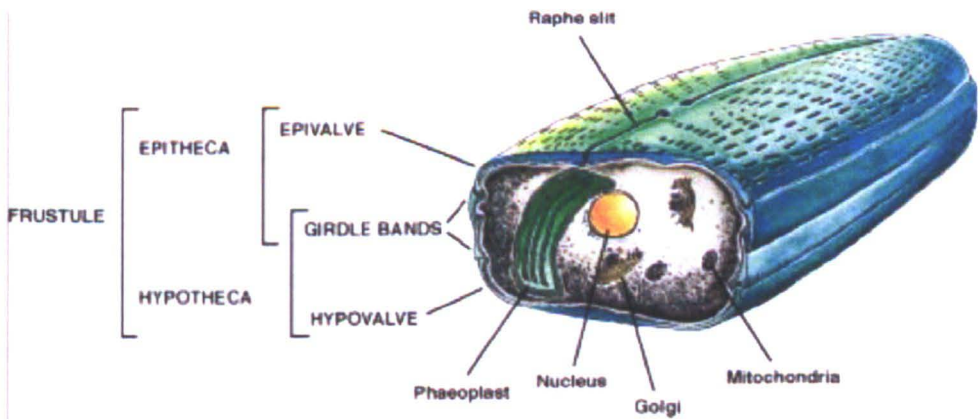


Figure 1.1. Schematic overview of the structure of a pennate diatom (from Falcatore and Bowler 2002).

Diatoms are autotrophic protists and are responsible for a large fraction of carbon fixation in the world’s oceans (about 1/5 of the global carbon fixation Mann 1999, Smetacek

1999). However, diatoms do not only live in the water column of the oceans but they are abundant in lakes and rivers, as well as present in the soil, if enough humidity is present. It is estimated that diatoms include about 200,000 species, the majority of which have a benthic habit and live as epilithic on sand and stones or epiphytic on the aquatic vegetation (Kooistra *et al.* 2007). The study of diatom fossil records showed that the first diatoms appeared in the early Jurassic (ca. 190 millions of years B.P.). The oldest diatoms were radial centrics and a major diversification, with the appearance of multipolar centrics and pennates, occurred in the Cretaceous (about 145-65 millions years B.P.). Molecular phylogenetic studies conducted by analyzing the small subunit of the ribosomal rDNA (SSU-rDNA) confirmed this evolutionary sequence: radial centric diatoms are the most primitive lineage, followed by bi- and multipolar centric, then araphid pennates and finally raphid pennates, which are the youngest lineage (Fig. 1.2) (Kooistra *et al.* 2007). Marine planktonic diatoms mostly belong to the centric lineages but there are some genera of pennate diatoms – e.g. *Pseudo-nitzschia*, *Fragilariopsis*, *Thalassiothrix*, *Asterionellopsis* - that have a planktonic habit and are an important component of the marine plankton.

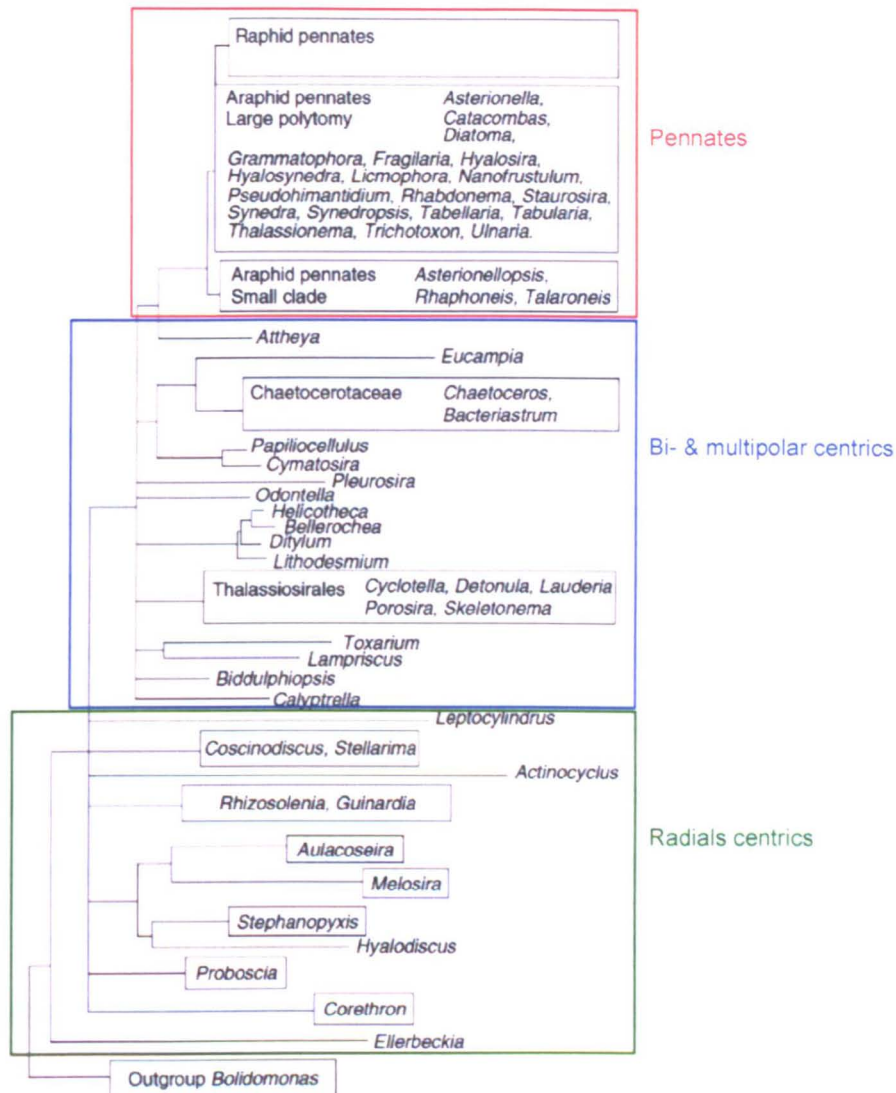


Figure 1.2. Phylogenetic tree of diatoms based on SSU rDNA (modified from Kooistra *et al.* 2007).

The capability to biomineralize silicon, i.e. to take up the silicic acid dissolved in the water and build the glass frustule, makes diatoms the key organisms governing the silicon biogeochemical cycle in aquatic environment. This element is dissolved from the rocks into the rivers and the sea, is taken up mostly by diatoms and, when they die and sink through the water column, it is either dissolved (entering again the dissolved Si pool) or buried on the sea floor. The largest deposit of siliceous diatom frustules is located around Antarctica and it is

largely constituted by the heavily silicified diatom *Fragilariopsis kerguelensis*, together with remnants of other large and thick-walled species that live in the area (Smetacek *et al.* 2004).

Diatoms also play an important role in the biogeochemical cycle of carbon (Smetacek 1999). They are responsible for a considerable fraction of the primary production in the ocean; they take up the inorganic carbon dissolved in the seawater and transform it into organic matter *via* the photosynthetic process. The threshold for diatom growth is set by the availability of light and nutrients. Diatoms generally dominate the spring blooms in temperate and polar regions, when day-length increases and remineralized inorganic nutrients become available in the upper portion of the water column after the deep winter mixing. Diatoms dominate these large blooms because they can grow in dim light (when the water column is mixed for tens of meters) and have a high efficiency for the uptake of the main inorganic nutrients (Smetacek 1999). When the blooms are over (generally due to the exhaustion of nutrients or by natural death of the populations), diatoms sink through the water column and export the organic carbon to the deep layers of the ocean, where it provides food for benthic organisms and is respired by the bacteria. It has been calculated that about one third of the global primary production is exported away from the photic zone, but only about 1% gets sequestered in the deep sediments in areas with the highest primary production (coastal areas, upwelling regions, frontal areas etc.). The fact that diatoms dominate blooms can be explained by their physiology but also by the fact that the biomineralized frustule protects them from grazers. This might be the reason why they tend to accumulate in the water column and suddenly collapse at the end of the bloom.

1.2 The life cycle of diatoms: what do we know from laboratory studies?

Diatoms have a diplontic life cycle; this means that they are diploid ($2N$) during most of their life with the exception of the gametes – the products of meiosis – that are haploid (N). Diatoms spend the majority of their life history going through repeated mitotic (asexual) divisions, but a short and quick sexual phase including meiosis, gametogenesis and fertilization is reported for many species (Chepurnov *et al.* 2004, Edlund and Stoermer 1997, Mann and Marchant 1989, Round *et al.* 1990 5742). The life cycle of diatoms is very peculiar because it is characterized by a strong link with the cell size: cells can in fact undergo specific transformations only in defined size windows.

1.2.1 Vegetative division

Before undergoing vegetative division, diatoms must increase about twofold their cell volume, double the mitochondria, plastids and other organelles, replicate the chromosomes and then segregate full components in each daughter cell. This increase in cytoplasm material is associated with an increase in cell size but, because of the constraint represented by the rigid frustule, they can increase in size only in one direction, as hypotheca and epitheca slide apart through the deposition of extra cingular bands (Round *et al.* 1990).

The expansion could be continuous or discontinuous and restricted to a particular phase of the cell cycle. For instance, *Thalassiosira weissflogii* and *Lauderia borealis* increase in size continuously during the cell cycle (Olson *et al.* 1986), while other species expand only at a particular time. As an example, in *Chaetoceros didymus* and in *Stephanopyxis turris* the expansion takes place during the end of interphase and during the mitotic prophase. In

Sellaphora pupula the main phase of expansion is after the completion of valve formation of the daughter cells (Round *et al.* 1990).

During interphase, the nucleus is usually accompanied by a small organelle, the centrosome, which is rarely visible in the light microscope, except for large diatoms such as *Surirella capronii* (Round *et al.* 1990). During prophase, the nuclear membrane disintegrates, and the centrosome (also named microtubule centre, MC) starts radiating numerous microtubules that move to the side of the cell and to the middle of the girdle. The nucleus is led from the side of the valve to the middle of the girdle of the cell, apparently through the interaction with the system of microtubules. However the nucleus does not always move before mitosis. In some diatoms, as *Cymbella* sp. and *Amphora ovalis*, there is no nuclear migration, because the nucleus has already moved to the center of the girdle during interphase (Round *et al.* 1990). In the pre-mitotic cell, a new structure, the polar complex (PC), appears next to the MC. It is still not known if the PC is produced by the MC or whether it is formed very close to it (De Martino *et al.* 2009). The MC disappears as the PC is divided into two parallel structures (the polar plates) that constitute the pole of the mitotic spindle. During pro-metaphase, the spindle, which is located outside the nucleus, sinks into it and at the same time, the nucleus enlarges markedly. At this point the condensed chromosomes start to arrange around the spindle attaching to it in a way not yet understood. Later, the spindle poles slide apart by the elongation of microtubules and separate the condensed chromosomes, the nucleus membrane reconstitutes itself and a new centrosome is formed. While the nucleus is dividing, a cleavage furrow appears and cuts the cell in two (De Martino *et al.* 2009, Round *et al.* 1990). Following the formation of the cell cleavage, the new valves are formed within the frustule of the mother cell, each with a single silica deposition vesicle (SDV). Silica deposition occurs under acid conditions and the SDV becomes more acid during the process of valve maturation (Vrieling *et al.* 1999). Silica deposition vesicles are produced by the Golgi apparatus and

migrate close to the plasmalemma through the connection to various systems of microtubules, some of which are connected to the centrosome (Mann and Marchant 1989, Round *et al.* 1990). To complete cell division, cytokinesis takes place at the middle of the girdle.

Diatom life cycle has been studied since the middle of XIX century. During this period, different researchers recognized that diatoms decrease in cell size during the vegetative reproduction (e.g. MacDonald 1869, Pfitzer 1869). Diatoms are surrounded by a rigid silica wall, called frustule that consists in two overlapping halves, called thecae, with unequal size, as a box (hypotheca) with the lid (epitheca). During vegetative division, each daughter cell inherits one maternal theca, which becomes the large epitheca, and builds *ex novo* the smaller one, which becomes the hypotheca. So, one daughter cell has the same mother size while the other one will be smaller (Fig. 1.3). This peculiar mechanism of cell division causes a progressive cell size reduction of the population, known as the 'MacDonald-Pfitzer rule' (MacDonald 1869, Pfitzer 1869). Consequently, repeated cell divisions are responsible for a decrease in the average cell size - length in pennates and diameter in centrics - of the population over time and a corresponding increase of the standard deviation (Round 1972). The cell size of diatom species is thus not constant and can vary considerably. For example, in *Sellaphora pupula* it ranges between 19 and 57 μm in length (Mann *et al.* 1999), in *Leptocilyndrus danicus* between 6 to 42 μm in diameter (French III and Hargraves 1985), in *Pseudo-nitzschia multistriata* between 26 and 82 μm (D'Alelio *et al.* 2009a) and in *P. delicatissima* between 8 and 80 μm in length (Amato *et al.* 2005).

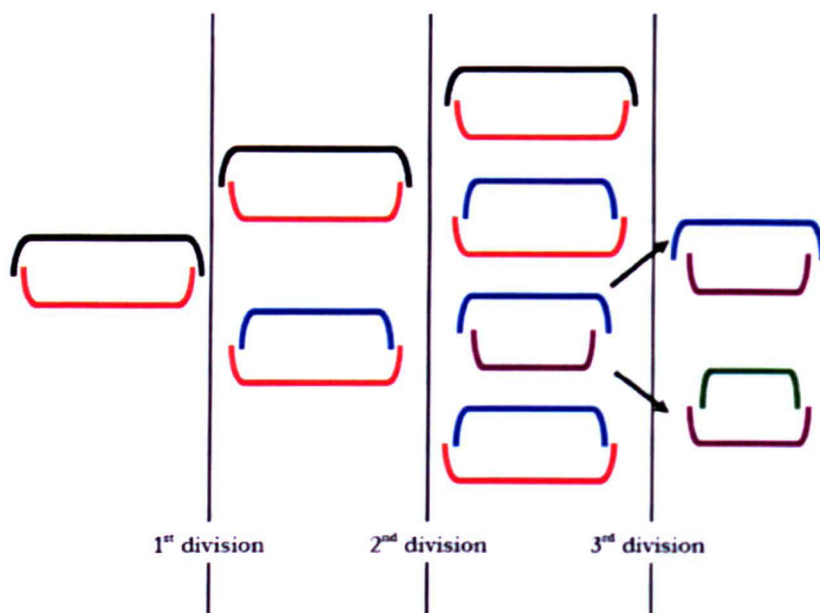


Figure 1.3. Cell size reduction of diatom cells due to mitotic divisions.

The largest cell size reduction per cell division has been recorded in large cells. The decrease in size is at times accompanied by a modification of the valve outline. In multipolar centric diatoms the diameter decreases equally, while in bipolar centric diatoms and in many pennate diatoms the reduction of the apical axis is not associated to a decrease in the transapical axis e.g. *Synedra* spp. and *Nitzschia* spp. (Round 1972). Continued mitotic divisions will eventually result in critically small cells that will die (Amato *et al.* 2005, D'Alelio *et al.* 2009a). It has been observed that in culture cells can become considerably small and reach cell sizes that are rarely recorded in the natural environment (Drebes 1977).

The formation of a daughter cell much smaller than the mother cell has been found to occur occasionally in *Pseudo-nitzschia pungens* (Chepurnov *et al.* 2005). This process is called 'abrupt size reduction' and occurs in two possible ways; 1) by the formation of a much shorter initial cell due to the abortion of a part of the enlarged auxospore, or 2) by the formation of shorter cells during a series of mitotic divisions in which one cell much smaller than the mother cell is formed (Chepurnov *et al.* 2005). In *Aulacoseira subarctica* reduction in

cells size up to 1 μm was found under unfavorable environmental conditions (Jewson 1992a). In *Stephanodiscus neoastraea* the largest decrease in cell diameter was observed in summer under nutrient limited conditions and in autumn under low light (Jewson 1992b). So, environmental conditions seem to affect the rate of cell size reduction. Since the reduction of valves along with cell division has been discovered, it has become clear that not all diatoms do exhibit reduction of cell size (e.g. *Eunotia pectinalis* var. *minor*; *Navicula pelliculosa* and some *Nitzschia*) and where it occurs such reduction is not always constant (reviewed in Mann and Marchant 1989, Round *et al.* 1990). The cell size of natural populations of *Stephanodiscus* sp. showed an inconstant decrease in cell diameter: at times it decreased and at times it remained constant (Round 1982). In *Phaeodactylum tricornutum* cell size reduction does not take place in any of the morphotypes (fusiform, triradiate and oval) because this species does not have a proper silica frustule. In fact, the three morphotypes are able to grow in absence of silicic acid because the cells are surrounded only by thin, poorly silicified, stripes; while only oval cells grown in the presence of silicic acid possessed a silicified cell wall organized into a typical frustules (De Martino *et al.* 2007).

1.2.2 The sexual phase

Sexual reproduction in diatoms is not only the life cycle phase in which genetic recombination occurs but it is also the phase in which the maximum cell size is restored. The lack of cell size reduction is apparently rare in diatoms. However, the distribution of this life cycle modality within the diatom lineages suggests that the possession of a sexual cell size reduction-restitution cycle is the primitive condition and that the asexual species are evolutionary ‘dead-ends’ (Mann and Marchant 1989). Sexual reproduction includes meiosis, gametogenesis, fertilization and formation of specialized zygote – the auxospore – within which the initial cell is produced (Chepurnov *et al.* 2004). The zygote lacks the rigid siliceous wall, so it is free to

expand and form the auxospore. The auxospore starts expanding by the formation of a composite organic-siliceous wall, called the perizonium, consisting of bands made of an organic matrix in which some silica is incorporated. After the auxospore has reached the maximum species-specific size, the two valves of the initial cell are formed following two 'special' mitotic nuclear divisions that are not accompanied by cytokinesis. Each mitotic division results in the formation of one valve. The uninucleate stage is maintained by the degeneration of one daughter nucleus following each mitotic division (Chepurnov *et al.* 2004). The size of the initial cell and the cell size threshold at which sex can occur are called 'cardinal points' (Geitler 1932) of the diatom life cycle. This synthesizes the strong link between cell size and the progression of the diatom life cycle. In the two main groups of diatoms, centric and pennate, two very different modalities of sexual reproduction are present.

1.2.2.1 *The sexual phase: centric diatoms*

Centric diatoms are always homothallic – gametes of opposite mating type (+) and (-) are produced in the same clonal culture – and they have an oogamous sexual reproduction (Fig. 1.4). Within the '-' (female) gametangium they form one or two sessile macro-gametes (egg cell/s) and within the '+' (male) gametangium, they produce numerous small uni-flagellate gametes (sperm cells).

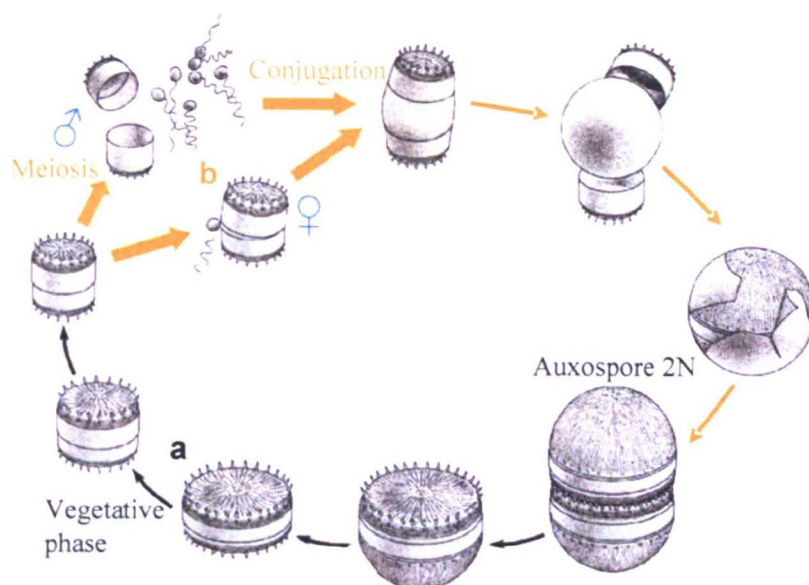


Figure 1.4. Scheme of the life cycle of a centric diatom. a) vegetative phase (black arrows), b) sexual phase (orange arrows). (Modified from Round *et al.* 1990).

Cells that start to become (-) gametangia (oogonia) can be recognized by their enlarged nucleus in prophase of meiosis I, the deeper pigmentation due to an increased number or size of plastids, and the elongation of the girdle region. In most species only one haploid egg is produced, so meiosis I and II proceed without cytokinesis and, after each nuclear division, one nucleus becomes pycnotic. In some species - as *Odontella mobiliensis* - two egg cells per oogonium are produced and cytokinesis follows meiosis I (Chepurnov *et al.* 2004). The formation of (-) gametangia has been described in e.g. *Thalassiosira punctigera* (Chepurnov *et al.* 2006) and *Stephanopyxis palmeriana* (Drebes 1966). The development of oogonia involves the elongation of the cell, followed by a gradual separation of the thecae and partial exposure of the protoplast (Chepurnov *et al.* 2006). Usually (-) gametes are not released from the oogonium – e.g. *Thalassiosira punctigera* (Chepurnov *et al.* 2006) and *Stephanopyxis palmeriana* (Drebes 1966) – but in *Lithodesmium* (-) gametes are released in the medium (Chepurnov *et al.* 2004).

Spermatogenesis is more variable and apparently more complex than oogenesis. Spermatogenesis starts with a series – the number can differ amongst species – of “special” mitotic divisions during which the cells do not expand as they do through the normal mitotic cell cycle (Drebes 1977). This special mitosis results in progressive reduction in cell size and plastid number per cell. In some diatoms such as *Thalassiosira punctigera* (Chepurnov *et al.* 2006), new siliceous thecae are deposited after some or all these mitotic divisions, but the thecae are reduced and weakly silicified. No thecae are produced in other diatoms, as in *Coscinodiscus granii*, in which the small diploid spermatogonia products remain enclosed by the parental frustule until meiosis occurs (Schmid 1995). In *Guinardia flaccida* and *Aulacodiscus argus*, spermatogonia are multinucleate because the special mitoses are acytokinetic (Drebes 1977). Sometimes spermatozooids of centric diatoms lack chloroplasts, and a residual body containing chloroplast was found in the spermatogonia frustule after spermatozooids were released. This is the case of *Thalassiosira punctigera* (Chepurnov *et al.* 2006), *Stephanopyxis palmeriana* (Drebes 1966) and *Coscinodiscus granii* (Schmid 1995). After the spermatozooids are released, they swim actively towards the egg cell but the mechanisms of attraction and recognition between sperms and eggs are poorly known. After fertilization of the egg cell, the zygote is wrapped by an organic wall and becomes an auxospore. In centric diatoms, the auxospore starts to expand isodiametrically and remains more or less spherical (Chepurnov *et al.* 2004). The auxospore wall can be unsilicified (Round 1982) or can include small siliceous scales embedded in the organic matrix (Crawford *et al.* 2001). When auxospore expansion is completed, the new frustule of the initial cell is synthesized inside the auxospore.

The life cycle of *Leptocylindrus danicus* constitutes an exception within diatoms because the auxospore develops into a resting spore, i.e. a quiescent stage that subsequently germinates into a vegetative cell (French III and Hargraves 1985).

1.2.2.2 The sexual phase: pennate diatoms

Pennate diatoms are generally heterothallic; (-) and (+) gametes are produced in different clones. Most raphid diatoms are isogamous, i.e. gametes are similar in shape and size but functionally distinct (Chepurnov *et al.* 2004, Drebes 1966, Round *et al.* 1990). The gametes of pennate diatoms are non-flagellate and have limited capacity of movement, so the two gametangia must be positioned close enough to allow conjugation (Fig. 1.5). In fact, interaction between opposite mating types is required to start meiosis and gametogenesis and sexual reproduction were never found in monoclonal heterothallic species. However, there are several exceptions, as in the case of *Pseudo-nitzschia brasiliensis* where homothallic auxosporulation was found in monoclonal cultures (Quijano-Scheggia *et al.* 2009a). Another ‘exception’ is the presence of motile gametes in the araphid pennate *Pseudostaurosira trainorii*; male gametes move by the extrusion and retrieval of filamentous threads, structures that have not been previously reported in heterokontophyta (Sato *et al.* 2011).

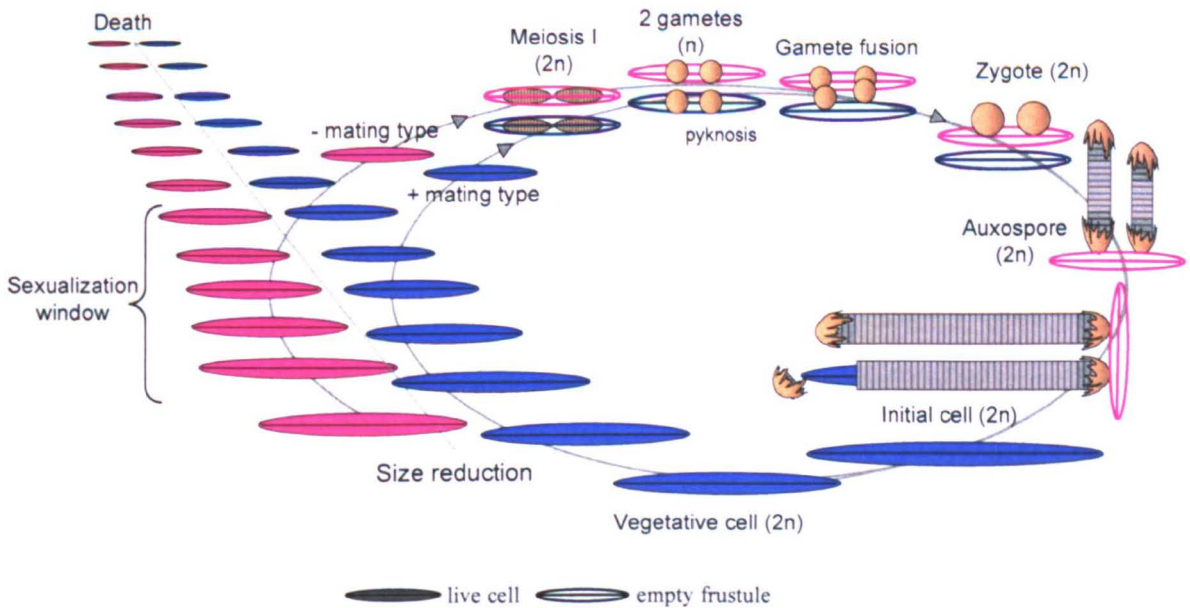


Figure 1.5. Scheme of the life cycle of a *Pseudo-nitzschia* species (pennate diatom).

In pennate diatoms, only one or two gametes are produced for each gametangium and the number of gametes is the same for both mating types (Chepurnov *et al.* 2004, Round *et al.* 1990 5742). A detailed description of gametogenesis has been reported for several species e.g. *Amphora* sp. (Sabbe *et al.* 2004b), *Navicula cryptocephala* (Poulickova and Mann 2006) and *Pseudo-nitzschia pungens* (Chepurnov *et al.* 2005).

When only one gamete is produced per gametangium, as in *Navicula cryptocephala* (Poulickova and Mann 2006), no cytokinesis occurs after the first meiotic division, nor after the second. It was not clear, however, when the 3 nuclei disappeared and left only one. In *Amphora* sp., unequal cytokinesis follows meiosis II and a residual body containing a small protoplast, a haploid nucleus and, rarely, also a small fragment of chloroplast is produced; this residual body subsequently aborts and the final product is thus only one gamete per gametangium (Sabbe *et al.* 2004b). When two gametes per gametangium are produced, an equal plasto- and cytokinesis follows the first meiotic division. In meiosis II, only karyokinesis is involved and two gametes, each one with one normal and one pycnotic nucleus, are produced. The pycnotic nucleus subsequently degenerates and 2 haploid nuclei are thus produced (Chepurnov *et al.* 2005, Mann 1993a).

Vegetative cells of raphid pennate diatoms could contain one, two or four plastids (Round *et al.* 1990 5742) and each vegetative cell can produce one or two gametes with one or two chloroplast each, depending on the species (e.g. Amato *et al.* 2005, Mann and Stickle 1989, Mann 1993a, Poulickova and Mann 2006). The number of chloroplasts depends on whether one or two gametes are formed per gametangium and, in diatoms producing two gametes, on whether or not chloroplast division occurs before the cytokinesis of meiosis I (Amato *et al.* 2005, Chepurnov *et al.* 2004, Levialdi Ghiron *et al.* 2008). This means that, in species that produce two gametes per gametangium with the same numbers of chloroplast as in vegetative cells, chloroplast division generally takes place during meiosis I (Mann 1993a,

Poulickova and Mann 2006). However, sometimes the auxospores of pennate diatoms have as many chloroplasts as vegetative cells (Chepurnov *et al.* 2002, Mann and Stickle 1989).

When gametangia of opposite mating type pair, meiosis takes place. Different fertilization behaviours have been reported in pennate diatoms (Mann 1993b). One of them is known as type IA, when two gametes are produced per gametangium and they are functionally anisogamous. Fertilization can be '*trans-type*' or '*cis-type*' (Mann 1993b). In the first one (IA1 = '*trans-type*') each gametangium produces one motile and one non motile gamete, migration of active gametes occurs in opposite directions and one auxospore develops on each gametangium, e.g. *Nitzschia sigmoidea* (Mann 1986). In the second one (IA2 = '*cis-type*') one gametangium produces passive (-) gametes that remain attached to the empty gametangium and the other gametangium produces active (+) gametes that escape from gametangium and migrate toward the passive gametes to fuse (Mann 1993b), e.g. *Pseudo-nitzschia* (Amato *et al.* 2005, Davidovich and Bates 1998) and *Amphora* cf. *laevissima* (Mann 1993b). The presence of a pheromone that induces the migration of the motile '+' (male) gametes towards the '-' (female) ones has been demonstrated for the araphid diatom *Pseudostaurosira trainorii*, that orientates motility of the '+' gametes after an initial 'random walk' (Sato *et al.* 2011). This is the first documented report of a pheromone in a diatom. During fertilization, only plasmogamy takes place and results in the formation of a zygote with two haploid nuclei and four chloroplasts. The zygote/s remains attached to the mother, empty gametangium and starts to elongate into an auxospore. During elongation the outer zygote membrane is broken, and the two halves (=caps) remain on the extremities of the auxospore. A new cell wall - the perizonium - is formed inside the original zygote membrane (Chepurnov *et al.* 2004, Wiese 1969). The major phase of expansion involves the formation of a new set of elements: the transverse perizonial bands and elongation can be unipolar (in one direction) or bi-polar (in both directions). When the elongation is completed, karyogamy takes place and the auxospore

contracts away from the perizonium (Chepurnov *et al.* 2005). The two thecae of the initial cell are subsequently synthesized, with the epivalve first and then the hypovalve (Chepurnov *et al.* 2005). Each valve deposition is preceded by acytokinetic mitosis: this means that each nuclear division corresponds to the deposition of one valve, and each time one of the two newly divided nuclei becomes pycnotic (Drebes 1977, Wiese 1969). When the initial cell escapes from the perizonium, it has four chloroplasts that will segregate into each daughter cell during the first mitotic division (Amato 2010, Chepurnov *et al.* 2004, Drebes 1977, Poulickova and Mann 2006, Round *et al.* 1990 5742). In *Pseudo-nitzschia delicatissima*, it seems that the auxospore contains four chloroplasts but, during its development, two of them disappear and the initial cell emerging from the auxospore appears to contain only two (Levialdi Ghiron *et al.* 2008). Occasionally, auxospores are produced from sexual reproduction occurring in a single gametangium; this process is called 'automixis'. In automixis, the two nuclei produced after meiosis in a single gametangium fuse and produce a zygote (Chepurnov *et al.* 2004, Mann 1993b). Two main types of automixis have been described. In the first type, e.g. in *Pinnularia nodosa* (Poulicková and Mann 2008), a pseudo-zygote is produced without any meiotic cytokinesis: two of the four nuclei fuse (autogamy), the other two nuclei degenerate. In the second type, e.g. in *Gomphonema angustatum* (Mann 1993b) and in *Sellaphora marvenii* (Mann *et al.* 2011), two normally differentiated gametes are produced in a gametangium after meiotic cytokinesis and fuse (paedogamy). In both types of automixis, the pseudo-zygote develops as an auxospore and it is surrounded by the normal perizonium typical of auxospores (Mann 1993b, Mann *et al.* 2011, Poulicková and Mann 2008).

1.2.3 Vegetative cell enlargement and asexual auxosporulation

In most diatoms, cell size restoration occurs only through sexual reproduction, but some species can restore the maximum cells size by vegetative cell enlargement or asexual

auxosporulation. In both processes, an auxospore-like structure is produced and within it a large vegetative cell is formed; however, the two processes differ because during vegetative enlargement, the cells lack the special envelopes (perizonia) characteristic of auxospores, while these envelopes are present in auxospore-like structures produced following apomictic auxosporulation (Chepurnov *et al.* 2004, von Stosch 1965). Asexual auxosporulation occurs usually in diatom genera in which sexual lineages predominate; this indicates that asexual auxosporulation is a secondary modification of a fundamentally sexual pathway of development (Chepurnov *et al.* 2004). Vegetative cell enlargement has been reported in some centric diatoms as *Coscinodiscus wailesii* (Nagai *et al.* 1995); *Ditylum brighwellii* (Koester *et al.* 2007), *Leptocylindrus danicus* var. *apora* (French III and Hargraves 1986) and *Skeletonema costatum* (Gallagher 1983). Asexual auxosporulation is known to occur in a few pennates such as *Achnanthes cf. subsessilis* (Sabbe *et al.* 2004a). Vegetative enlargement includes the formation of an auxospore-like structure, by partial or complete extrusion of protoplast from a vegetative cell. The auxospore is thus not the product of the conjugation between two gametes but is produced following a mitotic division. In the *Achnantes* species, a whole range of reproductive system has been reported, including asexual auxosporulation in *A. cf. subsessilis* (Sabbe *et al.* 2004a). The auxospore is produced following an acytokinetic mitotic division, followed by the degeneration of one (pycnotic) nucleus; the auxospore then expands surrounded by a longitudinal perizonium.

1.2.4 The resting phase

The life cycle of many diatoms also includes the formation of resting stages, either spores, which are morphologically differentiated from vegetative cells and have a thick wall, or resting cells, which are morphologically similar to vegetative cells, but physiologically differentiated (Hargraves 1976). Resting stages can be quiescent in the sediments for years and

might serve as survival stages for the population during adverse conditions for growth (McQuoid and Hobson 1996). In *Chaetoceros diadema*, spore formation does not seem to be linked with cells size (French III and Hargraves 1985); but in *Stephanopyxis palmeriana* only small cells produce spores (Round *et al.* 1990). A number of external factors have been found to induce spore formation. As an example, low nutrient concentration, especially nitrogen, induces spore formation in *Chaetoceros diadema*, although low temperature can positively influence the process (French III and Hargraves 1985).

Only for *Leptocylindrus danicus* there is evidence that the resting spore is the product of sexual reproduction, because it is the auxospore that transforms into a resting spore. It follows that the cell size window in which spores are produced depends on the size window in which sexual reproduction can be induced (French III and Hargraves 1985). The resting spores of diatoms as *Leptocylindrus danicus*, *Chaetoceros diadema* and *Chaetoceros socialis* show higher carbon content than vegetative cells (French and Hargraves 1980).

1.3 Factors influencing the sexual phase of diatoms life cycle

Sexual reproduction is a crucial phase in the diatom life cycle: it is the phase in which meiosis – and thus genetic recombination – occurs and also the phase in which large sized cells are produced, allowing the persistence of natural populations. Sex can occur only after two general conditions are met: i) cells must reach the cell size threshold within which gametes can be produced, typically 30-75% of the size of the initial cells; ii) favourable environmental conditions should be met, which might include combinations of temperature, light, nutrients, etc. (Chepurnov *et al.* 2004). In heterothallic species, it is the presence of the right mating types. The onset of sex, therefore, depends on a combination of endogenous and exogenous factors.

1.3.1 Endogenous factors

The initiation of the sexual phase is size-dependent and it is closely related to the age of the clones due to the MacDonald-Pfitzer rule: cultures have to reach a certain ‘age’, i.e. they have to go through a certain number of vegetative divisions before undergoing the sexual phase. Nevertheless it is important to point out that the onset of sex cannot be necessarily related to the ‘age’ of the clone. In fact, some diatoms can change cell size abruptly and produce cells with smaller size but with the same ‘age’, or with the same number of cell division that separate them from the initial cell. This is the case of *Pseudo-nitzschia pungens* (Chepurnov *et al.* 2005) and *Eunotia bilunaris* (Mann *et al.* 2003). The fact that the differentiation of gametes occurs in cells with a species-specific cell size would imply that these unicellular algae do have a mechanisms to monitor their size (Chepurnov *et al.* 2004). This mechanism might be a way to count the number of divisions between the initial cell and the first cardinal point.

Nevertheless, the fact that cells that underwent abrupt cell size reduction can undergo sex 'earlier', would exclude this explanation. The onset of sex might thus depend from a mechanism through which cells perceive their volume; nevertheless, it is surprising that only 'some' of the cells with the same volume undergo sex, while the others keep a normal cell growth.

In centric diatoms, it was found that there is often a different cell size range for oogenesis and spermatogenesis (Chepurnov *et al.* 2004). This is the case of *Ditylum brightwellii*, where strains of the smallest cell size produced mostly spermatogonangia, while strains of average cells size either produced oogonia and spermatogonangia with similar proportions or produced mostly oogonia (Koester *et al.* 2007). In *Thalassiosira weissflogii* the formation of sperms was detected in strains whose volume was below the 50% of the maximum cell size. However, the formation of oogonia could not be detected and only in small sized strains the formation of bent cells that could be interpreted as oogonia was detected but could not be confirmed by conjugation (von Dassow *et al.* 2006).

In heterothallic pennate diatoms sexual reproduction occurs when cells of compatible mating type are cultured together (e.g. Amato *et al.* 2005, Chepurnov *et al.* 2004, D'Alelio *et al.* 2009a). Cell-cell interactions between compatible cells seem to determine when and where sexual reproduction occurs. This suggests that the density of the populations will also be important in inducing sexual reproduction, not only to permit the contact between cells (Bates *et al.* 1998), but also to allow communication mediated by chemical compounds (pheromone-like substances). The presence of sex pheromones that induce gametogenesis in compatible clones of *Pseudostaurosira trainorii* has been demonstrated recently (Sato *et al.* 2011). The sexualization of '+' clones – i.e. the formation of gametes - is triggered by a '-' sex pheromone-like molecule. This compound seems to be secreted continuously by '-' strains in

the sexual size range. Once ‘+’ cells are sexualized, they secrete another sex pheromone, which stimulates the sexualization of ‘-’ cells.

Another important endogenous factor seems to be the cell cycle phase in which the diatom cells reside. Armbrust *et al.* (1990) showed that cells of *Thalassiosira weissflogii* respond to induction of gametogenesis only during a narrow portion of their cell cycle, the G1 phase. Cells in early G1 phase and in the right cells size window were induced to form male gametes when cells kept at to saturating levels of continuous light were exposed to dim light or dark, while cells in the remaining portion of the cell cycle ignored the signal and continued to divide mitotically (Armbrust *et al.* 1990). It is also important that cells are in a good physiological condition to be capable of reproducing sexually. This means that they must be in the exponential growth phase, e.g. 3-6 days from the inoculum, in batch culture. In nature, one would, therefore, expect to find sexualized cells only when conditions are favourable for growth.

1.3.2 Exogenous factors

Most reports of auxosporulation in diatoms are based on isolated laboratory experiments (Chepurnov *et al.* 2004). The role of different environmental parameters (irradiance, photoperiod and light spectral composition, temperature, salinity, nutrient concentration) on the occurrence of sexual reproduction has been tested on species belonging to different lineages (radial and multipolar centrics, raphid and araphid pennates) and life styles (planktonic and benthic), providing a rather complex picture from which it is difficult to extract general rules. It is plausible that different species have different requirements for sex, and that these differences might be further modulated by the environmental conditions of the sites in which they live. The different experimental setups and differences in the experimental

details provided by the authors contribute to difficulty of comparing results obtained with different species.

A series of experiments have tested the role of light (as irradiance, composition or photoperiod), at times coupled with the effect of temperature, in inducing the sexual phase. Most of these experiments have been carried out on centric planktonic diatoms. In *Stephanopyxis turris* and in *Coscinodiscus asteromphalus* it has been demonstrated that increasing irradiance (from 200-300 to 2000-4000 lux) induced sexualization; a greater effect was obtained when the increase in irradiance was associated to a temperature rise (reported in Drebes 1977). A similar result was obtained with *Stephanopyxis palmeriana*, where the increase of irradiance together with a simultaneous increase in temperature (from 15° to 21 °C) induced a massive sexual reproduction; in this case the temperature rise was required for the induction of gametogenesis (reported in Drebes 1977). Further experiments with *Stephanopyxis palmeriana* demonstrated that sexualization did not occur when cells were exposed to a mix of different wavelengths (white, red and far red light). The increase in temperature, from 15 to 24 °C, combined with an increase in irradiance and the inoculation of strains into fresh medium induced gametogenesis also in *Lithodesmium undulatum*, *Helicotheca tamesis* and *Bellerochea malleus* (Drebes 1977). A positive relationship between long day-lengths and sexual reproduction was also recorded for the planktonic *Chaetoceros curvisetus*, where the abundance of 4- and 8-cell stages (precursor stages of sperm cells) was 10-50 times higher at long day-length conditions. In this species *spermatogenesis* appeared also synchronized with the beginning of the light period (Furnas 1985). However, an opposite relationship with day-length was recorded for the benthic pennate *Cocconeis scutellum*, where sexual reproductions was promoted by short day-lengths and irradiance conditions that favoured auxosporulation were suboptimal for vegetative growth (Mizuno and Okuda 1985). Mouget *et al.* (2009) provided evidence that light (irradiance, photoperiod and spectral

composition) is a key factor for sexualization also in the marine planktonic pennate diatom *Haslea ostrearia*. Also in this case, the highest sexualization was obtained with low photoperiod (8:16 L:D cycle) and low irradiance ($60 \mu\text{mol photons m}^{-2}\text{s}^{-1}$). Also the quality of the light played a role: when white and red light was provided sexualization occurred, but it never occurred under monochromatic blue and green light, in continuous light or in darkness. Therefore, it seems that this diatom uses day-length and the spectral composition of light as cues for regulating the occurrence of sexual reproduction. Short day-lengths are recorded during the winter months and red wavelengths should be detected by photoreceptors mostly in the surface layers of the water column.

In centric diatoms, where the production of gametes of opposite type occurs in the same culture, the production of '+' and '-' gametes seems to respond to different cues. The effect of 64 different combinations of light (irradiance and photoperiod) and temperature on sexualisation of the marine planktonic centric diatom *Coscinodiscus concinnus* was tested (Holmes 1966). In this diatom '+' gametes were produced in a broad range and combination of irradiance and temperature, but higher numbers were produced when the photoperiod was short (8:16 L:D cycle). The '-' gametes were produced in a more restricted range of irradiance and temperature, i.e. at high irradiance and temperature associated with low or high day-length. It follows that auxospores were only detected in the latter conditions (Holmes 1966).

In *Nitzschia lanceolata*, sexual reproduction is partially inhibited under continuous light (reported in Davidovich 1998). When compatible strains in which sexual reproduction was induced were transferred into darkness, initial cells were formed only if the sexualized cells had received a certain critical amount of light before being placed in the dark (Davidovich 1998). Gametogenesis and conjugation took place independently from the quantity of energy provided, but auxosporulation and the formation of initial cell requires

energy to be completed (Davidovich 1998). A decrease in temperature stimulated sexual reproduction in *Chaetoceros decipiens* and *C. constrictus* (Drebes 1977).

In older studies, there are reports on the possible role of osmotic changes in inducing sexualization (reported in Drebes 1977). For example, an increase of Na^+ concentration induced gametogenesis and auxosporulation in two species of the estuarine centric planktonic diatom *Cyclotella* (Schultz and Trainor 1968). In *Ditylum brightwellii* it seems that the concentration of oligoelements might have a role in controlling sexual reproduction: the lack of manganese in artificial sea water induced sexualization, but also day length and irradiance played a role (Steele 1965). Gross (1937) was able to induce sexual reproduction in most of *Ditylum brightwellii* cells simply diluting cultures with new medium (as reported in Steele 1965). Koester *et al.* (2007) confirmed the requirement of nutrients for sexual reproduction in *Ditylum brightwellii*: sex did not occur in nutrient depleted conditions and during the stationary phase, when this species underwent vegetative enlargement or produced resting spores. Davis *et al.* (1973) reported that *Skeletonema costatum* in continuous culture and under silicate-limited conditions was able to synchronize the sexual phase by a change in growth kinetics (growth rate was lower). Finally, the use of a nitrogen-depleted medium induced sexual reproduction in *Leptocylindrus danicus*, where the auxospore is transformed into a resting spore (French III and Hargraves 1986).

In recent years, it has been found that bacteria might also play an important role in the sexual reproduction of phytoplanktonic species. In fact, it was found that the presence of the bacterium *Alcaligenes* sp. promoted spermatogenesis in *Coscinodiscus wailesii*, where the maximum sperm formation was found during the early and middle phases of exponential growth (Nagai *et al.* 1996, Nagai and Imai 1998, Nagai and Imai 2001).

1.4 The sexual cycle of diatoms: what do we know from the observation of natural populations?

Evidence for sexual reproduction in natural marine planktonic diatom populations is extremely sparse (Assmy *et al.* 2006, Crawford 1995, Holtermann *et al.* 2010, Sarno *et al.* 2010). This is most probably due to the fact that sex only involves a limited fraction of vegetative populations, or to the fact that sex is an ephemeral event that occurs over a short time interval, or that sexual stages cannot be identified by researchers who carry out species identification and enumeration. In *Corethron pennatum* (= *C. criophilum*), a large diatom abundant in the Southern Ocean, the sexual phase involved a considerable fraction of the population and affected the sedimentation dynamics (Crawford 1995). The massive sinking of siliceous frustules was attributed to the empty gametangia, as indicated by their size fingerprint (gamete formation only occurs within a defined size window) in the sediment traps and on the sea floor.

Auxospores of the chain forming pennate diatom *Fragilariopsis kerguelensis* have been recorded in natural samples collected during an iron-fertilization experiment carried out in the Southern Ocean. These sexual stages accounted only for a minute percentage (up to 0.4 %) of the whole diatom population, without remarkable differences between the ‘in-’ and the ‘out-bloom’ sampling stations (Assmy *et al.* 2006). Recently, a massive sexual reproduction of *Pseudo-nitzschia* cf. *delicatissima* and *P.* cf. *calliantha* was recorded at the same time in the in the Gulf of Naples (Italy) (Sarno *et al.* 2010). A massive sexual reproduction involving another two *Pseudo-nitzschia* species, *P. australis* and *P. pungens*, was observed along the Washington coast (USA) (Holtermann *et al.* 2010). In this latter case, sexual stages were

recorded on aggregates of surf-zone diatoms and it was hypothesized that *Pseudo-nitzschia* cells could use other species as substrate to move towards each other and perform fertilization. The sexual phase only involves cells in a defined cell size window and sexual reproduction is followed by the formation of large initial cells. Therefore, monitoring cell size in natural populations can represent a valuable approach to estimate the occurrence of sexual reproduction: it should be theoretically possible to follow cell size reduction, as a consequence of vegetative growth, and the appearance of cohorts of larger cells, as a consequence of sexual reproduction. The few datasets available for freshwater species indicate that sex is surprisingly timed, with a periodicity spanning from 1 to almost 40 years has been estimated (Mann 1988). The first attempt to trace the occurrence of sexual events in natural populations was carried out examining cell size distribution of *Tabellaria fenestrata* in laminated sediments of the Lake Zürich, over a period of almost 30 years (Nipkov 1927 in Mann 1988). A progressive gradual decrease in the population cell size was observed over time and – in some years – large sized cells, indicative of the occurrence of sexual reproduction, were detected.

Cells size distribution over two years were also followed for two centric diatoms, *Stephanodiscus neoastraea* (Jewson 1992b) and *Aulacoseira subarctica* (Jewson 1992a), where sexual reproduction event was always followed by the detection of cells with large diameter. In the planktonic *Stephanodiscus* cf. *neoastraea*, sexual reproduction was observed every year following the increase of nitrate concentration in late summer (Jewson 1992b). Cells started to divide asexually at the same time in which auxosporulation was observed, however the population density did not increase markedly. The evidence for sexual reproduction was provided both by the detection of auxospores and the appearance of large-sized cells. In the freshwater *Aulacoseira subarctica*, asynchronous sexual reproduction, with relatively frequent but low numbers (4 %) of sexual stages was observed over a period of 6-7

months. Gametogenesis was observed after the interruption of vegetative growth by a decrease in light availability but in presence of nutrients (Jewson 1992a).

The life history of the marine *Pseudo-nitzschia multistriata* natural populations was studied in the Gulf of Naples over 10 years by the analysis of cells abundance and cells size patterns. The species has been recorded in late summer-autumn and the sexual phase, inferred by the appearance of large-sized cell cohorts, recurred every two years (D'Alelio *et al.* 2010). The length of the life cycle, from the production of the initial cells to the reach of extremely small cell size was estimated to last about 4 years.

1.4.1 *Resting stages in sediments*

The formation of thick-walled spores is reported for several centric diatoms, but some species (e.g. *Skeletonema* species) can survive in the sediments for years as apparently undifferentiated resting cells (McQuoid and Hobson 1996). These cells should have peculiar - but still unknown - physiological features to cope with prolonged periods in the dark. Species of the genus *Chaetoceros* are key-players of upwelling-related blooms and large numbers of spores settle to the sediments after the blooms from which they are re-suspended by the nutrient-rich subsequent upwelling, thus seeding the water column with vegetative cells. Different *Chaetoceros* species have been reported as responsible for the spring bloom at different latitudes and environmental settings. It has been noticed that the onset of these blooms is related to the increase in day-length, and this environmental parameter has been suggested as a possible cue regulating spore germination and population growth (Eilertsen *et al.* 1995). The transition between vegetative cells and resting spores can be very rapid and might get overlooked, if the sampling resolution is not appropriate. Davis *et al.* (1980) monitored the development and sinking of a *Leptocylindrus danicus* bloom in a large enclosure that excluded adjective processes, thus allowing the assessment of quantitative

changes in a population secluded in a homogeneous parcel of water. The demise of the bloom was accompanied by massive spore formation, and *L. danicus* sank out of the surface layer in a few days.

1.5 The genus *Pseudo-nitzschia*

The genus *Pseudo-nitzschia* includes 37 species of marine diatoms (Table 1.1) that can be responsible for blooms in both coastal waters and open oceans. Species of the genus *Pseudo-nitzschia* can be distinguished from those of the closely related genus *Nitzschia* by their capability to form chains of cells joined together at their ends, and by the ultrastructure of the raphe system. However, there are exceptions, because some species, such as *P. americana*, have only been recorded as single cells (Lundholm *et al.* 2002). Indeed, most species in culture produce both single cells and long chains and chain formation might be stimulated by the growth phase of the cells and nutrient availability (Lelong *et al.* 2012).

The frustule of *Pseudo-nitzschia* includes (as that of all pennate raphid diatoms) two valves with a series of cingular bands. A raphe, reinforced by a series of fibulae, runs on the lateral side of each valve and in some species it is interrupted by a larger interspace. The surface of the valve includes a series of striae – portions ornamented by perforations with different shapes and organization – and interstriae, i.e. the non-ornamented portion of the valve (Fig. 1.6). *Pseudo-nitzschia* species are identified based on the presence/absence and combination of different morphological and ultrastructural characters: cell shape and width, density of striae and fibulae (number per 10 μm), morphology and density of perforations (areolae) (e.g.; Amato and Montresor 2008, Lundholm *et al.* 2003, Lundholm *et al.* 2006, Lundholm *et al.* 2012).

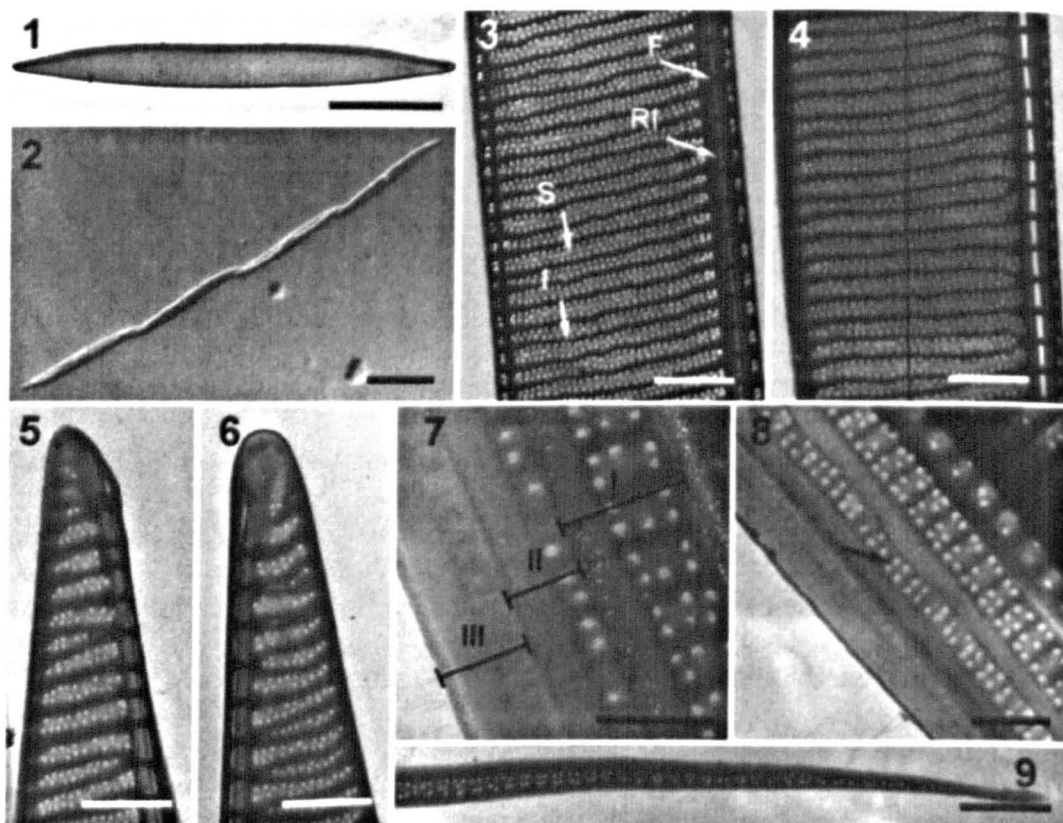


Figure 1.6. Light and electron micrographs of *Pseudo-nitzschia multistriata*. (panels 1, 3-9: TEM; panel 2: LM). Panel 1. *P. multistriata* valve in valvar view. Panel 2. A chain of cells in girdle view; note the undulate shape. Panel 3. Central part of the valve; striae (S), interstriae (I), raphe interspaces (RI) and fibulae (F) are arrowed. Panel 4. Central part of the valve with raphe and proximal mantle; note the different pattern of the striae of the proximal mantle. Panels 5, 6. Opposite ends of the same valve. Note the difference in the structure of the terminal striae. Panel 7. Cingulum with first band (=valvocopula) (I), second band (II) with a single row of poroids in the perforated part, and a third (III) non-areolated band. Panel 8. A similar cingulum with the second band showing a double row of poroids (arrowed). Panel 9. Terminal part of a first cingular band (=valvocopula). Scale bars represent: panels 1, 10 μm ; panel 2, 20 μm ; panels 3-6, 9, 1 μm ; panels 7, 8, 0.5 μm (from Orsini *et al.* 2002).

It follows that the identification at the species level often requires detailed investigations using transmission electron microscopy, which cannot be applied to identify and enumerate species in monitoring and/or ecological programs. At the present, in light microscopy, it is often possible only to distinguish between thin species (cell width < 3 μm , *P. delicatissima*-like) and

large ones (cell width >3 μm , *P. seriata*-like). In future molecular investigations will hopefully provide alternative tools to identify the species present in a certain area (e.g. McDonald *et al.* 2007). Studies on the genetic diversity of *Pseudo-nitzschia* species have been carried out using different molecular markers, such as ITS, LSU, rbcL (e.g. Amato *et al.* 2007, Amato and Montresor 2008, Casteleyn *et al.* 2008, Lundholm *et al.* 2003, Lundholm *et al.* 2006, Lundholm *et al.* 2012, Quijano-Scheggia *et al.* 2009b). These investigations have shown that genetically distinct species are often present behind a single morpho-species as identified in light microscopy (cryptic species). In some cases, the different genotypes can be distinguished only on the bases of very minor ultrastructural characters (pseudo-cryptic species). This is the case of the *P. delicatissima*-species complex, for which it was possible to distinguish three genetically distinct and reproductively isolated species - *P. delicatissima*, *P. arenysensis* (= *P. delicatissima*1) and *P. dolorosa*- whilst for *P. pseudodelicatissima*-species complex up to five different cryptic species - *P. cuspidata*, *P. calliantha*, *P. mannii* (= *P. calliantha*2), *P. caciaantha* and *P. pseudodelicatissima* were recorded (Amato *et al.* 2007). The application of molecular tools such as microarrays, clone libraries and targeted genomic approaches is under way to increase the detection capability of the different species.

The genus *Pseudo-nitzschia* does not only have an ecological importance, but also an economic one. In fact, the interest in this genus increased after the Amnesic Shellfish Poisoning (ASP) event that in 1987 caused the death of several people and illnesses in Canada (Bates *et al.* 1998). The cause of this event was the toxin domoic acid, a small amino-acid that acts as an analogue of the neurotransmitter glutamic acid. Domoic acid binds to the neuron membrane, and causes a strong and long depolarization that increases intra-neuronal calcium concentration, which eventually causes the death of the neuron. In mammals, neurons located in the hippocampus are affected, causing memory losses from which the name of the intoxication derives. Domoic acid also affected wildlife, such as birds and sea lions (Scholin *et*

al. 2000), showing that the toxin can be transmitted through the food web. The presence of the toxin is now regularly tested in seafood monitoring programs and the threshold amount for food consumption is $\geq 20 \text{ mg} \cdot \text{g}^{-1}$. Not all *Pseudo-nitzschia* species produce the toxin (Table 1.1) and the amount of toxin production can vary considerably amongst different isolates of the same species and/or under different physiological conditions (Lelong *et al.* 2012).

Blooms of *Pseudo-nitzschia* are a regular component of the phytoplankton assemblage. Nevertheless, when recurrent blooms of toxic species occur – as along the western US coast, Atlantic coast of Spain, and in the U.K. – they can cause severe economic damage to the regional economy (Lelong *et al.* 2012). No toxic *Pseudo-nitzschia* have been recorded up to now from Antarctic waters. However, there has been concern following the detection of domoic acid in open ocean populations of *Pseudo-nitzschia* that developed after iron addition (Silver *et al.* 2010). In the Mediterranean Sea, there have been no reports of ASP intoxications up to now, notwithstanding the presence of a number of species capable of producing domoic acid (Cerino *et al.* 2005, Orsini *et al.* 2002, Sahraoui *et al.* 2011) (see Table 1.1).

In the Gulf of Naples various species of *Pseudo-nitzschia* alternate over the annual cycle at the Long Term Ecological Research station MareChiara (Ribera d'Alcalà *et al.* 2004, Zingone *et al.* 2003), with species of the *P. delicatissima* complex often abundant in spring and again in autumn, *P. galaxiae* during the summer period, *P. multistriata* in summer and early autumn, and *P. pseudodelicatissima*-complex over a larger interval spanning from summer to autumn.

Table 1.1. List of *Pseudo-nitzschia* species described up to now with information on their toxicity. Species present in the Mediterranean Sea are marked with ‘*’ and species for which information on the life cycle is available are marked with ‘§’. Yes/no was used when toxicity was detected only in some of the strains tested.

Species	Toxicity
<i>P. americana</i>	no
<i>P. antarctica</i>	not tested
<i>P. arenysensis</i> * § (as <i>P. delicatissima</i> In Amato <i>et al.</i> 2005) (as <i>P. delicatissima</i> clade 1 in Amato <i>et al.</i> 2007) (Quijano-Scheggia <i>et al.</i> 2009b)	no
<i>P. australis</i> § (Holtermann <i>et al.</i> 2010)	yes/no
<i>P. brasiliiana</i> * § (Quijano-Scheggia <i>et al.</i> 2009a)	yes/no
<i>P. caciantha</i> *	no
<i>P. calliantha</i> * § (Amato <i>et al.</i> 2007) (as <i>P. cf. calliantha</i> in Sarno <i>et al.</i> 2010)	yes/no
<i>P. cuspidata</i> § (Amato <i>et al.</i> 2007, Lundholm <i>et al.</i> 2012)	yes/no
<i>P. decipiens</i>	no
<i>P. delicatissima</i> * § (as <i>P. cf. delicatissima</i> in Sarno <i>et al.</i> 2010)	yes/no
<i>P. dolorosa</i> § (Amato <i>et al.</i> 2007)	no
<i>P. fraudulenta</i> * § (Chepurnov <i>et al.</i> 2004)	yes/no
<i>P. fryxelliana</i>	not tested
<i>P. galaxie</i> *	yes/no

<i>P. granii</i>	yes/no
<i>P. hasleana</i>	no
<i>P. heimii</i>	no
<i>P. inflatula</i>	no
<i>P. linea</i> *	not tested
<i>P. lineola</i>	no
<i>P. mannii</i> * § (Amato and Montresor 2008)	not tested
<i>P. micropora</i>	not tested
<i>P. multiseries</i> § (Davidovich and Bates 1998, Kaczmarska <i>et al.</i> 2000, Hiltz <i>et al.</i> 2000)	yes
<i>P. multistriata</i> * § (D'Alelio <i>et al.</i> 2009a)	yes
<i>P. obtusa</i>	no
<i>P. prolongatoides</i>	not tested
<i>P. pseudodelicatissima</i> * § (Davidovich and Bates 1998) ⁽¹⁾ (Amato <i>et al.</i> 2007)	yes/no
<i>P. pungens</i> * § (Chepurnov <i>et al.</i> 2005, Holtermann <i>et al.</i> 2010)	yes/no
<i>P. pungiformis</i>	not tested
<i>P. roundi</i>	not tested
<i>P. seriata</i>	yes/no
<i>P. sinica</i>	not tested
<i>P. subcurvata</i> § (Fryxell <i>et al.</i> 1991)	no
<i>P. subfraudulenta</i>	no
<i>P. subpacifica</i>	no
<i>P. turgidula</i>	yes

<i>P. turgiduloides</i>	no
-------------------------	----

⁽¹⁾the species identification is not certain, see (Lelong *et al.* 2012)

1.5.1 *The life cycle of Pseudo-nitzschia species and the factors inducing sexual reproduction*

The first description of the life cycle of a *Pseudo-nitzschia* species was provided in 1991, when gametogenesis was described for *Nitzschia pungens* f. *multiseries* (now *P. multiseries*) by a study carried out in flow cytometry (Subba Rao *et al.* 1991). This study reported the formation of flagellate gametes – it would have been the first report for a pennate diatom – but this record turned out to be a contamination of the culture by parasitic fungi (chytrids) (Rosowski *et al.* 1992). Investigations in light microscopy provided the description of the life cycle of *P. multiseries* and *P. pseudodelicatissima* (Davidovich and Bates 1998) demonstrating that the two species have a heterothallic life cycle and that sexual reproduction is obtained by mixing strains of compatible mating type. The formation of gametes, the fertilization process, and the development of the auxospore and the production of a large initial cell was described for the two species. The ultrastructure of the sexual stages of *P. multiseries* was subsequently described in scanning electron microscopy, illustrating the structure of the auxospore surrounded by transversal perizonial bands and presenting two caps at the apex covered by thin siliceous scales (Kaczmarska *et al.* 2000). The effect of daylength on the sexual reproduction of this species was also investigated (Hiltz *et al.* 2000 see below). Amato *et al.* (2005) described the life cycle of *P. delicatissima* (now *P. arenysensis*) in both light and electron microscopy, showing a basically similar life cycle pattern. The authors also studied the cell size reduction dynamics of this species, demonstrating differences in growth rate in cells of different size. *Pseudo-nitzschia pungens* also has a similar life cycle pattern,

nuclear behaviour during gametogenesis, chloroplast dynamics, as well as abrupt cell size reduction (Chepurnov *et al.* 2005). Amato *et al.* (2007) carried out a large number of crosses involving different species in the *P. delicatissima* and *P. pseudodelicatissima* species complexes. The presence of a heterothallic life cycle, conforming to the one described for the other species has been reported for *P. arenysensis* (as *P. delicatissima* clade 1), *P. dolorosa*, *P. pseudodelicatissima*, *P. cuspidata* and *P. calliantha*. Notwithstanding the high number of attempts, the authors could not induce sexual reproduction in *P. delicatissima sensu stricto* (= *P. delicatissima* clade 2). The presence of intraclonal auxosporulation, i.e. a heterothallic life cycle, has been subsequently described for *P. brasiliiana* (Quijano-Scheggia *et al.* 2009a). Up to now, this is the only species for which this kind of life cycle has been proved but it might be present also in *P. subcurvata* (Fryxell *et al.* 1991). The life cycle of the heterothallic *P. multistriata* was studied together with cell size reduction process by (D'Alelio *et al.* 2009a) and sexual reproduction was found in four different species (*P. australis*, *P. pungens*, *P. cf. delicatissima* and *P. cf. calliantha*) that have been detected in the natural environment (Holtermann *et al.* 2010, Sarno *et al.* 2010). Successful crosses among multiple strains of *P. cuspidata* showed that also this species has a heterothallic life cycle (Lundholm *et al.* 2012), as is the case for *P. mannii* (Amato and Montresor 2008). The occurrence of sexual reproduction in *P. arenysensis* was recently confirmed by (Quijano-Scheggia *et al.* 2009b). Also, they reported unsuccessful attempts to induce the sexual phase in *P. delicatissima sensu stricto*, confirming the findings of Amato *et al.* (2007).

Almost all the studies mentioned above, in which sexual reproduction of various *Pseudo-nitzschia* species has been described or in which mating experiments have been carried out, mentioned that the sexual phase was induced when crossing compatible strains in the exponential growth phase. Very little experimental work has been carried out to detect the factors that influence the occurrence of the sexual phase in species of this genus. The effect of

different daylength conditions on the onset of the sexual phase has been studied in *P. multiseriata* cultures of different age, i.e. cell size (Hiltz *et al.* 2000). The population fertilization success (as the ratio (zygotes/0.5xgametes)x100) was similar between the couples: 68 and 91% for the younger and older couples, respectively. However, population fecundity, calculated as the number of gametes/vegetative cells x 100, was different: 49 and 4% for the younger and older cultures, respectively. In the younger cultures, a positive correlation was recorded between daylength and sexual cell production, suggesting that higher levels of photosynthesis might be required for the successful development of sexual stages.

In *Pseudo-nitzschia multistriata*, the maximum percentage of gametangia over the total number of cells was very low in crossing tests carried out at 20 °C, 40 $\mu\text{mol photons m}^{-2} \text{ s}^{-1}$ and 12:12 h L:D (around 1–2% D'Alelio *et al.* 2009a). In natural populations, the average percentage of sexual stages was of 9.2% for *Pseudo-nitzschia cf. delicatissima* and 14.3% for *P. cf. calliantha* (Sarno *et al.* 2010).

1.6 *Pseudo-nitzschia multistriata*

Pseudo-nitzschia multistriata (Takano) Takano is a planktonic, raphid pennate, diatom described from Japanese waters as *Nitzschia multistriata* (Takano 1993) and subsequently transferred to the genus *Pseudo-nitzschia* (Takano 1995). *Pseudo-nitzschia multistriata* cells are recorded as solitary or joined in short chains. They show a lanceolate shape in valve view and a peculiar sigmoid shape in girdle view. The sigmoid shape makes this species relatively easy to identified in light microscopy. The cell apical length varies between 35 and 77.5 μm and the trans-apical axis varies between 3 and 3.5 μm . The valves have striae with two rows of circular poroids (Orsini *et al.* 2002, Takano 1995). *Pseudo-nitzschia multistriata* has a heterothallic life cycle first described by D'Alelio *et al.* (2009a).

Pseudo-nitzschia multistriata has been recorded in temperate and tropical regions (reviewed in (Lelong *et al.* 2012). At the Long Term Station in the Gulf of Naples (Tyrrhenian Sea, Italy), *P. multistriata* was first recorded in 1995, and it reaches higher abundances in late summer-autumn (D'Alelio *et al.* 2009b, Ribera d'Alcalà *et al.* 2004). Cell abundances vary between $10 \cdot 10^3$ and $70 \cdot 10^4$ cells·L⁻¹ (D'Alelio *et al.* 2010). *Pseudo-nitzschia multistriata* produces the toxin domoic acid, the causative agent of ASP (Amnesic Shellfish Poison) (Orsini *et al.* 2002).

1.7 Aims of the thesis

The general aim of this thesis was to investigate endogenous and exogenous factors that influence the transitions amongst life cycle phases in the marine planktonic diatom *Pseudo-nitzschia multistriata*. As in the vast majority of diatoms, *P. multistriata* undergoes a progressive reduction in the average cell size of its populations as consequence of vegetative growth. There is then a restitution of cell size and the formation of large-sized cells occurs following the sexual phase. This species has a heterothallic life cycle (D'Alelio *et al.* 2009a) and strains of the opposite mating type have to get in contact to allow sexual reproduction to occur.

Why it is important to gain information on the different life cycle phases of a diatom species? Diatoms are important components of the marine phytoplankton, they are characterized by a considerable phylogenetic diversity, with thousands of species with distinct biogeographic distribution and often distinct seasonal timing. They are photosynthetic organisms and their growth is thus regulated by the availability of light and inorganic nutrients. Diatoms also have a complex life cycle, with a basic general pattern on which a series of different variations exist (Chapter 1). A relevant, but still poorly explored, aspect is the link between the different life cycle phases and the environmental characteristics of the environment in which the different species live. The distribution ranges, success, timing of growth of a diatom species thus also depends on its life cycle and on how the transitions between the different life cycle phases are regulated by the environment. The questions addressed in the course of my study have been mostly focused on the transition between the vegetative growth phase and the sexual phase.

There is also considerable interest for the biotechnological use of diatoms, to produce lipids, pharmaceuticals and other molecules of economic interest. This is based on the possibility to successfully cultivate diatoms, often in high biomass and for long time periods. Again, detailed information of the species life cycle is extremely important to evaluate the feasibility of long term maintenance and identify the best conditions for growth. Last but not least, we are now in the genomic era and new approaches to understand the molecular mechanisms that regulate the physiology and the life cycle of diatoms become available. A solid experimental knowledge of the factors that regulate transitions amongst diatom life stages is an important prerequisite to address old questions with new molecular tools.

Why focus on *P. multistriata*? This species is a member of an ecologically important genus of marine planktonic diatoms that includes species capable of producing the neurotoxin domoic acid (Lelong *et al.* 2012, Trainer *et al.* 2012). Different aspects of the biology of this species have been studied in recent years at the laboratory of Ecology and Evolution of Plankton of the Stazione Zoologica Anton Dohrn (Chapter 1) and, therefore, it is a good model organism to address specific questions on its life cycle. The species is present at the Long Term Ecological Research station MareChiara in the coastal portion of the Gulf of Naples and is also amenable to investigations in the natural environment. Recently, this species has been selected as the candidate for a genome sequencing project (Gypsy project lead by dr. Maria Immacolata Ferrante, SZN); this will open the possibility to address in the future various questions with genomic approaches.

The first aim of my thesis was to study the details of the life cycle of *P. multistriata* in confocal and time lapse microscopy (Chapter 2). The general morphological features of the life cycle stages of this species have been described by D'Alelio *et al.* (2009a). However no

information at the cytological level was available. The use of fluorescent nuclear markers in confocal microscopy and the possibility of observing the critical phases of the life cycle in real time, made it possible to gain information on the operation and timing of the different life cycle phases and to produce a detailed description. In the Appendix section (Appendix I), some results on the process of sexual reproduction in *Fragilariopsis kerguelensis* (another pennate raphid diatom phylogenetically related to the genus *Pseudo-nitzschia*) are reported.

The second part of my thesis was based on experimental work in the laboratory and the following main questions have been addressed.

- a) *Pseudo-nitzschia multistriata* is heterothallic, having cells belonging to two different mating types. No information exists on their relative distribution in the natural environment, although departures from a 50:50 ratio might have important consequences for population dynamics. An extensive number of crosses have been carried out with strains isolated over 3 years to gain information on their mating type (Chapter 2).
- b) The onset of the sexual phase in a heterothallic species implies that strains of compatible mating type are mixed together. While the general recommendation is to mix them when in the exponential growth phase, no quantitative data are available to support this statement. In a more general perspective, I planned to test the effect of cell density on the success and timing of sexual reproduction (Chapter 3).
- c) In Chapter 3, evidence supporting the fact that sexual reproduction is a density-dependent event are provided. Experiments were designed to detect the presence of a chemical mediator that induces the differentiation of vegetative cells into gametes using culture media conditioned by the growth of strains of opposite mating type.

Strains were grown in a common vessel but with a permeable membrane that prevents cell contacts (Chapter 4).

- d) The requirement of a threshold cell concentration for sex and the apparent presence of a chemical mediator that induces sexualization raise the question on where does sex occur in the natural environment. The effect on the timing and success of sexual reproduction of still water conditions, which allow the settling of cells at the bottom of the culture plates to form a micro-layer with higher cell concentration, and mixed conditions, where the formation of temporary layers should be inhibited, was compared (Chapter 5).

Chapter 2

The life cycle of *Pseudo-nitzschia multistriata*:
investigation in confocal and time lapse microscopy

2.1 Introduction

D'Alelio *et al.* (2009a) provided the first description of the life cycle of *Pseudo-nitzschia multistriata* using clonal cultures isolated from the Gulf of Naples (Tyrrhenian Sea, Mediterranean Sea). The authors performed a matrix of crosses of different strains and established that the species has a heterothallic life cycle, i.e. sexual reproduction was obtained only when mixing together strains with complementary mating type. The sexual phase was induced when parental cultures reached an average apical length between 39 and 55 μm , and the size of the initial cells produced at the end of the sexual phase ranged between 72 and 82 μm . Therefore, sexual reproduction was recorded within a cell size window corresponding to 39–71% of the maximum cell apical length of *P. multistriata*. The authors presented light and scanning electron micrographs of gametangia, zygotes and auxospores, whose general morphology fits with what has been reported previously for other *Pseudo-nitzschia* species (e.g. Amato *et al.* 2005, Amato and Montresor 2008, Chepurnov *et al.* 2005, Davidovich and Bates 1998, Kaczmarek *et al.* 2000). A detailed overview of the life cycle of *Pseudo-nitzschia* species is reported in Chapter 1. In *P. multistriata*, the gametes showed behavioural anisogamy, i.e. the gametes produced in the two gametangia behave differently: the two active gametes (+) glided towards the two sessile (-) ones (auxosporulation cis-type IA2 modality *sensu* Geitler 1973). Both growth performances and cell size reduction rates were related to cell size in *P. multistriata*: the largest cells showed slower growth rates and larger size reduction rates, while the relationship was opposite for cells smaller than 60% of the maximum size (D'Alelio *et al.* 2009a). At high light and temperature, the growth rates of *P. multistriata* strains ranged between 1.27 and 1.75 division $\cdot\text{day}^{-1}$ for large cell size (80–70 μm). The smaller cells (60–40 μm) showed higher growth rate (up to 2.40 divisions $\cdot\text{day}^{-1}$) (D'Alelio *et al.* 2009a).

The aims of the research illustrated in this chapter were to gain additional information on various cytological aspects of the life cycle of this species:

- i) follow gametogenesis, gamete conjugation and auxospore development in time lapse microscopy to gain information on the process and timing of these key life cycle phases;
- ii) study the nuclear behaviour during the different phases of the life cycle, with special attention to gametogenesis and conjugation; to this end, I have used the fluorochrome SYBR Green I to stain the nuclei and I have observed the different stages in confocal microscopy;
- iii) test if the size of initial cells is related to the size of the parental strains;
- iv) estimate the distribution of mating types in a large number of strains to gain insights on their ratio in natural populations.

2.2 Material and Methods

2.2.1 Cultures

Single cells or short chains of *Pseudo-nitzschia multistriata* were isolated with a micropipette from net samples collected at the Long Term Ecological Research station MareChiara (LTER-MC) in the Gulf of Naples (40°47' 33"N, 14°11' 18"E) from 2008 to 2010 (Table 2.1). All strains have been genotyped with micro-satellites by Sylvie Tesson (Tesson 2010) and Donatella Florio (Florio 2011). The single cells or short chains were each placed in wells of a 24-wells Costar tissue culture plates (Corning Inc., NY, USA) filled with 2 ml of culture medium; after about one week, cultures were transferred in 70 ml culture flasks Costar tissue culture plates (Corning Inc., NY, USA) filled with 25 ml of culture medium. The cultures were grown in f/2 culture medium (Guillard 1975) prepared with oligotrophic Mediterranean seawater collected offshore in the Gulf of Naples. The sea water was filtered over a 0.45 µm pore-size filter (Millipore S.p.A., nitrocellulose membrane, Milano, Italy) and then autoclaved. Salinity was adjusted to 36 psu by adding sterile milli-Q water, and f/2 was obtained through addition of 20 ml of Guillard's (f/2) marine water enrichment solution 50x (G9903, Sigma Aldrich S.r.l.) per litre. The f/2 medium was filtered over a 0.22 µm pore-size filter (Millipore, Filter Stericup- GP SCGPU05RE, Billerica, MA, USA) just before the use, in order to eliminate precipitates. To carry out mating experiments and to perform observations on the life cycle, a subsample of the stock cultures maintained at the Laboratory of Ecology and Evolution of Plankton were maintained in a growth chamber at a temperature of 18 °C, a photoperiod of 12L:12D h, and a photon flux density of 60 µmol photons m⁻²s⁻¹ provided by cool white fluorescent tubes (Philips TLD 36W/950). Light was measured by an interchanging sensor photometer (LI-185B, LI-COR, U.S.A.) equipped with a white lamp (SPAERICAL: SPAQ033A, LI-COR, U.S.A.).

Table 2.1. Strains of *Pseudo-nitzschia multistriata* used for the experiments to assess the mating type. For each strain are reported: the strain code, the isolation date, the LTER-MC sample code, the average length of the apical axis at the time when the cultures were established, and, when available, the average cell size at the time when the crosses were carried out (in parenthesis); an asterisk (*) marks the strains isolated in 2009 that were crossed with only one member of the reference couple; n.a. = data not available.

Strain code	Isolation date	LTER-MC code	Apical axis (µm)
Sy014	29/07/2008	823	60
Sy016	29/07/2008	823	48
Sy017	29/07/2008	823	48 (27 ± 1.37)
Sy019	28/08/2008	827	n.a.
Sy020	02/09/2008	828	n.a.
Sy021	02/09/2008	828	45
Sy023	17/09/2008	830	n.a.
Sy025	17/09/2008	830	48
Sy027	17/09/2008	830	48
Sy033	17/09/2008	830	45
Sy036	17/09/2008	830	n.a.
Sy039	17/09/2008	830	48
Sy040	17/09/2008	830	45
Sy043	17/09/2008	830	45
Sy044	17/09/2008	830	42
Sy046	17/09/2008	830	42
Sy047	17/09/2008	830	48
Sy050	17/09/2008	830	42
Sy055	17/09/2008	830	n.a.
Sy058	17/09/2008	830	42
Sy070	17/09/2008	830	n.a. (26 ± 1.20)
Sy084	23/09/2008	831	n.a.
Sy087	23/09/2008	831	45
Sy089	23/09/2008	831	45
Sy093	23/09/2008	831	n.a.
Sy096	23/09/2008	831	n.a.
Sy097	23/09/2008	831	45
Sy098	23/09/2008	831	45
Sy103	23/09/2008	831	42
Sy114	23/09/2008	831	39
Sy117	23/09/2008	831	42
Sy131	23/09/2008	831	45

Sy134	23/09/2008	831	42
Sy138	23/09/2008	831	36
Sy145	23/09/2008	831	42
Sy146	23/09/2008	831	42
Sy147	23/09/2008	831	43
Sy149	23/09/2008	831	43
Sy151	23/09/2008	831	43
Sy152	23/09/2008	831	42
Sy156	23/09/2008	831	42
Sy157	23/09/2008	831	42
Sy164	23/09/2008	831	n.a.
Sy165	30/09/2008	832	n.a.
Sy166	30/09/2008	832	n.a.
Sy168	30/09/2008	832	41
Sy171	30/09/2008	832	49
Sy172	30/09/2008	832	43
Sy173	30/09/2008	832	48
Sy174	30/09/2008	832	44
Sy175	30/09/2008	832	n.a.
Sy176	30/09/2008	832	n.a.
Sy177	30/09/2008	832	43
Sy178	30/09/2008	832	n.a.
Sy180	30/09/2008	832	n.a.
Sy182	30/09/2008	832	42
Sy183	30/09/2008	832	44
Sy184	30/09/2008	832	41
Sy185	30/09/2008	832	42
Sy186	30/09/2008	832	44
Sy187	30/09/2008	832	n.a.
Sy191	30/09/2008	832	n.a.
Sy196	30/09/2008	832	42
Sy200	30/09/2008	832	n.a.
Sy203	30/09/2008	832	43
Sy206	30/09/2008	832	44
Sy207	30/09/2008	832	46
Sy211	30/09/2008	832	46
Sy217	30/09/2008	832	45
Sy218	30/09/2008	832	46
Sy219	30/09/2008	832	46
Sy222	11/11/2008	838	n.a.
Sy234	21/11/2008	835	42

Sy236	21/11/2008	835	n.a.
Sy238	14/10/2008	834	42
Sy239	14/10/2008	834	41
Sy241	14/10/2008	834	42
Sy243	14/10/2008	834	41
Sy244	14/10/2008	834	41
Sy246	14/10/2008	834	39
Sy248	14/10/2008	834	42
Sy250	14/10/2008	834	42
Sy252	14/10/2008	834	42
Sy254	14/10/2008	834	45
Sy256	14/10/2008	834	44
Sy278	04/11/2008	837	40
Sy279	04/11/2008	837	42
Sy281	04/11/2008	837	43
Sy284	04/11/2008	837	n.a.
Sy290	11/11/2008	838	41
Sy297	11/11/2008	838	41
Sy299	11/11/2008	838	40
Sy301	11/11/2008	838	43
Sy302	18/11/2008	839	41
Sy303	18/11/2008	839	n.a.
Sy304	18/11/2008	839	n.a.
Sy305	18/11/2008	839	36
Sy306	18/11/2008	839	41
Sy307	18/11/2008	839	36
Sy308	18/11/2008	839	43
Sy309	18/11/2008	839	37
Sy310	09/12/2008	842	42
Sy319*	30/06/2009	868	48
Sy321*	30/06/2009	868	50
Sy323*	30/06/2009	868	49
Sy324 *	30/06/2009	868	50
Sy326*	30/06/2009	868	49
Sy327	30/06/2009	868	48
Sy329*	30/06/2009	868	50
Sy330*	30/06/2009	868	50
Sy331*	30/06/2009	868	48
Sy334	30/06/2009	868	47 (38 ± 2.17)
Sy336*	30/06/2009	868	48
Sy338*	30/06/2009	868	47

Sy340	30/06/2009	868	54 (41 ± 3.05)
Sy344*	30/06/2009	868	48
Sy345*	30/06/2009	868	43
Sy346*	07/07/2009	869	48
Sy347	07/07/2009	869	50 (43 ± 2.77)
Sy348*	07/07/2009	869	49
Sy349*	07/07/2009	869	52
Sy350*	07/07/2009	869	50
Sy351	07/07/2009	869	46
Sy353*	07/07/2009	869	40
Sy355*	07/07/2009	869	47
Sy357*	07/07/2009	869	50
Sy358*	07/07/2009	869	48
Sy359*	07/07/2009	869	43
Sy361	07/07/2009	869	47
Sy363*	07/07/2009	869	46
Sy365*	07/07/2009	869	40
Sy366*	07/07/2009	869	50
Sy368*	07/07/2009	869	50
Sy369*	07/07/2009	869	49
Sy370	07/07/2009	869	48
Sy373	07/07/2009	869	45 (39 ± 1.44)
Sy375	07/07/2009	869	53
Sy376*	07/07/2009	869	43
Sy377*	07/07/2009	869	49
Sy378	07/07/2009	869	48
Sy379	07/07/2009	869	50 (40 ± 2.66)
Sy380	07/07/2009	869	49
Sy382	07/07/2009	869	52
Sy383*	07/07/2009	869	53
Sy384	07/07/2009	869	47
Sy385*	07/07/2009	869	48
Sy386	07/07/2009	869	44
Sy387	07/07/2009	869	48 (38 ± 2.86)
Sy388*	07/07/2009	869	48
Sy389*	14/07/2009	870	49
Sy391*	14/07/2009	870	45
Sy392*	14/07/2009	870	49
Sy394	14/07/2009	870	49
Sy395*	14/07/2009	870	47
Sy397	14/07/2009	870	51 (39 ± 1.91)

Sy399	14/07/2009	870	46 (40 ± 1.72)
Sy400	14/07/2009	870	45 (37 ± 2.28)
Sy401*	14/07/2009	870	46
Sy402	14/07/2009	870	45
Sy403	14/07/2009	870	47
Sy404	14/07/2009	870	47
Sy405	14/07/2009	870	43
Sy406	14/07/2009	870	44
Sy407	14/07/2009	870	44
Sy408*	14/07/2009	870	46
Sy409*	14/07/2009	870	47
Sy445	29/09/2009	881	38 (38 ± 2.15)
Sy602	06/07/2010	920	47
Sy608	06/07/2010	920	61 (29 ± 1.79)
Sy627	10/08/2010	925	51 (44 ± 1.74)
Sy644	10/08/2010	925	48 (39 ± 3.32)
Sy653	10/08/2010	925	41
Sy659	10/08/2010	925	48
Sy664	07/09/2010	929	53 (49 ± 2.01)
Sy665	07/09/2010	929	49
Sy667	07/09/2010	929	53 (49 ± 1.99)
Sy668	07/09/2010	929	52 (48 ± 1.19)
Sy676	07/09/2010	929	49
Sy679	07/09/2010	929	52
Sy680	07/09/2010	929	46
Sy681	07/09/2010	929	53 (44 ± 8.69)
Sy683	07/09/2010	929	47
Sy684	07/09/2010	929	48
Sy685	07/09/2010	929	48
Sy686	07/09/2010	929	49 (37 ± 5.34)
Sy691	07/09/2010	929	53
Sy692	07/09/2010	929	51
Sy696	07/09/2010	929	46
Sy697	07/09/2010	929	52
Sy698	07/09/2010	929	57 (53 ± 3.03)
Sy701	07/09/2010	929	51
Sy707	07/09/2010	929	57
Sy710	07/09/2010	929	47 (43 ± 1.14)
Sy713	07/09/2010	929	48
Sy714	07/09/2010	929	48
Sy717	07/09/2010	929	50

Sy718	07/09/2010	929	45
Sy719	07/09/2010	929	44
Sy720	07/09/2010	929	45
Sy722	07/09/2010	929	51
Sy723	14/09/2010	930	53
Sy724	14/09/2010	930	53 (48 \pm 7.87)
Sy727	14/09/2010	930	49
Sy731	14/09/2010	930	55
Sy735	14/09/2010	930	55
St736	14/09/2010	930	50
Sy738	14/09/2010	930	43
Sy741	14/09/2010	930	59
Sy745	14/09/2010	930	43
Sy748	14/09/2010	930	54
Sy770	21/09/2010	931	40
Sy772	21/09/2010	931	34
Sy774	21/09/2010	931	36
Sy776	21/09/2010	931	40 (31 \pm 0.93)
Sy777	21/09/2010	931	34
Sy778	21/09/2010	931	33
Sy779	21/09/2010	931	49
Sy781	21/09/2010	931	37 (34 \pm 1.80)
Sy782	21/09/2010	931	31 (15 \pm 2.32)
Sy783	21/09/2010	931	50 (38 \pm 3.26)
Sy785	21/09/2010	931	32
Sy789	21/09/2010	931	41 (37 \pm 2.25)
Sy791	21/09/2010	931	45
Sy792	21/09/2010	931	50
Sy793	21/09/2010	931	34 (30 \pm 2.13)
Sy794	21/09/2010	931	36 (30 \pm 1.13)
Sy795	21/09/2010	931	37
Sy796	21/09/2010	931	36
Sy797	21/09/2010	931	36
Sy799	21/09/2010	931	53 (50 \pm 3.19)
Sy800	21/09/2010	931	40 (37 \pm 1.35)
Sy801	21/09/2010	931	51
Sy806	21/09/2010	931	54

2.2.2 *Observations in time-lapse microscopy*

The development and timing of the different life cycle phases during vegetative growth and the sexual phase were followed with time lapse microscopy. Observations were carried out at 200x magnifications with a Leica-DMI 6000B time-lapse microscope (Leica Microsystems, Wetzlar, Germany) equipped with a Leica DFC360FX photcamera. Strains Sy373 (mating type '+', male; average cell size $23 \pm 2 \mu\text{m}$) and Sy800 (mating type '-', female; average cell size $34 \pm 3 \mu\text{m}$) were used. A flask Canted Neck vent cap (Corning Inc., NY, USA) filled with 25 ml of f/2 medium was inoculated with $5,000 \text{ cells}\cdot\text{ml}^{-1}$ of each parental strain. The results of the experiments illustrated in Chapter 3 showed that at this cell concentration of parental strains, sexual reproduction should start within 1-2 days. Aliquots of 3 ml were dispensed in seven Petri-dishes with glass bottom (WillCo Well BV, Amsterdam, The Netherlands). The Petri-dishes were incubated in a growth chamber at a temperature of 18°C , a photoperiod of 12L:12D h and an irradiance of $60 \mu\text{mol photons m}^{-2}\text{s}^{-1}$.

Every evening, starting from the inoculum day and for 4 consecutive days, one Petri-dish was placed on the Leica-DMI 6000B microscope and the time lapse series were set in bright field (BF) to take a picture every 45 seconds for a total of 16 hours; the 'best-focus' option was selected. Two controls were carried out: i) one Petri-dish was kept in the growth chamber at the conditions illustrated above, to be sure that strains underwent sexual reproduction with the expected timing; ii) another Petri-dish was placed in the microscope room but it was wrapped in aluminium foil to avoid the exposition to the periodical flashes of the time-lapse and confirm that the condition in the microscopy room did not impair the success and timing of sexual reproduction. Both control Petri-dishes were inspected daily shortly after the onset of the light phase of the photocycle at 400x magnification using a Zeiss Axiovert 200 light microscope to check for the presence of gametes, zygotes and auxospores.

2.2.3 Observations in confocal microscopy

Confocal laser scanning microscopy (CLSM) is an optical imaging technique used to increase optical resolution and contrast of a micrograph by using point illumination and a spatial pinhole to eliminate out-of-focus light in specimens that are thicker than the focal plane (Fig. 2.1). It enables the reconstruction of three-dimensional structures from the obtained images. In a conventional (i.e. wide-field) fluorescence microscope, the entire specimen is flooded evenly in light from a light source. All parts of the specimen in the optical path are excited at the same time and the resulting fluorescence is detected by the microscope's photo-detector or camera including a large unfocused background part. In contrast, a confocal microscope (Fig. 2.1) uses point illumination and a pinhole in an optically conjugate plane in front of the detector to eliminate out-of-focus signal; the name "confocal" stems from this configuration. As only light produced by fluorescence very close to the focal plane can be detected, the image's optical resolution, particularly in the sample depth direction, is much better than that of wide-field microscopes. However, as much of the light from sample fluorescence is blocked at the pinhole, this increased resolution is at the cost of decreased signal intensity, so long exposures are often required. The confocal microscope is really efficient at rejecting out of focus fluorescent light by a confocal pinhole. The advantage of this is that the image comes from a thin section of the sample (there is a small depth of field). By scanning many thin sections through the sample, it is possible to build up a very clean three-dimensional image of the sample.

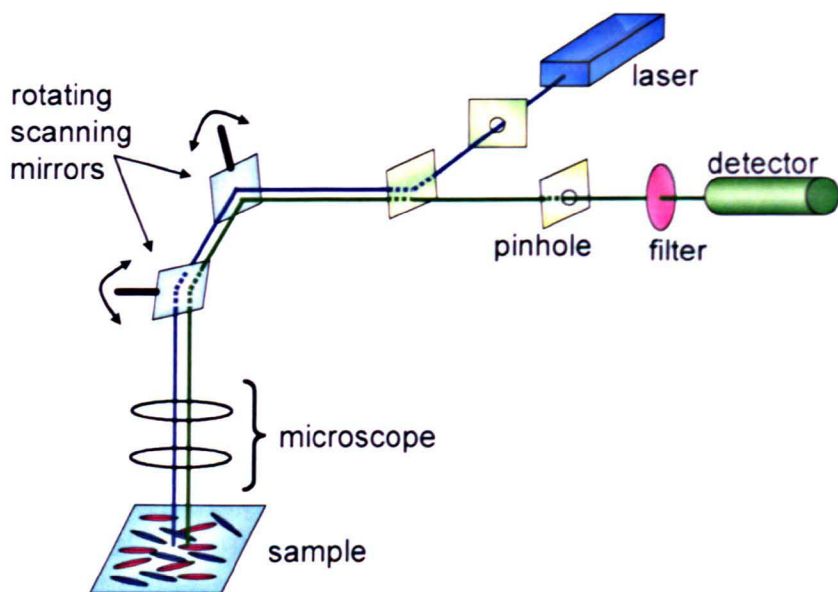


Figure 2.1. Schematic drawings of the confocal laser scanning microscope. The laser emits the light; the rotating scanning mirrors direct light; the pinhole, a single small aperture, permits the passage of the light; the filter selects the wavelengths required for the excitation of the specific fluorochrome and the detector for the signal detects the specific wavelengths emitted by the stained/autoepifluorescent sample.

The different life stages of *Pseudo-nitzschia multistriata* were studied in CLSM. For these experiments, two couples of parental strains were used: Sy373 ('+' mating type) and Sy800 ('-' mating type) and Sy793 ('+' mating type) and Sy799 ('-' mating type) (Table 2.2). The parental strains differ markedly in their average cell size, to make it easier to distinguish the two mating types under the microscope.

Table 2.2. Parental strains used during the confocal analysis. For each strain are indicated: the mating type ('+', male; '-', female) and the average cell size (\pm st. dev.) at the time when crosses were made.

Strains	Mating type	Apical axis (μm)
Sy373	+	23 ± 2
Sy793	+	23 ± 3
Sy799	-	30 ± 2
Sy800	-	34 ± 3

Particular attention has been paid to describe the nucleus arrangement during mitosis and meiosis, and to better characterize the sexual stages. An initial set of experiments was carried out to test the suitability of the different nuclear stains for observations in confocal microscopy. For this purpose, I prepared a mix of parental strains and inoculated it into 3 petri dishes. When sexual reproduction started, aliquots of the samples were stained as illustrated below and examined under the confocal microscope Zeiss-LSM 510 META (Carl Zeiss, Oberkochen, Germany) through appropriate combination of lasers excitation and acquisition filters (Table 2.3). Some material stained with SYBR Green I was also examined in light microscopy with a Zeiss Axiovert 200 epifluorescence microscope equipped with the FITC filter FS09 (excitation, 450 to 490 nm; emission, 515 nm).

SYBR Green I (S7567 - liquid, Molecular Probes, Invitrogen, Milano, Italy). Stock solution: as a stock solution was used the SYBR Green I stock already prepared from Invitrogen. Working solution: it was prepared by diluting 1:10 the SYBR Green I stock solution in MOPS (4-Morpholinepropanesulfonic acid) buffer 200 nM, pH 7.5-8. Aliquots of 200 μ l of working solution were placed in 0.5 ml Eppendorf vials and kept at -20 °C in the dark. One μ l of working solution was added to each ml of culture, to reach a final dilution of 1:10,000, and the culture was incubated for 15 min before observation. Cultures stained with SYBR Green I were also examined with the epifluorescence FITC filter FS09 (excitation, 450 to 490 nm; emission, 515 nm) at different magnifications using a Zeiss Axiovert 200 light microscope.

DAPI (4',6-Diamidino-2-phenylindole dihydrochloride; code: D9542, Sigma-Aldrich S.r.l., Milano, Italy). Stock solution: it was prepared by adding 10 mg of DAPI to 1 ml of MilliQ water (10 mg·ml⁻¹) and kept at -20°C in the dark. Working solution: it was prepared by adding 1 ml of DAPI stock solution to 19 ml of MilliQ water, to reach a final concentration of 0.5 mg·ml⁻¹. The working solution was filtered through a MILLEX-GS

filter unit with a 0.2 μm pore size (MILLIPORE, Carrantuohill, Co. Cork, Ireland). Aliquots of 0.5 ml were placed in 1.5 ml Eppendorf vials and kept at $-20\text{ }^{\circ}\text{C}$ in the dark. One μl of working solution was added to each ml of fixed sample and incubated 15 min in the dark before observation.

Hoechst (Code 33342, Molecular Probes, Invitrogen, Milano, Italy). Stock solution: it was prepared by adding 10 mg of Hoechst to 10 ml of MilliQ water, to reach a final concentration of $1\text{ mg}\cdot\text{ml}^{-1}$. Working solution: it was prepared by diluting 10 ml of stock solution in 90 ml of MilliQ water, to reach a final concentration of 0.1 mg ml^{-1} . Aliquots of 0.5 ml were placed in 1.5 ml Eppendorf vials and kept at $-20\text{ }^{\circ}\text{C}$ in the dark. Five μl of working solution are added to each ml of live sample and incubated for 15 min before observation.

Table 2.3. Combination of excitation laser (Ex. laser), percentage of laser intensity (%) and filter of acquisition (Filter Ac.) used for each dye for observations in confocal microscopy. The absorbance (Abs.) and emission (Em) wavelength range for the different fluorochromes is also indicated.

	Ex. laser (nm)	%	Filter Ac.	Abs. (nm)	Em. (nm)
SYBR Green I	488	1-2	BP 500-550	290-380	497-520
DAPI	405	5-13	BP 420-480	340-364	454-488
Hoechst	405	7-49	BP 420-480	± 350	± 461
Chlorophyll	405	1-8	BP 650-710	400-450 and 625-645	650-750

SYBR Green I turned out to be the better nuclear stain for my research purposes. Crosses with about $5,000\text{ cells}\cdot\text{ml}^{-1}$ for each parental strain were prepared in a flask. Aliquots of 3 ml were placed in 36 petri-dishes with glass bottom (WillCo-dish®, Amsterdam, The Netherlands) and incubated in a growth chamber at a temperature of $18\text{ }^{\circ}\text{C}$, a photoperiod of 12L:12D h and an irradiance of $60\text{ }\mu\text{mol photons m}^{-2}\text{s}^{-1}$. Starting from the first day after the inoculum and for 6 consecutive days, six petri-dishes were fixed with formaldehyde solution at a final concentration of 1.6 %. Each day, the material contained

in each pair of petri-dishes was stained with SYBR Green I. Images of vegetative cells, mitotic and meiotic cells with segregate cytoplasm (MSC cells), gametes, zygotes, auxospores and initial cells were captured at different magnifications with the CLSM Zeiss-LSM 510 META through the combination of lasers excitation and acquisition filters for the selected nuclear stain (Table 2.3).

2.2.4 Size of initial cells

In order to estimate the range of size of initial cells produced by parental strains of different size (Table 2.4), six crosses were carried out using the protocol illustrated in the next paragraph 2.2.5. The initial cells produced in all crosses were measured at 400 x magnifications using an Axiophot light microscope (Carl Zeiss, Oberkochen, Germany) equipped with an ocular micrometer.

Table 2.4. Parental strains used to test the size of the initial cells. For each strain are indicated: the strain code, the mating type ('+'; '-') and the average apical axis length (\pm st. dev.) at the moment in which crosses were carried out.

Strains	Mating type	Apical axis (μ m)
Sy373 (I)	+	39.0 \pm 1.4
Sy373 (II)	+	18.3 \pm 4.2
Sy379 (I)	-	43.9 \pm 2.6
Sy379 (II)	-	22.2 \pm 4.9
Sy627	+	31.7 \pm 3.6
Sy664	+	29.5 \pm 4.0
Sy776	-	20.8 \pm 1.6
Sy789	-	26.6 \pm 2.2
Sy793	+	22.7 \pm 2.9
Sy799	-	29.8 \pm 2.5
ES814	+	37.0 \pm 1.7
VF2.5	-	48.4 \pm 6.0

2.2.5 Mating experiments

In order to estimate the composition of mating types in natural populations, mating experiments were carried out using a total of 233 strains isolated at the LTER station MareChiara between 2008 and 2010 (Table 2.1). Experiments have been carried out in different steps, each time using a subset of strains. The data relative to strains collected in 2008 have been produced by Christophe Legrand (Stazione Zoologica Anton Dohrn, Napoli). For strains isolated in 2008 and 2009, only the average cell size at the time of strain isolation was available; for strains isolated in 2010, the average value and the maximum and minimum cell size was available. Crosses were carried out always within a few months from strain isolation; cell size was thus smaller as compared to that at the moment of culture establishment, but not significantly different. For some strains, cell size was measured also before running the experiments; for each parental strain, twenty cells were measured at 400x magnification using an Axiophot light microscope equipped with an ocular micrometer. Strains were crossed pairwise following a standard protocol: a few drops of exponentially growing culture were inoculated in 12-wells Costar tissue culture plates (Corning Inc., NY, USA) filled with 2 ml of f/2 medium. Plates were incubated in a growth chamber at a temperature of 18 °C, a photoperiod of 12L:12D h and an irradiance of 60 $\mu\text{mol photons m}^{-2}\text{s}^{-1}$. The culture plates were inspected every day with a Leica DMIL inverted microscope (Leica Microsystems, Wetzlar, Germany) to check for the presence of zygotes and auxospores.

In order to attribute the correct mating type to all the tested strains, reference crosses with strains markedly different in size have been carried out, so to be able to discriminate easily to which gametangium the auxospores were attached. The gametangium to which the auxospores are attached is the '-' mating type, following the terminology proposed by (Chepurnov *et al.* 2005). All strains isolated in 2008 have been crossed with both strains of a reference couple, Sy17 '-' and Sy172 '+'. Only a fraction of

the strains isolated in 2009 have been crossed with both Sy17‘-’ and Sy70‘+’; the remaining strains have been crossed only with one reference strain (marked with an asterisk on Table 2.1). In this latter case, the attribution of the mating type is certain when sexual reproduction was observed in the cross, but it was not certain when sexual reproduction was not observed (the lack of evidence is not a proof that the two strains belong to the same mating type); all strains isolated in 2010 have been crossed with two reference couples, Sy373‘+’ and Sy800‘-’ and Sy793‘+’ and Sy799‘-’. Reference strains were crossed amongst themselves to double check the mating type attribution.

2.3 Results

2.3.1 *The life cycle of P. multistriata in time lapse-microscopy*

The observations in time lapse microscopy were carried out with two parental strains different in size (small '+' strain Sy373 and large '-' strain Sy800), to make it possible to distinguish the behaviours of the two mating types. Sexual reproduction occurred regularly and with the same timing in all the 5 Petri-dishes used for the recordings in time lapse microscopy and in the two controls kept in the dark during the period in which recordings were carried out (one vessel in the incubation chamber and another vessel in the microscope room), from the evening to the morning of the next day. Therefore, the repeated flashing of the microscope light did not impair the progression of the life cycle. In the following section, the different life cycle phases are described from various frame pictures taken from the recordings in time-lapse microscopy. The following movies (movie serie_053a, gametogenesis and gamete conjugation; movie serie_015, gamete conjugation; movie serie_087, auxospore elongation) have been added as electronic Supplementary Information (non-book components) to this thesis.

2.3.1.1 *Gametogenesis and conjugation*

During the first day of observation, only vegetative cells and chains were observed. The majority of vegetative cells were on the bottom of the Petri-dish and moved around with apparently random trajectories. *Pseudo-nitzschia multistriata* is a raphid diatom and, therefore, it has the capacity of gliding on substrates, in similar way to benthic species. To change direction, vegetative cells stopped their movement, made a slight change in position (between few to 30°) and then moved back in a different direction. The '-' cells were more active and covered long distances along the slide surface, while the small '+' cells were less motile.

Day 2: When I started recording, there were no paired cells in the selected optical field but, after about half an hour, a sort of ‘courtship’ behaviour was observed as ‘-’ cells went repeatedly close to ‘+’ cells. A first contact, lasting only a few seconds, was observed after 30 min (Fig. 2.2a). After about 45 min, two other ‘-’ cells made contact with the small ‘+’ one (Fig. 2.2b); they moved randomly around it for almost 1 hour until one of the two ‘-’ cells made closer contact. The cells of the two different mating types remained in contact for almost 30 min, but then separated. After another 1.5 h, five ‘-’ cells went closer to the ‘+’ cell and moved randomly for about 30 min (Fig. 2.2c). One ‘-’ finally separated from the group, stopped moving, and paired with the ‘+’ cell (Fig. 2.2d).

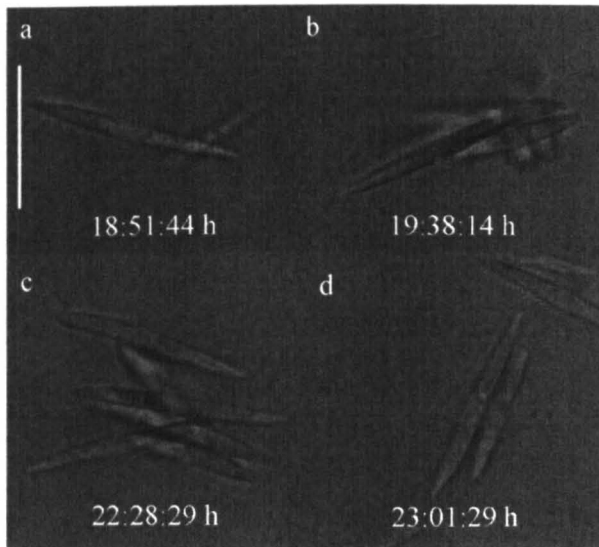


Figure 2.2. Time lapse bright field (BF) micrograph frames selected from a movie serie_053d that show the contact between opposite mating type cells. (a-c) One ‘+’ (small) cell and one (a), two (b) or five (c) ‘-’ cells (big) close to each other. (d) Pair of ‘+’ and a ‘-’ gametangia. Note that the time in hours (h), from the beginning of the experiment, is indicated on each sequence. Scale bar = 25 μ m.

Once the two cells paired, no other large ‘-’ cell came close and the two gametangia were paired for about 5 h before the rearrangement of the cytoplasm – indicative of gametogenesis - became evident (Fig. 2.3a). The cytoplasm rearrangement consisted in rapid and repeated migrations probably of the 2 chloroplasts along the perivalvar axis of the

cell in each gametangium, lasting for almost 5 hrs (Fig. 2.3*b-c*). At this point, the cytoplasm of the '+' gametangium underwent cytokinesis and separated into two distinct portions, while the cytoplasm of the '-' gametangium was still undivided (Fig. 2.3*d-e*). The '-' gametangium underwent cytokinesis, and separated into two protoplasts (Fig. 2.3*f-g*) with a time shift of about 20 min as compared to the '+' gametangium, showing that gametogenesis was not completely synchronized between the two gametangia. At the time at which '-' gametangium started cytokinesis, the two '+' protoplasts started to contract away from the tips of the frustule (Fig. 2.3*f-g*), becoming progressively rounded (Fig. 2.3*h*), until the two gametes were formed. The two gametes were close to each other, in the middle of the gametangia frustule, which was open (Fig. 2.3*i*). The same sequence of events occurred in the '-' gametangium (Fig. 2.3*h-i; j-k* and 2.3*l*). When the formation of the gametes in the two gametangia was completed, the lower '+' gamete started moving towards the upper '-' gamete (Fig. 2.3 *l-m*) and remained there for a long time (about 8 hours) before conjugation between the two gametes took place (Fig. 2.3 *n-p*). Conjugation was rapid and was completed in about 30 min. Unfortunately the recording time stopped before the conjugation of the second gamete could be followed.

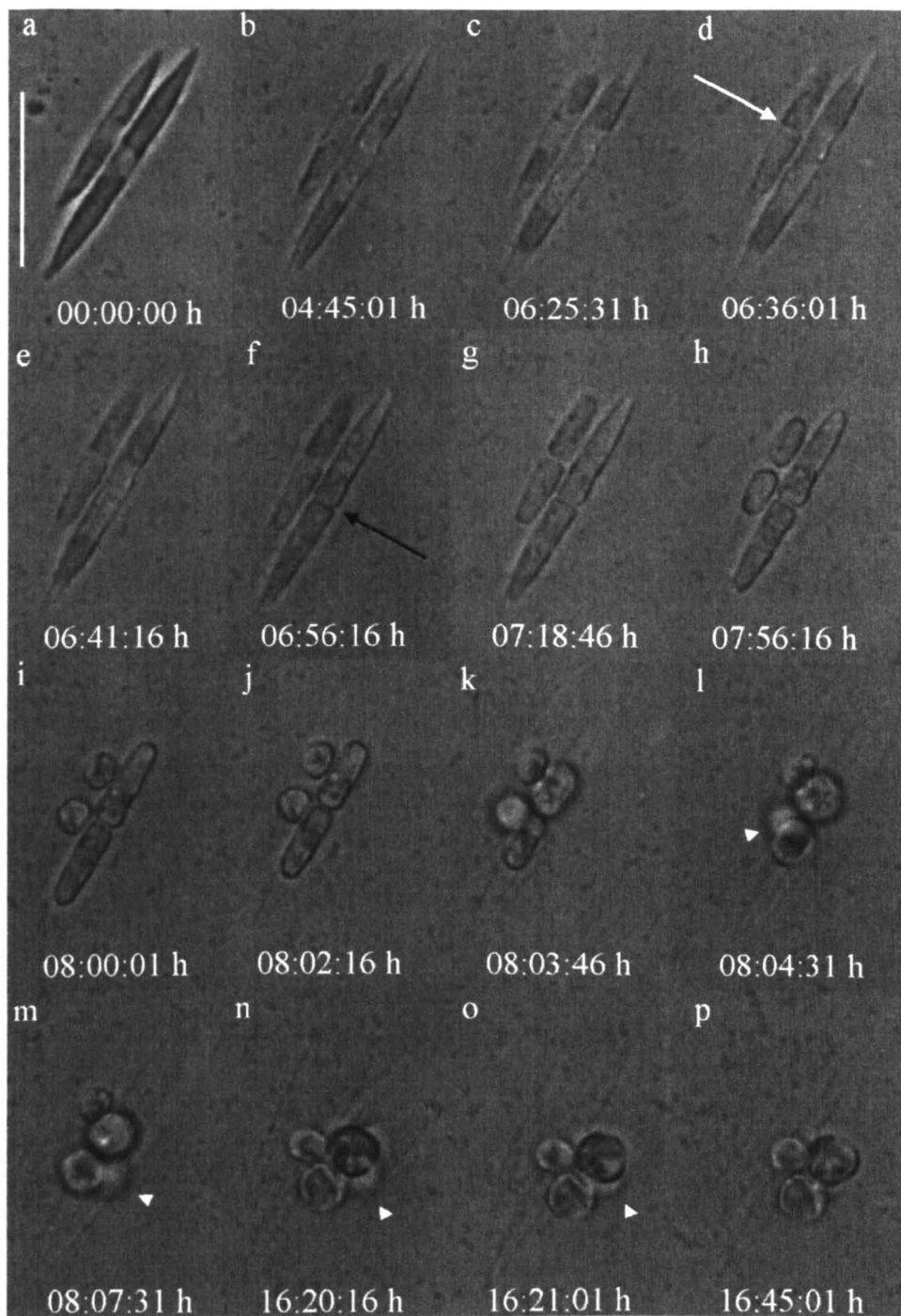


Figure 2.3. Time lapse BF micrograph frames selection from a movie serie_053a; gametogenesis and conjugation. (a) Pairing of '+' (left) and '-' (right) gametangia. (b-c) Cytoplasm rearrangement inside of each gametangium. (d-e) Cytokinesis within the '+' (white arrow) and (f) the '-' (black arrow) gametangia. (f-g) Cytoplasm contraction, within the small '+' and (h-k) big '-' gametangia, from the tips of the frustule to the central area before the formation of '+' (j) and '-' (l) rounded gametes respectively. (l-m) Movement of one '+' gamete (white arrowhead) towards the '-' one (n-p) previous the conjugation. Note that the time in hours (h), from the beginning of the experiment, is indicated on each sequence. Scale bar = 25 μ m.

Day 3: In the optical field selected for the third observation it was possible to follow the conjugation of the second gamete. The two pairing gametangia had already concluded gametogenesis and two of the four gametes already produced a zygote, the slightly larger spherical body attached to the large ‘-’ gametangium marked with an arrow on figure Fig. 32a. The other ‘+’ gamete was visible in the lower position still attached to the ‘+’ gametangium and the ‘-’ gamete was placed above the zygote attached to the large ‘-’ gametangium (Fig. 2.4a). After about 50 min from the beginning of the record, the ‘+’ gamete moved towards the ‘-’ one (Fig. 2.4b-c). The conjugation of the two gametes is illustrated from Fig. 2.4d to Fig. 2.4j. Also in this case conjugation was very rapid and was completed within 3 min and 30 s.

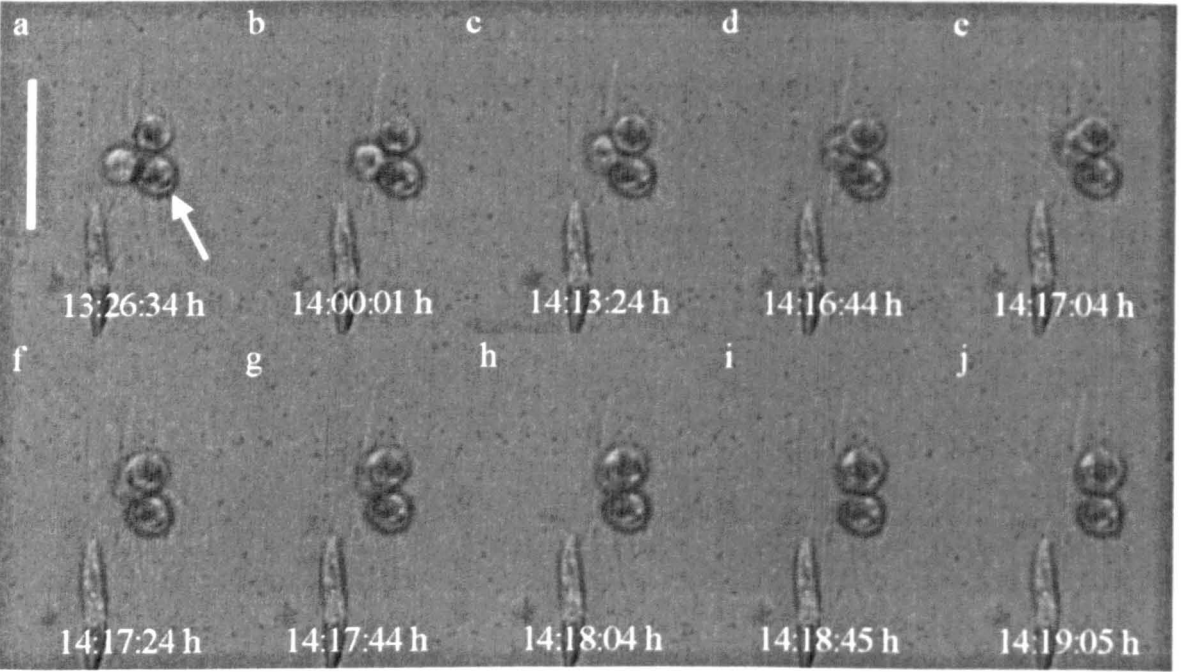


Figure 2.4. Selection of BF micrograph frames from a movie Series_015; gamete conjugation. (a) A zygote – the slightly larger spherical body (arrow) – and a ‘-’ gamete (upper part) are joined on the right side of the ‘-’ gametangium whereas the ‘+’ gamete is attached to the left side of the ‘+’ gametangium. (b-d) The ‘+’ gamete moved toward the ‘-’ one (e-j) prior the conjugation. Note that the time in hours (h), from the beginning of the experiment, is indicated on each sequence. Scale bar = 25 μ m.

2.3.1.2 *Anomalies during gametogenesis*

In a few cases, one of the two gametangia was not able to complete gametogenesis. The two paired gametangia started rearranging the cytoplasm and cytokinesis took place in the small '+' gametangium (Fig. 2.5*a-b*), where two normal spherical gametes were produced (Fig. 2.5*c-d*). Conversely in the large '-' gametangium, cytokinesis did not take place but the cytoplasm contracted within the frustule and one single, large, spherical body was produced. It was not possible to understand what occurred at the level of the nucleus, i.e. to understand if meiosis had occurred in the '-' gametangium, or to see the number of nuclei. The frustules opened and the rounded anomalous gamete came out from the gametangium (Fig. 2.5*e-g*). The two rounded '+' gametes detached from their gametangium and moved around but not near to the '-' spherical body and conjugation did not take place (Fig. 2.5*f-g*).

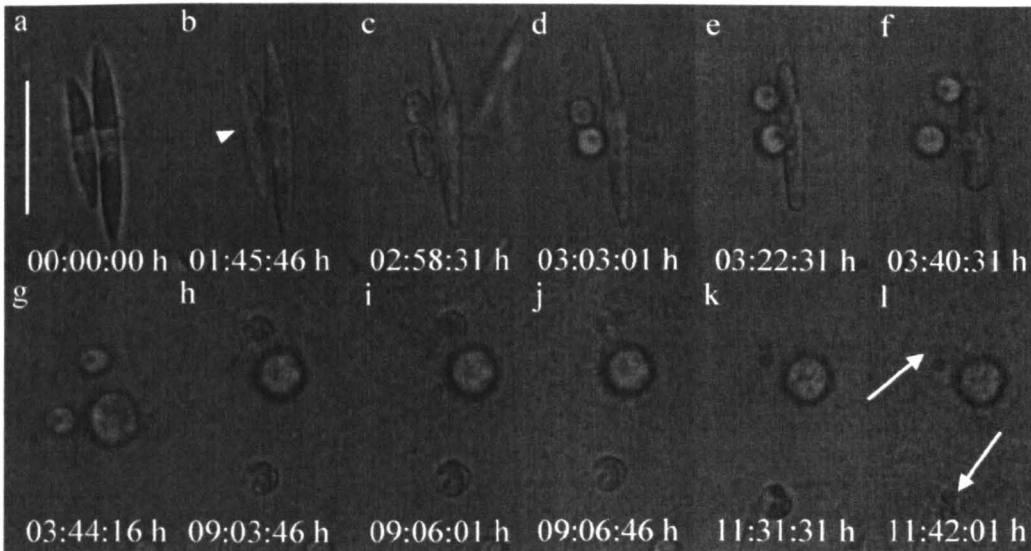


Figure 2.5. Selection of BF micrograph frames from a movie serie_053c; gametogenesis and gamete destruction by bacteria. (a) Paired gametangia of opposite mating types. (b) Cytokinesis in the '+' gametangium (arrowhead), followed by (c-d) the contraction and formation of the two '+' gametes. Rearrangement (b-d) and contraction (e-f) of the cytoplasm in the '-' gametangium with the formation of a single large spherical body (anomalous gamete) (g). The '+' gametes were attacked by bacteria (h-j). Two dark small bodies remained after the gamete destruction (arrows) (k-l). Note that the time in hours (h), from the beginning of the experiment, is indicated on each sequence. Scale bar = 25 μ m.

2.3.1.3 *Auxospore development and formation of the initial cell*

Auxospore expansion is illustrated in Figure 2.6. Two auxospores were attached perpendicularly to the ‘-’ empty gametangium (Fig. 2.6a). Generally they both develop into initial cells, in the case that we recorded only one was able to complete the elongation. The auxospore in the upper position started to expand in a bi-polar way and perpendicular to the gametangium (Fig. 2.6b-e). The central portion of the auxospore was slightly enlarged (Fig. 2.6c). The four chloroplasts inside of the auxospore became clearly visible when elongation proceeded (Fig. 2.6g-h). They moved up and down within the auxospores, but without a clear pattern. The other auxospore did not develop further: it extruded a spherical body containing some cytoplasm that started to expand (Fig. 2.6c). Both the spherical body and the second auxospore were destroyed by bacteria (Figure 2.6f). The destruction of the auxospore took about 20 min and only a globular mass remained attached to the gametangium close to the normally developed auxospores (Fig. 2.6h). When auxospore expansion was completed, the cytoplasm detached from the perizonium and the new silica walls were synthesized (Fig. 2.7a-b).

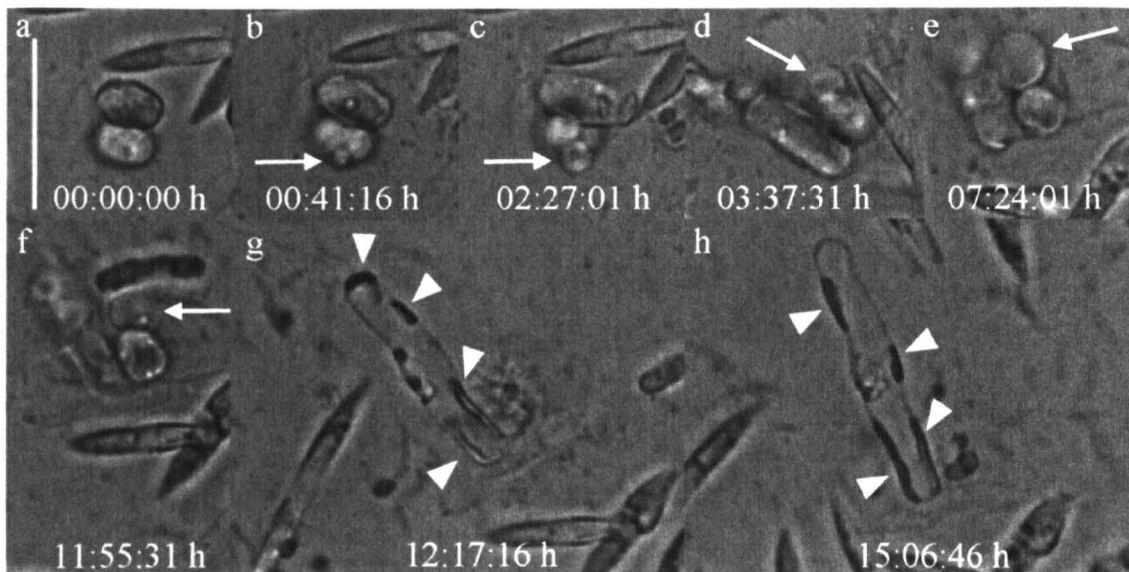


Figure 2.6. Selection of BF micrograph frames from a movie series_087; auxospore formation. (a) Two auxospores attached to an empty ‘-’ gametangium as generally produced in this species. (b) One auxospore starts to elongate while in the other a small spherical body (arrow) is extruded. (c-h) The elongation and the expansion of the normal auxospore are illustrated; the four chloroplasts were also visible (arrowheads) (g-h). The small spherical body of the other auxospore expand and (c-e) but was destroyed by bacteria. Note that the time in hours (h), from the beginning of the experiment, is indicated on each sequence. Scale bar = 25 μm .

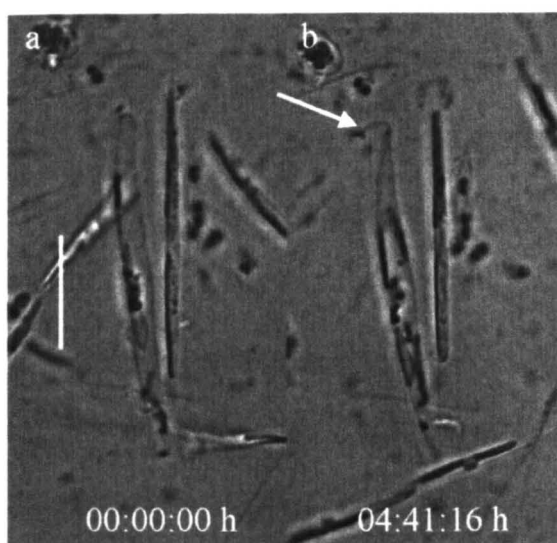


Figure 2.7. Selection of BF micrograph frames from a movie series_03. Initial cell formation. The detachment of the auxospore cytoplasm from the perizonium membrane (arrow) (a) and the production of the first valve of the initial cell (b) are shown. Note that the time in hours (h), from the beginning of the experiment, is indicated on each sequence. Scale bar = 25 μm .

2.3.1.4 *Bacteria*

The strains used for observations in time lapse microscopy were not axenic and several bacteria were present and visible on the bottom of the Petri-dish. Their number considerably increased during the period of observation, from day 1 to day 4, probably due to the fact that organic material is excreted from the cells during gametogenesis/conjugation. It was also possible to observe repeated attacks by bacteria sexual stages, which eventually died producing additional organic material in the culture. One example of bacterial attack on two '+' gametes is illustrated in Figures 2.5*h* - 2.5*n*. The bacteria started moving towards the '+' gametes – indicated with an arrow – and the gamete collapsed leaving two black rounded bodies (Fig. 2.5*h*). This bacterial attack was very rapid and took about 4 min for the destruction of the first '+' gamete and about 13 min for the second '+' gamete (frame *j* and *l*). The two small dark bodies that remain from the destruction of the gametes might be the remnants of the two chloroplasts.

2.3.2 *The life cycle of P. multistriata in confocal microscopy*

The preliminary experiment aimed at testing the performance of the different nuclear stains showed that SYBR Green I performed better. With this staining, I was able to use a lower light intensity for excitation and the staining bleached much slower as compared to DAPI and Hoechst. This was probably also due to the use of MOPS buffer that helped to stabilize the dye. I have used this staining for observations in both epifluorescence and confocal microscopy. I was planning to use Hoechst to carry out time lapse observations in confocal microscopy, to have the possibility to follow in real time the nuclear behaviour in different life cycle phases (e.g. formation of gametes, conjugation etc.). The Hoechst dye is a vital dye, but the UV light pulses needed to excite the fluorochrome in the time-lapse setting on the confocal microscope was used for a long time (4-5 hours) and damaged the cells.

Moreover, the Hoechst dye produced precipitates in the growth medium, which impaired image acquisition.

The crosses and observations in confocal microscopy were conducted in two different periods and using two different couples of strains. Both couples were able to undergo sexual reproduction in 24-36 hours from the inoculum. In the following, I provide a description of the life cycle stages and phases, with special attention to the behaviour of the nuclei and chloroplasts.

2.3.2.1 *Vegetative cells and mitotic division*

Vegetative cells have a sigmoid shape when observed in girdle view because their ends are slightly bent (Fig. 2.8). When cell size decreases (roughly below 24 μm), cells have a more straight morphology and often show a slight constriction in their central part (Figs 2.8 and 2.9). The nucleus was located in the central portion of the cell and two elongate chloroplasts were visible on each side of the nucleus (Fig. 2.10). In Figure 2.11, a cell that undergoes mitotic division is illustrated. The two chloroplasts just duplicated and are positioned side by side and the two nuclei are visible and positioned perpendicularly to the longitudinal axis of the cell. When karyokinesis is completed, the synthesis of the valves of the daughter cells started and – when completed – the two sister cells were aligned side by side along their longitudinal axis (Fig. 2.12a). *Pseudo-nitzschia multistriata* often forms chains where cells are joined end to end; the two daughter cells thus slide along their frustules after division, but generally remain attached to the apex of one cell and the antapex of the sister cell. In Figure 2.12b, a chain of cells that divided synchronously is illustrated. Abrupt cell size reduction, i.e. the formation of considerably smaller cells following a constriction produced during mitotic division (see Chepurnov *et al.* 2005) was never observed in cultures of *P. multistriata*.

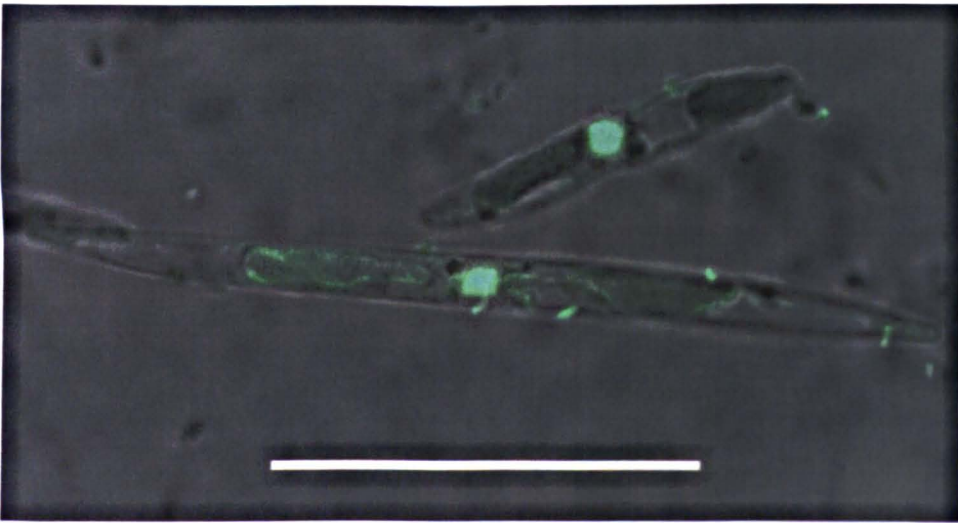


Figure 2.8. Confocal laser scanning (CLS) micrographs of two vegetative cells those are different in size (small strain Sy373 '+' and large strain Sy800 '-'). The SYBR Green I (green) stained nuclei were visible in the central part of the cell. Scale bar = 25 μ m.



Figure 2.9. Phase contrast (PC) micrograph of a small '+' vegetative cell (strain Sy373) with a constriction in its central part. Scale bar = 25 μ m.

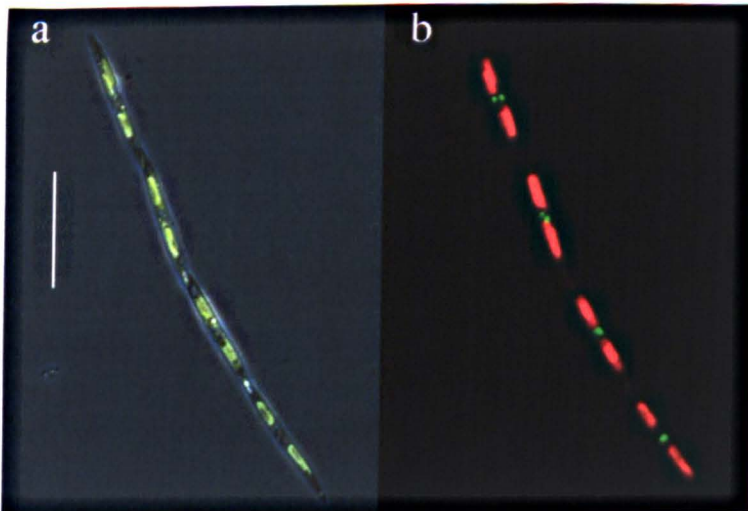


Figure 2.10. PC (a) and epifluorescence (b) micrographs of '-' vegetative cells in a chain (strain Sy800) in valve view. Nuclei (green), stained with SYBR Green I, were visible in the centre of the cells with the chloroplasts (red) at both sides. Note that the first two cells were under mitotic division. Scale bar = 25 μ m.

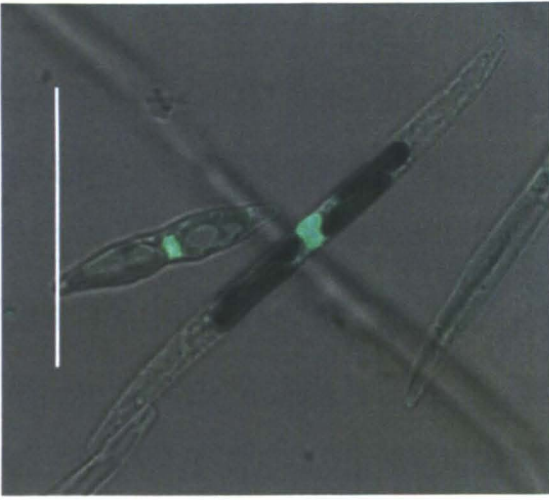


Figure 2.11. CLS micrograph of two vegetative cells different in size (small strain Sy373 '+' and large strain Sy800 '-'). The nuclei, stained with SYBR Green I (green), were visible in the central part of the cell. The large cell was undergoing mitotic division. Scale bar = 25 μ m.

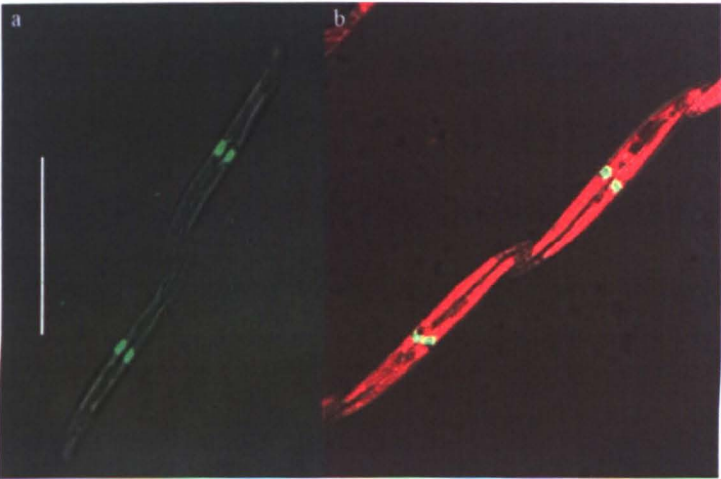


Figure 2.12. CLS micrographs of recently divided vegetative cells (strain Sy800 '-'). Nuclei, stained with SYBR Green I (green), were perpendicular to the length of the cells (*a-b*) chloroplasts (red) were placed on each side of the nucleus (*b*). Scale bar = 25 μ m.

2.3.2.2 *Gametogenesis*

Sexual reproduction never occurred in monoclonal cultures. The use of strains with markedly different cell size (Table 2.2) made it possible to distinguish the two mating types on the microscope.

Two cells of the opposite mating type (gametangia) paired and underwent meiosis (Fig. 2.13). The examination of several samples suggested that meiosis occurred most of the time asynchronously in the two mating types with the '+' mating type starting Meiosis I. In Figure 2.13, two paired gametangia are illustrated; the nucleus of the smaller cell ('+' mating type) is elongated and has started the 1st meiotic division, while the nucleus of the large '-' mating type still has a rounded shape. In Figure 2.14, different stages of meiotic divisions are illustrated. After Meiosis I, cytokinesis took place and during Meiosis II, only karyokinesis took place with the formation of 2 haploid nuclei in each protoplasm; subsequently, one of the two nuclei degenerated as a pyknotic nucleus. After that, the two protoplasts of each gametangium started to contract into gametes that contained only one nucleus each. Figure 2.14*a-b* shows two paired gametangia in which the large '+' gametangium is approaching Meiosis I division, as suggested by the fact that the nucleus has lost the rounded shape and is elongate. In the small '-' gametangium, the protoplast division was already completed and one nucleus was present inside each protoplast. In a slightly advanced phase, the two protoplasts of the small '-' gametangium went through Meiosis II and two nuclei are visible inside each protoplast (Figure 2.14*c-d*). Also in this figure the nucleus of the large '-' gametangium had lost the rounded shape and begun to expand; it was at the early stage of meiotic prophase. In Figure 2.14*e-f* the smaller '+' gametangium contains two protoplasts with one nucleus each, indicating that pyknosis had already taken place. The large '-' gametangium is now in Meiosis II, with two haploid nuclei in each protoplast.

In some cases, meiosis seemed to proceed synchronously in the two gametangia (Figure 2.14g-h). The two paired gametangia had already gone through plasmokinesis and the segregated cytoplasm was visible. Both the small '+' and the large '-' gametangium were undergoing Meiosis II: nuclear division was completed in the lower protoplasts (2 nuclei are visible) while in the upper protoplasts only one nucleus is visible. It is possible that nuclear division still had to start or that one of the two nuclei had already become pycnotic; this possibility seems to be supported by the presence of a faint green mark in the upper part of the large gametangium. Figure 2.15a illustrates two gametes in a gametangium in the process of contracting the protoplasm and becoming rounded. Two nuclei were present in the lower gamete, while only one nucleus was present in the upper gamete; the other nucleus had most probably already degenerated, as suggested by the fact that the protoplasts had already detached from the gametangium frustule; however, the pyknotic nucleus was not visible. At the end of meiosis, each gametangium contained two rounded gametes with one nucleus and with probably two chloroplasts each (Fig. 2.15b). The number of chloroplasts could not be assessed accurately because of the very small size of the gametes and the bright fluorescence of the chloroplast/s. Another fact that supports the presence of two chloroplasts for each gamete is the fact that the auxospore has four chloroplasts (see below). The majority of gametangia observed in confocal microscopy remained paired until the completion of gametogenesis. Once formed, gametes remained attached to the '-' gametangium but some free gametes were also observed.

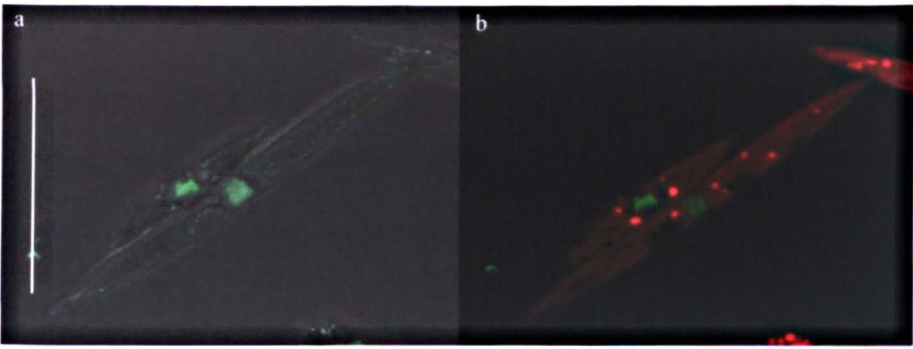


Figure 2.13. CLS micrographs of two paired gametangia (small '+' strain Sy373; and large '-' strain Sy800). The SYBR Green I stained nuclei (green) were visible in the central portion of the cell; note that the nucleus of the smaller cell (left) has started to undergo the first meiotic division (*a, b*); two chloroplasts (red) were visible inside each cell (*b*). Scale bar = 25 μ m.

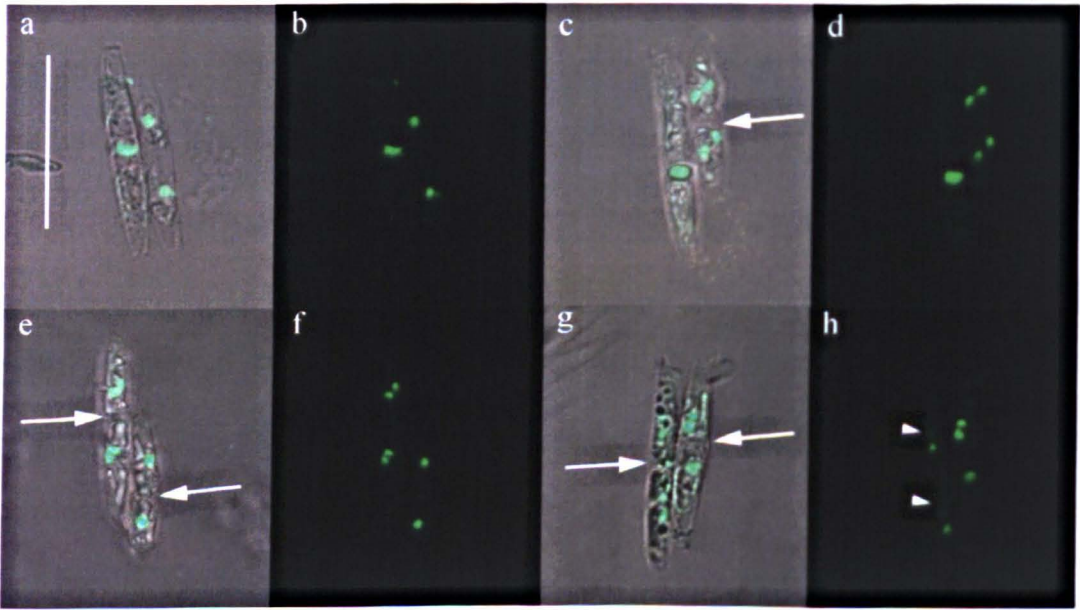


Figure 2.14. Confocal Z-stack projection onto CLSM micrographs of different pairing gametangia showing asynchronous gametogenesis (small '+' strain Sy793 and large '-' strain Sy799); nuclei were stained with SYBR Green I (green). (*a-b*) The small gametangium in Meiosis I with a nucleus inside each protoplast. (*a-d*) The nucleus of the large gametangium has lost the rounded shape and was starting Meiosis I. (*c-f*) The small gametangium was in Meiosis II where the 4 nuclei - 2 inside each protoplast – and the segregation of the cytoplasm (arrow) were visible. The small gametangium was at the end of Meiosis I with 1 (*c-d*) or 2 (*e-f*) nuclei inside each protoplast. (*g-h*) Both gametangia are in Meiosis II; two nuclei are present in the gametangium on the right, while only one nucleus with a possible pycnotic one (arrowhead) was present on the other cell. Note that the segregated cytoplasm is marked with an arrow. Scale bar = 25 μ m.

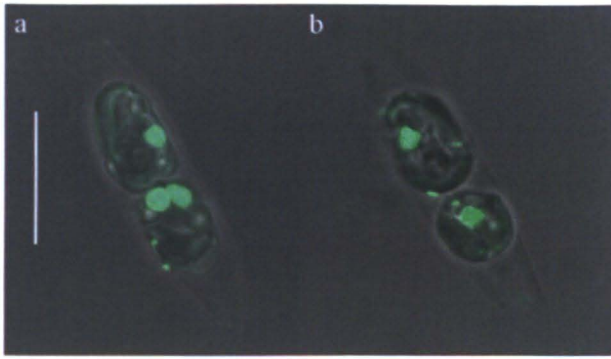


Figure 2.15. Confocal Z-stack projection onto CLSM micrographs of gametes at different sexual stages within a small '+' gametangium (strain Sy379), their nuclei were stained with SYBR Green I (green). (a) Bi- and uni-nucleate elongated gametes and (b) rounded uni-nucleate gametes. Scale bar = 25 μ m.

2.3.2.3 *Gamete conjugation, auxospore development and formation of initial cell*

When gametogenesis was completed, gametes from the '+' gametangium migrated towards the '-' gametes (see the information gained in time lapse microscopy illustrated above) and conjugation occurred between the two compatible gametes, followed by the formation of a zygote that contained two nuclei (Fig. 2.16). When observing samples stained with SYBR Green I in confocal microscopy or in epifluorescence microscopy, gametes were recognizable as uninucleate rounded bodies in contact with their gametangium. Most of the times, four gametes – two in each paired gametangia – were visible. However, at times, gametangia were detached and/or gametes were detached from their gametangium, due to the fact that the sample was mixed with a pipette; in any case, rounded protoplasts with one nucleus were considered gametes. The zygotes were also generally still attached to the '-' gametangium; besides the presence of the two nuclei, they had a well-defined rounded shape and cell wall, due to the presence of the primary zygote wall. The zygote started to expand into an auxospore with four chloroplasts clearly distinguishable; the chloroplasts become very elongate as auxospore expansion proceeded (Fig. 2.17). The two nuclei were close to each other and located in the middle of the auxospore (Fig 2.18). The two nuclei were still visible until the completion of expansion (Figs 2.19a). At this point, the cytoplasm started to contract away from the perizonium. The two haploid nuclei fused to

form the diploid nucleus and the new silica frustule was synthesized (Fig. 2.19*b*). In raphid pennate diatoms, the synthesis of the two valves of the initial cell is accompanied by two acytokinetic mitotic divisions that are followed by the degeneration of one nucleus. This process could, however, not be clearly documented during the observations in confocal microscopy. When completed, the initial cell can escape from the perizonium or it can undergo a mitotic division while still inside the perizonium. This first mitotic division is peculiar because it is not accompanied by plastokinesis and the four chloroplasts of the initial cell are split up, two in each daughter cell. In Figure 2.20 two daughter cells still surrounded by the perizonium are illustrated: they had completed the first mitotic division and each daughter cell contained two chloroplasts and one nucleus.

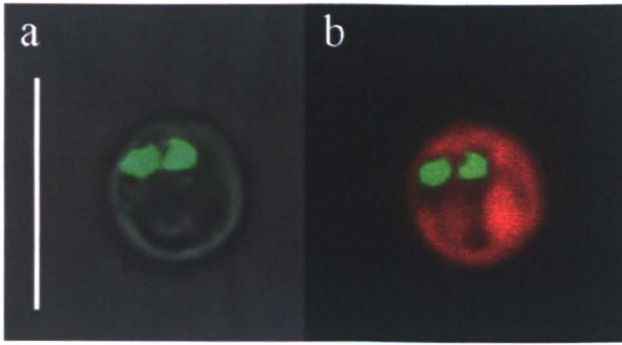


Figure 2.16. CLSM micrographs of a binucleated zygote. Both nuclei, SYBR Green I (green) stained (*a-b*) and, the red auto-fluorescence of the chlorophyll, were visible (*b*). Scale bar = 10 μm .



Figure 2.17. PC micrograph of an auxospore attached to the empty ‘-’ gametangium; its four chloroplasts were visible. Scale bar = 25 μm .

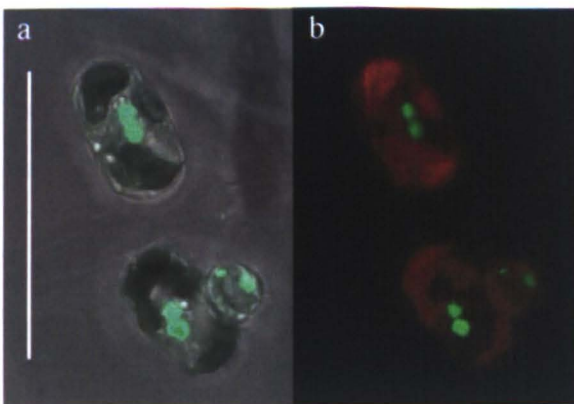


Figure 2.18. Confocal Z-stack projection onto CLSM micrographs of auxospores. Stained nuclei, with SYBR Green I (green) and the red auto-fluorescence of chlorophyll were visible (*a-b*). The round globule on the left auxospore is a free gamete. Scale bar = 25 μm .

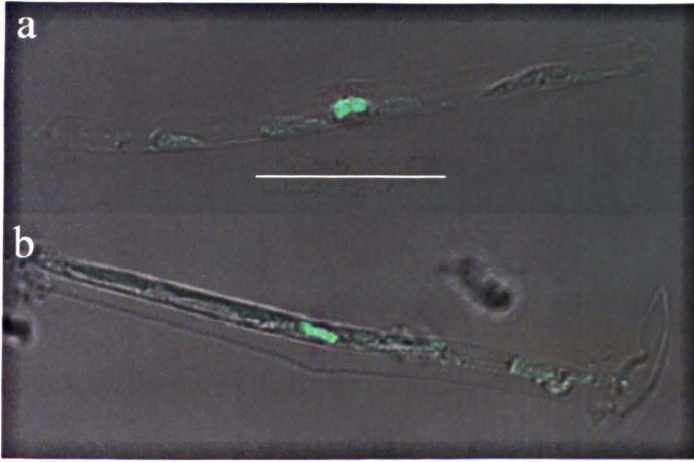


Figure 2.19. CLSM micrographs of the initial cell formation. (a) Binucleated auxospore, stained with SYBR Green I (green), at the end of the expansion, and (b) a complete initial cell inside the perizonium with its nucleus at the centre. Scale bar = 25 μm .

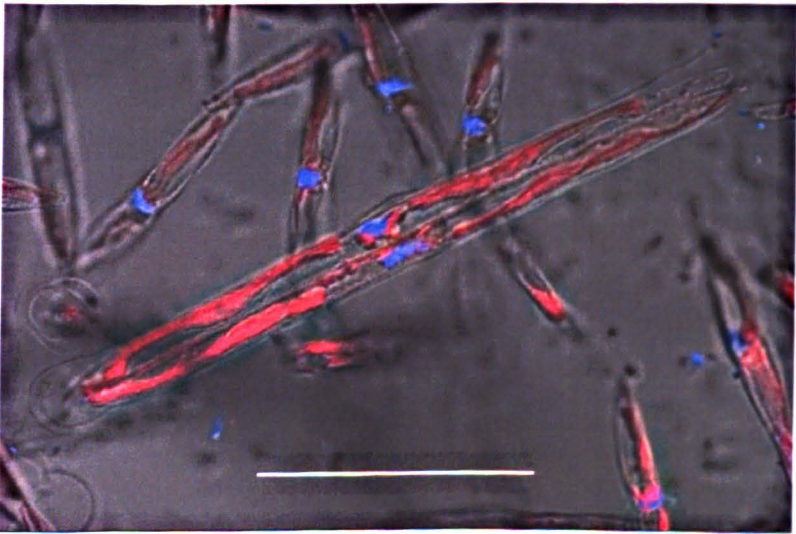


Figure 2.20. CLSM micrograph of the first mitotic division undertaken in an initial cell inside the perizonium membrane. Two chloroplasts (red) and one nucleus, stained with DAPI (blue), were visible inside each daughter cell. Scale bar = 25 μm .

2.3.2.4 *Atypical stages during sexual reproduction*

During sexual reproduction some atypical arrangements of nuclei and chloroplasts were found in some cells. Two rounded zygotes with three nuclei each were found attached to one ‘-’ gametangium (Fig. 2.21). When the single frames of the Z-stack image were checked, it was possible to visualize the two paired empty frustules of the gametangia, supporting the fact that the two rounded protoplasts were indeed zygotes (not shown). Once I found an expanding auxospore with four nuclei and four chloroplasts (Fig. 2.22).

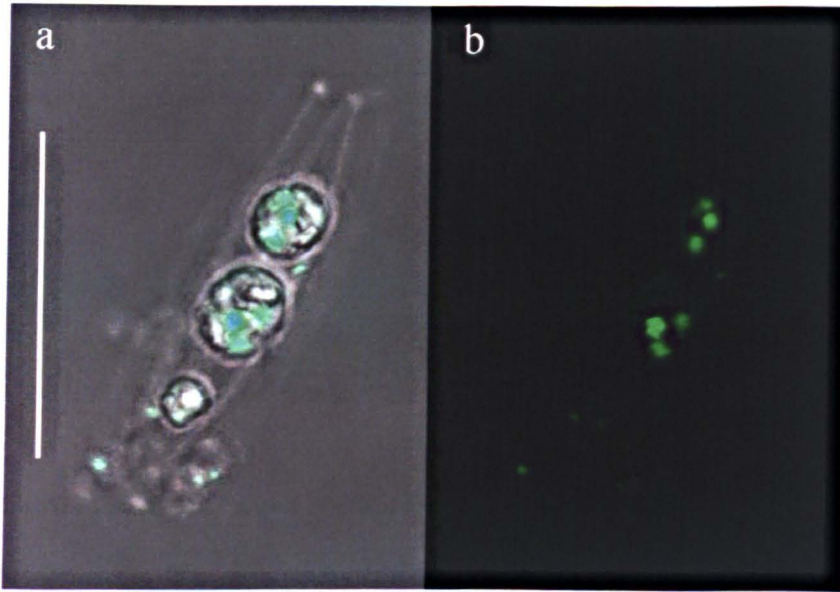


Figure 2.21. Confocal Z-stack projection onto CLSM micrographs of two zygotes with three nuclei (stained with SYBR Green I) each; a polar body is visible in the lower part of the gametangium. Scale bar = 25 μm .

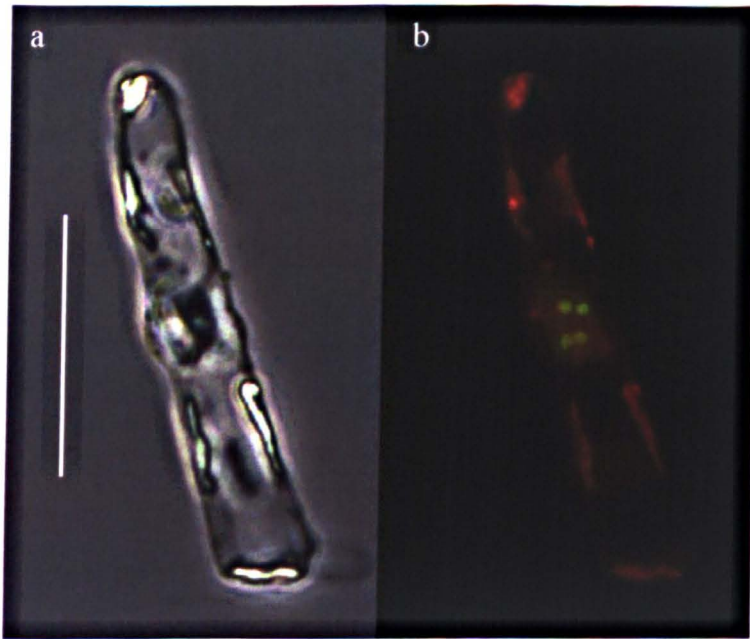


Figure 2.22. PC (a) and epifluorescence (b) micrographs of an auxospore in which four nuclei, stained with SYBR Green I (green), and 8 chloroplasts (red) were visible. Scale bar = 25 μm .

2.3.3 The size of initial cells

The crosses carried out with different combinations of six parental strains of different size, produced initial cells spanning from 67 to 90 μm in length (Table 2.5). The first cross involving small parental strains (SxS 1) produced rather small initial cells, with an average length of 63.3 μm . The initial cells produced by the other crosses had similar average and median values; the cell size range varied amongst the different crosses, but no relation with the parental cell size was evident (Fig. 2.23). The cross, involving strain Sy373 and Sy379, was repeated twice, the first time when they had longer size (L), the second time when they were much shorter (S); the cell size produced in the two crosses was very similar.

Table 2.5. Size of initial cells produced by parental strains of different cell size (S=small, M=medium, L=large size). For each parental strain, the mating type ('+'; '-') and the average size (μm) at the moment in which crosses were carried out are reported; the average size of initial cells (μm) is reported together with st. dev., 20 initial cells were measured for each cross.

Strains	Sy373 '+'	Sy793 '+'	Sy664 '+'	Sy627 '+'	ES814 '+'	Sy373 '+'
crossed	18.3 (S)	22.7 (S)	29.5 (M)	31.7 (M)	37.0 (L)	39.0 (L)
Sy776 '-' 20.8 (S)		69.3 \pm 3.1 SxS (1)				
Sy379 '-' 22.2(S)	79.0 \pm 2.3 SxS (2)		77.7 \pm 3.3 SxM (1)			
Sy789 '-' 26.6 (M)				76.0 \pm 2.6 MxM (1)		
Sy799 '-' 29.8 (M)	79.6 \pm 4.1 SxM (2)		80.7 \pm 3.6 MxM (2)	77.4 \pm 3.5 MxM (3)		
Sy379 '-' 43.9 (L)						77.6 \pm 2.5 LxL (1)
VF2.5 '-' L 48.4 (L)					78.1 \pm 3.5 LxL (2)	

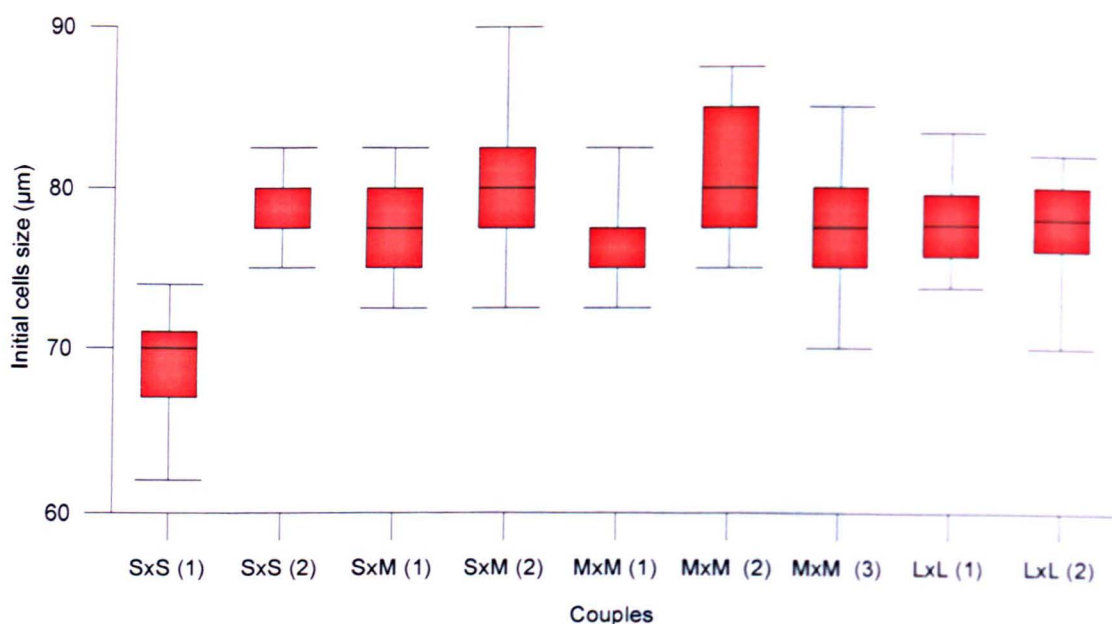


Figure 2.23. Box plot distribution of the initial cells size produced under different parental strains (x axis) crosses as listed in Table 2.5.

2.3.4 Mating experiments

The results of all mating experiments carried out with *Pseudo-nitzschia multistriata* strains isolated in different years showed that sexual stages were detected when crossing parental strains with an average apical length comprised between 55 µm and 55 µm (Tables 2.1 and 2.6). The strains isolated in 2008 were all crossed with Sy172 '+' strain and Sy17 '-' strain. A strain was defined '-' when it produced sexual stages when crossed with the reference '+' strain but not with the reference '-' strain. A vast majority (94 over 102) belonged to the '+' mating type and only 2 strains to the '-' mating type (Table 2.7). It has not been possible to assign the mating type to six strains because they did not undergo sexual reproduction when crossed with either '+' or '-' strains. Unfortunately, cell size data at the time at which crosses were performed were not available and it cannot be verified if strains were above the cell size for sexualisation. In 2009, some of the tested strains were crossed with two reference strains ('+' and '-') and the assignment of the mating type was consistent between the two tests. Some other strains (marked with an asterisk on Table 2.1) were crossed only with one of the two mating types; if they did produce sexual stages the

assignment to the mating type was certain, if they did not, we assigned them the same mating type as the one of the strain with whom they were crossed. However, this assignment is not certain and it has been marked with a question mark (?) on Table 2.6. About a half of the strains tested (30 over 65) belonged to the ‘-’ mating type and 13 strains belonged to the ‘+’ mating type (Table 2.7). If we consider also the uncertain mating type assignments illustrated above, we have 13 more ‘+’ strains and 4 more ‘-’ strains, that will bring the figures to 34 ‘-’ and 26 ‘+’. Out of the 66 strains isolated in 2010, 25 turned out to be of the ‘+’ mating type and 37 of the ‘-’, and it was not possible to assign the mating type to 4 strains because they did not undergo sexual reproduction when crossed with either ‘+’ and ‘-’ strains, notwithstanding the fact they should have been within the size window for sexualisation, i.e. <51 µm (Table 2.6).

Table 2.6. Attribution of the mating type (‘+’ and ‘-’ strains; ‘+’? and ‘-’? for when it uncertain whether male or female strains; n.a. = not assigned); an asterisk (*) marks the strains isolated in 2009 that were crossed with only one member of the reference couple to the strains tested in the different years (See Table 2.1 for the details on isolation dates and cell size).

Year 2008 (102 strains)					
Strain code	Mating type	Strain code	Mating type	Strain code	Mating type
Sy014	+	Sy145	+	Sy217	+
Sy016	+	Sy146	+	Sy218	+
Sy017	-	Sy147	+	Sy219	+
Sy019	+	Sy149	+	Sy222	+
Sy020	+	Sy151	+	Sy234	+
Sy021	+	Sy152	+	Sy236	+
Sy023	+	Sy156	+	Sy238	+
Sy025	+	Sy157	+	Sy239	+
Sy027	+	Sy164	n.a.	Sy241	+
Sy033	+	Sy165	+	Sy243	+
Sy036	+	Sy166	n.a.	Sy244	+
Sy039	+	Sy168	+	Sy246	+
Sy040	+	Sy171	+	Sy248	+
Sy043	+	Sy172	+	Sy250	+
Sy044	+	Sy173	+	Sy252	+

Sy046	+	Sy174	+	Sy254	+
Sy047	+	Sy175	+	Sy256	+
Sy050	+	Sy176	+	Sy278	+
Sy055	+	Sy177	-	Sy279	+
Sy058	+	Sy178	+	Sy281	+
Sy070	+	Sy180	+	Sy284	+
Sy084	+	Sy182	+	Sy290	+
Sy087	+	Sy183	+	Sy297	+
Sy089	+	Sy184	+	Sy299	+
Sy093	+	Sy185	+	Sy301	+
Sy096	+	Sy186	+	Sy302	+
Sy097	+	Sy187	+	Sy303	+
Sy098	+	Sy191	n.a.	Sy304	n.a.
Sy103	+	Sy196	+	Sy305	+
Sy114	+	Sy200	n.a.	Sy306	+
Sy117	+	Sy203	+	Sy307	+
Sy131	+	Sy206	+	Sy308	+
Sy134	+	Sy207	+	Sy309	+
Sy138	+	Sy211	+	Sy310	+

Year 2009 (65 strains)

Sy319*	+	Sy355*	-	Sy386	-
Sy321*	-	Sy357*	+	Sy387	-
Sy323*	-	Sy358*	+	Sy388*	+
Sy324 *	-	Sy359*	-	Sy389*	+
Sy326*	+	Sy361	-	Sy391*	+
Sy327	-	Sy363*	+	Sy392*	+
Sy329*	+	Sy365*	+	Sy394	-
Sy330*	-	Sy366*	+	Sy395*	+
Sy331*	+	Sy368*	+	Sy397	+
Sy334	+	Sy369*	+	Sy399	-
Sy336*	+	Sy370	-	Sy400	-
Sy338*	-?	Sy373	+	Sy401*	-
Sy340	+	Sy375	+	Sy402	-
Sy344*	+	Sy376*	+	Sy403	-
Sy345*	+	Sy377*	-?	Sy404	+
Sy346*	-	Sy378	-	Sy405	+
Sy347	-	Sy379	-	Sy406	+
Sy348*	-	Sy380	-	Sy407	+
Sy349*	-	Sy382	+	Sy408*	-?
Sy350*	+	Sy383*	-	Sy409*	-?

Sy351	-	Sy384	-	Sy445	-
Sy353*	+?	Sy385*	-		
Year 2010 (66 strains)					
Sy602	-	Sy698	+	Sy772	-
Sy608	-	Sy701	+	Sy774	+
Sy627	+	Sy707	+	Sy776	-
Sy644	-	Sy710	+	Sy777	+
Sy653	-	Sy713	n.a.	Sy778	-
Sy659	-	Sy714	-	Sy779	+
Sy664	+	Sy717	-	Sy781	-
Sy665	-	Sy718	+	Sy782	+
Sy667	-	Sy719	-	Sy783	-
Sy668	+	Sy720	-	Sy785	-
Sy676	-	Sy722	-	Sy789	-
Sy679	-	Sy723	-	Sy791	-
Sy680	-	Sy724	+	Sy792	+
Sy681	+	Sy727	+	Sy793	+
Sy683	-	Sy731	-	Sy794	n.a.
Sy684	+	Sy735	-	Sy795	-
Sy685	-	St736	+	Sy796	-
Sy686	-	Sy738	+	Sy797	n.a.
Sy691	-	Sy741	+	Sy799	-
Sy692	n.a.	Sy745	-	Sy800	-
Sy696	-	Sy748	+	Sy801	+
Sy697	+	Sy770	-	Sy806	+

Table 2.7. Synthesis of the assignment of mating type to strains of *P. multistriata* isolated over three consecutive years. For each year, the total number of tested strains (N) are reported, as well as the number and percentage of '+' and '-' mating type, of mating type assigned with uncertainty '+?', '-?', and of the non-assigned mating types (NA).

Year	N	‘+’	‘-’	‘+’?	‘-’?	NA	% ‘+’	% ‘-’	% ‘+’?	% ‘-’?	% NA
2008	102	94	2	-	-	6	92.2	2.0	-	-	5.9
2009	65	13	30	18	4	-	21.3	49.2	29.5	6.6	-
2010	66	25	37	-	-	4	37.9	56.1	-	-	6.1

2.4 DISCUSSION

Pseudo-nitzschia multistriata has a heterothallic life cycle: '+' and '-' gametes are produced in gametangia belonging to different clonal strains. The species has isogamous gametes, they are similar in shape and size but functionally distinct (D'Alelio *et al.* 2009a and present study). The study of the life cycle stages of *Pseudo-nitzschia multistriata* in time-lapse and confocal microscopy and the large number of crosses carried out has increased the information on the life cycle of this species. In particular, the details of cell pairing, formation of gametes, gamete conjugation and auxospore formation were described, allowing comparison with what has been reported for other congeneric species and other raphid diatoms. More detailed information on the 'cardinal points' of the life cycle of this species has also been achieved. The high number of crosses carried out over three years showed that the percentage of mating types was rather comparable in 2009 and 2010, while in 2008 the population was surprisingly dominated by '+' mating types.

The life cycle of diatoms is characterized by a general pattern that is common to many species across their diversity (Chepurnov *et al.* 2004); however, there are important minor variations that characterize different genera and even species within the genera. In the following, the life cycle characteristics recorded for *P. multistriata* will be compared with what is known for other congeneric species and other raphid diatoms.

2.4.1 Vegetative division

The cell size of *P. multistriata* in culture spanned from 15 to 90 μm . This is a broader size range than has been recorded in the natural environment. In a study carried out at the LTER station MareChiara in the Gulf of Naples, where the cell size of natural populations has been measured over 10 years, the cell size was comprised between 30 and 75 μm (D'Alelio *et al.* 2010). It is not surprising that the larger cells, i.e. the initial cells or those

deriving from the first divisions of them, are not frequently recorded. Sexual reproduction occurs rarely and these cells are obviously difficult to find. What is interesting is the fact that the cell size reached in cultures is considerably lower than recorded in nature. It has to be pointed out that in culture it is very frequent to find cells with anomalous morphology, usually when cells are below 30 μm in length. These cells show a constriction in their middle portion, but they are vital, can divide and can produce gametes. It might be that the anomalous morphology is an indicator for other physiological weaknesses that cause the death of the cells in the natural environment at a larger cell size as compared with what happens in culture. The formation of lobate cells has been also reported in *P. pungens* (Subba Rao *et al.* 1991). In *Thalassiosira weissiflogii*, cultures that reached the lower cell size started to produce cells with abnormal shape and/or multinucleate (von Dassow *et al.* 2006). The authors hypothesized that physical constraints imposed by the lower valve diameter may affect cytoskeleton structure; interfere with mitosis, cytokinesis or normal valve deposition.

2.4.2 Gametogenesis and gamete conjugation

A detailed description of gametogenesis has been obtained for *P. pungens*, where cultures of opposite mating type have been studied in light microscopy and some pictures of nuclei stained with the fluorochrome DAPI were provided (Chepurnov *et al.* 2005). The observations carried out in time lapse and confocal microscopy for *P. multistriata* confirm the same general life cycle pattern described for *P. pungens*. However, some differences were observed. The sequence of meiotic divisions in the two gametes developing in the gametangia was not always synchronous. Meiosis seems to be completed first in the '+' gametangium and slightly later in the '-' one. The observations in time lapse microscopy also showed that conjugation between the two gametes was not synchronous, but slightly offset in time.

This study has shown that the migration of gametes towards those of the opposite mating type and their subsequent conjugation is a rather quick process taking between a few to 30 min. The time elapsing from the pairing of gametangia and the first evidence for gamete formation in time lapse microscopy, i.e. the separation of the two protoplasts, was about 3 hours. This is reasonable because the two meiotic divisions and the reorganization of the cytoplasm have to take place within the gametangium. A rather long time interval elapsed between the completion of gamete formation and the conjugation process. It has been possible to follow only once the whole process in a single record and it cannot be confirmed if this long time interval is a characteristic of the life cycle or if it was due to the conditions in culture and/or to the fact that the repeated flashes of the microscope light might have negatively affected the process.

Pseudo-nitzschia multistriata undergoes a IA2 cis-type auxosporulation process (i.e. two active '+' gametes move towards the two '-' passive gametes), which has been reported for other *Pseudo-nitzschia* species (*P. delicatissima* in Amato *et al.* 2005, *P. multiseries* and *P. pseudodelicatissima* in Davidovich and Bates 1998, *P. pungens* in Chepurnov *et al.* 2005). The observations in time lapse microscopy made it possible to see that the conjugation pattern between the two gametes is not between the two gametes facing each other, but it occurs with an 'X' pattern, i.e. the gamete positioned in the lower part of the '+' gametangium conjugates with the gamete in the upper part of the '-' gametangium and *viceversa* for the other gamete. A consequence of a 'cis-type' life cycle in which two gametes are produced in each gametangium is that the two auxospores develop on the '-' gametangium. However, a 'trans-type' life cycle has been reported for raphid diatoms. In this case, one active and one passive gamete are produced within each gametangium and the migration of the active gametes occurs in opposite directions, so that one auxospore develops within each gametangium (Chepurnov *et al.* 2004). The conjugation modality observed in *Fragilariopsis kerguelensis* occurs between one '+' and

one ‘-’ gamete in a criss-crossed fashion, so that each gametangium bears one auxospore. This conjugation modality has been reported for other raphid diatoms such as *Petronopsis* (Jones *et al.* 2005).

In raphid diatoms, the degeneration of the meiotic nuclei has been reported to occur in the gametes – as in *P. multistriata* (this study) and *P. pungens* (Chepurnov *et al.* 2005)- or in the zygote. This is the case of the phylogenetically closely related raphid diatom *Fragilariopsis kerguelensis* (see Appendix I). In this latter species – the only *Fragilariopsis* for which some information on the life cycle is available – the gametes keep the two haploid nuclei produced during Meiosis II, the auxospore is quadrinucleate and the degeneration of two out of the four nuclei occurs in the early-stage auxospore. This pattern has been observed in other raphid diatoms, such as *Seminavis robusta* (Chepurnov *et al.* 2002) *Navicula sensu stricto* (Mann and Stickle 1989) and in *Pinnularia cf. gibba* (Poulickova *et al.* 2007).

In raphid diatoms, homotallic reproduction has been reported in some species. In *Navicula cryptocephala* only one gamete per gametangium is produced and cytokinesis does not occur after Meiosis I (Poulickova and Mann 2006). In *Amphora* sp. unequal cytokinesis follows Meiosis II and a polar body is produced and subsequently aborts (Sabbe *et al.* 2004b).

It was not possible to clearly detect the number of chloroplast present in the gametes of *P. multistriata*; however, when the auxospores expanded it was possible to clearly recognize four chloroplasts. It could thus be reasonable to assume that each gamete contains two chloroplasts. Two chloroplasts per gamete were reported for *P. delicatissima* (Levialdi Ghiron *et al.* 2008) and *P. pungens* (Chepurnov *et al.* 2005). Vegetative cells of raphid pennate diatoms could contain one, two or four plastids (Round *et al.* 1990 5742); they can produce one or two gametes per gametangium with one or two chloroplast each, depending from the species (Amato *et al.* 2005, Mann and Stickle 1989, Mann 1993,

Poulickova and Mann 2006). The number of chloroplasts in the gametes thus depends on the number of chloroplasts in the vegetative cell, on the number of gametes formed per gametangium and on whether or not chloroplast division occurs before cytokinesis of Meiosis I (Amato *et al.* 2005, Chepurnov *et al.* 2004, Levialdi Ghiron *et al.* 2008). This means that, in species that produce two gametes per gametangium with the same number of chloroplast as in vegetative cells, chloroplast division generally takes place during Meiosis I (Mann 1993, Poulickova and Mann 2006). This should be the case for *P. multistriata*.

2.4.3 The auxospore

After the bi-nucleate auxospore of *P. multistriata* completed expansion, karyogamy took place before the synthesis of the valves of the initial cell. The auxospore contained four chloroplasts as reported for other *Pseudo-nitzschia* species such as *P. australis* (Holtermann *et al.* 2010), *P. delicatissima* (Amato *et al.* 2005), *P. mannii* (Amato and Montresor 2008), *P. multiseriis* (Davidovich and Bates 1998), *P. pseudodelicatissima* (Davidovich and Bates 1998) and *P. pungens* (Chepurnov *et al.* 2005). The auxospore of *P. multistriata* is surrounded by a transverse perizonium consisting of thin transversal bands (D'Alelio *et al.* 2009a) and two caps – deriving from the rupture of the primary zygote wall – present at both ends of the auxospore.

2.4.4 The initial cells

I could not follow the nuclear divisions that accompany the deposition of the two valves of the initial cell. The general pattern reported for many pennate diatoms is that the two thecae of the initial cell are subsequently synthesized after acytokinetic mitosis and the degradation of one of the two nuclei: this means that each nuclear division corresponds to the deposition of one valve (Drebes 1977, Round *et al.* 1990 5742). As reported for

P. delicatissima (Amato *et al.* 2005) and *P. pungens* (Chepurnov *et al.* 2005), I also observed that the first mitotic division can take place when the initial cell is still inside the perizonium or when it is outside it. The initial cell of *P. multistriata* contains one nucleus and four chloroplasts that will segregate into each daughter cell during the first mitotic division. In *P. delicatissima* the initial cell produced inside the auxospore seemed to contain only two chloroplasts, as in vegetative cells (Amato *et al.* 2005, Levialdi Ghiron *et al.* 2008). The authors could not determine whether two of the four chloroplasts degenerated or if they fused two by two, yielding the two chloroplasts located on each side of the nucleus (Amato *et al.* 2005).

2.4.5 Abnormal stages

Sometimes ‘abnormal’ zygotes and/or auxospores were observed in *P. multistriata*. During this study were found zygotes with 3 nuclei and one auxospore with 4 nuclei and 8 chloroplasts. Similar atypical stages during sexual reproduction were already reported for *P. pungens* (Chepurnov *et al.* 2005). In this species, triploid auxospores were found and the authors suggest that they probably derived from the conjugation of three gametes. In *P. pungens*, an expanding auxospore with only two plastids and a single nucleus was also found and it has been hypothesized that it has been presumably developed from a single unfertilized gamete (Chepurnov *et al.* 2005).

2.4.6 The size of initial cells

The size of initial cells is one of the ‘cardinal points’ of the life cycle of a diatom species and it is a species-specific character. In *P. arenysensis* (= *P. delicatissima* in Amato *et al.* 2005) their size varied between 78 and 94 μm ; in *P. multiseries* the initial cell length was 146 (± 8.9) μm and in *P. pseudodelicatissima* was 126.4 (± 5.5) μm (Davidovich and Bates 1998); in *P. mannii* the initial cells length varied between 120 and 130 μm (Amato and

Montresor 2008) and in *P. pungens* between 157.1 and 176.3 μm (Chepurnov *et al.* 2005). In the two auxosporulating events observed in the natural environment, the initial cell length varied between 140 and 170 μm for *P. australis* and between 155 and 185 μm for *P. pungens* (Holtermann *et al.* 2010); and between 75 and 92.5 μm for *P. cf. delicatissima* and between 110 and 113 μm for *P. cf. calliantha* (Sarno *et al.* 2010).

The size of initial cell length might determine the length of time between the 'origin' of the initial cell and the time at which the cohort of daughter cells reach the cardinal point for sexualisation and the cardinal point at which cells die. The larger the initial cell, the longer the time (i.e. the number of divisions) required to reach the two key-points of their life cycle. However, this relationship assumes that the cell size reduction rate, i.e. the cell size reduction at each cell division, along the life cycle of the different species is comparable.

The apical length of the initial cells of *Pseudo-nitzschia multistriata* reported by (D'Alelio *et al.* 2009a), where the data were gained from 40 measurements without information on the cell size of the parental strains, was between 72 and 82 μm . In this study, a broader size range of initial cells, between 67 and 90 μm , was recorded. Data were obtained from a total of 180 measurements of initial cells obtained from crosses involving 9 pairs of parental strains covering the size range for sexualisation in this species (from 18.3 ± 4.2 to 48.4 ± 6.0 μm in cell length). The average values were comparable between the two studies – 76.8 ± 2.4 (D'Alelio *et al.* 2009a) and 77.2 ± 4.5 in this study – but I have recorded both smaller and longer initial cells. The range of initial cell length as related to the cell size of the parental strains shows a wide range of variation within and between species (Edlund and Bixby 2001). Auxospore expansion, and thus the size of initial cells, is probably influenced by numerous factors such as the size of gametangia, genetic differences between strains, and environmental factors (reported in Edlund and Bixby 2001). In the present study, a significant correlation was not found between the length of initial cells and the average length of parental strains. The average and median values were

very similar and only the initial cells derived from a couple of small parental strains produced smaller initial cells. The size of initial cells produced by the same couple but at different times of their 'life', i.e. at different cell size, was very similar.

In other diatom species - such as the heterothallic planktonic raphids *Haslea subagnita*, *Nitzschia lanceolata*, *Nitzschia longissima* and *Striatella unipunctata* (Davidovich 1994) - a positive correlation between the length of initial cells and the length of gametangia was observed. In the centric diatom *Coscinodiscus wailesii*, the diameter of initial cell formed by large parental cells was significantly higher as compared to the one formed by small parental cells (Nagai *et al.* 1995). A significant positive correlation between the size of gametangia and that of initial cells was found in several other centric and pennate diatoms such as *Aulacoseira spp*, *Cocconeis placentula*, *Gomphonema parvulum*, *Melosira moniliformis*, *Skeletonema costatum* (reported in Edlund and Bixby 2001). In four species of centric diatoms (*Chaetoceros didymus*, *Ditylum brightwellii*, *Melosira borreri* and *Skeletonema costatum*) it was instead reported that the diameter of the initial cells varies considerably and the range of variation increases with the decrease of the initial cell diameter (Gross 1937). Still in other species, the length of initial cells was independent from the length of the parental cells and no significant relationship was observed; this is the case of e.g. *Coscinodiscus granii* (Schmid 1995) and *Thalassiosira weissflogii* (Armbrust and Chisholm 1992).

2.4.7 Factors modulating the success of sexual reproduction

The success of sexual reproduction can be estimated as the number of successfully developed initial cells produced by a certain population. No quantitative estimates of sexual stage production was carried out during observations in time lapse and confocal microscopy, however, some aspects of the results obtained are worth discussion.

In the observations carried out in time-lapse microscopy, a number of rounded protoplasts were observed free in the culture medium during the second day of observation; nuclear stains were not used and it was, therefore, not possible to determine with certainty if they were fully formed gametes (they should be uninucleate) or zygotes (they should be bi-nucleate). Nevertheless, due to the fact that conjugation was observed in the second day, we can assume that these rounded protoplasts were mostly gametes. These naked protoplasts often had bacteria attached that caused their implosion and death. Sexual reproduction is thus the 'Achille's heel' in the life cycle of diatoms. In fact, these microalgae are always protected by their siliceous frustule that surrounds the cell also during vegetative division. Gametes are instead the least protected stages in the life cycle of *P. multistriata* and pennate diatoms in general and can be prone to attack by algicidal bacteria. The auxospore is also not surrounded by the silica frustule; however, the perizonial bands contain some silica (Amato *et al.* 2005) and it might provide a more valuable protection to this stage as compared to the simple organic membrane that surrounds the gametes. It would be interesting to determine which are the bacteria present in cultures of *P. multistriata* and test if the capability to attack gametes is a prerequisite of some or of all bacteria present in culture. It will also be interesting to test the presence and abundance of these bacteria in the natural environment. A massive attack of gametes might in fact impair sexual reproduction success and the formation of large cells in a population.

Another critical phase in the life cycle of diatoms is the successful development of the auxospore into an initial cell. The observation carried out in time-lapse microscopy showed that both gametogenesis and auxospore development can take place under repeated flashes of the microscope light during the dark phase of the photocycle. It can be thus postulated that a dark phase is not strictly necessary for the development of these stages. The development of auxospores in *Nitzschia lanceolata* has been studied in cultures placed in the dark after mixing compatible parental strains. Auxospores were able to develop and

produce initial cells, although only auxospores that reached a critical length ($> 100 \mu\text{m}$) were able to form the initial valve (Davidovich 1994, Davidovich 1998). The author concluded that the elongation of the auxospores and their development into initial cells depends on the reserve material present in the parental cells/gametes.

As discussed above, there is no clear relationship between the cell size of parental strains and that of initial cells in *P. multistriata*. Moreover, a considerable variability has been detected amongst different diatom species. Other factors than the size of parental strains might influence the size of initial cells. The effect of total daily irradiance and salinity on the size of initial cells formed by *Coscinodiscus wailesii* has been studied and a positive correlation between the diameters of initial cells and the total daily irradiance was recorded. The same relationship was recorded with salinity (Nagai and Imai 1997, Nagai and Imai 1999). Similar experiments have been carried out testing the effect of different photoperiod conditions and irradiance on the size of initial cells of the pennate diatoms *Haslea subagnita*, *Nitzschia lanceolata*, *Nitzschia longissima* and *Striatella unipunctata*; in this case, none of the tested conditions seemed to affect the length of initial cells (Davidovich 1994).

Future experiments might consider the following factors. First of all, it is important to relate the size of initial cells to the gametangia from which they originate. The cell size range of parental strains provides some information, but has a broad range of variability. Moreover, it is important to determine the cell size of initial cells at experimental conditions that include some nutrient limitation. The point raised by (Davidovich 1994), that the expansion of the auxospore and the successful development of the initial cell can depend on the physiological conditions of the parental strains and gametes is very plausible. The deposition of the valves of the initial cells requires silica, and the concentration of this element is thus critical. The expansion of the auxospore also requires

the synthesis of organic material, from the synthesis of perizonial bands, to the elongation of chloroplasts and possible synthesis of other cytoplasmic organelles.

2.4.8 Mating experiments

In the paper by (D'Alelio *et al.* 2009a), sexual reproduction in *P. multistriata* was observed in strains with an average cell size range spanning from 39% to 71% to the maximum size, i.e. from 39 to 55 μm of average cell apical length. In this study a broader window for sexualization was detected; in fact, strains with an average cell size spanning from 15 to 55 μm in apical length were capable of undergoing sexual reproduction. In the smallest parental strains, gametangia as small as 6 μm in length were observed, therefore, suggesting that the lowest cardinal point for sexualisation in *P. multistriata* might coincide with the minimum cell size compatible with life.

The cell size threshold for sexualization is not universal and seems to be species-specific. In some species, e.g. *P. delicatissima* (20–90% of the maximum size, Amato *et al.* 2005); *P. multiseriata* (23–70% of the maximum size, Hiltz *et al.* 2000) and *P. pungens* (20–60% Chepurnov *et al.* 2005) this range is wide. In a field study, the upper size thresholds for sexual induction were 62% and 75% of the maximum cell size for *P. pungens* and *P. australis*, respectively (Holtermann *et al.* 2010). A narrower size range of gametangia (10–31 μm corresponding to about 11–34% of the initial cell size) was instead reported for the phylogenetically closely related raphid diatom *Fragilariopsis kerguelensis* from observations carried out on natural populations (Assmy *et al.* 2006). A total of 233 strains collected in the Gulf of Naples over 3 years were crossed to assess their mating type. Surprisingly in 2008 almost all the isolated strains belonged to '+' mating type, while in the other years there was a better balance between mating types. So far no studies have explored the attribution of mating type on such a high number of strains. It has been suggested that at least 7 strains should be used when testing the mating system in

heterothallic diatoms; this assumes that in nature the ratio between mating types should be roughly 50:50 (Chepurnov *et al.* 2002). However, there are cases in which crosses amongst many more strains did not provide any successful sexual event. This is the case for one genotype of *P. delicatissima* (*P. delicatissima* clade 2 = *P. delicatissima sensu stricto* in Amato *et al.* 2007) where 25 genetically homogeneous strains were tested at different experimental conditions for a total of 723 crosses. The same negative result was obtained with the same species by (Quijano-Scheggia *et al.* 2009b). It might be that also in these cases a marked unbalance of mating type could have been present in the Gulf of Naples and along the Catalan coast, from which strains have been isolated. A balanced ratio of mating types is crucial to allow sexual reproduction to occur and thus permit the persistence of the population. It was not possible to assign the mating type to small number of strains because they did not undergo sexual reproduction with both '+' and '-' strains. Only for some of these strains cell size was available and they were within the size range for sexualization. In 2009 most of the strains have been crossed only with one reference strain; the mating type attribution is thus only 'orientative'.

Most of the 233 strains of *P. multistriata* used for the mating experiments were genotyped with microsatellites to investigate if a single or multiple populations were present within this species in the Gulf of Naples (Tesson, Montresor, Kooistra and Procaccini in preparation; Tesson 2010). Three genetically different populations were recorded; one dominated the bloom in 2008, and the other two were mostly present in 2009 and 2010. Genetic differences between the three populations were not high and a series of 'hybrid' genotypes were recorded, suggesting that gene flow was still occurring amongst the 3 populations. The results of the crosses could be used to further support this point and confirm that sexual reproduction was still occurring between the populations and that a viable F1 progeny could be obtained. In Table 2.8 the assignment to the different populations has been listed. The strains used for the crosses in all three years represent a

subset of the population tested with the microsatellite markers. As expected, the majority of the strains used for the 2008 crosses and genotyped belonged to population 1. In 2009, the majority of genotyped strains belonged to the ‘hybrid’ group, which was sexually compatible with both strains of population 2 and 3. The highest number of tested combinations was possible in 2010 where the reproductive compatibility was tested also between strains of population 2 and 3, between hybrid strains and population 2 and 3, and at least between one strain of population 1 and one of population 3 (Table 2.9).

Table 2.8. Attribution of the microsatellite populations (pop1, pop2, pop3 and hybrid; n.a. = data not available) and the mating type (‘+’ and ‘-’ strains; n.a. = not assigned) to the strains tested in the different years (See Table 2.1 for the details on isolation dates and cell size).

Year 2008 (102 strains)					
Strain code	Mating type	Population	Strain code	Mating type	Population
Sy014	+	n.a.	Sy176	+	n.a.
Sy016	+	n.a.	Sy177	-	n.a.
Sy017	-	n.a.	Sy178	+	n.a.
Sy019	+	n.a.	Sy180	+	n.a.
Sy020	+	n.a.	Sy182	+	pop1
Sy021	+	n.a.	Sy183	+	pop1
Sy023	+	n.a.	Sy184	+	hybrid
Sy025	+	n.a.	Sy185	+	pop1
Sy027	+	pop1	Sy186	+	pop1
Sy033	+	n.a.	Sy187	+	n.a.
Sy036	+	n.a.	Sy191	n.a.	n.a.
Sy039	+	hybrid	Sy196	+	hybrid
Sy040	+	pop1	Sy200	n.a.	pop1
Sy043	+	pop3	Sy203	+	pop1
Sy044	+	pop1	Sy206	+	pop1
Sy046	+	hybrid	Sy207	+	pop1
Sy047	+	pop1	Sy211	+	n.a.
Sy050	+	pop1	Sy217	+	pop1
Sy055	+	n.a.	Sy218	+	pop1
Sy058	+	pop1	Sy219	+	pop1
Sy070	+	n.a.	Sy222	+	n.a.
Sy084	+	n.a.	Sy234	+	n.a.

Sy087	+	pop1	Sy236	+	n.a.
Sy089	+	n.a.	Sy238	+	pop1
Sy093	+	n.a.	Sy239	+	pop1
Sy096	+	n.a.	Sy241	+	pop1
Sy097	+	pop1	Sy243	+	hybrid
Sy098	+	pop1	Sy244	+	pop1
Syl103	+	pop1	Sy246	+	pop1
Syl114	+	pop1	Sy248	+	pop1
Syl117	+	pop1	Sy250	+	pop3
Syl131	+	pop1	Sy252	+	hybrid
Syl134	+	pop1	Sy254	+	pop1
Syl138	+	pop2	Sy256	+	pop1
Syl145	+	pop1	Sy278	+	hybrid
Syl146	+	pop1	Sy279	+	pop1
Syl147	+	pop1	Sy281	+	pop1
Syl149	+	n.a.	Sy284	+	n.a.
Syl151	+	n.a.	Sy290	+	pop1
Syl152	+	pop1	Sy297	+	pop1
Syl156	+	pop1	Sy299	+	hybrid
Syl157	+	pop1	Sy301	+	Hybrid
Syl164	n.a.	n.a.	Sy302	+	pop1
Syl165	+	n.a.	Sy303	+	n.a.
Syl166	n.a.	n.a.	Sy304	n.a.	hybrid
Syl168	+	pop1	Sy305	+	pop1
Syl171	+	pop3	Sy306	+	pop1
Syl172	+	pop1	Sy307	+	pop1
Syl173	+	pop1	Sy308	+	pop1
Syl174	+	pop1	Sy309	+	pop3
Syl175	+	n.a.	Sy310	+	n.a.
Year 2009 (65 strains)					
Sy319	+	hybrid	Sy373	+	hybrid
Sy321	-	hybrid	Sy375	+	hybrid
Sy323	-	n.a.	Sy376	+?	n.a.
Sy324	-	hybrid	Sy377	-?	n.a.
Sy326	+?	pop3	Sy378	-	pop3
Sy327	-	pop3	Sy379	-	pop3
Sy329	+?	pop3	Sy380	-	hybrid
Sy330	-	pop3	Sy382	+	hybrid
Sy331	+?	pop3	Sy383	-	hybrid
Sy334	+	hybrid	Sy384	-	pop2

Sy336	+	pop3	Sy385	-	hybrid
Sy338	-?	pop3	Sy386	-	hybrid
Sy340	+	n.a.	Sy387	-	n.a.
Sy344	+?	hybrid	Sy388	+?	pop3
Sy345	+?	n.a.	Sy389	+	hybrid
Sy346	-	hybrid	Sy391	+?	pop2
Sy347	-	pop2	Sy392	+?	pop3
Sy348	-	pop3	Sy394	-	pop2
Sy349	-	hybrid	Sy395	+?	pop2
Sy350	+?	hybrid	Sy397	+	hybrid
Sy351	-	n.a.	Sy399	-	pop2
Sy353	+?	pop3	Sy400	-	pop2
Sy355	-	pop2	Sy401	-	pop3
Sy357	+?	pop3	Sy402	-	pop2
Sy358	+?	pop3	Sy403	-	pop2
Sy359	-	hybrid	Sy404	+	n.a.
Sy361	-	hybrid	Sy405	+	hybrid
Sy363	+?	n.a.	Sy406	+	hybrid
Sy365	+?	pop2	Sy407	+	hybrid
Sy366	+?	pop3	Sy408	-?	pop2
Sy368	+?	hybrid	Sy409	-?	n.a.
Sy369	+	pop3	Sy445	-	pop2
Sy370	-	n.a.			
Year 2010 (66 strains)					
Sy602	-	hybrid	Sy723	-	n.a.
Sy608	-	hybrid	Sy724	+	pop2
Sy627	+	pop3	Sy727	+	pop2
Sy644	-	pop3	Sy731	-	pop2
Sy653	-	pop2	Sy735	-	pop2
Sy659	-	pop3	Sy736	+	hybrid
Sy664	+	hybrid	Sy738	+	n.a.
Sy665	-	hybrid	Sy741	+	hybrid
Sy667	-	hybrid	Sy745	-	n.a.
Sy668	+	hybrid	Sy748	+	hybrid
Sy676	-	hybrid	Sy770	-	n.a.
Sy679	-	pop2	Sy772	-	n.a.
Sy680	-	hybrid	Sy774	+	n.a.
Sy681	+	n.a.	Sy776	-	n.a.
Sy683	-	n.a.	Sy777	+	pop3
Sy684	+	n.a.	Sy778	-	n.a.

Sy685	-	hybrid	Sy779	+	pop2
Sy686	-	n.a.	Sy781	-	n.a.
Sy691	-	hybrid	Sy782	+	n.a.
Sy692	n.a.	pop3	Sy783	-	n.a.
Sy696	-	n.a.	Sy785	-	pop3
Sy697	+	hybrid	Sy789	-	n.a.
Sy698	+	pop2	Sy791	-	n.a.
Sy701	+	hybrid	Sy792	+	pop2
Sy707	+	n.a.	Sy793	+	pop3
Sy710	+	pop1	Sy794	n.a.	pop3
Sy713	n.a.	hybrid	Sy795	-	pop3
Sy714	-	hybrid	Sy796	-	n.a.
Sy717	-	pop2	Sy797	n.a.	pop3
Sy718	+	n.a.	Sy799	-	pop2
Sy719	-	n.a.	Sy800	-	pop3
Sy720	-	n.a.	Sy801	+	n.a.
Sy722	-	pop3	Sy806	+	n.a.

Table 2.9. For each year, it is reported the number of successful crosses between strains belonging to the 3 populations (pop1, pop2 and pop3) and for the ‘hybrid’ strains.

	2008				2009				2010			
	pop1	pop2	pop3	hybrid	pop1	pop2	pop3	hybrid	pop1	pop2	pop3	hybrid
pop1												
pop2										5		
pop3									1	12	10	
hybrid						17	8	3		13	22	15

Chapter 3

Parental cell density and growth phase as factors influencing the occurrence and success of sexual reproduction in *Pseudo-nitzschia multistriata*.

3.1 Introduction

An overview of the experimental work that has been carried out to detect the factors that induce sexual reproduction in diatoms has been presented in Chapter 1. Different diatom species seem to respond to different environmental cues and it is difficult to extract general rules on the conditions that trigger the onset of the sexual phase. External factors seem to play a more important role in modulating the sexual cycle of homothallic centric diatoms, while in pennate diatoms the mixing of two sexually compatible strains seems, at times, to be sufficient (Chepurnov *et al.* 2004). Nevertheless, light, both as irradiance and photoperiod, can influence the success of sexual reproduction in pennate diatoms; as an example, long day length increased the fertilization success in *Pseudo-nitzschia multiseries* (Hiltz *et al.* 2000). However, an opposite result was obtained for two other pennate diatoms, *Haslea ostrearia* and *Cocconeis scutellum*, where the highest success of sexual reproduction was observed at low irradiance and short photoperiod (Mizuno and Okuda 1985, Mouget *et al.* 2009).

In most publications dealing with the description of the sexual phase of pennate diatoms it is often stated ‘successful mating was obtained by mixing exponentially growing clonal cultures, of the appropriate cell size, in fresh medium’ (Amato *et al.* 2005, Amato *et al.* 2007, Amato and Montresor 2008, Chepurnov *et al.* 2005, D’Alelio *et al.* 2009a, D’Alelio *et al.* 2009b, Davidovich and Bates 1998, Quijano-Scheggia *et al.* 2009a, Quijano-Scheggia *et al.* 2009b, Gordon 2001). No auxosporulation was apparently observed in *Pseudo-nitzschia multiseries* and *P. pseudodelicatissima* when mixing parental strains that had reached the stationary growth phase (Davidovich and Bates 1998); however experimental data were not provided. The requirement for optimal growth conditions for sexual reproduction has been reported also for centric diatoms. In *Ditylum brightwellii* and *Chaetoceros didymus* sexual reproduction could be induced by diluting

cultures with new fresh medium (reported in Steele 1965). Koester *et al.* (2007) found that sexual reproduction in *Ditylum brightwellii* occurred in nutrient-repleted cultures, while this species underwent vegetative enlargement and resting stage production in stationary phase cultures.

In some eukaryote lineages, the induction of the sexual phase is related to stress conditions. In the unicellular, haploid, green microalga *Chlamydomonas reinhardtii* nitrogen starvation coupled with a blue light stimulus induces the differentiation of vegetative cells into gametes that conjugate and form into a zygote that transforms into a resting spore capable of withstanding adverse conditions (reported in Huang and Beck 2003). A stress condition, provided by a marked increase of temperature, induces the sexual phase in the haploid multicellular green alga *Volvox carteri* that includes the differentiation of gametes, which, upon fertilization, form a desiccation-resistant spore (Nedelcu and Michod 2003). Nutrient starvation also induces the differentiation of gametes in dinoflagellates and, in several species, the planozygote produced by gamete conjugation transforms into a resting cyst (Montresor and Lewis 2006). The alternation between the haplontic and diplontic phase in Prymnesiophyceae implies the conjugation of haploid cells, but nothing is known about the mechanisms and the factors that induce this life cycle transition (Montresor and Lewis 2006). The mechanism for sexual induction in the diploid diatoms seems to be completely different from the cases mentioned above: in diatoms sex is apparently induced in conditions that are optimal for growth. The only exception reported so far is *Leptocylindrus danicus* where sexual reproduction occurs when following nitrogen starvation (French III and Hargraves 1985).

The aim of the experiments reported in the present study was to investigate the link between the growth phase of the parental strains and the timing and success of sexual reproduction in the heterothallic pennate planktonic diatom *Pseudo-nitzschia multistriata*. There is some evidence that suggests that the growth phase of the parental strains plays a

role in the success of sexual reproduction but no detailed experimental studies have been carried out to test the extent to which this factor might be important. Another question addressed in the present study is to test for the presence of a threshold cell concentration for sexual reproduction. Sexual reproduction includes the differentiation of vegetative cells into gametes, which have to 'find each other' to allow conjugation to occur (see Chapter 2). The gametes of pennate diatoms do not have flagella and cannot swim towards the gametes of opposite mating type. It is, therefore, reasonable to hypothesize that sexual reproduction requires a threshold cell concentration to occur, either to favour the random encounter of cells of the opposite mating type or to favour the perception of chemical signals that induce gamete formation (e.g. Sato *et al.* 2011). The specific questions addressed in this chapter were: i) Does sexual reproduction only occur when crossing strains in their exponential growth phase, or can sex be induced also when crossing strains in late- or post-exponential growth phase? ii) What is the percentage of sexual stages produced, i.e. the success of sexual reproduction, when strains at different growth phases, and, therefore, at different cell concentrations, are mixed? iii) Do parental strains have to reach a threshold cell concentration before sex can be induced? Does a decrease in irradiance increase the success of sexual reproduction?

3.2 Material and Methods

3.2.1 Culture isolation and maintenance

Single cells or short chains of *Pseudo-nitzschia multistriata* were isolated with a micropipette from net samples collected at the Long-Term Ecological Research station Mare Chiara (LTER-MC) in the Gulf of Naples (Table 3.1). The cultures were established and maintained as illustrated in Chapter 2. When the cultures were established and before carrying out each experiment, 20 cells for each strain were measured at 400x magnification using a Zeiss Axiophot light microscope (Carl Zeiss, Oberkochen, Germany) equipped with an ocular micrometer.

Table 3.1. Strains of *Pseudo-nitzschia multistriata* used for the experiments illustrated in this chapter. For each strain are reported: the strain code and the mating type, the isolation date, the LTER-MC sample code, the average length of the apical axis at the moment in which the cultures were established (I), and the average length (\pm standard deviation) of the apical axis at the moment in which the experiments were carried out (II).

Experiment	Strain code	Isolation date	LTER-MC	Apical axis (μ m) I	Apical axis (μ m) II
Exp. 1	Sy373 (+)	07/07/2009	869	45	39.3 \pm 1.4
Exp. 1	Sy379 (-)	07/07/2009	869	50	44.0 \pm 2.7
Exp. 2	Sy373 (+)	07/07/2009	869	45	35.0 \pm 1.6
Exp. 2	Sy379 (-)	07/07/2009	869	50	39.0 \pm 2.0

3.2.2 Calculation of growth rate

Cell concentration was estimated on a sub-sample fixed with formaldehyde solution at a final concentration of 1.6 %. A 1-ml aliquot was used to fill a Sedgewick Rafter counting slide and cells were enumerated at the Zeiss Axiophot light microscope. Growth rate was expressed as divisions \cdot day⁻¹ and was estimated from a semi-log plot of successive counts (cells \cdot ml⁻¹) over time. This method permits a ready identification of the period of

exponential growth. A straight line was drawn to identify the slope of the portion of the graph representing the exponential growth. A least-squares regression was applied to the log (base10) data (K_{10}). A logarithmic transformation from log base10 to log base2, by multiplying $K_{10} \cdot 3.322$, was used to obtain the number of divisions·day⁻¹ (Guillard 1980).

3.2.3 *Growth rates of parental cultures in different culture vessels*

This preliminary experiment was planned to test if the maximum growth rate of parental strains grown in culture vessels of different volume, and sampled over time with a different strategy, were comparable. To test this question, a series of culture wells (6-wells culture plates, each with 8 ml volume, filled with 4 ml of culture) were used and the content of two wells was fixed at regular time intervals to estimate cell concentration; for the second set up, 250 ml polystyrene culture flask (filled with 150 ml of culture) were subsampled at regular time intervals to estimate cell concentration. Two stock flasks, one for each parental strain (Sy373 '+' mating type and Sy379 '-' mating type) containing 200 ml of f/2 filtered medium, were inoculated with an exponentially growing culture to reach a final concentration of about 300 cells·ml⁻¹. For each parental strain, 4 ml aliquots were dispensed into each well of two 6-wells culture plates and a 150 ml aliquot was dispensed into a single 250 ml flask. For each parental strain, the flask and the two plates were placed in a growth chamber at a temperature of 18°C, a photoperiod of 12L:12D h, and an irradiance of 110 $\mu\text{mol photons m}^{-2}\text{s}^{-1}$.

Every two days, and for a period of 10 days, 4 ml of culture for each strain grown in flasks were sub-sampled in duplicate and placed in Eppendorf vials. At the same time, the culture material of 2 wells for each parental strain was placed in Eppendorf vials. In this way, duplicate samples were collected at each time point for both experimental conditions. All subsamples were fixed with formaldehyde solution at a final concentration of 1.6 % and stored in the fridge at 4 °C. One ml of each sample was counted using a

Sedgewick Rafter counting slide on a ZEISS Axiophot light microscope. The growth curve was plotted for strains grown in the two types of culture vessels and the growth rate was estimated as illustrated in paragraph 3.2.2.

3.2.4 Sexual reproduction in crosses carried out with parental strains at different cell densities and growth phase (Experiment #1)

Parental strains Sy373 ('+' mating type) and Sy379 ('-' mating type) have been used for this experiment. Two flasks, one for each parental strain, containing 700 ml of f/2 filtered medium, were inoculated with cells at a final concentration of about 300 cells·ml⁻¹ and allowed to grow at a temperature of 18 °C, a photoperiod of 12L:12D h (light:dark) and an irradiance of 110 $\mu\text{mol photon m}^{-2}\text{s}^{-1}$. Cell concentration of the two parental strains was estimated every two days and crosses were carried out on day 0 (T0), 2 (T2), 4 (T4), 5 (T5), 6 (T6), 7 (T7) and 8 (T8).

At each time point, 50 ml of culture for each parental strain were mixed in a flask and aliquots of 4 ml were dispensed, after careful mixing, in four 6-wells culture plates (Fig. 3.1a). Plates were incubated in a growth chamber at a temperature of 18 °C and a photoperiod of 12L:12D h (light:dark); two plates were placed at an irradiance of 60 $\mu\text{mol photon m}^{-2}\text{s}^{-1}$ and the other two at a higher irradiance of 110 $\mu\text{mol photon m}^{-2}\text{s}^{-1}$ (the same irradiance at which parental strains were grown). The culture plates were inspected every day with an inverted microscope to check for the presence of gametes. Starting from the day at which gametes were first observed, and for 4 consecutive days, the content of 3 wells was fixed to estimate the time course of the formation of sexual stages. The culture material of the 3 wells was placed in 3 Eppendorf vials and fixed with formaldehyde solution at a final concentration of 1.6 %. One ml of fixed culture was placed in a Sedgewick Rafter counting slide and vegetative cells, gametes or zygotes (the two stages cannot be always differentiated in light microscopy without using a nuclear stain, see

Chapter 2, or when the stages get detached from the gametangia), auxospores, initial cells (still surrounded by the perizonium), and F1 generation cells (long vegetative cells) were enumerated (Fig 3.2).

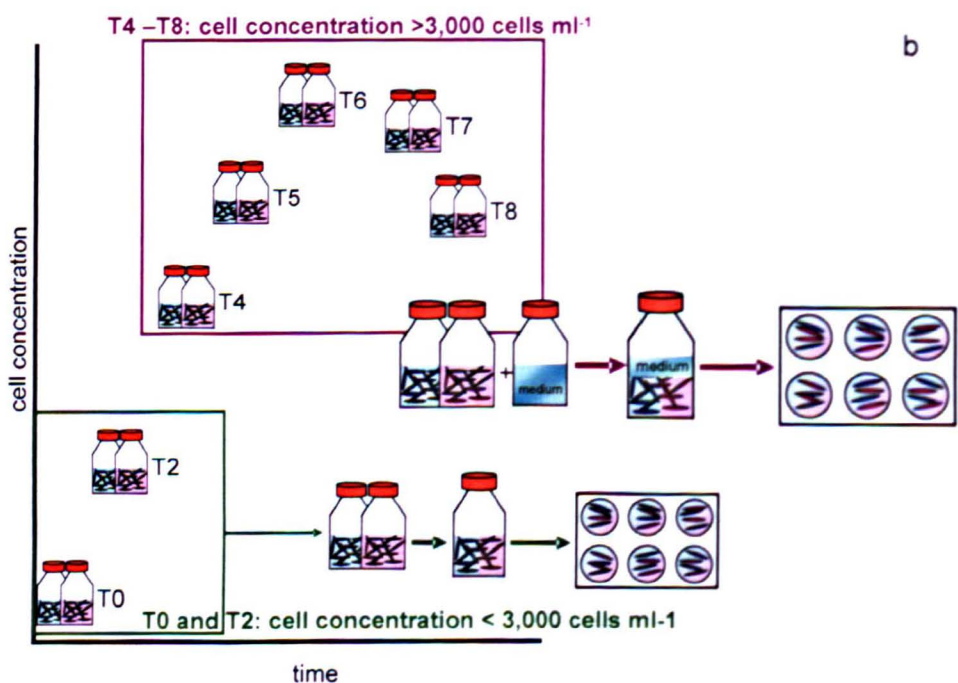
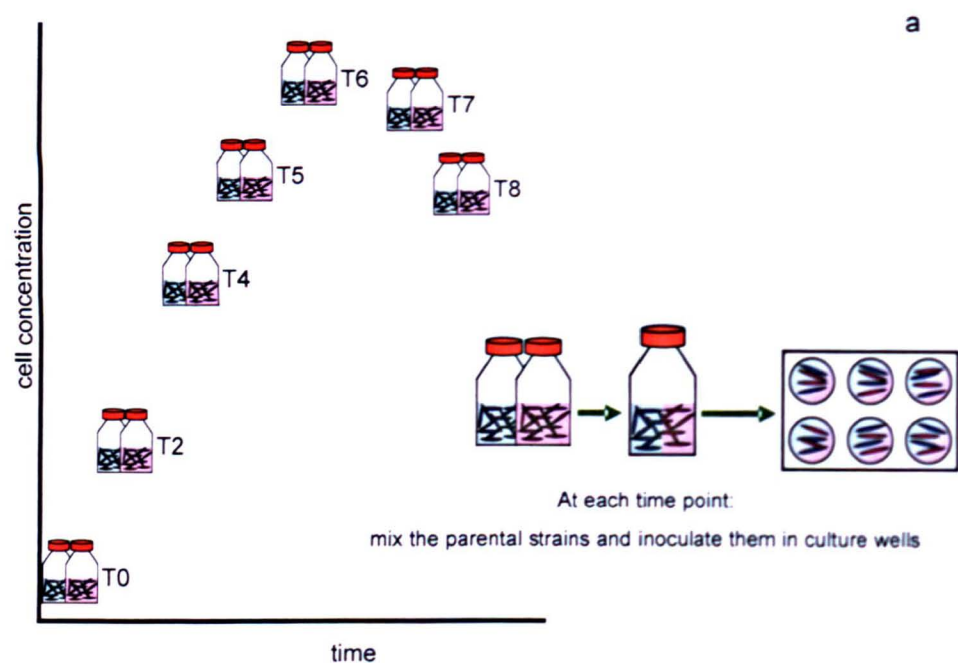


Figure 3.1. Schematic drawings of the experimental set up of Experiment #1 (a) and #2 (b). See the text for explanation.

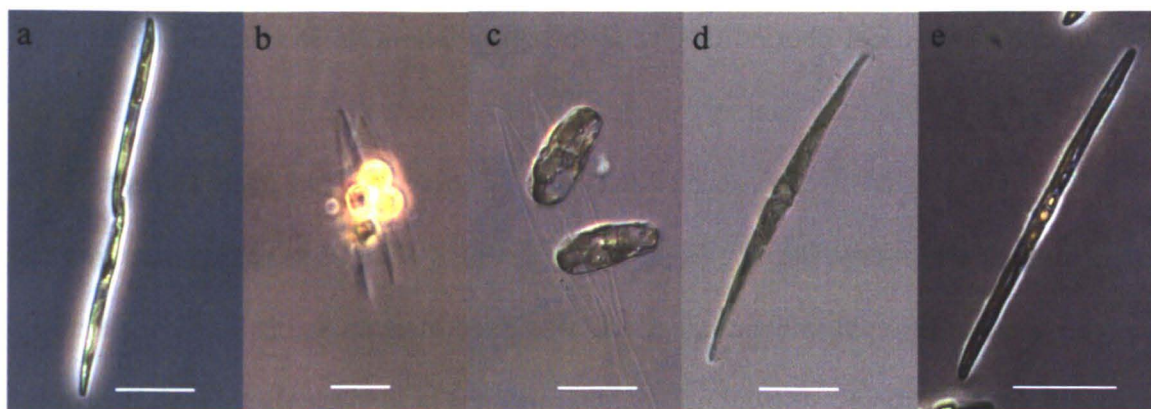


Figure 3.2. The different life stages that were enumerated in the experiments: (a) vegetative cells, (b) gametes or zygotes, (c) auxospores, (d) initial cells and (e) large F1 generation cells. Bright field (a, b and e) and differential interference contrast (DIC; c and e) micrographs; scale bars = 20 μm .

3.2.5 Sexual reproduction in crosses carried out with parental strains from different growth phases, but diluted at the same cell concentration (Experiment #2)

Two flasks, one for each parental strain, were prepared and grown at the same conditions as in Experiment #1. Crosses were carried out at day 0 (T0), 2 (T2), 4 (T4), 5 (T5), 6 (T6), 7 (T7) and 8 (T8). Crosses were started with cell concentrations $\leq 1,500 \text{ cells}\cdot\text{ml}^{-1}$ for each parental strain. At T0 and T2 cell concentration of parental strains was lower than $3,000 \text{ cells}\cdot\text{ml}^{-1}$ and they were crossed without diluting them. At both time points, 50 ml of each parental strain were mixed in a flask and 4 ml were dispensed, after careful mixing, in four 6-wells culture plates (Fig. 3.1b). From T4 onwards, cell concentration of parental strains was higher than $3,000 \text{ cells}\cdot\text{ml}^{-1}$. Cell concentration of parental strains was estimated by placing 1 ml of fixed (with formaldehyde solution at a final concentration of 1.6 %) culture, in a Sedgewick Rafter counting slide. The required amounts of each parental strain needed to reach a final concentration of $1,500 \text{ cell}\cdot\text{ml}^{-1}$ were calculated, they were placed in flasks filled with 100 ml of f/2 filtered medium, and 4 ml were dispensed in four 6-wells culture plates (24 wells for each cross). Plates were incubated in a growth chamber at a temperature of 18 °C, a photoperiod of 12L:12D h (light:dark); two plates were placed at

an irradiance of $60 \mu\text{mol photon m}^{-2}\text{s}^{-1}$ and the other two at an irradiance of $110 \mu\text{mol photon m}^{-2}\text{s}^{-1}$.

The culture plates were inspected every day with an inverted microscope to check for the presence of zygotes. Starting from the day at which gametes were first observed and for 4 consecutive days, the content of 3 wells was fixed to estimate the time course of the formation of sexual stages. The culture material of the 3 wells was placed in 3 Eppendorf vials and fixed with formaldehyde solution at a final concentration of 1.6 %. One ml of the fixed culture was placed in a Sedgewick Rafter counting slide and vegetative cells, gametes and zygotes (see 3.2.4), auxospores, initial cells and F1 generation (long vegetative cell escaped from the perizonium) were enumerated (Fig 3.2).

One of the results of these experiments was the arrest of growth induced by the start of the sexual phase. In order to allow the comparison between the temporal trend of cell concentration of parental strains and that of the co-cultures in which sex was observed, a growth curve of the parental strains at the irradiance of $60 \mu\text{mol photon m}^{-2}\text{s}^{-1}$ was needed. This growth curve was obtained immediately after the completion of the two experiments by growing monoclonal cultures of the parental strain Sy373 ('+' mating type) and Sy379 ('-' mating type) as described in paragraph 3.2.3, but flasks were incubated at 60 instead of $110 \mu\text{mol photon m}^{-2}\text{s}^{-1}$.

3.3 Results

3.3.1 *Growth rates in different culture vessels*

The two parental strains Sy373 '+' and Sy379 '-' reached the maximum cell concentration after 6 days from the inoculum in both culture vessels, i.e. culture flasks and multi-well tissue culture plates (Fig 3.3). The maximum cell concentration reached in flasks was between 169,300 and 195,700 cells·ml⁻¹ for '+' strain and 132,850 and 140,000 cells·ml⁻¹ for '-' strain. The maximum cell concentration reached in plates was between 256,250 and 341,600 cells·ml⁻¹ for '+' strain and 183,550 and 249,300 cells·ml⁻¹ for '-' strain. The maximum growth rate estimated in flasks was between 1.44 and 1.56 divisions·day⁻¹ for '+' strain and 1.51 divisions·day⁻¹ for '-' strain; and the maximum growth rate estimated in plates was between 1.55 and 1.70 division·day⁻¹ for '+' strain and between 1.57 and 1.66 divisions·day⁻¹ for '-' strain (Table 3.2). Growth rates were very similar between the two parental strains, as confirmed by Student t-test ($p > 0.9$). Also the differences between maximum growth rates measured in the two culture vessels were not significant ($p > 0.03$). Therefore, the two methods of estimating growth rates give similar results.

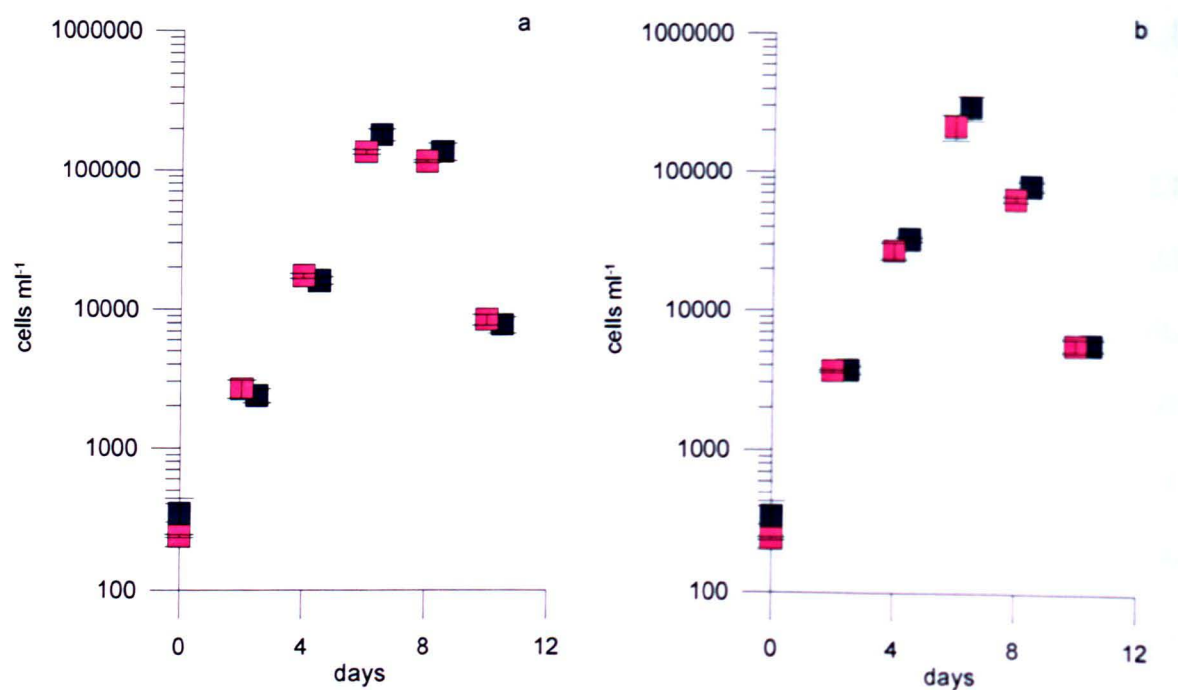


Figure 3.3. Growth curve of Sy373 '+' (blue) and Sy379 '-' (pink) parental strains grown in flasks (a) and in culture plates (b). Each point represents the average value of duplicate counts; maximum and minimum values are represented with vertical bars.

Table 3.2. Maximum cell density (cells·ml⁻¹) and maximum growth rate (divisions·day⁻¹) of the two parental strains grown in different vessels.

Vessels type	Sy373 '+'		Sy379 '-'	
	cell·ml ⁻¹	div·day ⁻¹	cell·ml ⁻¹	div·day ⁻¹
Flask	195,700	1.56	140,000	1.51
	169,300	1.44	132,850	1.51
Well	341,600	1.70	249,300	1.66
	256,250	1.55	183,550	1.57

3.3.2 Sexual reproduction in crosses carried out with parental strains at different cell density and growth phase (Experiment #1)

The maximum growth rates of the '+' and '-' parental strains were similar; however, differences were detected when comparing the values obtained at the two irradiance conditions of 60 and 110 μmol photons m⁻²s⁻¹. Sy373 '+' had an average maximum growth

rate of 0.93 and 1.56 divisions·day⁻¹ at 60 and 110 $\mu\text{mol photons m}^{-2}\text{s}^{-1}$, respectively, and Sy379 '-' had an average maximum growth rate of 0.98 and 1.70 divisions·day⁻¹ at 60 and 110 $\mu\text{mol photons m}^{-2}\text{s}^{-1}$, respectively. The two parental strains reached similar maximum cell concentrations when grown at the same irradiance and their maximum cell density was lower at low irradiance (Figs 3.4 and 3.5). The exponential phase of the growth curve for both mating types was comprised between day 0 and day 10 and between day 0 and day 6, for the low and high irradiances, respectively.

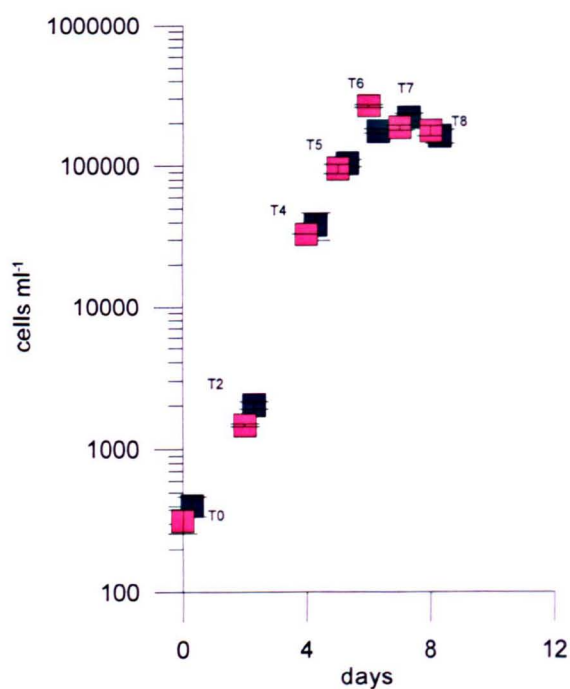


Figure 3.4. Growth curve of Sy373 '+' (blue) and Sy379 '-' (pink) parental strains grown in flasks at 110 $\mu\text{mol photons m}^{-2}\text{s}^{-1}$. Each point represents the average value of duplicate counts; maximum and minimum values are reported by the vertical bars (Experiment #1).

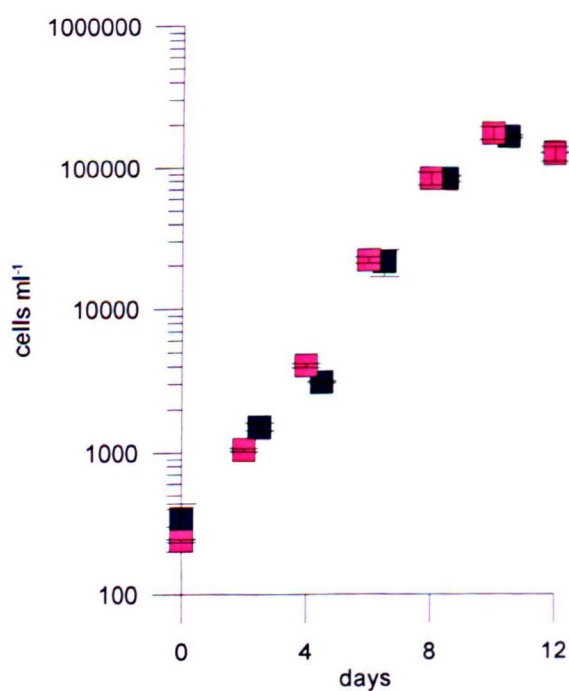
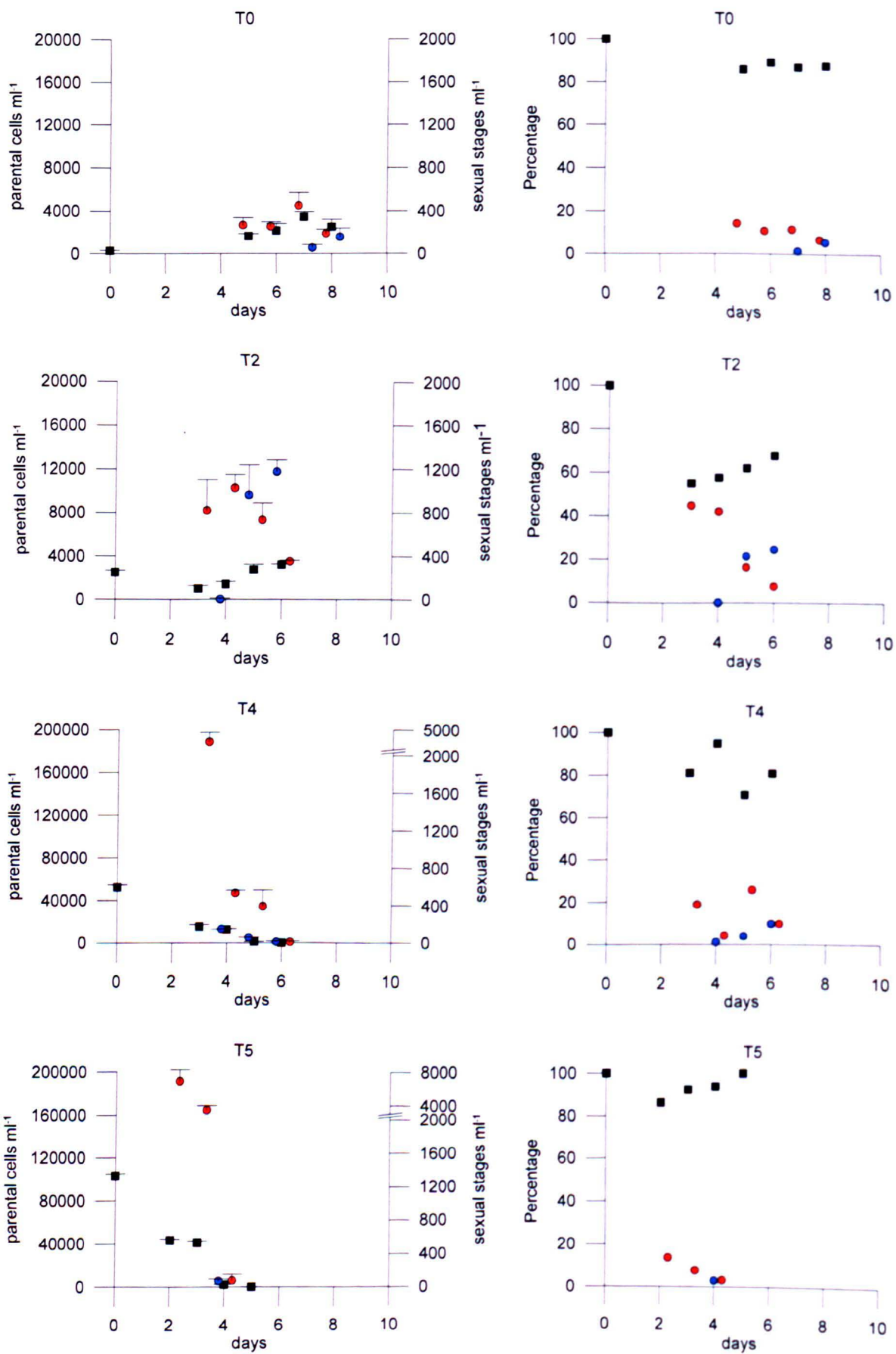


Figure 3.5. Growth curve of Sy373 '+' (blue) and Sy379 '-' (pink) parental strains grown in flasks at 60 $\mu\text{mol photons m}^{-2}\text{s}^{-1}$. Each point represents the average value of duplicate counts; maximum and minimum values are reported by the vertical bars.

Experiment #1 was aimed at testing the occurrence and success of sexual reproduction when crossing parental strains from different phases of the growth curve, thus differing in cell concentration, growth phase and, presumably, nutrient availability in the culture medium. Sexual reproduction occurred in all crosses carried out at both irradiances but with variable timing and success, depending on the time at which the co-culture of the two parental strains started and thus on their cell concentration (Figs 3.6 and 3.7). In all figures, the number of gametes, zygotes, auxospores and initial cells were pooled together, in order to avoid confusion due to the presence of many different symbols.

At $60 \mu\text{mol photons m}^{-2}\text{s}^{-1}$ and in the experiments in which parental strains from T0 (at low concentration) were mixed together, sexual stages were first recorded after 5 days from the inoculum (Figs 3.6 and 3.8a). The timing of appearance of sexual stages gradually decreased in the crosses carried out in the following days, which were started with progressively higher cell concentrations. In the crosses carried out on T5 and T6, sexual stages were in fact recorded on day 2 from the inoculum. The highest percentage of sexual stages over the total number of cells (about 40%, Fig. 3.6) in the co-cultures started on T2, and was reached when the average parental cell concentration was about $2,000 \text{ cells}\cdot\text{ml}^{-1}$. The percentage of sexual stages was also relatively high in experiment at T4 and T5, but this was due to the fact that the concentration of vegetative cells notably decreased after a couple of days from the inoculum. In experiments from T0 to T4 the number of sexual stages generally decreased after a couple of days from their appearance and large F1 cells started to appear. In the co-cultures started later (from T5 onwards) gametes were recorded after 2 days from the inoculum, but they did not develop into auxospores most probably due to nutrient limitation.



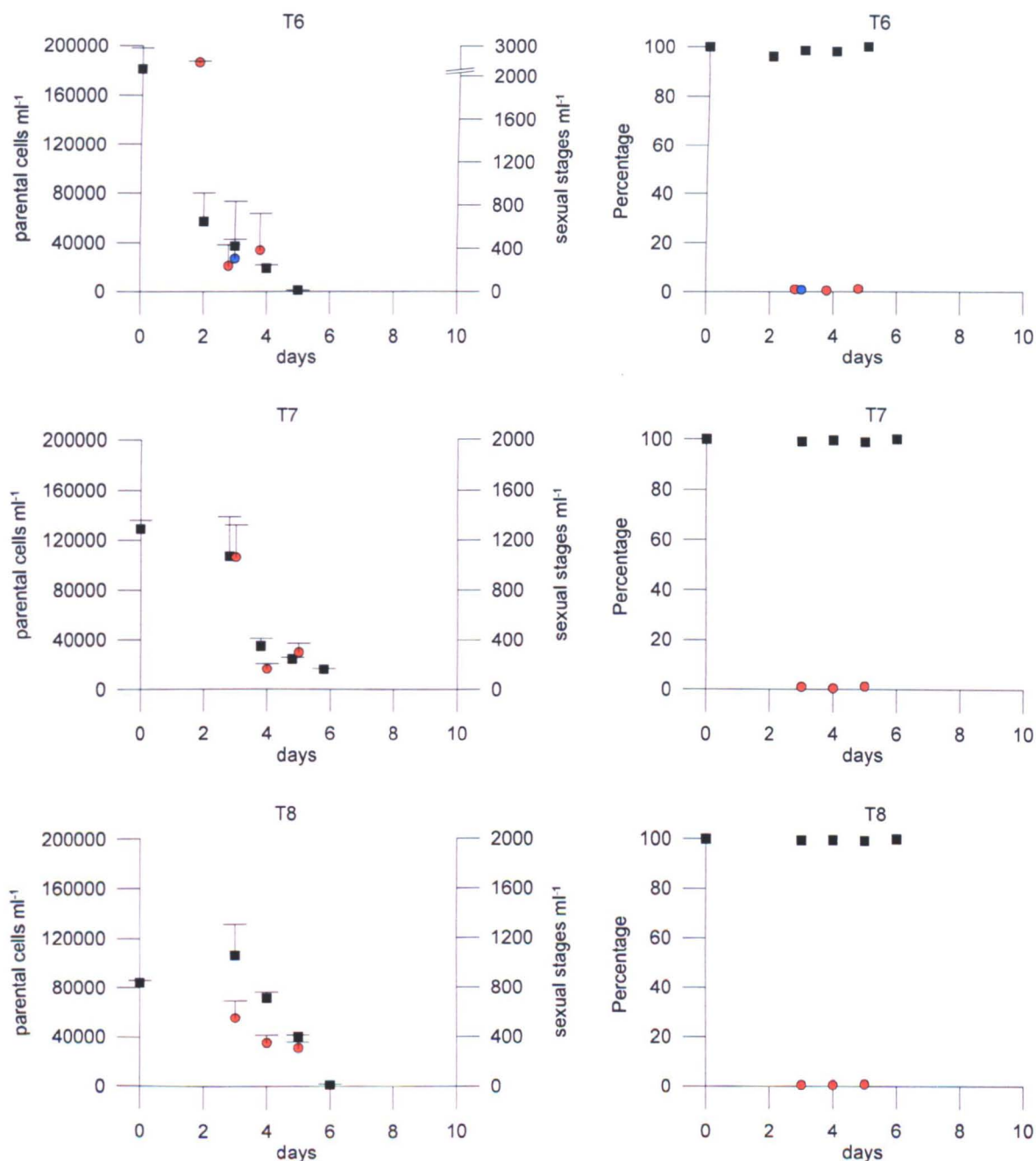
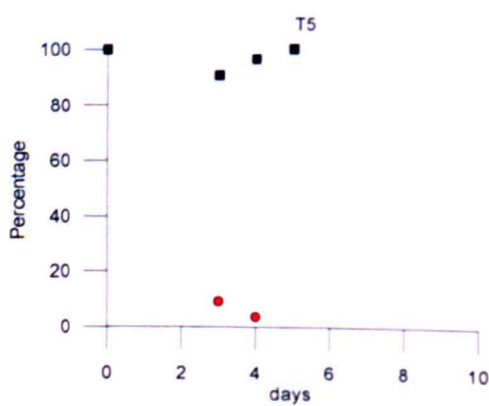
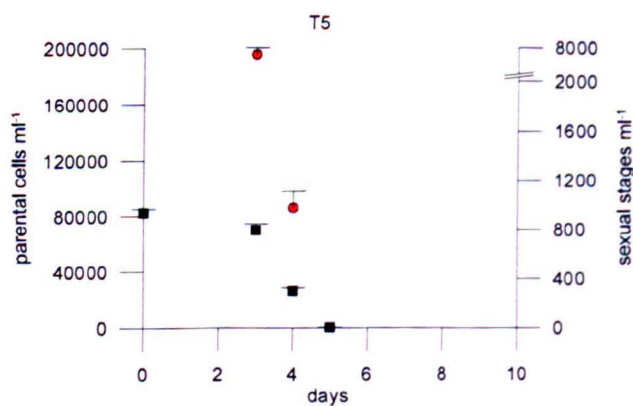
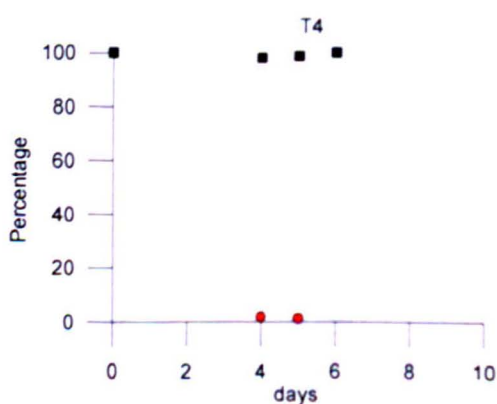
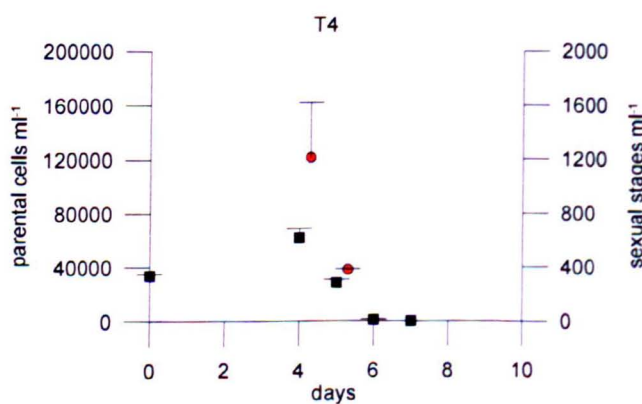
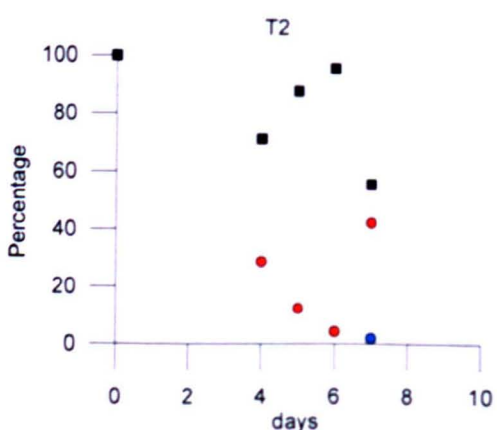
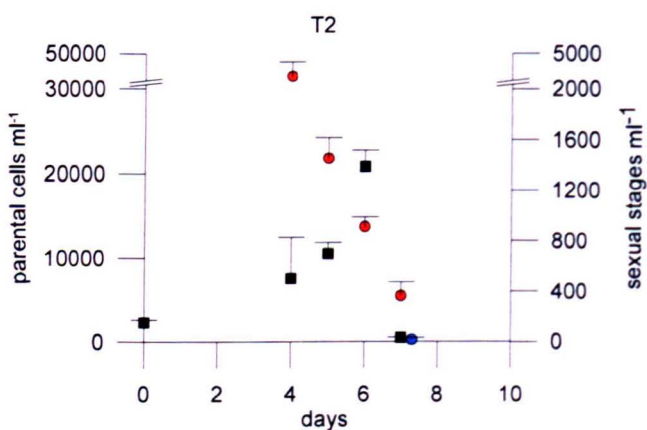
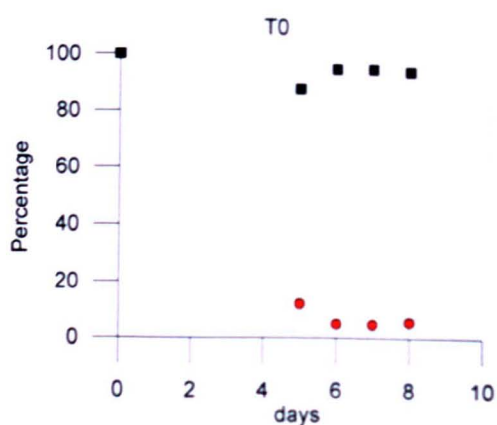
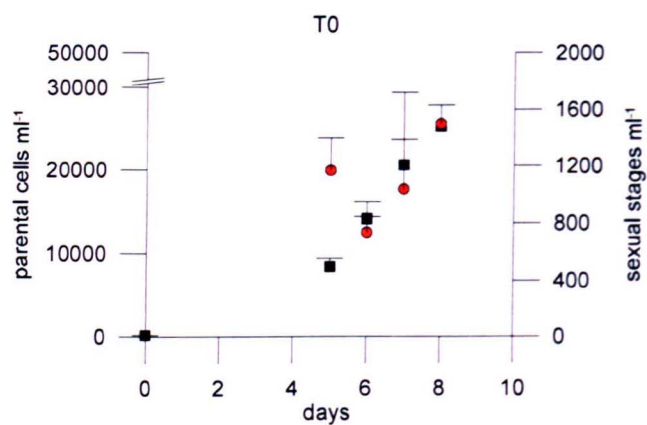


Figure 3.6. Variation of cell concentration ($\text{cells} \cdot \text{ml}^{-1}$, on the left panels) and average percentage values (on the right panels) of parental strains (black squares), sexual stages (gametes, zygotes, auxospores and initial cells: orange circles) and large F1 cells (light-blue circles) with time in Experiment #1 at $60 \mu\text{mol photons m}^{-2} \text{s}^{-1}$. Note the different scales on the y axes.



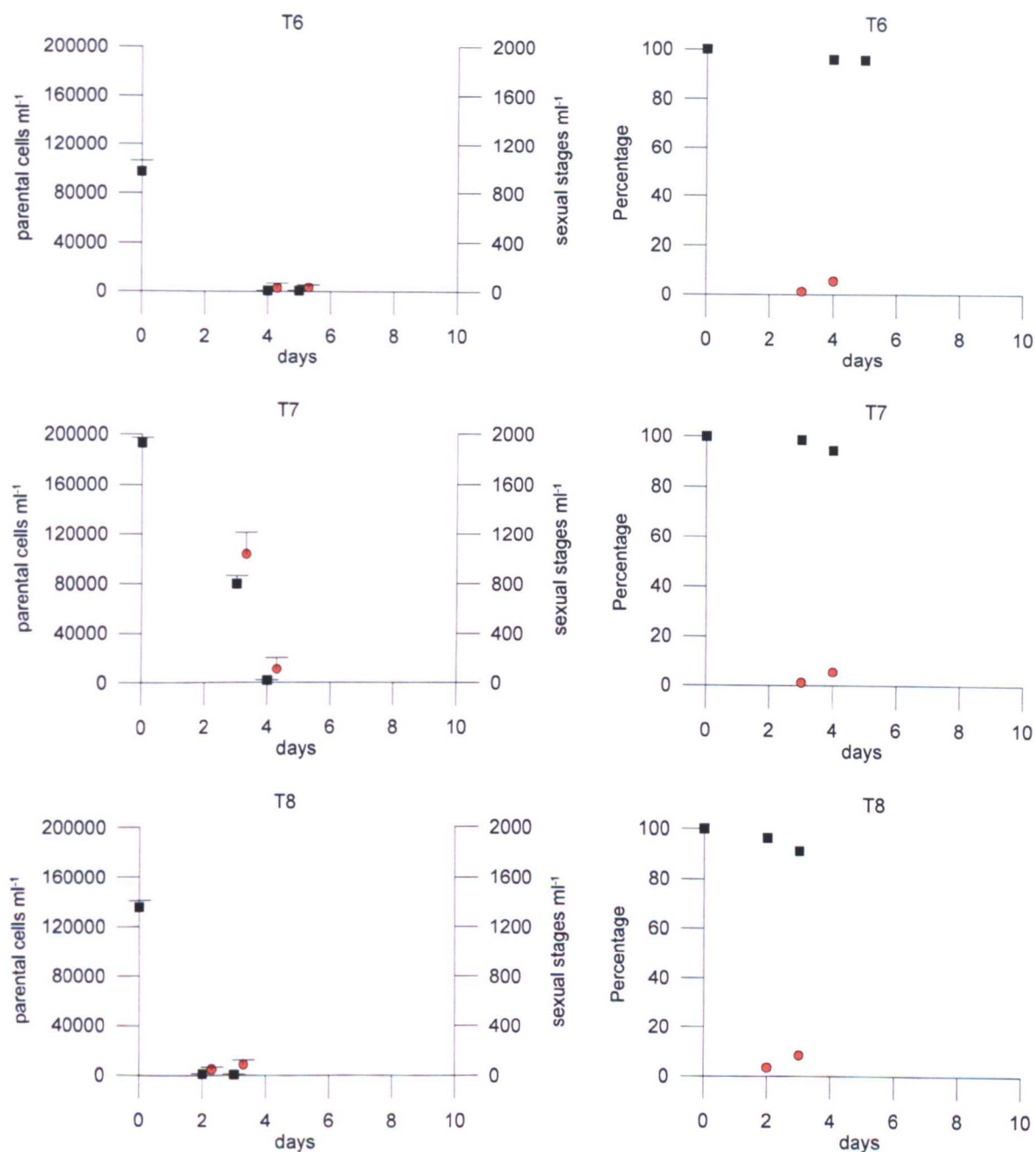


Figure 3.7. Variation of cell concentration (cells·ml⁻¹, on the left panels) and average percentage values (on the right panels) of parental strains (black squares), sexual stages (gametes, zygotes, auxospores and initial cells: orange circles) and large F1 cells (light-blue circles) with time in Experiment #1 at 110 $\mu\text{mol photons m}^{-2}\text{s}^{-1}$. Note the different scales on the y axes.

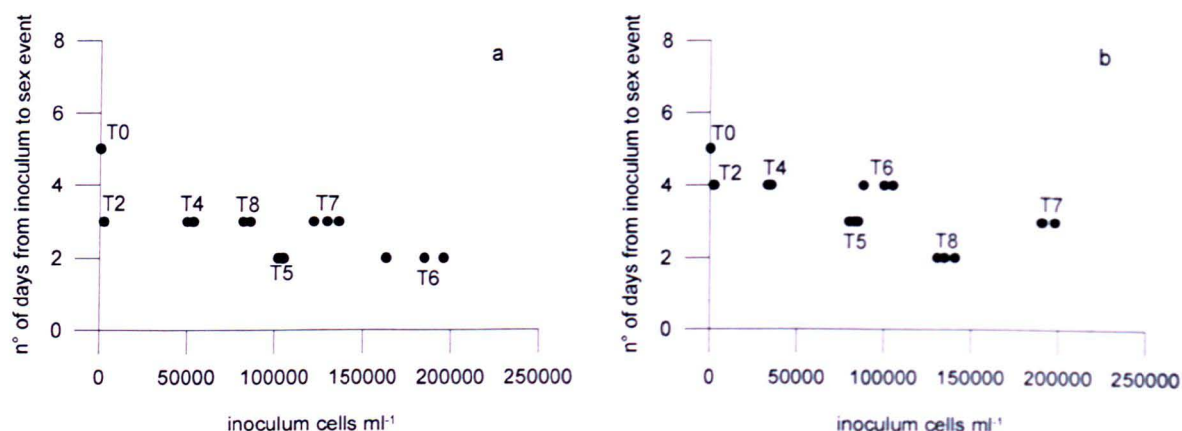


Figure 3.8. Time of appearance of the first sexual stages (gametes) as related to the inoculum size (cells·ml⁻¹ of the two parental strains). The points represent the different replicate for each cross, from T0 to T8, in Experiment #1 at low (a) and high (b) irradiances, respectively.

In the sister experiment carried out at slightly higher irradiance (110 $\mu\text{mol photons m}^{-2}\text{s}^{-1}$), the timing of production of sexual stages was similar (Figs 3.7 and 3.8b). In the experiments in which parental strains from T0 (at low concentration) were mixed together, sexual stages were first recorded after 5 days from the inoculum. The timing of appearance of sexual stages gradually decreased in the crosses carried out in the following days, which were started with progressively higher cell concentrations. In the co-cultures carried out on T2 and T4, sexual stages were recorded 4 days after the inoculum; while from T4 onwards, sexual stages were recorded on day 3 after the inoculum. The maximum percentage of sexual stages (28%) was recorded in co-cultures started on T2, when parental cell concentration was about 10,000 cells·ml⁻¹. In this experiment, the production of sexual stages decreased after a couple of days from their appearance, but in this case the formation of large F1 cells was only sporadically observed.

The decrease in concentration of vegetative cells observed in the co-cultures started from T5 onwards at both irradiances and was most probably due to nutrient exhaustion. This can be seen in the growth curves of parental strains, where the exponential phase ended after 6 or 10 days – depending on the irradiance - when cell concentration reached

about $200 \cdot 10^3 \text{ cells} \cdot \text{ml}^{-1}$. However, a markedly reduced growth rate was also observed in co-cultures started from T0 or T2, when the initial inoculum was lower. The difference between the growth curves of the mono-cultures of parental strains and those of the co-cultures in which sexual reproduction was occurring, can be appreciated when plotting the cell concentration data on the same graph (Fig. 3.9). From this graph, it is evident that co-cultures reach a cell concentration lower by 10 – 43%, as compared to the concentration of the strains grown in monoculture at the same time.

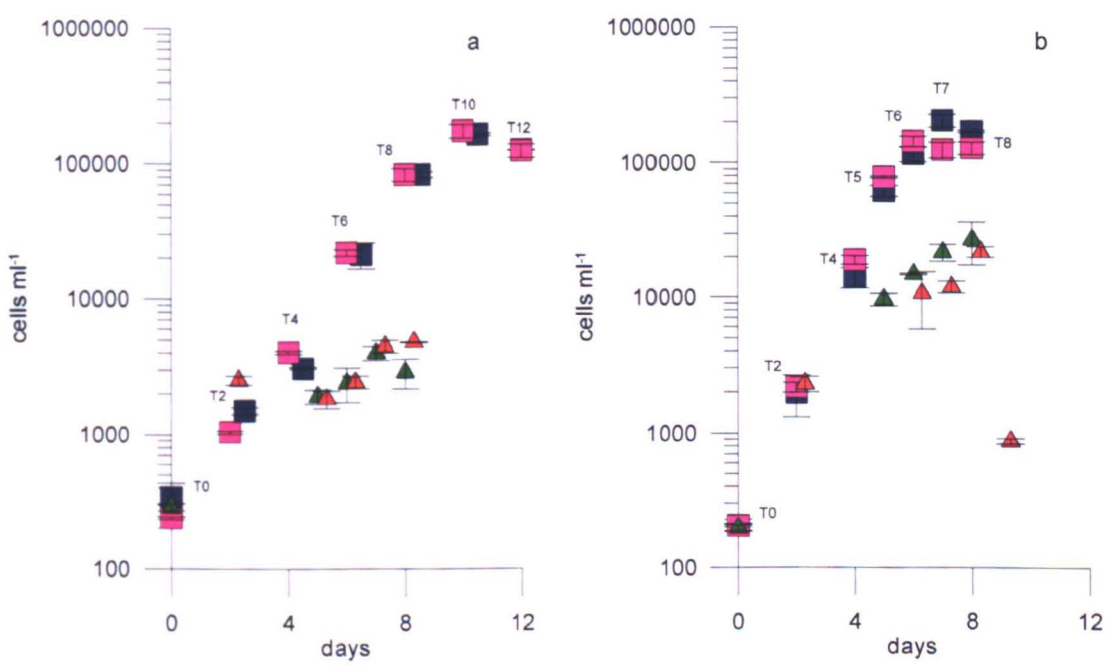


Figure 3.9. Time course of cell concentration for parental strain Sy373 '+' (blue), Sy379 '-' (pink), the total number of cells (parental vegetative cells, sexual stages, large F1 cells) in crosses carried out at T0 (green triangles) and T2 (red triangles) in Experiment #1. Panel (a) illustrates the results obtained at 60 and panel (b) at 110 $\mu\text{mol photons m}^{-2}\text{s}^{-1}$. Each co-culture was plotted at the time from which parental cells were sampled and mixed. Each point for the parental strains (squares) represents the average value of duplicate counts with maximum and minimum, each point for the crosses (triangles) represents the average of triplicate counts with standard deviation.

The results of Experiment #1 can be summarized in the following points:

- a) The formation of sexual stages occurred when co-culturing parental strains from all phases of their growth curve, i.e. exponential, post-exponential and senescent.
- b) The maximum success of sexual reproduction (28-44.8 % of sexual stages over the total number of cells) was obtained when co-culturing parental strains in the early-middle exponential growth phase, when their initial cell concentration was comprised between 2,000 and 10,000 cells·ml⁻¹.
- c) The number of sexual stages (mostly gametes) was very low in the crosses started with high cell concentrations of parental strains in their late exponential or post-exponential growth phase and gametes did not develop into auxospores.
- d) The time required to obtain the formation of the first sexual stages was longer when starting the crosses with low cell concentration of parental strains; the time progressively decreased when crosses were started with higher cell concentrations. .
- e) The growth of vegetative cells decreased in crosses undergoing the sexual phase.

3.3.3 Sexual reproduction in crosses carried out with parental strains from different growth phases, but diluted at the same cell concentration (Experiment#2)

The results of the previous experiment (Experiment #1) showed evidence that parental strains need to reach a threshold concentration before sexual reproduction starts and also showed that the 'optimal' cell concentration to gain a good percentage of sexual stages was comprised between 2,000 and 10,000 cells·ml⁻¹. Experiment #2 was aimed at i) repeating the crosses carried out with increasing initial cell concentration (from 300 to 2,000 cells·ml⁻¹, ie T0-T2) and ii) testing if the timing and success of sexual reproduction were comparable once the inocula of parental strains from T4 to T8 were diluted down to 3,000 cells·ml⁻¹ (1,500 cells·ml⁻¹ for each strain) with the addition of fresh medium. In this way, all crosses started with the same cell concentration – besides the first two – and were not

limited by nutrients. The expected result was that the dynamics and timing of appearance of the sexual stages should be comparable.

The maximum growth rates of the '+' and '-' parental strains were similar: Sy373 '+' had an average maximum growth rate of $1.52 \text{ divisions} \cdot \text{day}^{-1}$ and Sy379 '-' had an average maximum growth rate of $1.50 \text{ divisions} \cdot \text{day}^{-1}$. The two strains reached also similar maximum cells concentrations (Fig. 3.10).

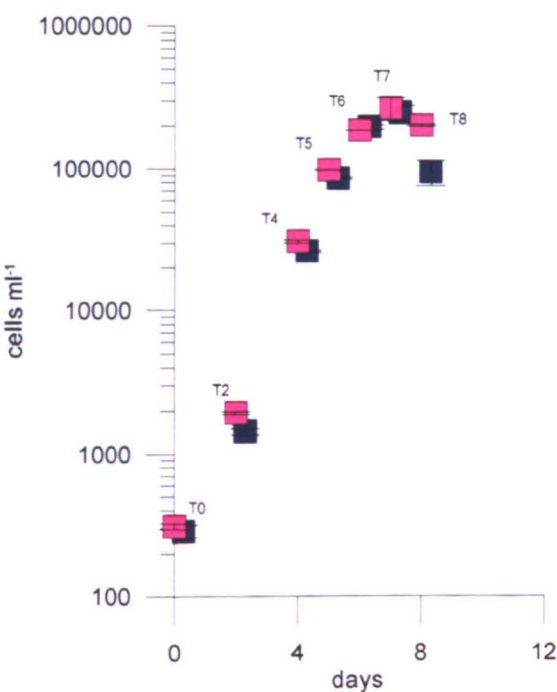
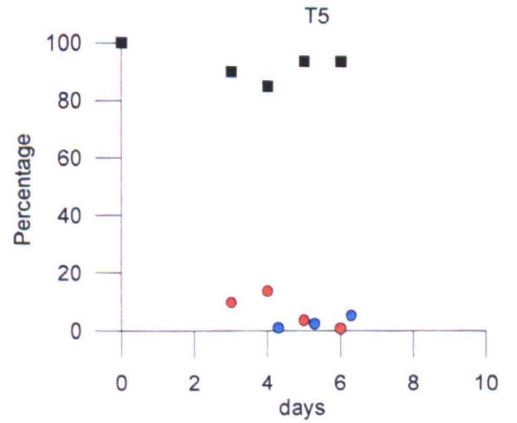
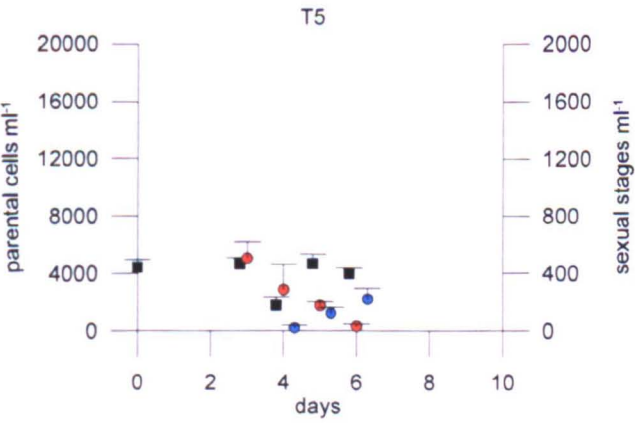
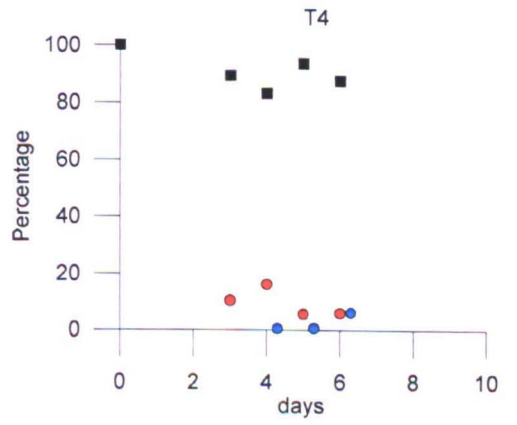
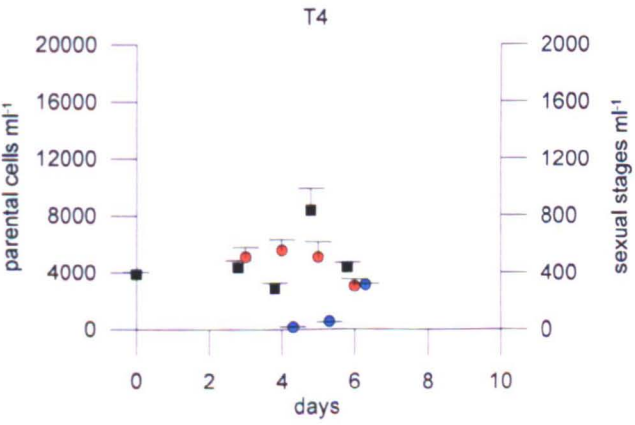
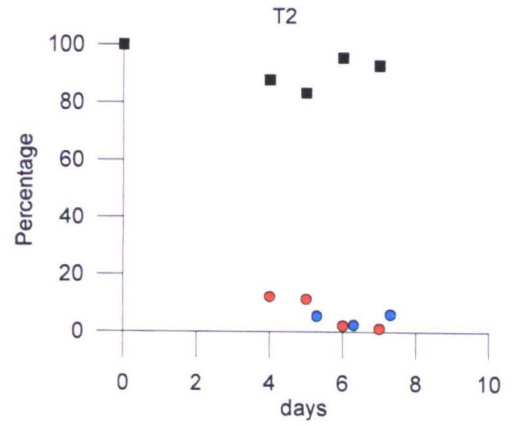
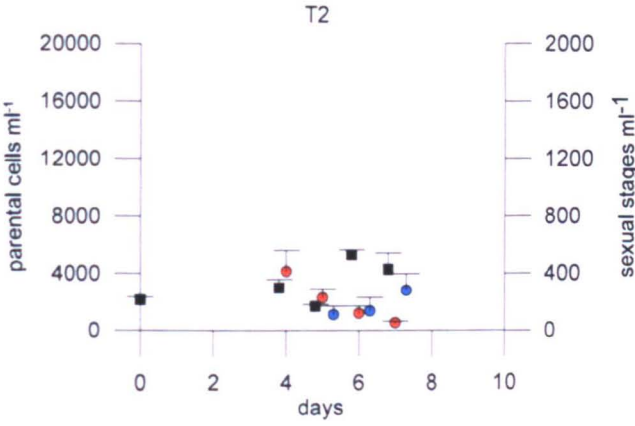
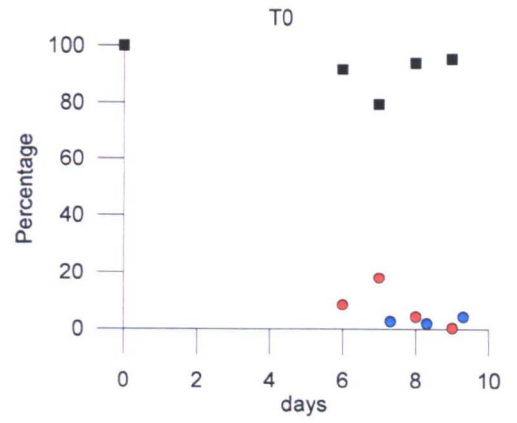
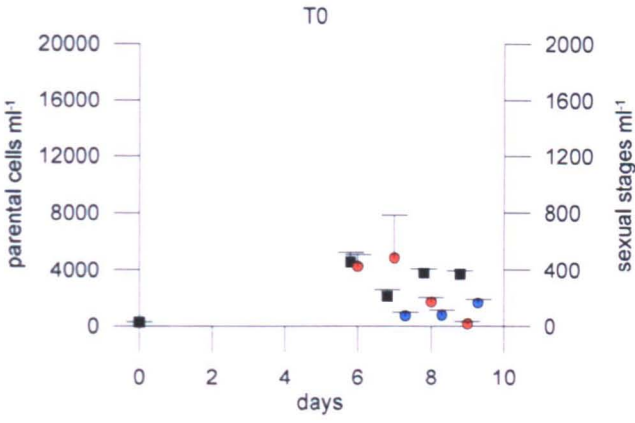


Figure 3.10. Growth curve of Sy373 '+' (blue) and Sy379 '-' (pink) parental strains grown in flasks at and $110 \mu\text{mol photons m}^{-2}\text{s}^{-1}$. Each point represents the average value of duplicate counts; maximum and minimum values are reported by the vertical bars (Experiment #2).

Sexual reproduction occurred in all crosses carried out at both irradiances but with variable timing, depending on the time at which the co-culture of the two parental strains started (Figs 3.11 and 3.12).

In all figures the number of gametes, zygotes, auxospores and initial cells were pooled together, as in Experiment #1. At $60 \mu\text{mol photon m}^{-2}\text{s}^{-1}$ and in the experiments in which parental strains from T0 (the lowest concentration) were mixed together, sexual

stages were first recorded after 6 days from the inoculum. In the crosses carried out on T2 (where average initial cell concentration was about $2,000 \text{ cells}\cdot\text{ml}^{-1}$) sexual stages were recorded on day 4 after the inoculum and in all the other crosses that were started with concentrations between $2,000$ and $4,500 \text{ cells}\cdot\text{ml}^{-1}$ sexual stages were recorded after 3 days from the inoculum (Figs 3.11, and 3.13a). The highest percentage of sexual stages, i.e. the percentage of gametes/zygotes + auxospores + initial cells over the total number of cells was similar (between 10 and 22%) within the different crosses. Sexual stages started to be recorded when the average parental cell concentration was comprised between $2,700$ and $6,000 \text{ cells}\cdot\text{ml}^{-1}$ (Fig. 3.11). In all the co-cultures the number of vegetative cells did not increase from the day in which gametes were first observed and for the four consecutive days of observation (Figs 3.11, 3.14a and 3.15a). The number of sexual stages generally decreased after a couple of days from their appearance and was followed by the appearance of large F1 initial cells. In all crosses gametes developed into auxospores and later into large F1 generation.



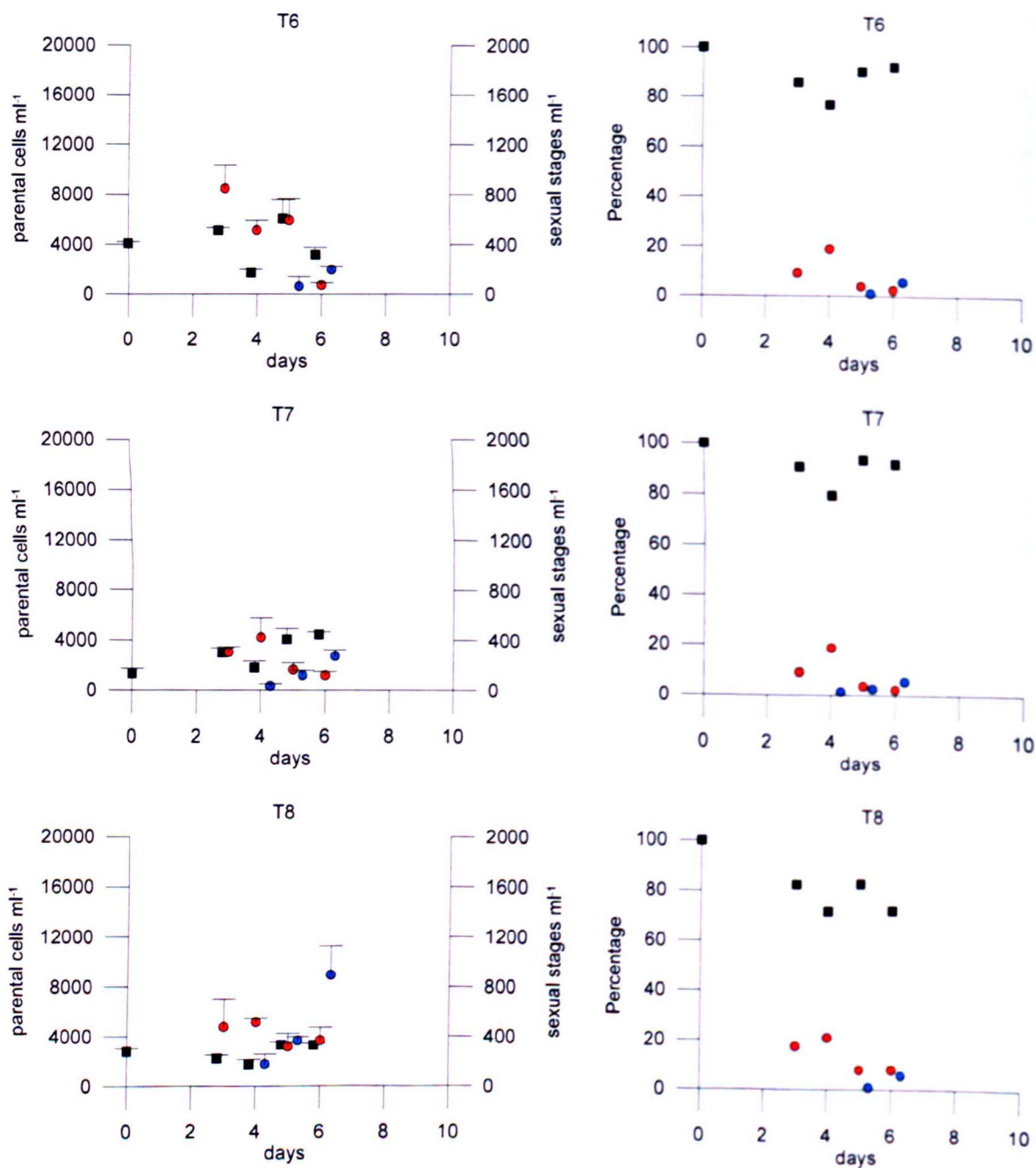
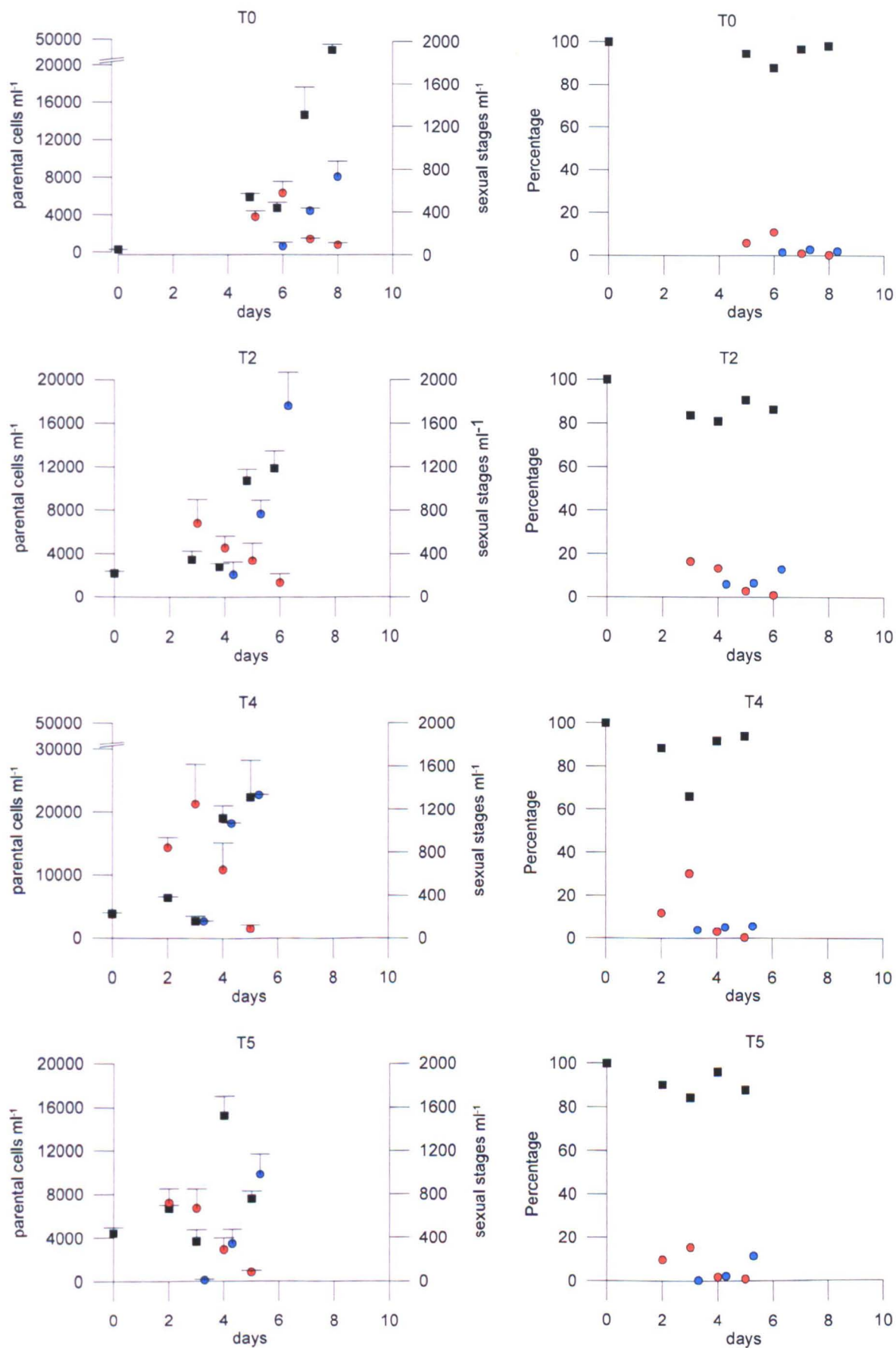


Figure 3.11. Variation of cell concentration (cells·ml⁻¹, on the left panels) and percentage values (on the right panels) of parental strains (black rectangles), sexual stages (gametes, zygotes, auxospores and initial cells: orange circles) and large F1 cells (light-blue circles) with time in Experiment #2 at 60 μmol photons m⁻²s⁻¹. Note the different scales on the y axes.



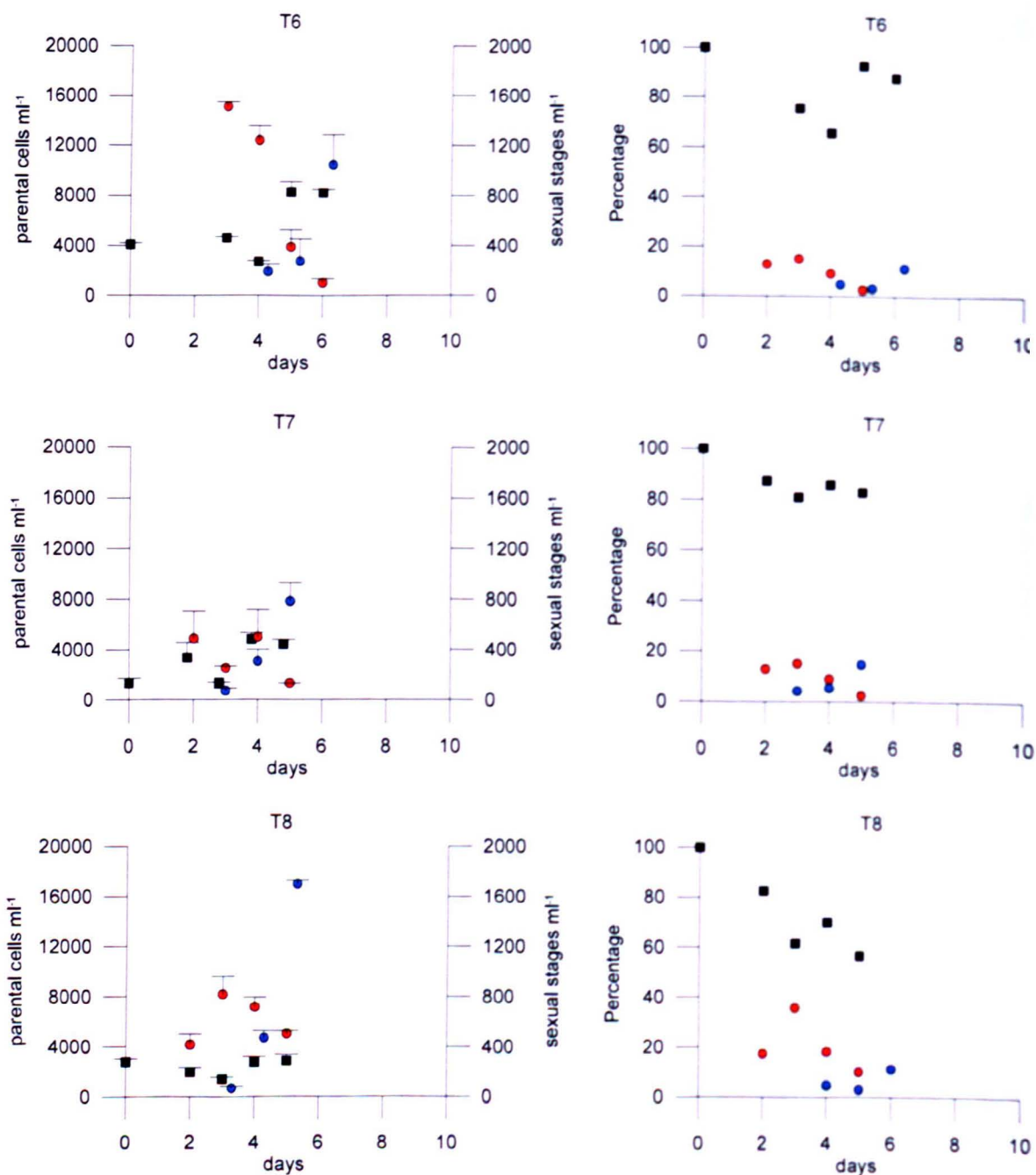


Figure 3.12. Variation of cell concentration (cells·ml⁻¹, on the left panels) and percentage values (on the right panels) of parental strains (black squares), sexual stages (gametes, zygotes, auxospores and initial cells: orange circles) and large F1 cells (light-blue circles) with time in Experiment #2 at 110 $\mu\text{mol photons m}^{-2}\text{s}^{-1}$. Note the different scales on the y axes.

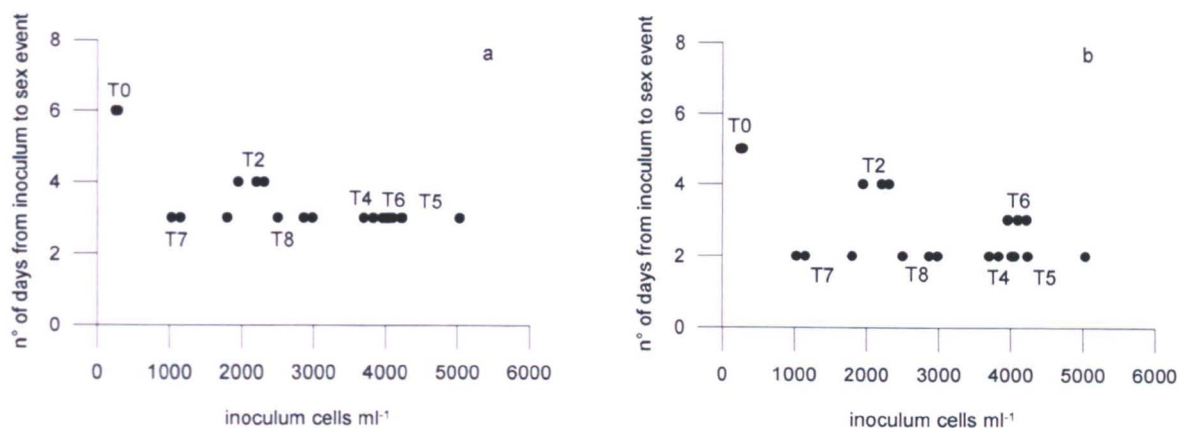


Figure 3.13. Day at which the formation of the first sexual stages (gametes) was observed plotted on the respective inoculum size (cells·ml⁻¹) of the two parental strains. The points represent the different triplicates for each cross, from T0 to T8, carried out in Experiment #2 at low (a) and high (b) irradiances.

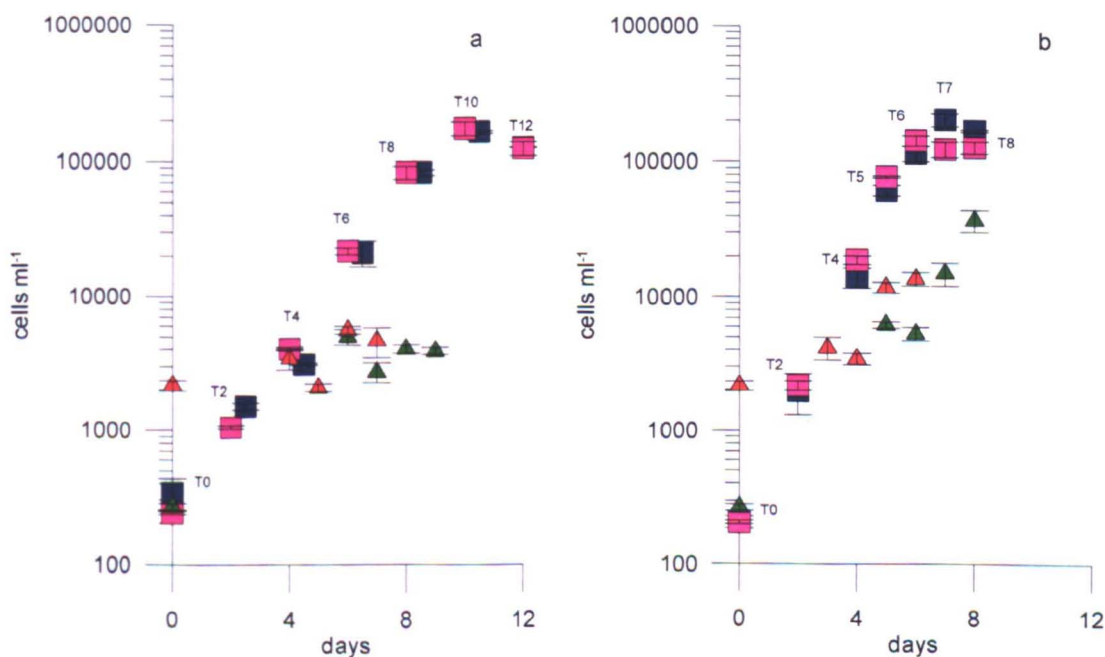


Figure 3.14. Time course of cell concentration for parental strain Sy373 '+' (blue), Sy379 '-' (pink), the total number of cells (parental vegetative cells, sexual stages, large F1 cells) in crosses carried out at T0 (green triangles) and T2 (red triangles) in Experiment #2. Panel (a) illustrates the results obtained at 60 and panel (b) at 110 μmol photons m⁻² s⁻¹. Each point for the parental strains (squares) represents the average value of duplicate counts with maximum and minimum, each point for the crosses (triangles) represents the average of triplicate counts with standard deviation.

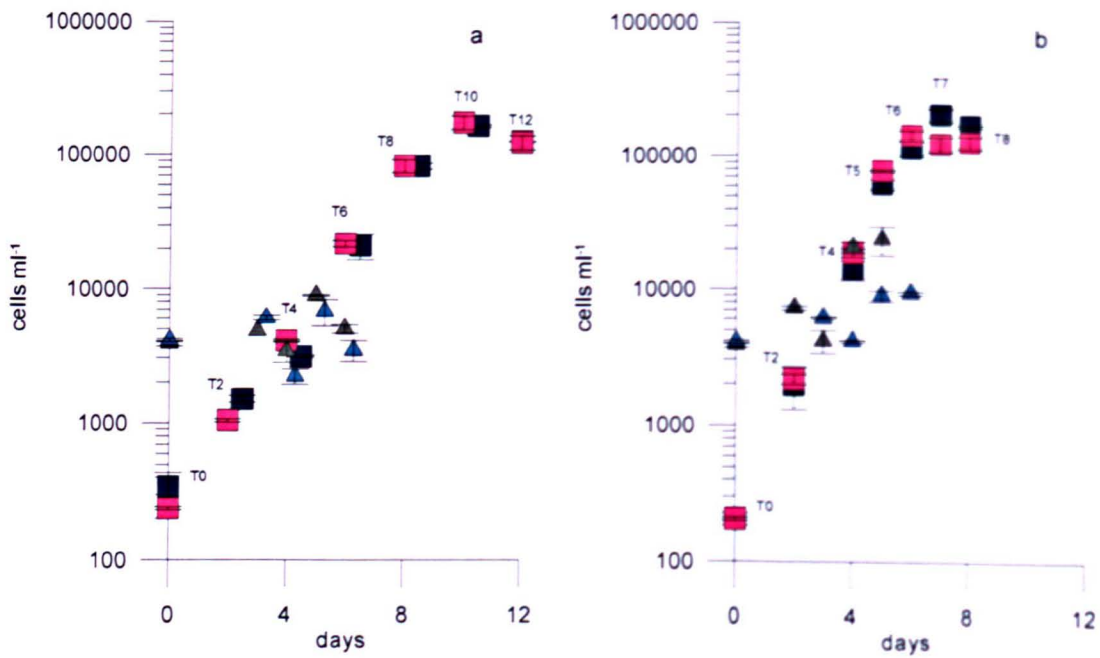


Figure 3.15. Time course of cell concentration for parental strain Sy373 '+' (blue), Sy379 '-' (pink), the total number of cells (parental vegetative cells, sexual stages, large F1 cells) in crosses carried out at T4 (grey triangles) and T6 (light-green triangles) in Experiment #2. Panel (a) illustrates the results obtained at 60 and panel (b) at 110 $\mu\text{mol photons m}^{-2}\text{s}^{-1}$. Each point for the parental strains (squares) represents the average value of duplicate counts with maximum and minimum, each point for the crosses (triangles) represents the average of triplicate counts with standard deviation.

In the sister experiment carried out at slightly higher irradiance (110 $\mu\text{mol photon m}^{-2}\text{s}^{-1}$), the timing of production of sexual stages was one day shorter. Gametes were recorded after 5 days in co-cultures started on T0, after 3 days in those started at T2 and T6, and after 2 days in the others (Figs 3.12 and 3.13a). Also in this experiment the maximum percentage of sexual stages over the total number of cells was similar (between 12 and 38%, Fig. 3.12) amongst the different crosses and was correlated with parental cell concentrations between 2,400 and 7,400 cells·ml⁻¹. The number of gametes, zygotes, auxospores and initial cells generally decreased after a couple of days from their appearance and was followed by the appearance of large F1 initial cells. In all crosses gametes/zygotes developed into auxospores and later into a large cell F1 generation. In all the crosses, started from T0 to T8, the total number of life stages (vegetative cells +

gametes/zygotes + auxospores + initial cells + large F1 generation cells) did not increase over the observation period compared to the cell concentrations recorded in the monocultures of the parental strains (Figs 3.14*b* and 3.15*b*). This reduction in growth is apparent when the cell concentration of the two parental strains and the cell concentration recorded in the crosses (vegetative cells + sexual stages + large F1 generation cells) are plotted on the same graph (Figs 3.14 and 3.15). It is evident from these results that co-cultures had cell concentrations lower by 7 – 52% compared to the concentrations of the strains grown in monoculture. As in the previous experiment, the reduction of growth of the vegetative cells when sexual reproduction was occurring was more evident under low irradiance (Figs 3.14 and 3.15).

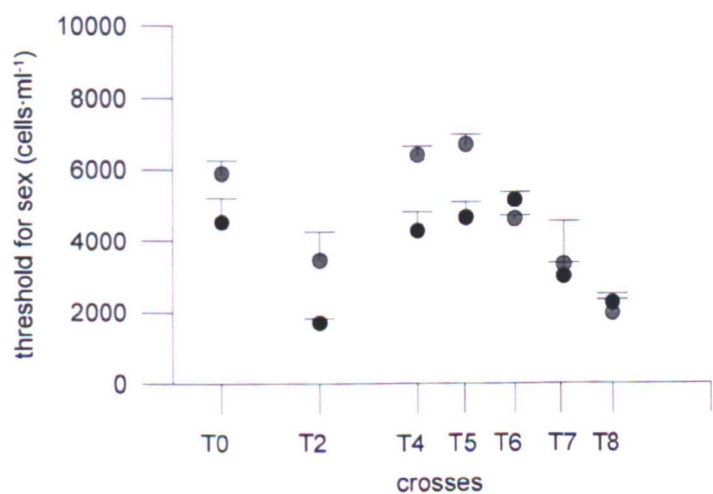


Figure 3.16. The cell density of parental cells on the first day in which sexual stages were detected in the crosses carried out at different times in Experiment #2; black circles: low irradiance, grey circles: high irradiance.

The results of Experiment #3 can be summarized in the following main points:

- a) The highest success of sexual reproduction (20-38 % of sexual stages over the total number of cells) was obtained with an initial concentration of parental strains of between 1,330 and 4,100 cells·ml⁻¹.

- b) Sexual reproduction started when the concentration of parental strains was between 2,400 and 7,400 cells·ml⁻¹ (Fig. 3.16).
- c) The time course of the experiments from T4 and T8, which started with the same cell concentration of parental strains, was similar.
- d) The decrease in cell concentration of vegetative cells at the same time as sexual reproduction (observed in Experiment #1) was confirmed.

3.4 Discussion

3.4.1 Sexual reproduction and growth phase of parental strains

Parental strains of *Pseudo-nitzschia multistriata* were able to undergo sexual reproduction not only when they were crossed in the early exponential phase, but also when they were crossed in the late- or post- exponential growth phase. This shows that within the parental cell population there were always some cells potentially able to differentiate into gametes, independent of the growth phase they were in. Nevertheless, when crosses were performed with parental strains in late- or post-exponential growth phase, the relative percentage of sexual stages was extremely low and the gametes could not develop into auxospores and subsequently into initial cells. This shows that a high concentration of vegetative cells of the two mating types within the cell size window for sexualisation is not the only condition required for a successful auxosporulation and formation of new initial cells. In fact, parental strains should be actively growing for a successful completion of the sexual phase. The concentration of nutrients was not measured in these experiments, but it is reasonable to assume that parental strains collected in the late exponential phase may be already at or close to nutrient limitation (see Chapter 5 for experiments in which nutrient concentration was estimated). The nutrient limitation became more severe in the days following the beginning of the crosses of T5 onwards. The collapse of vegetative cell concentration observed in these experiments, provides experimental evidence for that. The experimental evidence for the fact that *P. multistriata* strains need to be in the active growth phase to complete successful auxosporulation comes from the results of Experiment #2, where all the crosses carried out by diluting the parental strains with fresh medium were able to produce auxospores and F1 cells at similar timing and success. The role of a healthy physiological state of the parental strains for a successful completion of the sexual phase was pointed out by Davidovich (1998), and the results obtained in this chapter provide a

valid experimental support. The formation of an initial cell requires the synthesis of biomass that can be achieved only if nutrients are available. The average diameter of gametes ranges between 5 to 6 μm in diameter, that corresponds to an average carbon content of $7.20 \text{ pg C}\cdot\text{cell}^{-1}$; the average length of a complete auxospore is about 80 μm that corresponds to an average carbon content of $118.14 \text{ pg C}\cdot\text{cell}^{-1}$. As shown in Chapter 2, the process of gamete conjugation and formation of an auxospore is relatively rapid (about 20 minutes and 24 hours, respectively). In this time interval, a biomass increase of one order of magnitude occurs, with the synthesis of perizonial bands, frustule of the initial cell, most probably synthesis of cellular organelles (e.g. mitochondria) and the energy required to complete the nuclear divisions that accompany the deposition of the valves of the initial cell. Davidovich (1994) suggested that the mechanism of auxospore expansion depends on the increase of the vacuole volume, which in turn depends from the utilization of reserve material stored in the gametes. However, in my opinion, the considerable increase of biomass, cannot only sustained by the material present in the gametes and, therefore, nutrient assimilation and synthesis of new material has to be occurs.

In this respect, the case of *Leptocylindrus danicus* in which sex is induced by nutrient starvation, is very puzzling. In this species, in fact, nitrogen depletion promoted auxosporulation in about 100% of vegetative cells in the narrow valve diameter (8 μm or less) (French III and Hargraves 1985). The auxospore in this species is transformed into a resting spore and this link between the onset of sexual reproduction triggered by sex and the transformation of the zygote in a resting stage recalls what occurs in other lineages such as dinoflagellates and chlorophyceans. *Leptocylindrus danicus* is a very primitive centric diatom, at the base of the phylogenetic evolutionary tree of diatoms and its peculiar life cycle might be an ancestral character that was subsequently lost in diatom evolution.

As mentioned in the Introduction, both in unicellular (*Chlamidomonas reinhardtii*) and colonial (*Volvox carteri*) Chlorophyceae the induction of the sexual phase is linked to

stress conditions, either nitrogen starvation (Quarmby 1994) or temperature shock (Nedelcu and Michod 2003) and is followed by the formation of a resting stage. The same pattern seems to occur in dinoflagellates. In this group of protists, however, it has been recently shown that the planozygotes (the product of the conjugation of two gametes) can revert to the vegetative phase and does not necessarily transform into cysts (Figueroa *et al.* 2006). Therefore, it cannot be excluded that sexual reproduction in this lineage occurs more often and that the conjugation process and the production of planozygotes could have been overlooked. However, we also have to keep in mind that the formation of gametes and planozygotes in nutrient deprived media has been reported also in dinoflagellate species that do not form resting stages (e.g. *Ceratium furcoides* Hickel 1988).

3.4.2 The timing and cell density threshold for sex

The time required for the initiation of the sexual phase in *P. multistriata* showed an inverse correlation with the density of the inoculum of parental cells, i.e. the lower the inoculum size, the longer was the time required to initiate the sexual phase. This suggests that a threshold cell concentration has to be reached to allow sexual reproduction to occur. The highest percentage of sexual stages and F1 generation cells occurred with an inoculum of about 2-3,000 cells·ml⁻¹, which was the size of the inoculum in the crosses started at T2 in both Experiment #1 and #2. These relatively high percentages of sexual stages were also obtained in all tests carried out within Experiment #2 that were all started with cell concentrations around 3,000 cells·ml⁻¹. The cell concentration threshold at which gametes were first observed was rather broad and was comprised between 2,000 and 10,000 cells·ml⁻¹. The only cell concentration value which sex occurs in diatoms has been reported for *Pseudo-nitzschia brasiliiana*, the homothallic species, where auxospores were recorded in cultures with a cell density of between 10³ to 10⁷ cells·ml⁻¹ (Quijano-Scheggia *et al.* 2009a), which is an extremely broad range. The relatively broad range of cell concentration at which gametes were first observed in *P. multistriata* can be explained

either by the variability amongst experiments or by the fact that vegetative cells tend to settle to the bottom of the culture plates – possibly in variable percentages amongst the different replicates/experiments – where they produce a micro-aggregation that favours encounters and/or perception of chemical signals. The variability of these aggregations might explain the variability of threshold cell concentrations that we have recorded, considering that estimates of cell concentration were obtained after mixing the sample.

The results of the experiments illustrated in this chapter would suggest that sex in the diatom *P. multistriata* is a density-dependent event. The effect of density of multicellular organisms – either plants or animals – on various aspects of population dynamics, such as growth, reproduction and mortality has been broadly explored. The marine brown algae *Pterygophora californica* and *Macrocystis pyrifera* have a heteromorphic life cycle including a large sporofite and a minute gametophyte. In both species a negative correlation was observed between the density of spores settled per unit of surface and the growth of the gametophyte and the subsequent maturation of the gametes (Reed *et al.* 1991). The effect of cell density has been well studied also in bacteria, which perceive the density of the population *via* the production of small diffusible molecules that have a signalling role. This mechanism is known as ‘quorum sensing’ and includes the production of the signalling molecule, the capacity of recording its activation and the consequent activation or inhibition of different metabolic pathways in relation to the detection of specific density thresholds in the population (Keller and Surette 2006). Very little is known on density-dependent phenomena in the life history of unicellular eukaryotes. Examples are chrysophyte *Synura peterseni* where statospores are produced following conjugation between two heterothallic gametes (Sandgren and Flanagan 1986). The heterothallic strains have to be mixed at a sufficient cell concentration and the formation of statospore is a density-dependent process that occurs during periods of active vegetative cell population growth. The life cycle of unicellular marine dinoflagellate

Noctiluca scintillans consists of large vegetative cells and smaller 'swarmer' stages. After a number of binary fissions (19-29) vegetative cells turned into swarmer cells. This program could not be altered by changing abiotic conditions (temperature, salinity, light, nutrients or pH), but by the density of vegetative cells: the higher cell density was, the higher the percentage of cells that could escape the transformation into swarmers (Sato *et al.* 1998).

3.4.3 Sex and growth

When parental strains were inoculated in the same culture vessel, sexual reproduction was induced after a variable number of days depending from the inoculum size; the onset of sexual reproduction was accompanied by a reduction of cell concentration as compared to the cultures of the single parental strains. The clonal cultures of parental strains and the crosses were grown in the same culture medium and incubated at the same experimental conditions. Cultures of parental strains were grown in culture bottles, while the crosses were grown in culture wells; nevertheless, it has been demonstrated that the growth rates obtained in the two vessels is the same. The observed low cell concentration in the crosses as compared to the clonal parental strains can be explained by the following reasons: a) a high percentage of vegetative cells turned into gametes, because gametes are clearly distinguishable from vegetative cells b) the vegetative cells died at the onset of the sexual phase. Only live cells were enumerated but I can rule out a massive mortality during all tests in Experiment #2 and in T0 and T2 of Experiment #1, c) the growth rate of vegetative cells is arrested or reduced when the sexual reproduction starts. The sum of vegetative cells and sexual stages, i.e. the total biomass present in the cultures, has been represented in the graph. From the 'biomass' point of view, sexual reproduction does not represent a loss: two cells (gametangia) should provide two new initial cells. A decrease in the vegetative cell division rate, therefore, seems the most plausible explanation for what was observed.

To my knowledge, there are very few reports – mostly incidental – on the link between growth rates and occurrence of sexual reproduction in diatoms. It has been reported that in natural populations of the centric diatom *Stephanodiscus neoaestrea* the cell density did not increase markedly when sexual reproduction was observed, although nutrients were not limiting in the environment (Jewson 1992a). A decrease in growth rate in correspondence with the induction of sexual reproduction was also reported for the chrysophyte *Synura petersenii* (Sandgren and Flanagan 1986).

The possible arrest or decrease of vegetative division in concomitance with the onset of sexual reproduction is extremely interesting and deserves future investigations. It can be hypothesized that the population invests in sexual reproduction, minimizing the uptake of nutrients of the vegetative cells during this critical moment of the life cycle. This explanation however, implies a complex regulatory mechanism by which a) the whole population perceives a signal (a pheromone like molecule? A quorum sensing molecule?), b) some cells in the population differentiate into gametes, c) the other cells stop or reduce division rate. Another possible explanation is that the onset of sexual reproduction is mediated by a chemical cue and that this compound inhibits the cell cycle of vegetative stages. Experiments to test for the presence of a chemical mediator that induces sexualisation in *P. multistriata* will be illustrated in Chapter 4.

3.4.4 The success of sexual reproduction

The highest percentage of sexual stages (comprised between 10 and 38%) was recorded in the crosses started on T0 and T2 in Experiment#1 and in all crosses carried out in Experiment#2. There are very few studies in which the production of sexual stages in diatoms has been quantified. In *Pseudo-nitzschia multistriata* D'Alelio *et al.* (2009a) found that the fraction of gametangia over the total number of vegetative cells was about 1-2%. These values have been obtained at experimental conditions (20°C, 12L:12D, 40 µmol

photons $\text{m}^{-2}\text{s}^{-1}$) not very different from the ones used in these experiment. The differences might be explained either by genetic differences amongst the strains used for the experiments or by the fact that the irradiance values of $40 \mu\text{mol photons m}^{-2}\text{s}^{-1}$ are too low to permit the onset of sexual reproduction. In *Pseudo-nitzschia multiseriis* the fertilization success (expressed as the percentage of initial cells over 0.5-number of gametes) was similar between strains of different age, i.e. size, but the reproductive success (expressed as the percentage of initial cells over 0.5-number of gametes) was higher for longer/younger strains (Hiltz *et al.* 2000). In *Haslea ostrearia* the reproductive success spanned from 3 to 20%, depending on the different combination of irradiances and photoperiod (Mouget *et al.* 2009). In natural populations of *Pseudo-nitzschia* species, only a small fraction of vegetative cells underwent sexual reproduction during a sex event recorded in the Gulf of Naples (7.2% for *Pseudo-nitzschia* cf. *delicatissima*; 14.3% for *P.* cf. *calliantha*) (Sarno *et al.* 2010), while up to 59% of the cells were auxospores in a bloom of *P. australis* (Holtermann *et al.* 2010). In the pennate diatom *Fragilariopsis kerguelensis* the higher percentage of auxospores (0.4 %) was observed inside an iron-fertilized bloom, while outside it the percentage was lower (0.03%) (Assmy *et al.* 2006).

Very low percentages of sexual stages (0.16 %) were recorded for centric diatom *Aulacoseira subarctica* (Jewson 1992b) and for *Stephanodiscus neoastraea* (3-4 %) (Jewson 1992a). The figures provided above and the results obtained in the experiments illustrated in this chapter show that – with the exception of the extremely high values recorded for *P. australis* – only a limited fraction of the population differentiates into gametes that will be involved in the sexual cycle. This is a reasonable strategy if we consider that sexual reproduction is a costly process for an organism (Lewis 1983). In fact, energy has to be invested in the synthesis of gametes, gametes might be destroyed by bacterial or other pathogens (see Chapter 2), fertilization might not be successful and the successful formation of initial cells might not always occur.

Chapter 4

Is there a chemical cue that induces gametogenesis in

Pseudo-nitzschia multistriata?

4.1 Introduction

Marine organisms produce a wide variety of chemical compounds – called secondary metabolites – that have an important role as defence mechanisms, communication between organisms, deterrent systems against predators and allelopathic mechanisms that influence the interactions between organisms, e.g. inhibiting or enhancing growth (Ianora *et al.* 2006). Secondary metabolites are molecules that are not involved in the ‘basic’ metabolism of the organisms and their chemical diversity, biosynthesis and action mechanisms are still largely unknown.

There are different kinds of chemical interactions that involve bacteria, unicellular and multicellular marine organisms. Bacteria can perceive the density of their populations through a mechanism called ‘quorum sensing’. Bacterial cells synthesize molecules that diffuse in the water and can be detected by other bacterial cells. When a threshold concentration is reached, the signal is translated at the gene level and target genes can be activated. These genes can regulate different aspects of the biology of bacteria, such as their virulence, bioluminescence and various coordinated behaviours (Keller and Surette 2006). Quorum sensing mechanisms are known also for eukaryotes. As an example, in the social amoeba *Dictyostelium discoideum*, nutrient depleted cells secrete a signal molecule that, above a threshold level, induces cell aggregation and the formation of fruiting bodies, which release the amoebae and restart the cycle (Gregor *et al.* 2010). Different kinds of secondary metabolites with different functions are produced by unicellular eukaryotes. Examples are allelopathic compounds that inhibit the growth of other species (e.g. Rengefors and Legrand 2007, Yamasaki *et al.* 2007), or the polyunsaturated aldehydes synthesized by broken diatom cells that damage the reproductive biology of their main grazers, the copepods (e.g. Ianora *et al.* 2004), or can act as info-chemicals mediating bloom termination through the induction of cell death (Vardi *et al.* 2006).

It has been shown that the metabolic profile of the substances excreted by diatom species during different phases of their growth is different, and some compounds are only produced within very specific growth phases, which may have parallely with bacterial quorum sensing (Barofsky *et al.* 2009). The metabolic profile of exudates produced by two diatom species, *Skeletonema marinoi* and *Thalassiosira weissflogii*, grown in monoculture and in co-cultures that did not allow contact between the cells has shown that different compounds are produced when the species are in contact with the metabolites produced by the other species (Paul *et al.* 2009). Moreover, while the growth of *S. costatum* was not influenced by the presence or absence of *T. weissflogii*, the growth of this latter species was increased by the presence of *S. costatum*.

Sex pheromones are a particular category of secondary metabolites; they are volatile organic compounds and, in the aquatic ecosystems, they have been first detected in various brown macro algae (Fink 2007). Several molecules have been identified; they are produced by female gametes and have the function to attract the male gametes. Some of the compounds that function as sex pheromones in macroalgae have been also detected in diatoms. As an example, ectocarpene was extracted from *Skeletonema costatum* when cultures were exposed to a drastic increase in irradiance that resulted in the induction of gametogenesis (Derenbach and Pesando 1986). However, the role as a sex pheromone of this compound has not been demonstrated.

The evidence that diatoms can produce sex-pheromones during sexual reproduction has been provided very recently for the araphid pennate *Pseudostaurosira trainorii* (Sato *et al.* 2011). This heterothallic pennate diatom has a very peculiar life cycle in which the male gametes are motile. The motility is due to the presence of thin and extensible thread-like projections. The sexualisation seems to be a two-step process in which the female sex pheromone is continuously produced by the actively growing female and induces sexualisation in the male strains when exposed to the female filtrate medium. When the

male strain is sexualized, i.e. gametes are formed, it synthesizes a pheromone that induces sexualization in the female.

As illustrated in Chapter 1, in some unicellular lineages, sexual reproduction occurs in response to stress. This mechanism has been investigated in the chlorophycean *Volvox carteri* where the sexual phase is mediated by the cellular overproduction of reactive oxygen species (ROS) following a heat-shock (Nedelcu and Michod 2003, Nedelcu *et al.* 2004). The treatment of cultures that received a sex-inducing heat-shock with antioxidants, in fact, inhibited sexualisation.

The study by Sato *et al.* (2011) is, to my knowledge, the only indirect but convincing example that chemical mediators are involved in the sexual reproduction of diatoms. The results presented in Chapter 3, where a direct link between inoculum size and the timing of sexual reproduction has been demonstrated, support the fact that sexual reproduction is a density-dependent event in the life cycle of *P. multistriata* and, thus, it should be mediated by a chemical cue. In this chapter, this hypothesis will be tested by different approaches: inoculating strains of different mating types in culture media conditioned by the growth of the opposite mating type, and incubating strains in the same culture vessel but separated by a permeable membrane. Results presented in Chapter 3 also suggested that with the onset of sexual reproduction, the growth of vegetative stages seems inhibited. This hypothesis will be further tested by comparing crosses carried out with different inoculum size in which parental strains of different cell size were used. This provides a test to assess if the inhibition of growth affects only one or both mating types.

4.2 Material and Methods

4.2.1 Culture isolation and maintenance

The cultures of *Pseudo-nitzschia multistriata* used for the experiments in this chapter (Table 4.1) were isolated and maintained as described in Chapter 2. Before carrying out each experiment, 20 cells from each strain were measured at 400x magnification using a Zeiss Axiophot light microscope equipped with an ocular micrometer. The maximum growth rate was calculated as described in Chapter 3.

Table 4.1. Strains of *Pseudo-nitzschia multistriata* used for the experiments reported in Chapter 4. For each experiment, details are given of the strain code, the isolation date, the average length of the apical axis at the moment in which the culture was established (I), and the average length of the apical axis at the time when the experiments were carried out (II). The superscripts ^(a) and ^(b) denote the strains used in the first and second crosses, respectively, in Experiment#1.

Experiment	Strain code	Isolation date	Apical axis (μm) I	Apical axis (μm) II
Exp#1	Sy373 '+' S ^(a)	07/07/2009	45	23
	Sy800 '-' L ^(a)	21/09/2010	40	37
	Sy668 '+' L ^(a)	07/09/2010	52	48
	Sy379 '-' S ^(a)	07/07/2009	50	28
	Sy793 '+' S ^(b)	21/09/2010	34	25
	Sy686 '-' L ^(b)	07/09/2010	49	41
	Sy710 '+' L ^(b)	07/09/2010	47	40
	Sy776 '-' S ^(b)	21/09/2010	40	32
Exp#2a.1	Sy373 '+' S	07/07/2009	45	23
	Sy800 '-' L	21/09/2010	40	34
Exp#2a.2	Sy686 '-' L	07/09/2010	49	41
	Sy793 '+' S	21/09/2010	34	25
Exp#2a.3	Sy793 '+' S	21/09/2010	34	22.7

	Sy799 -' L	21/09/2010	53	30
Exp#2b	Sy793 '+' S	21/09/2010	34	22.7
	Sy799 -' L	21/09/2010	53	30
Exp#3	Sy686 -' L	07/09/2010	49	39
	Sy793 '+' S	21/09/2010	34	23

4.2.2 Effect of sexual reproduction on the growth rate of parental strains (Experiment #1)

This experiment was aimed at testing the results illustrated in Chapter 3 that showed how the occurrence of sexual reproduction seems to be linked to a decrease in growth of the vegetative cells. Eight parental strains with different average apical length were used to be able to recognize the different mating types when strains were co-cultured (Table 4.1). The experiment was run in two different runs in which 2 different couples were tested each time (marked with ⁽¹⁾ and ⁽²⁾ in Table 4.1) The growth curve of the single strains, of the strains of the same mating type grown together, and of the strains of opposite mating types grown together (crosses) were compared. For each couple of strains, a stock culture with about 150 cells·ml⁻¹ for each parental strain was prepared. Aliquots of 4 ml were placed in six 6-wells culture plates (36 well for each cross) and incubated in a growth chamber at a temperature of 18 °C, a photoperiod of 12L:12D h and an irradiance of 60 µmol photons m⁻²s⁻¹. Every day and for a period of 11 days, the culture material of 3 wells was placed in 3 Eppendorf vials, was fixed with formaldehyde solution at a final concentration of 1.6 % and stored in a fridge at 4 °C. The concentration of the following life cycle stages was estimated using a Sedgewick Rafter counting slide and a Zeiss Axiophot light microscope: large and small vegetative cells, gametes/zygotes (as described in Chapter 3, gametes and zygotes are unequivocally distinguished when they are connected to the gametangial frustules), auxospores, initial cells and large F1-generation cells. To obtain the growth curve of the individual parental strains, four flasks, one for each parental strain, containing

50 ml of f/2 filtered medium, were inoculated with about 300 cells·ml⁻¹. For each strain, aliquots of 4 ml were dispensed in two 6-well culture plates. Plates were placed in the same growth chamber as the crosses. Every two days and for a period of 10 days, the culture material of 2 wells for each parental strain was placed in 2 Eppendorf vials, fixed with formaldehyde solution at a final concentration of 1.6 % and stored in a fridge at 4°C. Cell concentration was estimated on 1 ml of each sample with a Sedgewick Rafter counting slide, using an Axiophot light microscope. The data were plotted and the maximum growth rate was estimated.

A control was set up co-culturing the two parental strains of the same mating type. For each couple of '+' and '-' strains, a culture flask was inoculated with about 150 cells·ml⁻¹ for each parental strain. Aliquots of 4 ml were placed in two 6-well culture plates and incubated. Plates were placed in the same growth chamber as the crosses.. Every two days and for a period of 10 days, the culture material of 2 wells for each couple were placed in 2 Eppendorf vials and fixed with formaldehyde solution at a final concentration of 1.6 %. Cell concentration the two parental strains different in size, was estimated using a Sedgewick Rafter counting slide and a Zeiss Axiophot light microscope. The growth rate was estimated as described in on Chapter 3, paragraph 3.2.2.

4.2.3 Test for the presence of a chemical cue inducing gametogenesis (Experiment #2)

This experiment was aimed at testing the presence of a chemical cue that can induce meiosis and gametogenesis. Two different approaches were taken. In Experiment#2a, the aim was to test if the culture medium conditioned by the growth of strains of the opposite mating type could induce the formation of gametes. In Experiment#2b, the aim was to test if the presence of a diffusible chemical compound could induce gametogenesis in strains of opposite mating type when incubated in a culture plate separated by a permeable membrane.

Experiment#2a. This experiment included three different tests using different couples of strains (Table 4.1). The experimental design of the first test (Experiment#2a.1) is illustrated in Figure 4.1 and summarized in Table 4.2 . Two flasks, one for each parental strain, containing 150 ml of f/2 filtered medium were inoculated with cells at a final concentration of about $500 \text{ cells}\cdot\text{ml}^{-1}$ and allowed to grow in a growth chamber at a temperature of 18°C , with a photoperiod of 12L:12D and an irradiance of $60 \mu\text{mol photon m}^{-2}\text{s}^{-1}$ (Fig. 4.1 aI, bI). Cell concentration was estimated every two days and, when cultures reached the late exponential growth phase ($194\cdot 10^3$ and $147\cdot 10^3 \text{ cells}\cdot\text{ml}^{-1}$ for '+' and '-' strains, respectively), 100 ml were filtered through a MILLEX-GS filter unit with a $0.22 \mu\text{m}$ pore size filter (MILLIPORE, Carrantuohill, co. Cork, Ireland) (Fig. 4.1 aII, bII). In this way, the culture medium conditioned by the two strains of different mating type to be used for the experiments was obtained. At the same time, the two parental strains were inoculated at a final concentration of $1.5\cdot 10^3 \text{ cells}\cdot\text{ml}^{-1}$ for each of them in a flask filled with 250 ml of f/2 filtered medium (Fig. 4.1 cI). The cross was allowed to grow at the experimental conditions illustrated above. The cross was inspected every day and, when auxospores were detected, i.e. when sexual reproduction started, 200 ml of culture were filtered through a MILLEX-GS filter unit (Fig. 4.1 cII), to be used in the experiments.

To test the effect of the conditioned medium on the parental strains of the opposite mating type, two culture flasks were filled with 50 ml of f/2 filtered medium plus 50 ml of the conditioned filtrate medium of one parental strain. The fresh medium was added in order to avoid nutrient depletion, which would have inhibited the onset of the sexual phase (see Chapter 3). Exponentially growing cells of the opposite mating type were inoculated in the conditioned medium to reach a cell concentration of $10\cdot 10^3 \text{ cells}\cdot\text{ml}^{-1}$ for each mating type (Fig. 4.1 aIII, bIII). This cell concentration was chosen because preliminary experiments showed that under these conditions the sexual phase was induced within 1-2 days (see Chapter 3). For each parental strain, aliquots of 4 ml were dispensed in four 6-

well culture plates, i.e. 24 wells for each mating type (Fig. 4.1 *aIV*, *bIV*). Two other flasks were prepared with 20 ml of *f*/2 filtered medium plus 80 ml of filtrate medium conditioned by both strains undergoing sexual reproduction. A different ratio of conditioned:fresh medium was used due to the fact that the sex-conditioned medium was obtained from strains at lower cell concentration – and thus with higher nutrient concentrations - as compared to the medium conditioned by the single parental strain. The parental strains (one for each bottle) were inoculated in the sex-conditioned medium to reach a cell concentration of $10 \cdot 10^3$ cells·ml⁻¹ for each mating type (Fig. 4.1 *cIII*). Aliquots of 4 ml were dispensed in four 6-well culture plates for each parental strain (Fig. 4.1 *cIV*).

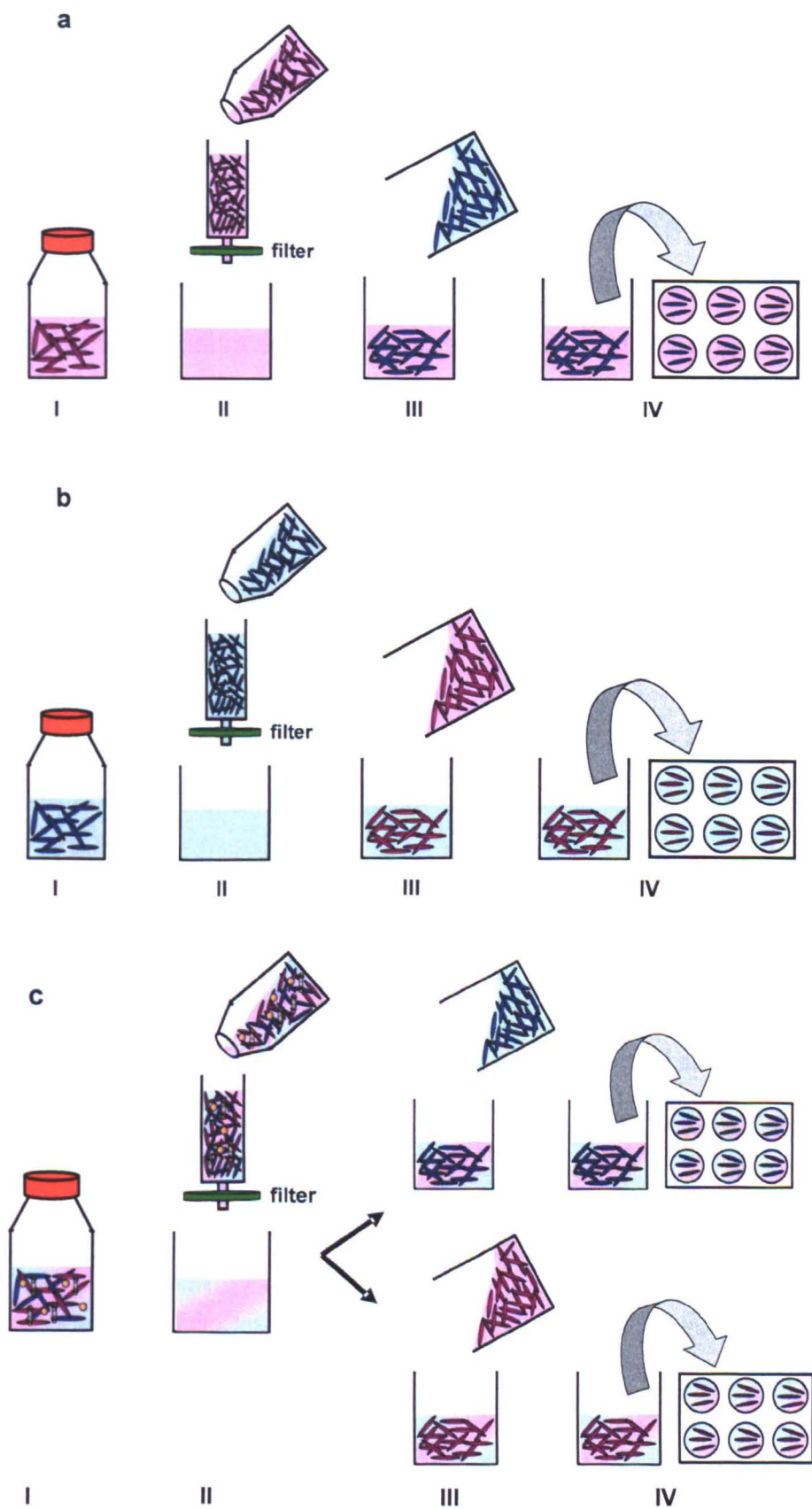


Figure 4.1. Schematic drawings illustrating the experimental setup for Experiment#2a.1. See the text for explanation.

A control was prepared by co-culturing the two parental strains of opposite mating type to test when the sexual reproduction could occur under the experimental conditions. A flask containing 100 ml of f/2 filtered medium was inoculated with a volume of exponentially growing culture to provide a final concentration of $10 \cdot 10^3 \text{ cells} \cdot \text{ml}^{-1}$ for each parental strain. Aliquots of 4 ml were dispensed in four 6-well culture plates, for a total of 24 wells. All plates (controls, plates with the medium conditioned by a single strain and plates with the sex-conditioned medium) were incubated in a growth chamber at the same temperature, photoperiod and irradiance conditions illustrated above. After 12, 16, 20, 24, 28, 36, 40 and 44 hours from the inoculum, the content of 3 wells for each culture type was placed in 3 Eppendorf vials and fixed with formaldehyde solution at a final concentration of 1.6 % and stored in the fridge.

In the second and third tests (Experiment#2a.2 and #2a.3), some modifications of the protocol were applied; a schematic representation of the experimental setting is provided in Figure 4.2 and summarized in Table 4.2. The modifications of the protocol included: i) the addition of a negative control in which exponentially growing cells of the two mating types were inoculated also in the conditioned medium of the same mating type; ii) the sex-conditioned medium was not tested; ii) the experiment lasted longer, i.e. 36 h instead of 48 h; iv) the sampling frequency was 12 h. The aim of the experiment was to detect the formation of gametes. As illustrated in Chapter 2, in the early stage of formation, gametes are enclosed in the gametangium. After the first meiotic division, the 2 nuclei are parallel to the longitudinal axis of the cell; plasmokinesis occurs and the two gametes become distinct within the gametangium. At this stage, meiosis II takes place followed by the subsequent degeneration of 2 of the nuclei and the rounding up of the gametes. In order to visualize the nuclei, all samples were analyzed as follows: 3 μl of SYBR Green I working solution (1:100) was added to the Eppendorf vials to reach a final concentration of 1:10,000, the sample was placed in an Utermöhl sedimentation chamber and examined

with a Zeiss Axiovert 200 epifluorescence microscope equipped with the filter FS09 (excitation, 450 to 490 nm; emission, 515 nm) at 400x magnification. Large and small vegetative cells, meiotic cells with segregated cytoplasm (MSC cells), rounded gametes, zygotes, auxospores and initial cells were enumerated (Fig. 4.3). Meiotic cells with segregated cytoplasm were those cells with two nuclei parallel to the longitudinal axis of the cell and evidence for the segregation of the cytoplasm (plasmokinesis); see Chapter 2 for a detailed description of these life stages.

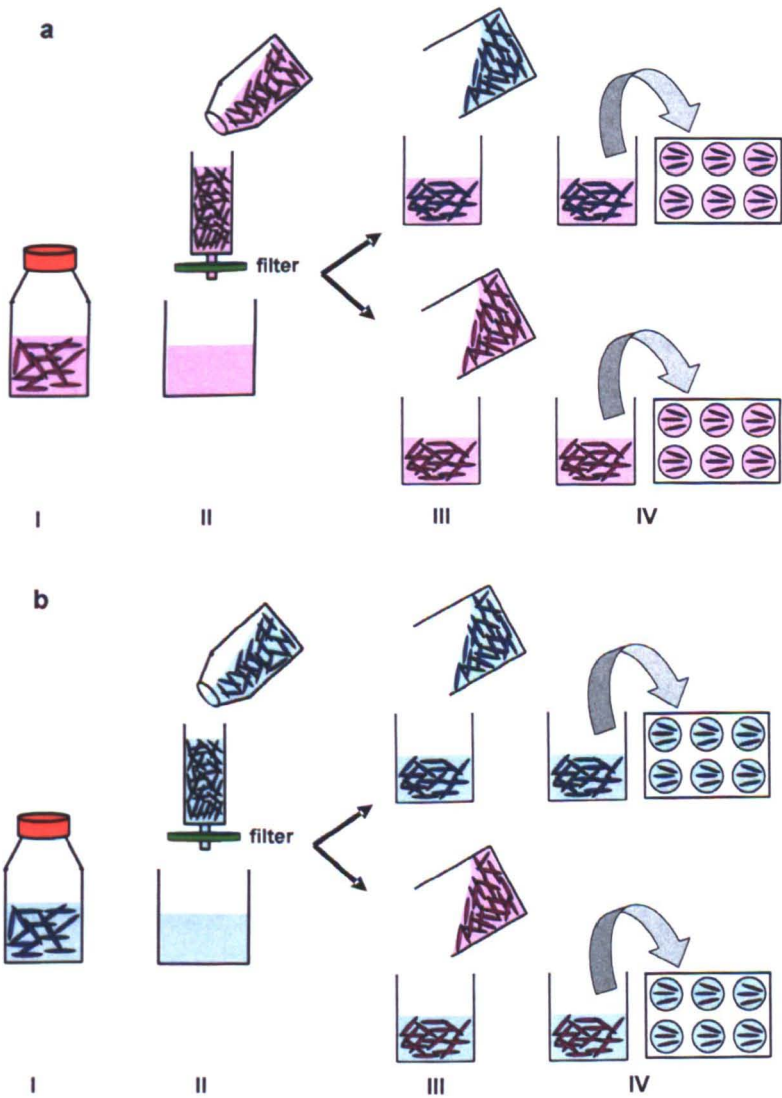
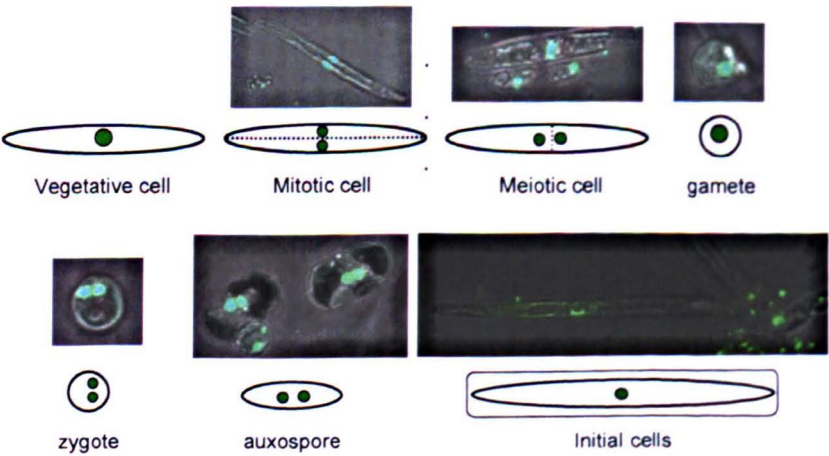


Figure 4.2. Schematic drawings illustrating the experimental setup for Experiment#2a.2 and #2a.3. See the text for explanation.

Table 4.2. Strains of *Pseudo-nitzschia multistriata* used in Experiment#2a. The mating type ('+' male mating type; '-' female mating type), the size of the cells (S = small; L = large), the cell concentration (cells·ml⁻¹) at the time in which cultures were filtered to obtain the conditioned medium, the strain inoculated in the conditioned medium.

Filtred medium from	Cells·ml ⁻¹	Inoculated strains
Sy800 '-' L	157·10 ³	Sy373 '+' S
Sy373 '+' S	196·10 ³	Sy800 '-' L
Sy373 '+' S	16,860	Sy373 '+' S
Sy800 '-' L (Cross)		Sy800 '-' L
Sy686 '-' L	155·10 ³	Sy793 '+' S
		Sy686 '-' L
Sy793 '+' S	162·10 ³	Sy793 '+' S
		Sy686 '-' L
Sy799 '-' L	258·10 ³	Sy793 '+' S
		Sy799 '-' L
Sy793 '+' S	322·10 ³	Sy793 '+' S
		Sy799 '-' L



Figures 4.3. Pictures and drawings showing the position of the nuclei in the different life stages.

Experiment #2b. The strains used for this experiment are listed in Table 4.1. The two parental strains were grown together but physically separated by a hanging cell culture insert (MILLIPORE, Carrantuohill, co. Cork, Ireland) that has a membrane with 0.22 μm pore size: this allows the passage of diffusible compounds but does not allow contact between cells of different strains. Stock cultures with a cell concentration of about 3,000 $\text{cells}\cdot\text{ml}^{-1}$ were prepared for each parental strain and aliquots were dispensed in two 6-well culture plates. In the first one, 3 ml of the '+' mating type were placed below the filter membrane and 3 ml of the '-' mating type was placed above it; the opposite was done in the other culture plate. The hanging insert fitted into the well, but the culture medium equilibrated so that above the insert there were 2 ml of medium and in the culture well below there were 4 ml. In the calculations, the cell concentration of the two mating types was thus referred to these volumes. A positive control was prepared co-culturing the two parental strains of opposite mating type, to have evidence that sexual reproduction was occurring under the tested experimental conditions. A flask containing 22 ml of f/2 filtered medium was inoculated with a volume of exponentially growing culture to provide a final concentration of $1.5\cdot 10^3$ $\text{cells}\cdot\text{ml}^{-1}$ for each parental strain. Aliquots of 6 ml were dispensed in 6-wells culture plates.

All plates were incubated in a growth chamber at the same temperature, photoperiod and irradiance conditions used for Experiment#2a. After 1, 2, 3, 4, 5 and 7 days from the inoculum, the content of one well, both above and below the membrane, was placed in Eppendorf vials and fixed with formaldehyde solution at a final concentration of 1.6 %. To visualize the nuclei, the samples were analyzed as described for Experiment#2a. The concentration of vegetative cells, MSC, and round gametes was estimated.

4.2.4 Test for the presence of oxidative stress during meiosis/gametogenesis (Experiment#3)

This experiment was planned to test for the possible presence of reactive oxygen species (ROS) during meiosis and gametogenesis in *Pseud-nitzschia multistriata*. Strains Sy793 '+' and Sy686 '-', different in size, were used for this experiment (Table 4.1). Two flasks, one for each parental strain, containing 20 ml of f/2 filtered medium were inoculated with cells at a final concentration of about $10 \cdot 10^3$ cells·ml⁻¹. For each parental strain, aliquots of 3 ml were dispensed in 7 petri dishes with glass bottom (test parental strains). Another flask was prepared with 50 ml of f/2 filtered medium and inoculated with a final concentration of $5 \cdot 10^3$ cells·ml⁻¹ for each parental strain. At this cell concentration, the formation of sexual stages is expected to occur after 1-2 days. Aliquots of 3 ml were dispensed in 7 petri dishes with glass bottom (test cross). All petri dishes were incubated in a growth chamber at a temperature of 18 °C, a photoperiod of 12L:12D h (light:dark) and an irradiance of 60 μ mol photon m⁻²s⁻¹. To detect the presence of ROS, one petri dish for each parental strain and one petri dish with the cross were treated, after 10 and 50 minutes, and after 16, 24 and 48 hours from the inoculum, with 1.5 μ l of dihydrorhodamine 123 (DHR 123) (D-632 Invitrogen) stock solution (5 mM DHR dissolved in DMSO) to reach a final concentration of 2.5 μ M. Auxosporulation was observed 48 hours after the inoculum. Controls were used to test the stain DHR123 in samples where oxidative stress was induced by the addition of H₂O₂ to each parental strain and to one cross, 150 μ l of H₂O₂ (H0904, SIGMA-ALDRICH) working solution was added. It was prepared by diluting H₂O₂ in MilliQ Water (1:200) to reach a final dilution of 1:10,000.

All samples were examined 10 minutes after staining with the dye DHR 123 with a Zeiss Axiovert 200 epifluorescence microscope equipped with the FITC filter FS09 (excitation, 450 to 490 nm; emission, 515 nm) at 400x magnification, looking for the

presence of large and small vegetative cells, meiotic cells with segregate cytoplasm (MSC cells), gametes and zygotes (Fig. 4.3).

4.3 Results

4.3.1 *Effect of sexual reproduction on the growth of parental strains (Experiment #1)*

When grown in mono-culture, the eight parental strains reached the maximum cell concentration after 6 or 8 days after the inoculum (Fig. 4.4 and Table 4.3). The maximum average cell density was between 74,900 and 217,166 cells·ml⁻¹, values recorded for the two large strains '+' Sy668 and '-' Sy686, respectively. The maximum growth rate of the strains was between 1.03 and 1.60 div·day⁻¹ for the large '-' Sy800 and the small '+' Sy793 strains, respectively. No significant difference ($p>0.02$) between the maximum growth rates of the strains belonging to different mating types or between strains of different cell size was detected. After reaching the maximum cell density a sudden collapse of vegetative cells was observed, which was particularly evident in the strains used in the second set of crosses (Fig. 4.4*b* and *c*).

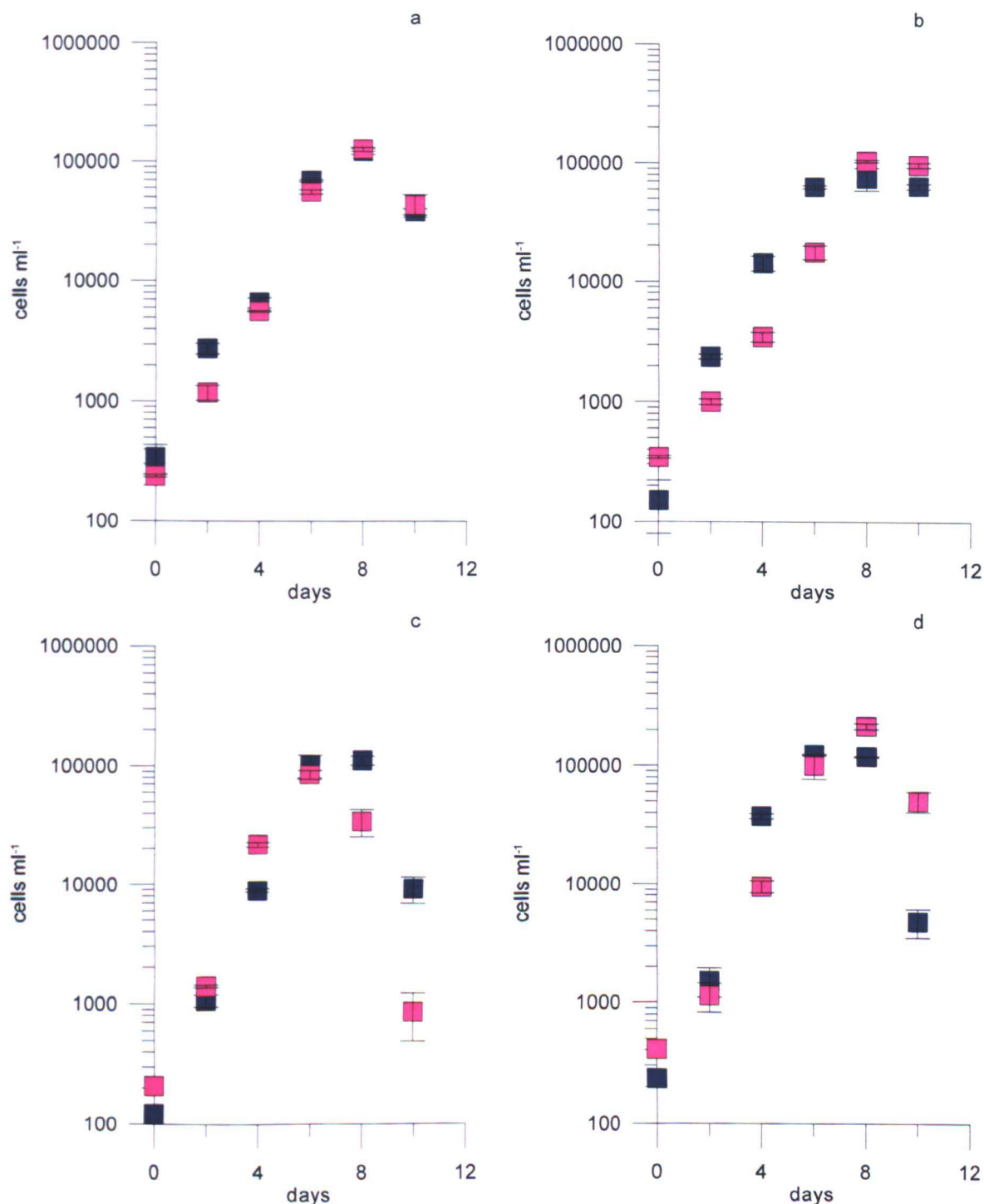


Figure 4.4. Experiment#1. Growth curve of '+' (blue) and '-' (pink) parental strains grown in single culture. a) Small parental strains Sy373 '+' and Sy379 '-', b) large parental strains Sy668 '+' and Sy800 '-', c) small parental strains Sy793 '+' and Sy776 '-', d) large parental strains Sy710 '+' and Sy686 '-'. (a) and (b) first experiment, (c) and (d) second experiment. Each point represents the average values of duplicate counts; maximum and minimum values are reported by vertical bars.

Table 4.3. Maximum growth rate (divisions·day⁻¹) and maximum cell concentration (cells·ml⁻¹) of the eight strains grown in mono-culture (A), in co-cultures with same mating type (B), and in co-culture with the opposite mating type (C). The superscript ^(a) and ^(b) mark the strains used in the first and second crosses, respectively, in Experiment#1.

Strain code		A	B	C
Sy373 '+' S ^(a)	div·day ⁻¹	1.08	1.49	1.01
	cells·ml ⁻¹	121,400 ± 6,930	89,167 ± 8,250	11,000± 3,606
Sy800 '-' L ^(a)	div·day ⁻¹	1.03	0.99	1.22
	cells·ml ⁻¹	104,000 ± 2,357	59,333 ± 4,243	147,500± 10,232
Sy668 '+' L ^(a)	div·day ⁻¹	1.45	1.33	1.43
	cells·ml ⁻¹	74,900 ± 16,558	91,000 ± 4,243	53,111 ± 7,784
Sy379 '-' S ^(a)	div·day ⁻¹	1.18	0.9	1.53
	cells·ml ⁻¹	127,000 ± 5,568	64,000 ± 7,543	139,333 ± 12,055
Sy793 '+' S ^(b)	div·day ⁻¹	1.6	1.27	1.26
	cell·ml ⁻¹	110,923± 9,402	105,664 ± 12,880	38,840± 4,548
Sy686 '-' L ^(b)	div·day ⁻¹	1.23	1.13	1.7
	cell·ml ⁻¹	217,166 ±12,063	95,177 ± 7,918	135,044 ± 21,001
Sy710 '+' L ^(b)	div·day ⁻¹	1.59	1.26	0.97
	cell·ml ⁻¹	124,887± 2,025	61,235 ± 7,793	33,597± 38,461
Sy776 '-' S ^(b)	div.day ⁻¹	1.49	1.16	2.06
	cell·ml ⁻¹	84,032± 7,051	88,703 ± 11,135	86,583± 31,983

When co-culturing strains of the same mating type, the '+' strains showed similar maximum growth rates spanning between 1.26 and 1.33 div·day⁻¹; in the '-' strains the maximum growth rates spanned from 0.90 to 1.16 div·day⁻¹ (Fig. 4.5 and Table 4.3). The Student t-test showed a significant difference (p< 0.0005) between the maximum growth rates of '+' versus '-' strains when grown with the same mating type: '+' strains grown faster as compared to '-' strains. No significant differences in maximum growth rates were observed between '+' strains grown in mono-culture and '+' strains co-cultured with the same mating type, and between '-' strains grown in mono-culture and '-' strains co-

cultured with the same mating type. These results show that there is no positive or negative effect on the growth rate, when strains of the same mating type are cultured together.

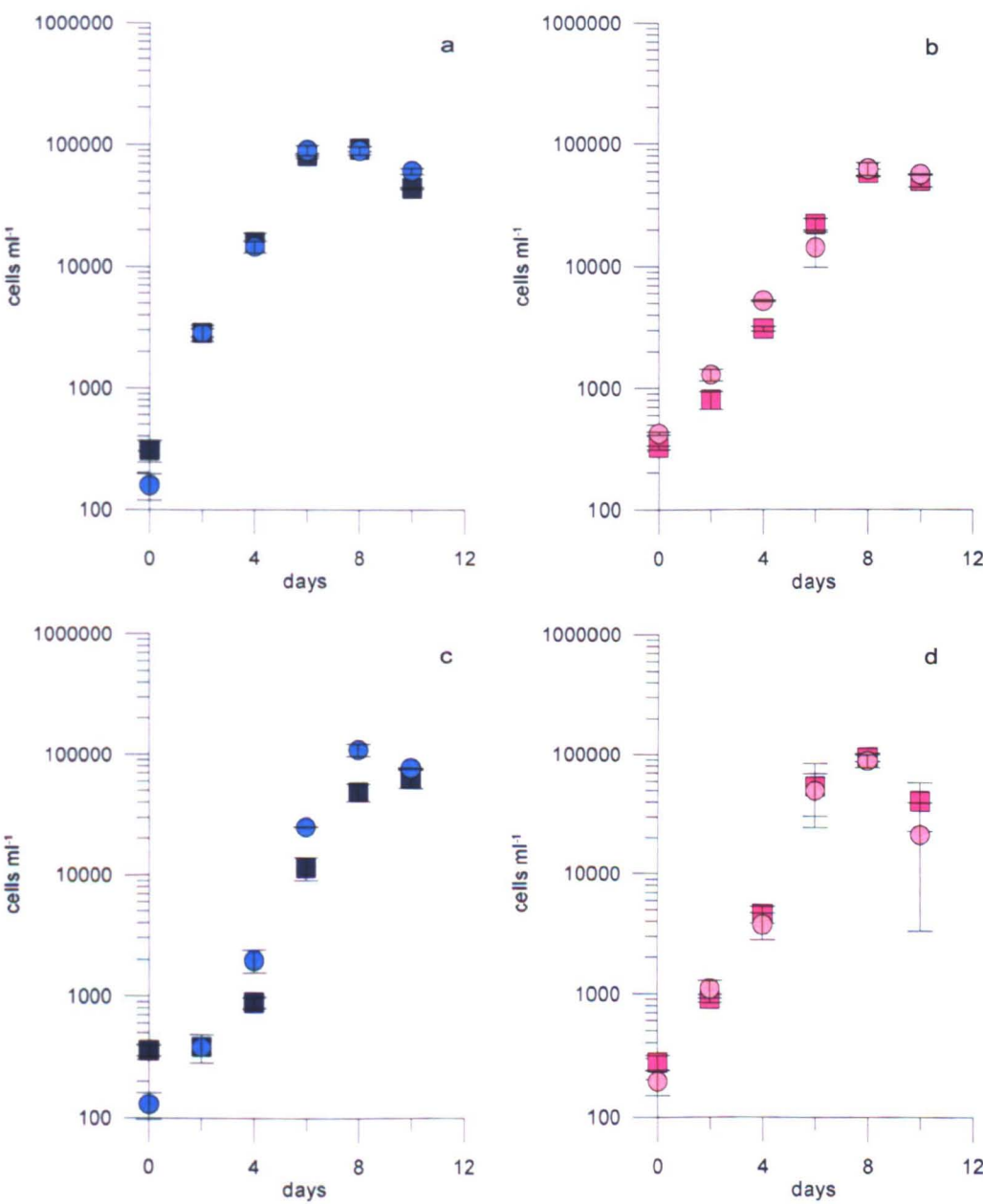


Figure 4.5. Experiment#1. Growth curve of '+' (blue) and '-' (pink) parental strains grown together with the same mating type. (a) Co-cultures of small (Sy373 circle) and large (Sy668 square) '+' strains; (b) co-cultures of large (Sy800 square) and small (Sy379 circle) '-' strains; (c) co-cultures of small (Sy793 circle) and large (Sy710 square) '+' strains; (d) co-cultures of small (Sy776 circle) and large (Sy686 square) '-' strains. (a) and (b) first experiment, (c) and (d) second experiment. Each point represents the average values of duplicate counts; maximum and minimum are reported by vertical bars.

When strains of opposite mating type were cultured together, sexual reproduction occurred and the formation of gametes was observed in all four crosses. However, their concentration was different, as was their development into zygotes/auxospores (see below) (Figs 4.6, 4.7). In all four crosses, '+' strains reached a much lower maximum cell density and had a lower maximum growth rate as compared to '-' strains (Table 4.3). In the first set of crosses (Experiment #1a), carried out with '+'Sy373S x '-'Sy800L and '+'Sy668L x '-'Sy379S, a similar timing in the appearance of the different sexual stages was observed (Fig. 4.6). Gametes started to appear on day 4, their number increased up to day 6 or 7, and then decreased. Auxospores appeared on day 5, increased up to day 7 and were followed by the appearance of initial cells and large F1 cells. These latter cells appeared on day 8 and started to grow till the end of the experiment.

In the second set of crosses (Experiment #2b), the production of sexual stages was much lower (Fig. 4.7a). In the cross involving '+'Sy793S x '-'Sy686L, gametes were first observed on day 4 and their number slightly increased up to day 6. However, they did not develop further into auxospores. The exponential growth phase of both parental strains was over on day 4, for the '+' strain and on day 5 for the '-' strain; a progressive collapse of their cell numbers occurred in the following days. The maximum growth rates and the maximum cell concentration were considerably different for the two parental strains, with the '+' strain showing lower values for both parameters (Table 4.3). The number of gamete produced in this cross '+'Sy710L x '-'Sy776S was higher as compared to the previous cross, however, very few gametes developed into auxospores. Also, in this case, the exponential growth phase of the two parental strains was over by day 5, but in this experiment, only the cell concentration of the '+' strain collapsed, while the '-' strain remained in a stationary growth phase.

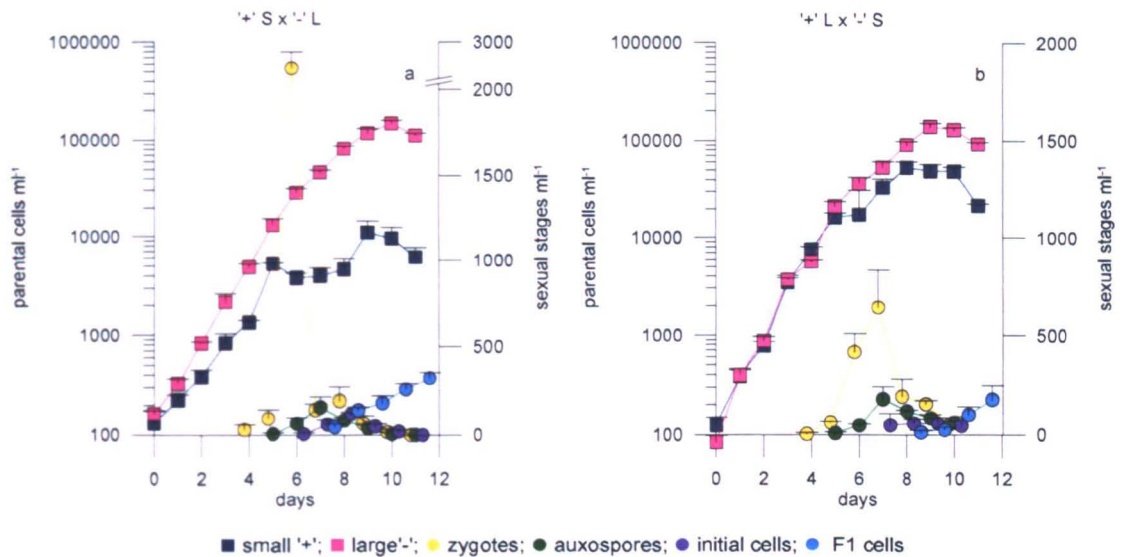


Figure 4.6. Experiment#1a. Cell concentration of parental strains and sexual stages obtained when co-culturing strains of opposite mating type with different cell size. Panel (a) Sy373 S'+ x Sy800 L'-; panel (b) Sy668 L'+ x Sy379 S'-'. On the left axis, parental cell concentration (cells·ml⁻¹; blue square for '+' and pink square for '-'); on the right axis concentration of sexual stages ml⁻¹ (yellow circles for gametes and zygotes; green circles for auxospores; violet circles for initial cells; light blue circles for large F1 cells. To allow the visualization of the different symbols of the sexual stages, they were plotted slightly apart.

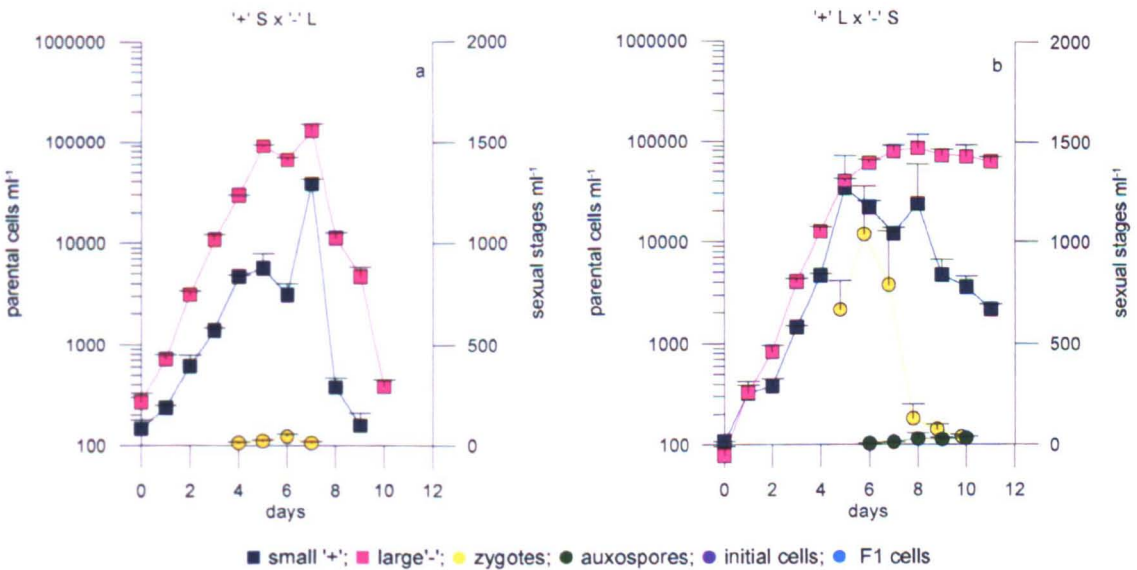


Figure 4.7. Experiment#1b. Cell concentration of parental strains and sexual stages obtained when co-culturing strains of opposite mating type with different cell size. Panel (a) Sy793 S'+ x Sy686 L'-; panel (b) Sy710 L'+ x Sy776 S'-'. On the left axis, parental cell concentration (cells·ml⁻¹; blue square for '+' and pink square for '-'); on the right axis concentration of sexual stages ml⁻¹ (yellow circles for gametes and zygotes; green circles for auxospores; violet circles for initial cells; light blue circles for large F1 cells). To allow the visualization of the different symbols of the sexual stages, they were plotted slightly apart.

4.3.2 Test for the presence of a chemical cue inducing gametogenesis (Experiment #2)

Experiment #2a. In two out of the three tests, evidence was provided on the presence of a chemical cue that induces the formation of gametes in strains of the opposite mating type. The third test failed and the possible reasons are discussed in the discussion section. In all the control crosses sexual reproduction occurred successfully, with only a slight shift in the timing of appearance of the different sexual stages (Figs 4.12, 4.13 and 4.14).

In the first test, gametangia with segregated cytoplasm and one or two (in the case of gametes undergoing the second meiotic division) nuclei for each protoplasm and also rounded gametes containing one nucleus were observed in strains of both mating types exposed to the culture medium conditioned by strains of the opposite mating type and by sex-conditioned medium (Figs 4.8 and 4.9). The initial stages of gametogenesis, i.e. meiotic cells with segregated cytoplasm (MSC cells) were recorded after 12 hours from the inoculum. Rounded gametes with one nucleus appeared later, about 24 hours after the inoculum. The highest density of MSC cells ($1,656$ and $1,562\text{ ml}^{-1}$, for '+' and '-' strains, respectively), and gametes ($1,004$ and 690 ml^{-1} , for '+' and '-' strains, respectively) were found towards the end of the observation period (Fig. 4.8). When both mating types were exposed to the sex-conditioned culture medium, a similar timing of appearance of MSC cells and gametes was recorded, although with slightly lower abundance (Fig. 4.9). In all four treatments both mating types did not increase markedly the population density, in '+' strains there was also a decreasing in cells density.

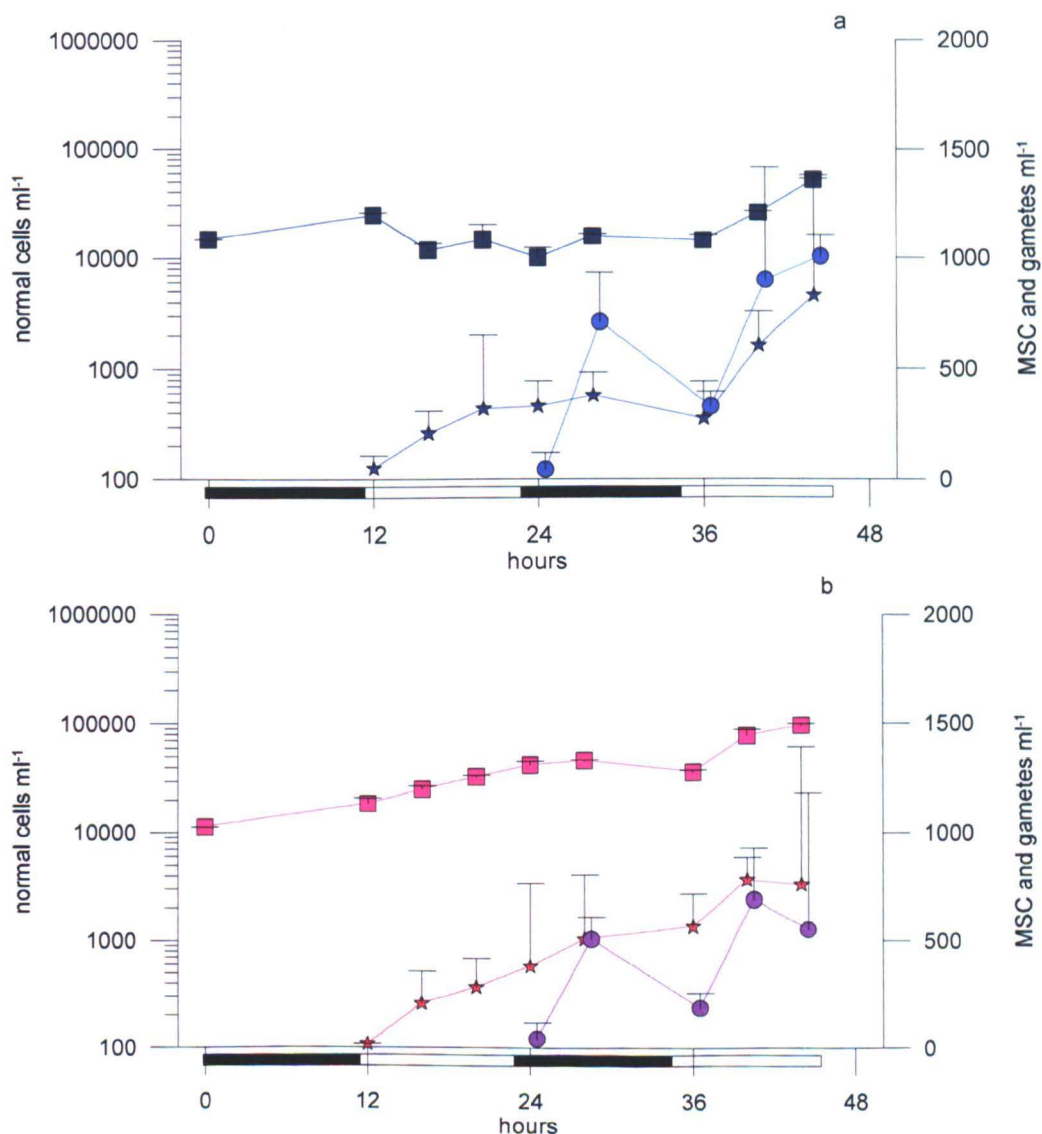


Figure 4.8. Experiment#2a. Production of gametes in strains incubated in the medium conditioned by the opposite mating type. (a) The '+' Sy373 S strain grown in '-' Sy800 L conditioned medium; (b) the '-' Sy800 L strain grown in '+' Sy373 S conditioned medium. On the left y axis cell concentration ($\text{cells}\cdot\text{ml}^{-1}$) of parental, strains (blue squares '+'; pink squares Sy800 L '-'), on the right y axis concentration of sexual stages (sexual stages ml^{-1}): blue stars '+' meiotic cells with segregated cytoplasm (MSC), pink stars '-' meiotic cells with segregated cytoplasm, blue circles '+' round gametes and pink circles '-' round gametes. The black and white bars below the x axis indicate the Light:Dark cycle.

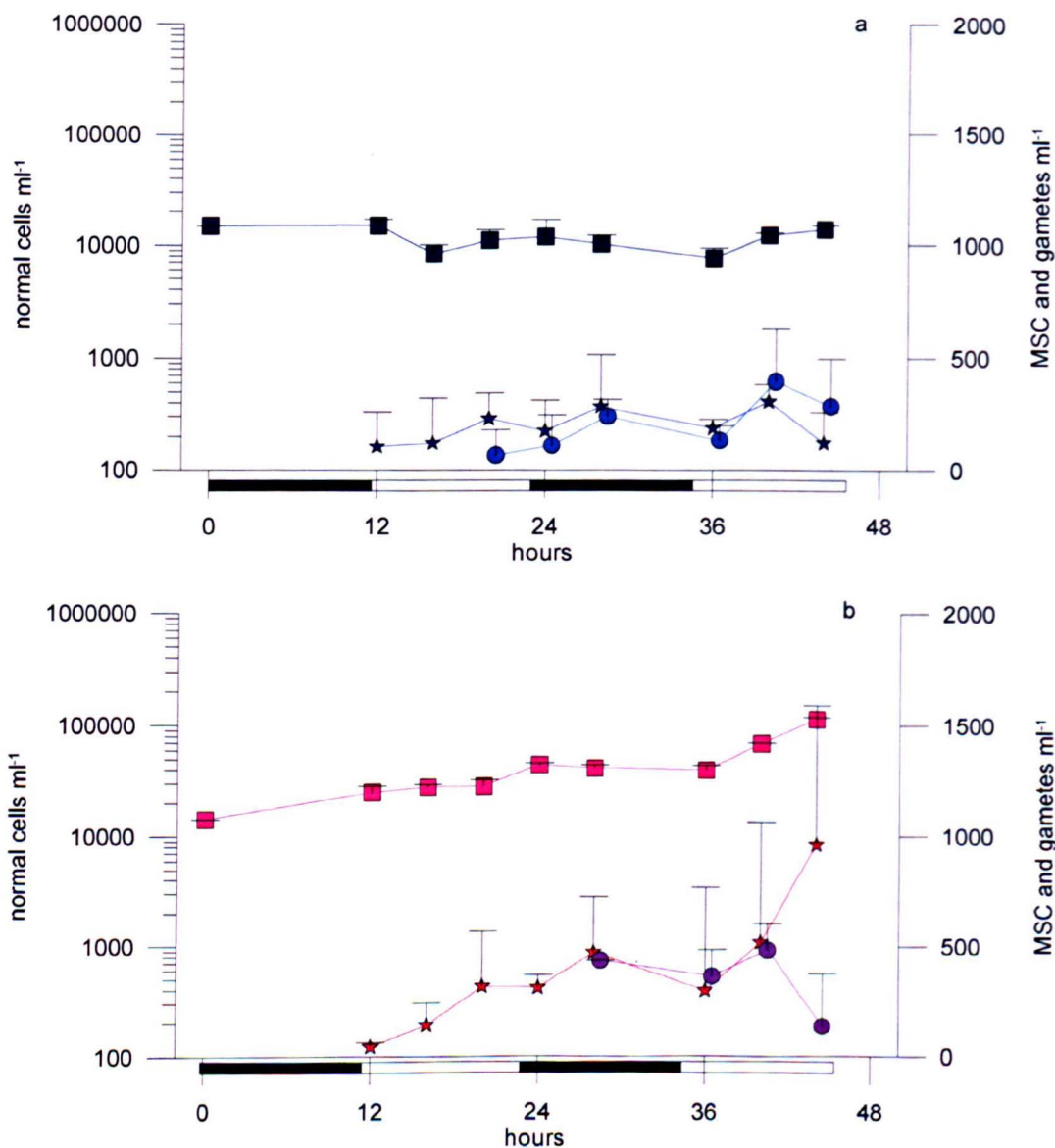


Figure 4.9. Experiment#2a. Production of gametes in strains incubated in the sex-conditioned medium. (a) The '+' Sy373 S grown in sex-conditioned medium; (b) the '-' Sy800 L strain grown in sex-conditioned medium. On the left y axis cell concentration (cells·ml⁻¹) of parental strains: blue squares Sy373 S '+', pink squares Sy800 L '-'; on the right y axis concentration of sexual stages (sexual stages ml⁻¹): blue stars: '+' meiotic cells with segregated cytoplasm (MSC), pink stars '-' meiotic cells with segregated cytoplasm (MSC), blue circles '+' round gametes and pink circles '-' round gametes. The black and white bars below the x axis indicate the Light:Dark cycle.

In the second test, performed with a different couple of strains ('+'Sy793S and '-'Sy686L), both mating types were able to undergo gametogenesis when exposed to the conditioned medium from the opposite mating type (Figs 4.10 and 4.11). In the two controls in which strains were grown in the medium conditioned by their own growth, the formation of gametes was not observed. Meiotic gametangia with segregated cytoplasm (MSC cells) were found after 12 hours also in this experiment, with concentrations comparable to those recorded in the previous test. However, fewer rounded gametes were recorded in both mating types in this experiment, and they only appeared the third day of observation (Figs 4.10*a* and 4.11*b*). In the third trial involving '+'Sy793S and '-'Sy799L, gametogenesis was not observed in both mating types when exposed to the conditioned medium from the opposite mating type as well as when they were exposed to their own conditioned medium (data not shown).

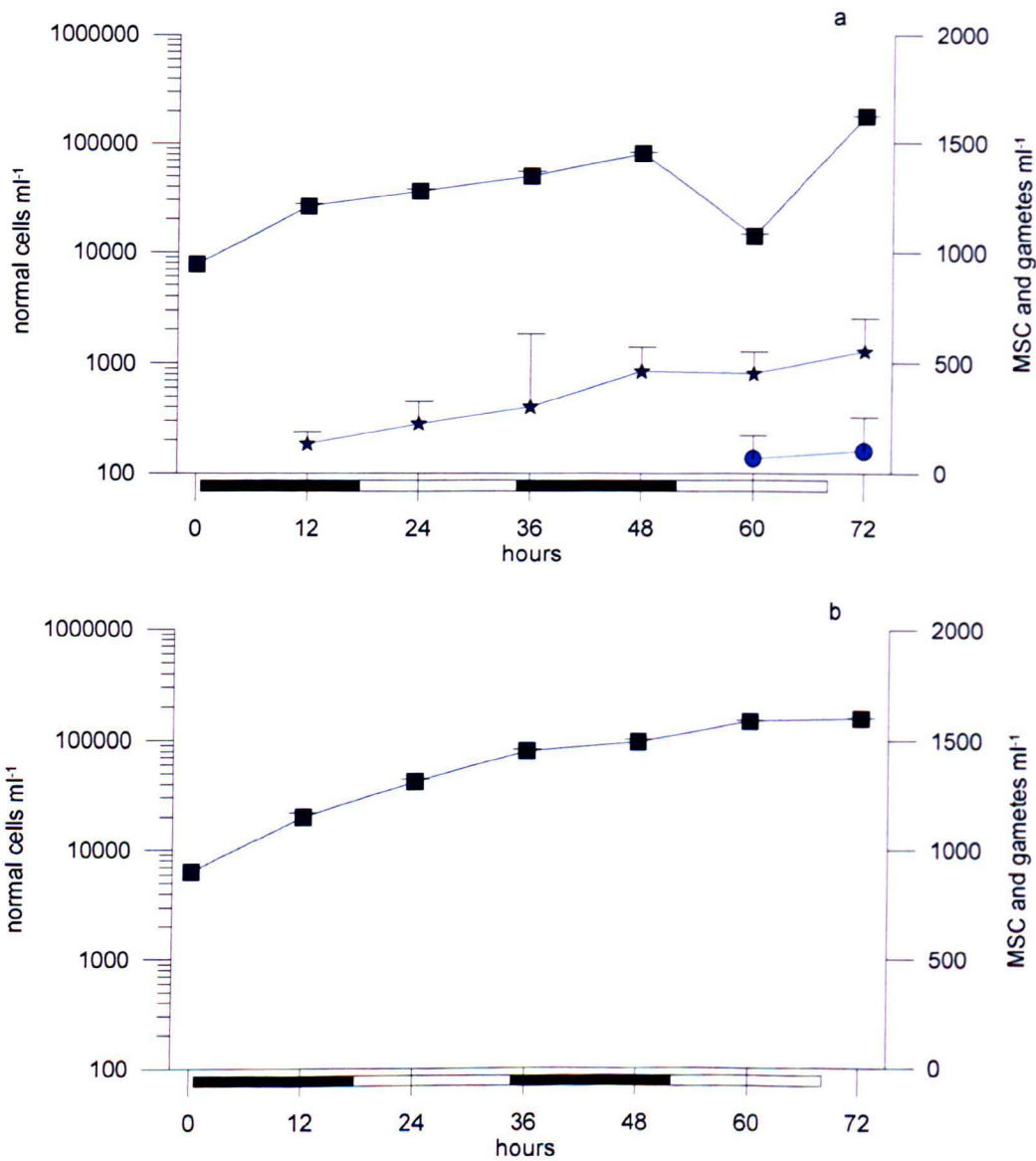


Figure 4.10. Experiment#2a. (a) Production of gametes in the ‘+’ Sy793S strain incubated in the medium conditioned by the opposite mating type ‘-’ Sy686 L and in (b) the medium conditioned by its own growth. On the left y axis, cell concentration ($\text{cells}\cdot\text{ml}^{-1}$) of the parental strains (blue squares); on the right y axis, concentration of sexual stages ($\text{sexual stages}\cdot\text{ml}^{-1}$): blue stars, ‘+’ meiotic cells with segregated cytoplasm (MSC); blue circles, ‘+’ round gametes. The black and white bars below the x axis indicate the Light:Dark cycle.

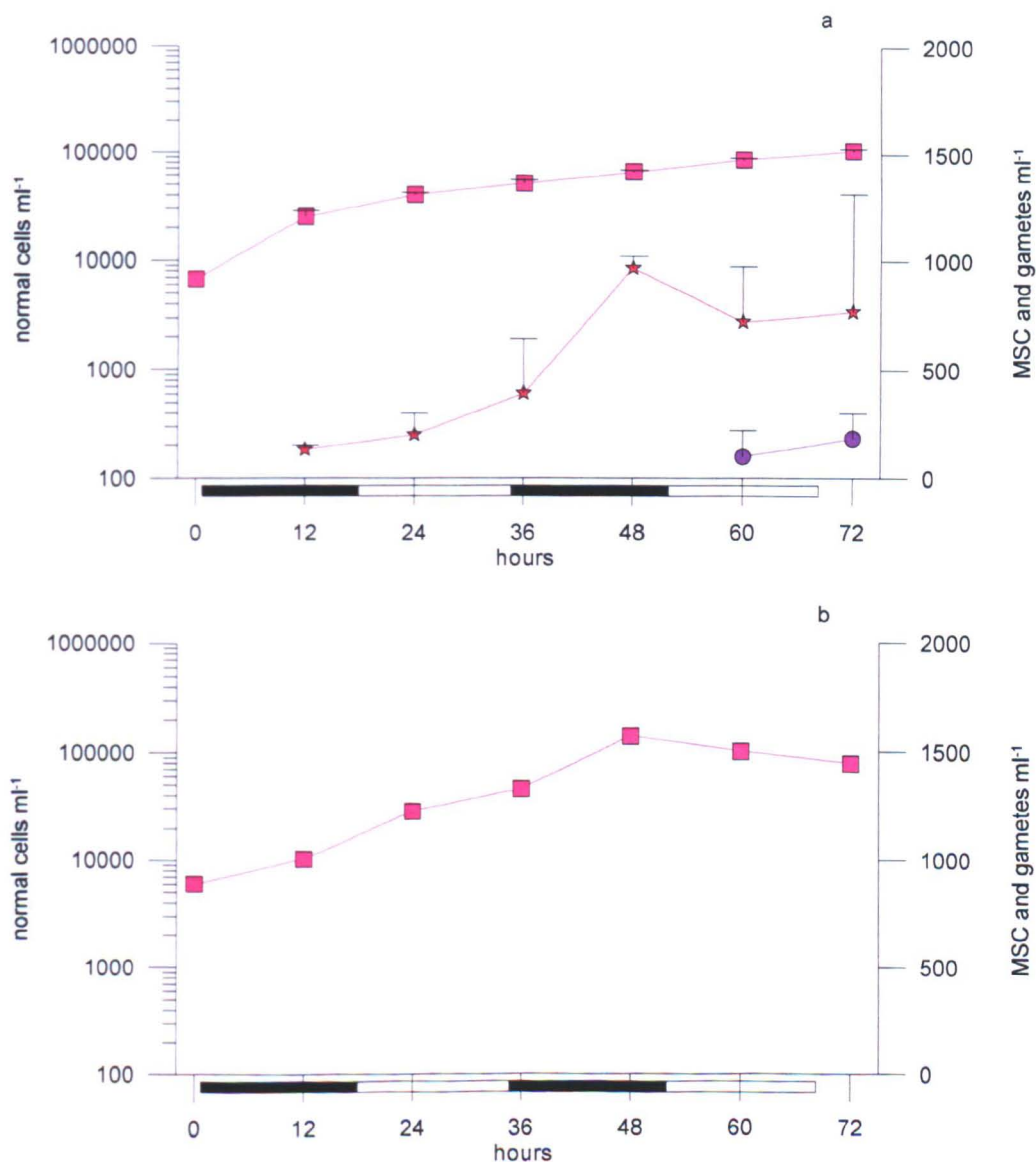


Figure 4.11. Experiment#2a. (a) Production of gametes in the '-' Sy686 L strain incubated in the medium conditioned by the opposite mating type '+' Sy793S and in (b) the medium conditioned by its own growth. On the left y axis, cell concentration ($\text{cells} \cdot \text{ml}^{-1}$) of the parental strains (pink squares); on the right y axis, concentration of sexual stages ($\text{sexual stages} \cdot \text{ml}^{-1}$): pink stars, '+' meiotic cells with segregated cytoplasm (MSC); pink circles, '+' round gametes. The black and white bars below the x axis indicate the Light:Dark cycle.

When comparing the controls of the three experiments, which were carried out under the same experimental conditions and starting with roughly the same inoculum of parental cells, slight differences in the timing and abundance of the sexual stages were detected. In the first cross, MSC cells were found after 12 h, the round gametes were detected after a few hours and started increasing on the second day, reaching an average concentration of $120 \text{ MSC cell}\cdot\text{ml}^{-1}$ for each parental strain (Fig. 4.12). Few gametes turned into zygotes and a few auxospores were detected only at the end of the second day. The concentration of both parental stages was about $34\cdot 10^3 \text{ cell}\cdot\text{ml}^{-1}$ when MSC cells were detected. In the second cross, MSC cells and round gametes started to be detected later, at the end of the second day, as compared to the previous cross (Fig. 4.13). More zygotes and auxospores were produced in this cross and initial cells were recorded on the third day; we have to keep in mind that this experiment lasted one more day. The concentration of both parental stages was about $14\cdot 10^3 \text{ cell}\cdot\text{ml}^{-1}$ at the moment when MSC cells were detected. In the third cross, the dynamics and abundance of sexual stages was very similar to the previous one (Fig. 4.14). This time, also the paired gametangia were enumerated; they appeared 12 h after the inoculum. In all crosses the concentration of both parental stages did not increase over the duration of the experiment. Daily growth rates were around zero or even negative during the first and second day, which coincided with the appearance of the sexual stages. An exception was the '-' strain of the second control, where a growth rate of $0.7 \text{ div}\cdot\text{day}^{-1}$ was recorded during the second day. A very slight increase in growth was detected during the third day in the second and third controls.

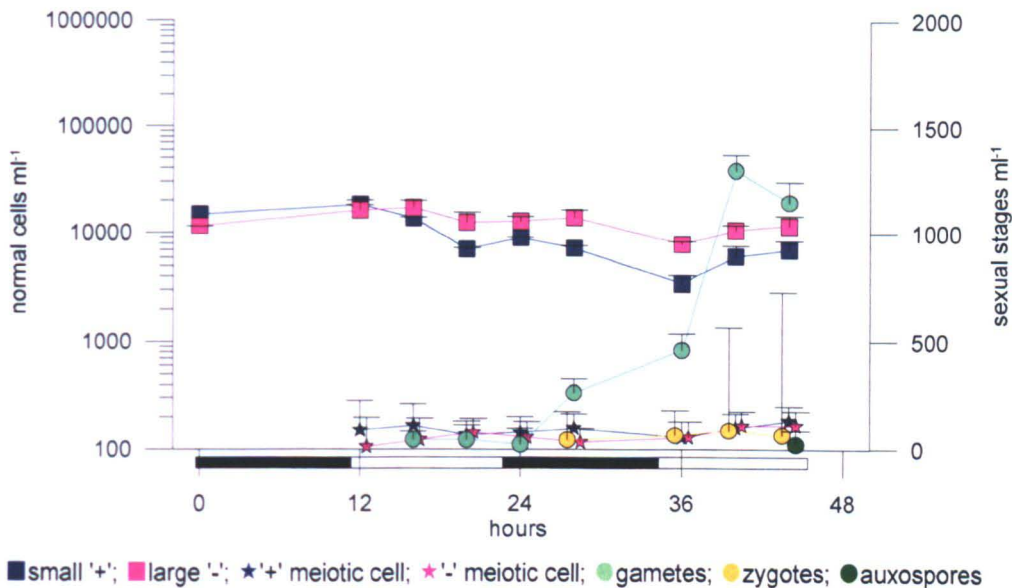


Figure 4.12. Experiment#2a.1. Control cross of the two parental strains (blue squares '+' Sy373 S, pink squares '-' Sy800 L). On the left y axis cell concentration of parental strains ($\text{cells}\cdot\text{ml}^{-1}$); on the right y axis concentration of the different sexual stages: blue stars, '+' meiotic cells with segregated cytoplasm (MSC); pink stars, '-' MCS cells; light green circles, round gametes; yellow circles, zygotes; green circles, auxospores. The black and white bars below the x axis indicate the Light:Dark cycle.

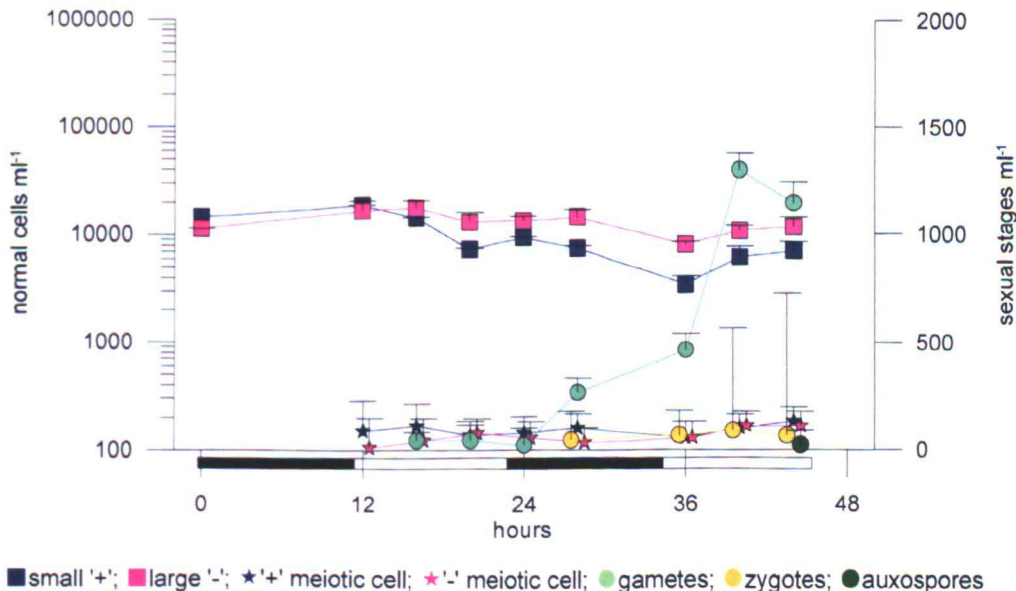


Figure 4.13. Experiment#2a.2. Control cross of the two parental strains (blue squares '+' Sy793 S, pink squares '-' Sy686 L). On the left y axis cell concentration of parental strains ($\text{cells}\cdot\text{ml}^{-1}$); on the right y axis concentration of the different sexual stages: blue stars, '+' meiotic cells with segregated cytoplasm (MSC); pink stars, '-' MCS cells; light green circles, round gametes; yellow circles, zygotes; green circles, auxospores; violet circles initial cells. The black and white bars below the x axis indicate the Light:Dark cycle.

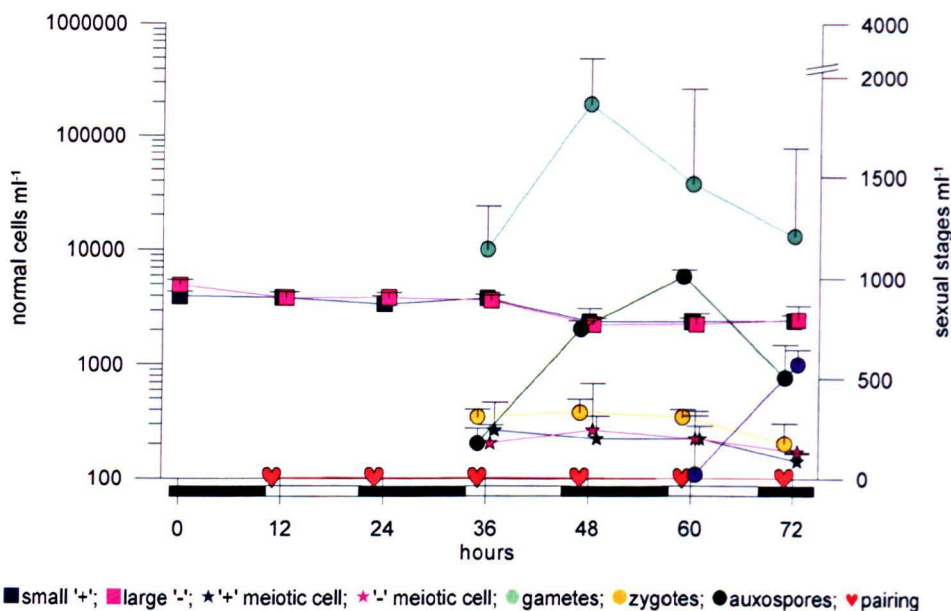


Figure 4.14. Experiment#2a.3. Control cross of the two parental strains (blue squares '+' Sy793S, pink squares '-' Sy799 L). On the left y axis cell concentration of parental strains ($\text{cells}\cdot\text{ml}^{-1}$); on the right y axis concentration of the different sexual stages: red hearths, paired gametangia; blue stars, '+' meiotic cells with segregated cytoplasm (MSC); pink stars, '-' MCS cells; light green circles, round gametes; yellow circles, zygotes; green circles, auxospores; violet circles, initial cells. The black and white bars below the x axis indicate the Light:Dark cycle.

In Experiment#2b the two mating types were physically separated by a membrane permeable to metabolites (Figs. 4.15 and 4.16). In the control cross, MSC cells and round gametes were detected starting from day 4, and the latter ones reached a concentration of 146 ml^{-1} on day 7. Fixed samples collected during the experiment were examined in epifluorescence microscopy to check for the presence of meiotic cells with segregated protoplasm and/or gametes. Cell counts were carried out starting from day 4. A considerable amount of meiotic cells with segregated protoplasm were detected in '+' strains, where a few round gametes were detected also on day7. The abundance of MSC stages in the '-' strains was, however, much smaller and these stages were not detected in all samples. These results suggest that the chemical compound secreted by the female is more powerful in inducing the formation of male gametes as compared to the male one.

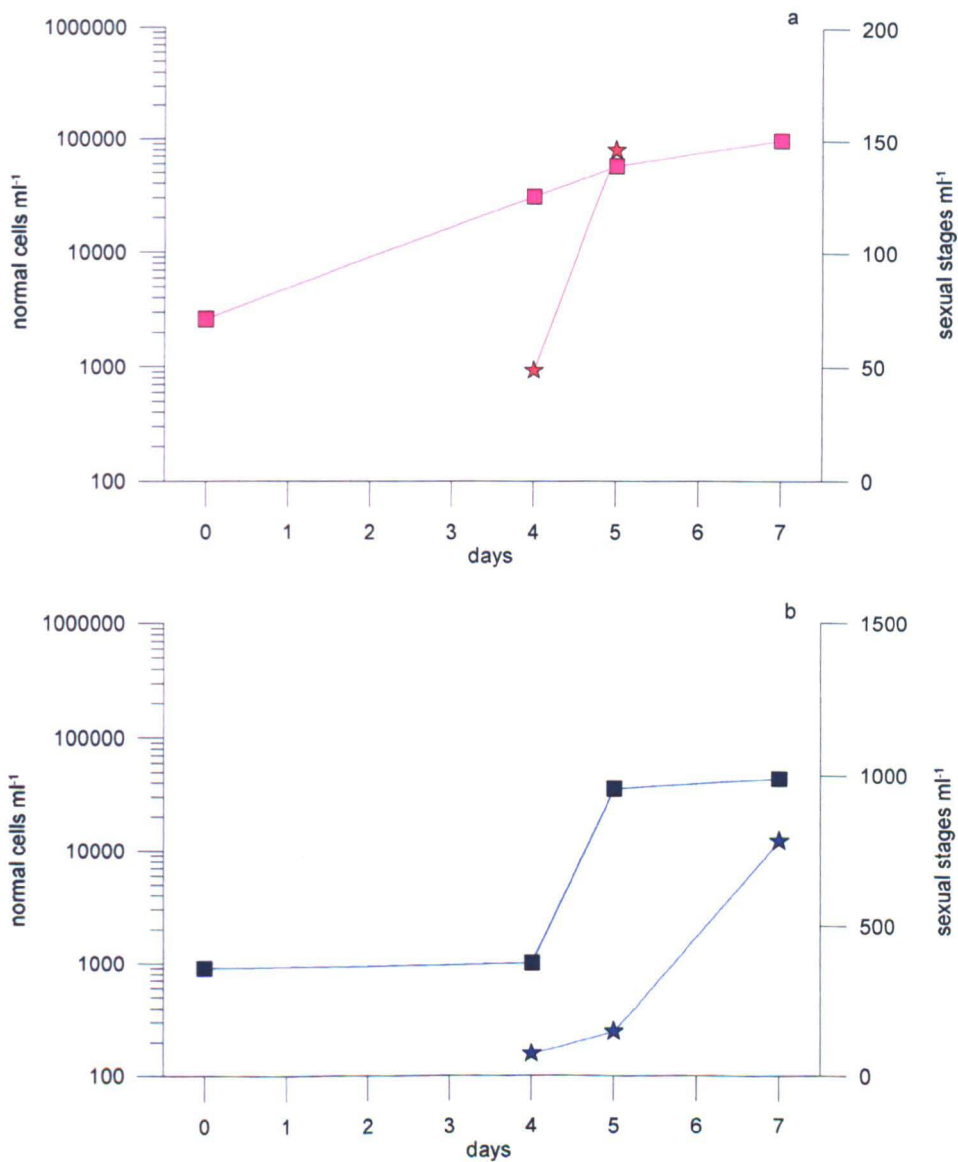


Figure 4.15. Experiment#2b. Concentration of the vegetative cells and the sexual stages of the two parental strains separated by the insert membrane: '-' Sy799 L (pink squares) above the insert and '+' Sy793S (blue squares) below the insert. On the left y axis, cell concentration (cells·ml⁻¹) of parental strains; on the right y axis, concentration of sexual stages (sexual stages ml⁻¹): blue stars, '+' meiotic cells with segregated cytoplasm (MSC); pink stars: '-' MSC cells, blue circles round '+' gametes and pink circles '-' round gametes.

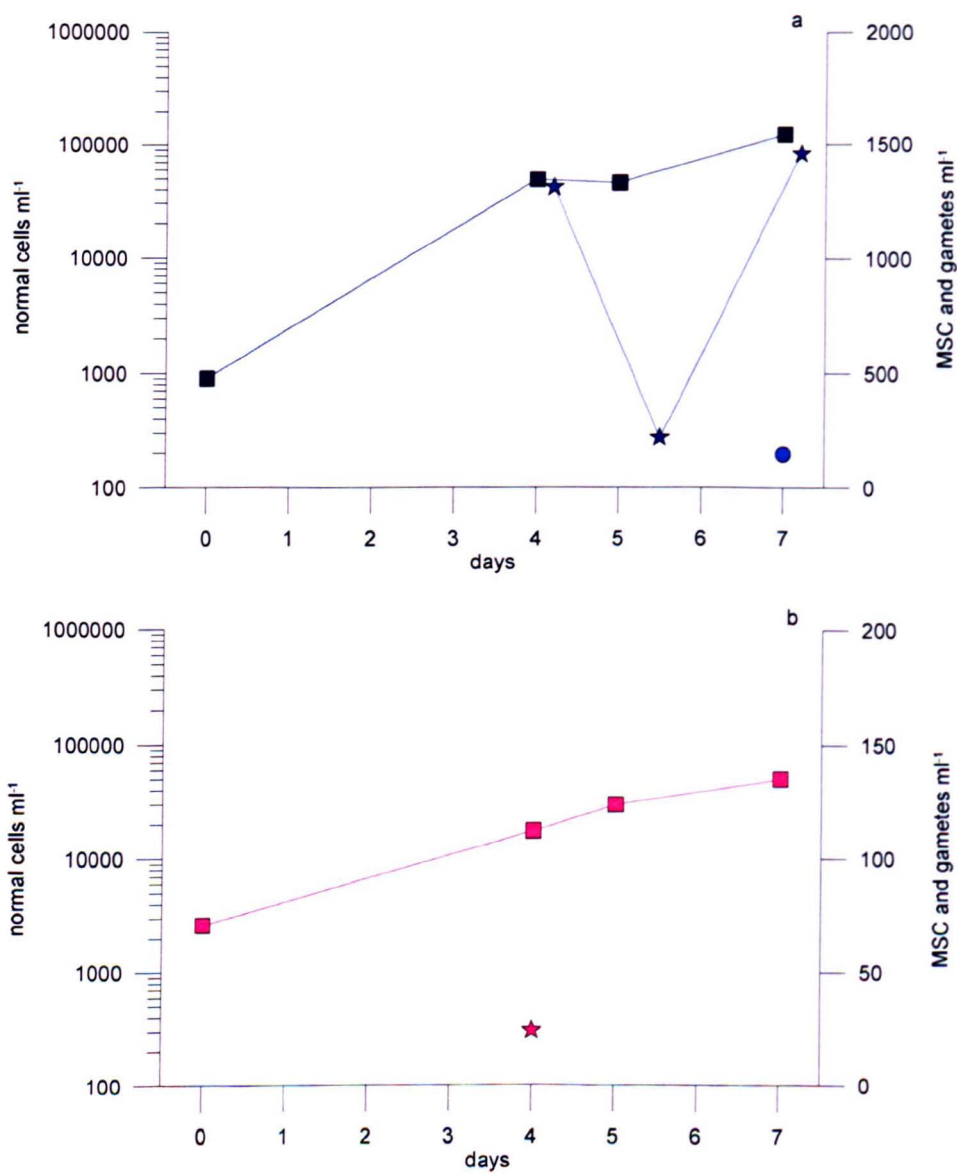


Figure 4.16. Experiment#2b. Concentration of the vegetative cells and the sexual stages of the two parental strains separated by the insert membrane: '+' Sy793S (blue squares) above the insert and '-' Sy799 L (pink squares) below the insert. On the left y axis, cell concentration (cells·ml⁻¹) of parental strains; on the right y axis, concentration of sexual stages (sexual stages ml⁻¹): blue stars, '+' meiotic cells with segregated cytoplasm (MSC); pink stars: '-' MSC cells, blue circles round '+' gametes and pink circles '-' round gametes.

4.3.3 Test for the presence of oxidative stress during meiosis/gametogenesis (Experiment#3)

The presence of reactive oxygen species (ROS) was not detected in the two monoclonal cultures of parental strains in exponential growth phase and in the crosses examined at various time intervals, including the one observed after 48 h after the inoculum in which sexual reproduction was ongoing. ROS were detected in the control treated with H_2O_2 , demonstrating that the staining protocol was working fine. A few cells stained with DH123 were detected only in the last sampling point of the exponentially-growing cultures, where dying cells with contracted cytoplasm were present (Fig. 4.17).

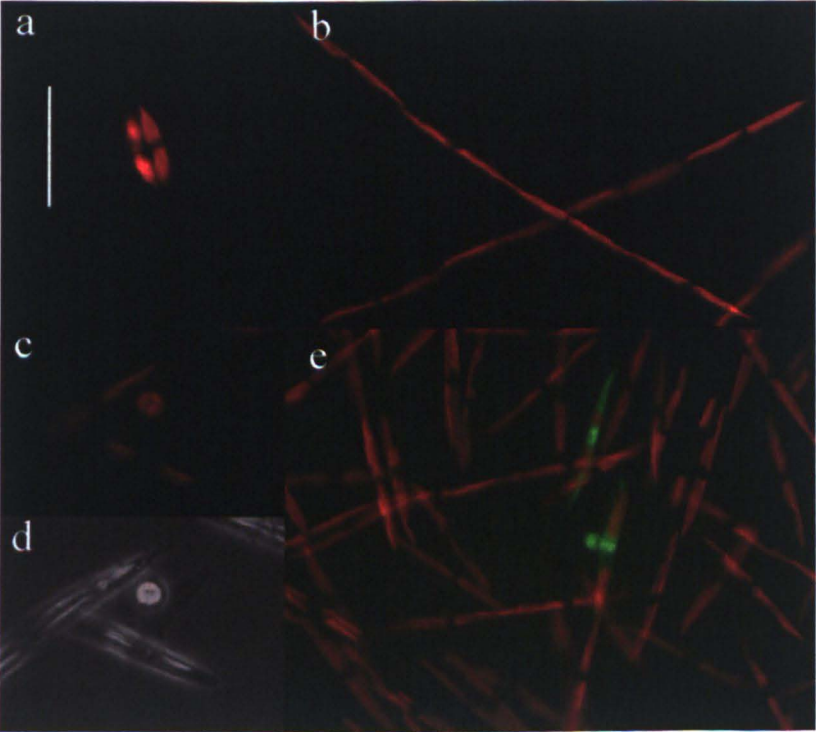


Figure 4.17. Micrographs of the two monoclonal cultures ‘+’ Sy793 (a), ‘-’ Sy686 (b, e), and the cross undergoing sexual reproduction (c and d) treated with the stain DHR123 that binds to reactive oxygen species (ROS) after 10’ (a), 40’ (b) and 48h (c, e) after the inoculum. Epifluorescence micrographs (a, b, c, e), bright field micrographs (d); scale bar = 25 μ m.

4.4 Discussion

The experiments described in this chapter provide evidence for the presence of a chemical mediator that induces the formation of gametes in *Pseudo-nitzschia multistriata* when strains are exposed to the medium of the opposite mating type. Nevertheless results provided by the two different approaches were quantitatively different (the results will be discussed in detail in the following sections). The arrest of growth of vegetative cells when sexual reproduction was initiated on other cells was much more evident in the experiments in which relatively high concentrations of the two mating types were inoculated together, while it was much less when co-cultures were started with lower concentrations of the two mating types.

4.4.1 *A diffusible compound promotes gametogenesis*

In the experiments carried out by incubating strains of the two mating types with medium from the opposite mating type and by the medium of a cross in which sexual reproduction was taking place, both gametangia containing gametes in the process of formation (the nuclei were parallel to the longitudinal axis of the cell and the cytoplasm was separate) as well as rounded gametes were observed. These results were obtained in two different experiments carried out with different strains. Neither gametangia in the process of gamete formation nor gametes were recorded in the controls in which parental strains were incubated with the culture medium conditioned by the presence of cells with the same mating type. This strongly suggests for the presence of a diffusible compound that induces gametogenesis in *P. multistriata*. However, the formation of gametes could not be observed in a third experiment carried out with another couple of strains. Possible explanations might be that: 1) the conditioned culture medium was collected at a very late stage of the growth phase and the pheromone-like compounds might have not been present, or their activity might have been masked by other compounds. The analysis of the exo-

metabolome of the diatom *Skeletonema marinoi* showed that the composition of the metabolites produced in culture vary considerably along over the growth phase of this diatom (Barofsky *et al.* 2009). Similar results were obtained when analysing the oxylipine composition of another diatom species, *Pseudo-nitzschia delicatissima* in which different ratios of oxylipines were detected along the growth curve, as well as the production of a specific compound towards the end of the growth phase of this diatom (d'Ippolito *et al.* 2009). 2) Another possibility is that the production of the pheromone-like compounds occurs with a different timing over the daily cell cycle. The collection of the medium to be used in the experiment was done during the day in all three experiments, but the precise timing cannot be reconstructed with precision. 3) Another possibility is that the compound was degraded in the third experiment due, probably to bacterial activity. The strains used in all experiments were not axenic and it might be that during the time between the medium collection and the beginning of the experiment (a few hours) the compounds were degraded.

Evidence for the presence of a chemical mediator inducing gametogenesis was also provided by the experiments in which strains were grown in the same medium but separated by a septum that prevented contact between cells. In this experiment, the number of gametes produced was higher in the male strains as compared to the female strains, suggesting a higher activity of the female strains in inducing the formation of gametes. This result was obtained both when the female strain was incubated in the upper portion of the culture well and also when incubated in the lower portion; therefore, a difference in the diffusivity can be ruled out.

The results of the experiments illustrated in this chapter suggest that two different compounds, with the same activity of inducing gamete formation are produced by the strains of opposite mating type in *P. multistriata*, or that both strains produce the same compound. The mechanism of gamete production in this raphid diatom seems to differ

from what has been reported in the araphid diatom *Pseudostaurosira trainorii* (Sato *et al.* 2011). In this species, the female strain produces a compound that induces the sexualisation of the male strain. Evidence for that was obtained by observing the production of gametes when incubating the males with the female filtrate, but not observing the production of gametes when incubating the female with the male filtrate. The formation of gametes in the female strain was only observed when incubating it with the filtrate of the male in which gamete formation was already induced. Therefore, in *Pseudostaurosira trainorii*, the sexualisation process includes two steps: first the induction of the formation of gametes in the male strain by the female and – only at this point – the male strain produces a compound that induces the formation of gametes in the female.

The production of pheromone-like compounds that mediate the induction of gametogenesis supports the observation that sexual reproduction in *P. multistriata* requires a threshold cell concentration to take place (Chapter 3). Almost no experimental data are available on the presence of chemical mediators inducing sexual reproduction in diatoms. In Bates and Davidovich (2002) there is mention of a thesis work in which a successful induction of gametogenesis was observed in a strain of *Pseudo-nitzschia multiseries* exposed to culture medium conditioned by a mixed cultures in which sexual reproduction was ongoing; unfortunately, data were not presented. In the review paper of Chepurnov *et al.* (2004), are reported the results of experiments carried out by Roshchin (1986) with the benthic diatom *Licmophora ehrenbergii*, where no auxosporulation was observed when cells of opposite mating type were inoculated on opposite sides of a Petri-dish. Gametogenesis was induced only when the distance between cells of opposite sex did not exceed the sum of their lengths. This is another indication that a threshold concentration is needed to induce sexual reproduction, i.e. to allow the perception of the chemical signal. It might be that this threshold concentration is different for benthic species that are attached

to a firm substrate and in planktonic species that live in a three-dimensional environment for which a 'strong' signal might be needed.

The production of pheromones has been detected in brown algae, which belong to the same Heterokontophyta lineage as the diatoms. In the brown algae, e.g. *Fucus*, *Ectocarpus*, the female gametes produce a pheromone that attracts the motile gametes (Kawai *et al.* 1994, Pohnert and Boland 2002). In these macroalgae it has been demonstrated that gametes from different species, *Fucus serratus* and *F. vesiculosus*, are mutually attracted, but cross fertilisation did not occur, although both use the same pheromone molecules. This suggests that species specific gamete recognition systems are present in these macroalgae to avoid cross fertilization between different species in the same environment. It would be interesting to investigate if similar systems also occur in diatoms. There are two reports of sexual reproduction in *Pseudo-nitzschia* species in the natural environment and in both of them sexual reproduction was observed in two species at the same time (Holtermann *et al.* 2010, Sarno *et al.* 2010). A possibility is that the pheromone-like compound that induces the production of gametes acts across species, but it would be interesting to test if barriers exist to avoid hybridization.

In this chapter, I also tested the possible presence of a mechanism based on the production of ROS in inducing the sexual phase in *P. multistriata*. This mechanism has been demonstrated for the colonial chlorophycean *Volvox carteri* where gametogenesis is induced by high levels of ROS (Nedelcu and Michod 2003, Nedelcu *et al.* 2004). The authors hypothesized that this is a demonstration that sex, and specifically meiosis, has been selected for the DNA-repair in eukaryotic lineages. However, no ROS production has been observed in *P. multistriata* crosses at different time from the inoculum, including the time at which sexual reproduction was occurring. This rules out that a similar mechanism exists for diatoms, or at least for *Pseudo-nitzschia* species.

4.4.2 *Cell density of vegetative cells during sexual reproduction*

In Chapter 3 it was shown that, in crosses in which sexual reproduction is taking place, the number of cells did not reach the concentrations comparable to those reached by the parental strains in monoculture. This observation was confirmed also by the three control tests of Experiment#2a. They were inoculated with roughly $10 \cdot 10^3$ cells·ml⁻¹ of each parental strain but almost no increase in cell concentration was observed after 2 or 3 days (depending on the length of the experiment). In Figure 4.4, which shows the growth curves of single strains, the exponential growth phase lasted until cell concentrations reached $1 - 200 \cdot 10^3$ cells·ml⁻¹. This is similar to values that were observed when co-culturing strains of the same mating type. The formation of sexual stages in the crosses only accounts for a limited percentage of the biomass and does not explain the marked differences in cell number. The apparent arrest of growth observed in the three control experiments can be compared with what was observed in the test of the T2 and T4 of Experiment#1 (the crosses carried out mixing parental strains at different growth phases/cell concentration, see Figs. 3.6, 3.7) and in the test at T2 – T8 of Experiment#2 (the crosses carried out mixing parental strains at different growth phases but same cell concentration, see Figs. 3.11, 3.12).

Experiment#1 of this chapter was planned to test the link between the occurrence of sexual reproduction and the growth of parental strains but, in this case, the initial cell concentration was set much lower, about 150 cells·ml⁻¹ for each strain, comparable to the starting conditions of the experiments begun at T0 and illustrated in Chapter 3 (see Figs 3.6, 3.7, 3.11 and 3.12). In these latter crosses, however, the reduction of growth of vegetative cells was more marked, although with variable rates between the 4 different tests. Nevertheless, Experiment#1 that was carried out with strains of different size, provided another puzzling piece of information: at the start of the co-culture, parental strains grew with similar rates but (coincident with the appearance of gametes) the ‘+’

strain showed lower growth and the biomass reached by this mating type was much smaller. This different response was observed when using both large and small '+' and it can, thus, rule out the fact that the slower growth rate could be attributed to cells size (D'Alelio *et al.* 2009a). If confirmed, this distinct response of the two mating types suggests that they are physiologically different and capable, for example, to perceive in a different way the effect of any compound excreted during sexual reproduction that can influence growth.

As mentioned before, the decrease in growth rate when two strains of opposite mating type are cultured together, seems to be connected to the cell concentration at which the cross was started, which in turn, is also connected to the success of sexual stages. When the inoculum was small, the percentage of sexual stages was not extremely high but the growth of the parental strains might be inhibited (see the different cases in the T0 experiments in Chapter 3, Figs 3.6, 3.7, 3.11 and 3.12); when the inoculum of the parental strains slightly increased, a sort of 'optimum' was reached where the highest percentages of sexual stages were produced. However, at this stage, the growth of the parental strains was also inhibited. At even higher abundances the percentages of sexual stages decreased again but, in this case, nutrient limitation might be an added complexity.

Chapter 5

Timing and success of sexual reproduction under
'mixed' and 'still' conditions

5.1 Introduction

The ecological and environmental conditions that favour the occurrence of sexual reproduction in diatoms, and more specifically in *Pseudo-nitzschia* species, are not fully understood (see Chapter 1 for an overview). The species belonging to the genus *Pseudo-nitzschia* have a heterothallic life cycle (Chapter 2): cells of two compatible mating types ('+' and '-') need to be in contact to allow sexual reproduction to occur. The only known exception is *Pseudo-nitzschia brasiliiana* that has a homothallic life cycle; this might represent an advantage, since it allows the production of auxospores and large sized initial cells without the need of finding cells of the opposite mating type (Quijano-Scheggia *et al.* 2009a). In *Pseudo-nitzschia multistriata*, the occurrence of sexual reproduction occurs later when the parental cell inoculum concentration in the cross is low, while it occurs sooner when it is more concentrated (Chapter 3). In experiments carried out with culture medium conditioned by the growth of the opposite mating type, the formation of gametes was induced, suggesting the presence of a chemical mediator (Chapter 4). Therefore, the results of this experimental work suggest that the onset of the sexual phase in heterothallic *Pseudo-nitzschia* species is a density-dependent event, i.e. the sexual differentiation starts in 'some' cells within a population only after a certain cell concentration is reached. The cell concentration should be linked to the production and perception of a chemical cue that acts as a signal of density.

Sexual reproduction of *Pseudo-nitzschia* species has been recorded also in the natural environment (Holtermann *et al.* 2010, Sarno *et al.* 2010). In both cases, the sexual event was recorded during a bloom and involved two different species, *P. australis* and *P. pungens* along the NW Pacific coast (Holtermann *et al.* 2010), and *P. cf. pseudodelicatissima* and *P. cf. calliantha* in the Gulf of Naples, Mediterranean Sea (Sarno *et al.* 2010). The density of *Pseudo-nitzschia* spp. during the sexual event spanned between

$187 \cdot 10^3$ and $929 \cdot 10^3$ cells \cdot L $^{-1}$ for both *P. australis* and *P. pungens* (cumulative values), while it was higher for *P. cf. pseudodelicatissima* (about $9.1 \cdot 10^6$ cells \cdot L $^{-1}$) and for *P. cf. calliantha* (about $7 \cdot 10^5$ cells \cdot L $^{-1}$). Although the vegetative cell concentration at which sexual events occurred in nature varied considerably, only the highest values - $9.1 \cdot 10^6$ cells \cdot L $^{-1}$ for *P. cf. pseudodelicatissima* - are similar to cell concentration values at which sexual reproduction occurs under controlled laboratory conditions ($2 - 10 \cdot 10^3$ cells \cdot ml $^{-1}$ that corresponds to $2 - 10 \cdot 10^6$ cells \cdot ml $^{-1}$, Chapters 3 and 4).

As a result, some questions arise: Where does sexual reproduction occur in the natural environment? Do cells often reach concentrations comparable to those recorded in the laboratory? The physical structure of the water column might be an important factor that helps reconciling the apparent mismatch between field and laboratory conditions. Recent studies showed that along the water column, thin layers (TLs) of phytoplankton cells can be present (Durham and Stocker 2012). Different mechanisms can be responsible for the formation of these layers such as accumulation due to physical processes (e.g. vertical gradients of horizontal velocity due to shear, advection), active accumulation of phytoplankton cells (as in the case of actively swimming dinoflagellates), active buoyancy regulation (as in the case of aggregates of the large diatoms *Rhizosolenia*) or active *in situ* growth due to e.g. optimal light or nutrient conditions coupled with vertical density gradients in the water column. Thin layers can have a thickness spanning from the order of centimetres to a few meters (<5 m), can extend horizontally for kilometres and persist for days. The TLs can be rapidly destroyed by turbulence due to wind and/or to changes in water density (salinity, temperature). The small vertical structure that characterizes TLs makes them difficult to detect by conventional sampling and profiling instruments (McManus *et al.* 2008). In fact, the discrete sampling with Niskin bottles averages out the fine scale vertical dimension of the water column (Rines *et al.* 2002).

Planktonic organisms in TLs are more abundant than in the water immediately above or below it (Rines *et al.* 2002, Velo Suárez *et al.* 2008). Several *Pseudo-nitzschia* species (*P. australis*, *P. cf. pseudodelicatissima*; *P. fraudulenta*; *P. multiseriata* and *P. pungens*) have been frequently recorded in TLs with cells density comprised between $5 \cdot 10^4$ and $3.3 \cdot 10^6$ cells·l⁻¹, which were between 2.8 and 3.3 times higher as outside the TLs (McManus *et al.* 2008, Rines *et al.* 2002, Ryan *et al.* 2005, Sullivan *et al.* 2005, Velo Suárez *et al.* 2008). Single cells and colonies of *P. cf. pseudodelicatissima* were observed together with colonies of *Chaetoceros socialis* (Rines *et al.* 2002, Velo Suárez *et al.* 2008); and this association persisted for 3 weeks (Rines *et al.* 2002). The aggregation of phytoplankton cells in TLs or in low turbulence environments can increase the probability of mating success, due to higher cell concentration, or to the fact that other species might provide the substrate on which cells can migrate towards to the opposite mating types (Lelong *et al.* 2012).

In this chapter, I present the results of an experiment aimed at testing differences in success and timing of sexual reproduction in crosses incubated on: i) a rotating wheel that induced a gentle mixing of the water and ii) on a shelf under unmixed, still, conditions. All the other experimental conditions (initial cell concentration, temperature, irradiance, and photoperiod) were identical. The hypothesis was that mixed conditions impair the conjugation of gametangia that would be facilitated in still conditions. In the latter conditions, cells settle on the bottom of the culture flask and reach higher concentrations, which thus increases the chances of either random encounters and/or success of chemical signalling. Monoclonal parental cultures were used, as controls in both conditions, to test the possible effect of the rotating wheel on growth dynamics. In this experiment, the concentration of the major nutrients, in the culture medium, was also tested over the time course of the experiment.

5.2 Material and methods

5.2.1 Culture isolation and maintenance

Single cells or short chains of *Pseudo-nitzschia multistriata* were isolated with a micropipette from net samples collected at the Long-Term Ecological Research station Mare Chiara (LTER-MC) in the Gulf of Naples in July 2010 (Table 5.1). The cultures were grown in f/2 culture medium (Guillard 1975) prepared with oligotrophic seawater collected offshore in the Gulf of Naples. The f/2 medium was filtered through a 0.22 μm pore-size filter (Millipore, Filter Stericup GP SCGPU05RE, Billerica, MA, USA) just before use in order to eliminate precipitates. The cultures were maintained in a growth chamber at a temperature of 18 °C, a photoperiod of 12L:12D h, and a photon flux density of 60 $\mu\text{mol photons m}^{-2}\text{s}^{-1}$ provided by cool white fluorescent tubes (Phillips TLD 36W/950). When the cultures were established and before carrying out each experiment, 20 cells for each strain were measured at 400x magnification using a Zeiss Axiophot light microscope (Carl Zeiss, Oberkochen, Germany) equipped with an ocular micrometer.

5.2.2 Calculation of growth rate

Cell concentration was estimated on a sub-sample fixed with formaldehyde solution at a final concentration of 1.6 %. A 1-ml aliquot was used to fill a Sedgewick Rafter counting slide and cells were enumerated on the Zeiss Axiophot light microscope. Growth rate was expressed as divisions $\cdot\text{day}^{-1}$ and was estimated from a semi-log plot of successive counts (cells $\cdot\text{ml}^{-1}$) over time. This method permits a ready identification of the period of exponential growth. A straight line was drawn to identify the slope of the portion of the graph representing the exponential growth. A least-squares regression was applied to the log (base10) data (K_{10}). A logarithmic transformation from log base10 to log base2, by multiplying $K_{10}\cdot 3.322$, was used to obtain the number of divisions $\cdot\text{day}^{-1}$ (Guillard 1980).

5.2.3 'Mixed' and 'calm' conditions

The aim of this experiment was to compare the timing of sexual reproduction and the abundance of sexual stages produced in two different conditions where the culture flasks were incubated i) on a rotating wheel that produced a slow and regular mixing avoiding the formation of stratification (mixed condition) and ii) on a shelf in complete absence of physical disturbance (calm condition). Parental strains Sy793 (small '+' mating type) and Sy799 (large '-' mating type) different in size have been used for this experiment (Table 5.1).

Table 5.1. Strains of *Pseudo-nitzschia multistriata* used for the experiments illustrated in this chapter. For each strain are reported: the strain code and the mating type, the isolation date, the LTER-MC sample code, the average length of the apical axis at the moment in which the cultures were established (I), and the average length (\pm standard deviation) of the apical axis at the moment in which the experiments were carried out (II).

Strain code	Isolation date	LTER-MC	Apical axis (μm) I	Apical axis (μm) II
Sy793 '+'	21/09/2010	931	34	22.7 ± 2.9
Sy799 '-'	21/09/2010	931	53	30.0 ± 2.5

Two 250 ml flasks, one for each parental strain, were filled with 240 ml of f/2 filtered medium and inoculated with cells at final concentration of about $3,000 \text{ cells}\cdot\text{ml}^{-1}$. Aliquots of 30 ml of were dispensed, after careful mixing, in 8 of 70 ml flasks. The stock co-culture of the two parental strains was prepared in a 1,200 ml flask filled with 1,140 ml of f/2 filtered medium and inoculated with cells at final concentration of about $1,500 \text{ cells}\cdot\text{ml}^{-1}$ for each parental strain ($3,000 \text{ cells}\cdot\text{ml}^{-1}$ in total). This initial cell concentration was optimal to get a high percentage of sexual stages (Chapter 3). Aliquots of 30 ml of were dispensed, after careful mixing, in 38 of 70 ml flasks. For each parental strain and for the crosses, half of the flasks were placed on the rotating wheel (RW) and the other half were placed on a shelf (SH). The rotating wheel and the shelf were located in a walk-in

climatic chamber at a temperature of 18°C and a photoperiod of 12L:12D h. The integrated irradiance at which cultures were exposed on the rotating wheel was 65 $\mu\text{mol photons m}^{-2}\text{s}^{-1}$ (110 $\mu\text{mol photons m}^{-2}\text{s}^{-1}$ at the top; 35 $\mu\text{mol photons m}^{-2}\text{s}^{-1}$ at the bottom), which was the same as the one on the shelf. The rotating wheel was set at a 0.1 rpm; this rotation velocity caused a gentle and constant mixing of the cultures.

To monitor the growth rate of the individual parental strains at the two different conditions (RW and SH), 2 ml of culture were sub-sampled from each parental strain every two days (= 10 sampling points) from one flask on the rotating wheel and from one on the shelf, they were placed in Eppendorf vials and fixed (Fig. 5.1). To monitor the growth rate and the production of sexual stages in the crosses, one flask from the RW and one from the SH were randomly collected every day (= 19 sampling points) (Fig. 5.1). From each flask, two subsamples of 3.5 ml were placed in two Eppendorf vials. All subsamples were fixed with formaldehyde solution at a final concentration of 1.6 % and stored in a fridge at 4 °C. For each parental strain, one ml of fixed culture was counted using a Sedgewick Rafter counting slide and live vegetative cells (cells with cytoplasm content) and dead cells (empty frustules) were enumerated using an Axiophot light microscope; the growth curve was plotted and the maximum growth rate was estimated as illustrated above. For the cross samples, one ml of fixed culture, in triplicate, was placed in a Sedgewick Rafter counting slide and the following stages were enumerated at the Axiophot light microscope: live vegetative cells (cells with cytoplasm content), gametes/zygotes, auxospores, initial cells, large F1 generation cells and dead cells (empty frustules). An empty frustule, recognised by absence of the chloroplasts, is composed by epi- and hypotheca and it was counted as a single dead cell. However, I cannot rule out the possibility to have counted a single theca as one dead cell.

Nutrient concentration in the monoclonal cultures was measured four times (T0, T6, T12 and T18), while in the crosses nutrient concentration was measured at each

sampling point. Twenty ml of each culture (from the bottle from which the sample for cell enumeration was collected) were filtered through a MILLEX-GS filter unit with a 0.22 μm pore size (MILLIPORE, Carrantuohill, Co. Cork, Ireland) using a 60 ml syringe. Filters, high density polyethylene vials, and syringes were washed with bi-distilled water (DDW) before the filtration and high density polyethylene vials were rinsed with the sample before filling them. The filtered samples were placed at $-20\text{ }^{\circ}\text{C}$ until the analysis. The samples were analysed for nitrate (NO_3^-), nitrite (NO_2^-), ammonia (NH_4^+), orthophosphates (PO_4^-) and silicate (SiO_4) using a FlowSys Systema Autoanalyzer, equipped with five continuous flux channels, following Hansen and Grasshoff (1983). The analyses have been carried out by Augusto Passarelli and Francesca Margiotta (MECA, Stazione Zoologica Anton Dohrn).

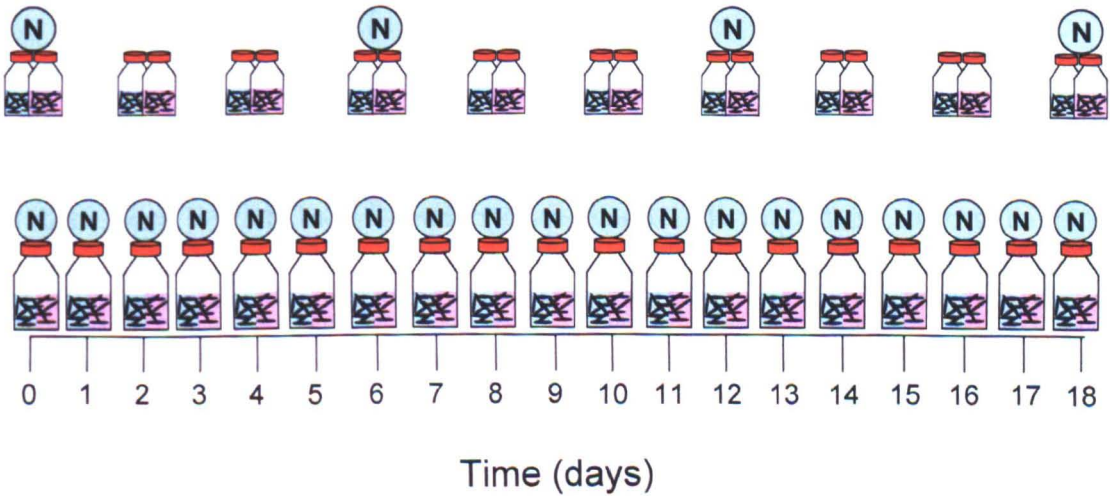


Figure 5.1. Schematic drawings of the experimental set-up. Two kinds of flasks were placed both on the rotating wheel and on a shelf and sampled in the same days: 20 flasks with monoclonal cultures (blue for '+' and pink for '-'), and 18 flasks with co-cultures/crosses of the two mating types (blue and pink). The circle with 'N' indicates the time at which the nutrient analyses were carried out.

5.3 Results

Sexual reproduction occurred in all crosses of *P. multistriata* incubated on the rotating wheel (RW) and on the shelf (SH). As hypothesized, the slow constant mixing given by the rotating wheel impaired sexual reproduction, but it did not impair the growth of monoclonal parental strains.

5.3.1 Growth dynamics of the individual parental strains on RW and SH

The two parental strains grown in monoculture showed a different growth dynamics on RW and SH (Figs 5.2 and 5.3). The small '+' strain reached the maximum cell concentration on days 10 ($526 \cdot 10^3$ cells·ml⁻¹) and 8 ($172.6 \cdot 10^3$ cells·ml⁻¹) on RW and SH, and, in RW and SH respectively. The exponential growth phase was similar between the two treatments for '+' strain: it lasted 8 days and maximum growth rate was 1.01 div·day⁻¹ on RW and 0.79 on SH). The large '-' strain reached the maximum cell concentration on day 4 in both conditions ($172.6 \cdot 10^3$ cells·ml⁻¹ on RW and $529.5 \cdot 10^3$ cells·ml⁻¹ on SH). The exponential growth phase was thus much shorter than that of the '+' stain, and the maximum growth rate was 1.69 div·day⁻¹ on RW and 1.99 on SH. In both strains, the exponential growth phase was followed by a more or less short stationary phase and then by a rapid decline of vegetative cell concentration.

Nitrate concentration in the f/2 medium is extremely high; this nutrient declined over the exponential growth phase but its concentration remained high. The concentration of silicate instead reached undetectable values on day 12 (with the exception of the '-' culture on RW), but possibly also before that day, considering that the sampling was done every 4 days. In all conditions silicate concentration slightly increased in the last sampling point (day 18) showing that this element became available due to frustule dissolution. Also the concentration of orthophosphate reached undetectable values at day 12. The

concentration of nitrite (NO_2^-) and ammonium (NH_4^+) showed an opposite trend to the other nutrients. Their concentration at time 0 was very low and started to increase in concomitance with the end of exponential phases of vegetative cells; nitrite between 3 and $15 \mu\text{mol}\cdot\text{L}^{-1}$, on both RW and SH; and ammonium between 25 and $80 \mu\text{mol}\cdot\text{L}^{-1}$, on RW and between 3 and $10 \mu\text{mol}\cdot\text{L}^{-1}$ on SH (data not shown).

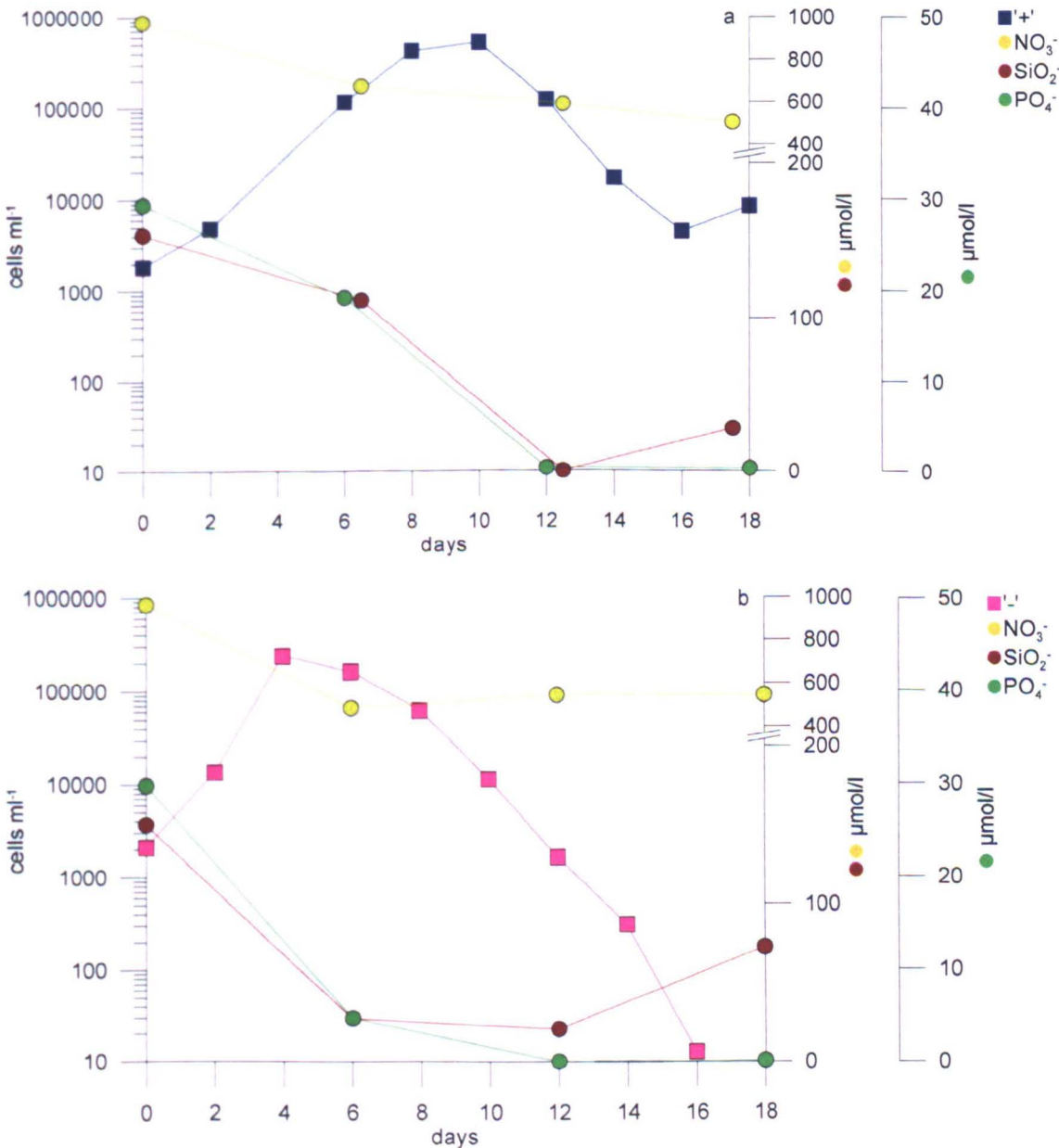


Figure 5.2. Cell concentration of the two parental strains in monoclonal culture and concentration of nutrients on the rotating wheel (RW); '+' strain (blue square, panel a) and '-' strain (pink square, panel b). On the left axis, cell concentration ($\text{cells}\cdot\text{ml}^{-1}$); on the two right axes, nutrient concentration with different scales ($\mu\text{mol}\cdot\text{L}^{-1}$; yellow circles nitrate, brown circles silicates, green circles orthophosphates).

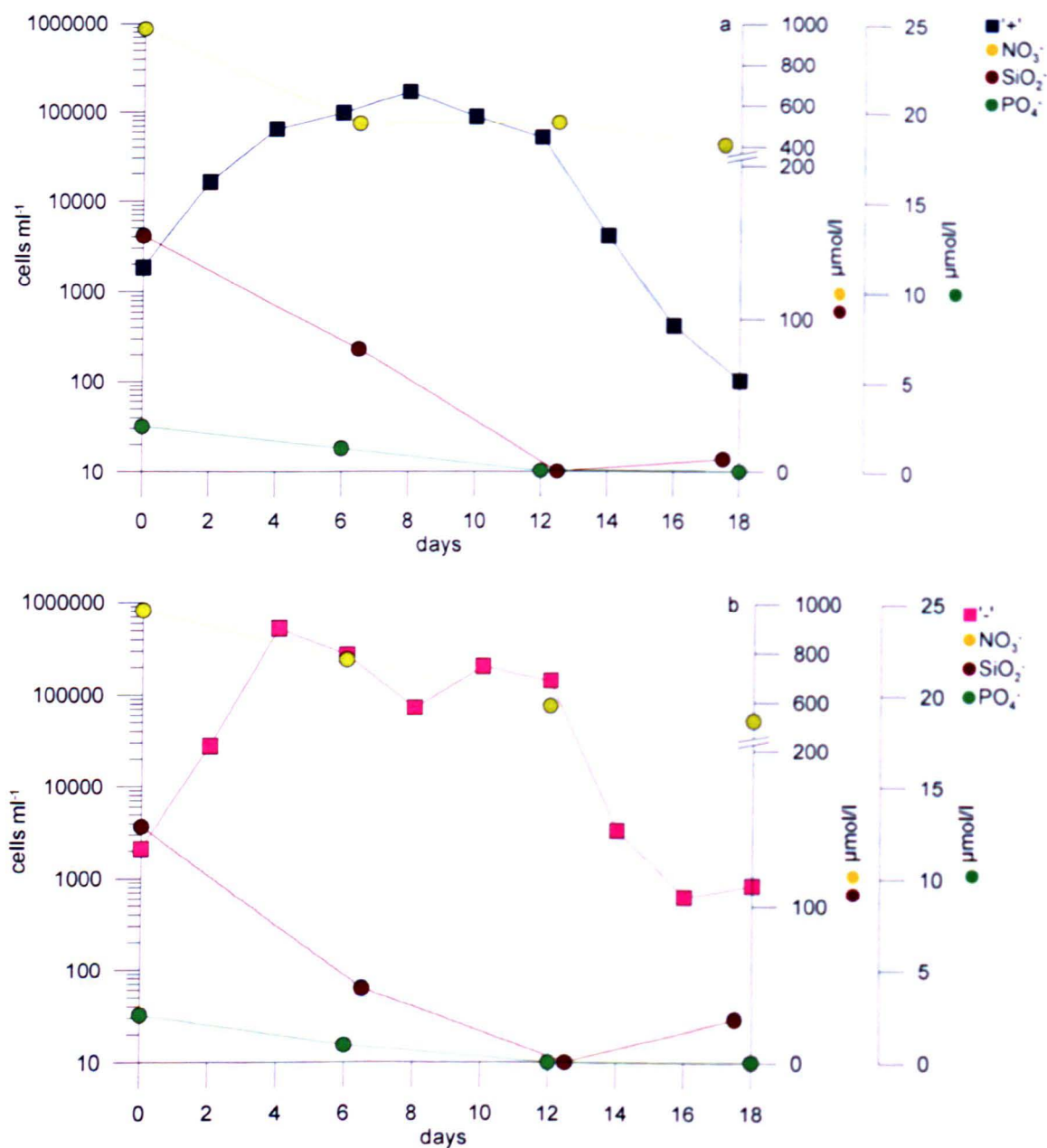


Figure 5.3. Cell concentration of the two parental strains in monoclonal culture and concentration of nutrients on the shelf (SH); '+' strain (blue square, panel a) and '-' strain (pink square, panel b). On the left axis, cell concentration (cells ml^{-1}) ; on the two right axes, nutrient concentration with different scales ($\mu\text{mol l}^{-1}$; yellow circles nitrate, brown circles silicates, green circles orthophosphates).

5.3.2 Growth dynamics and sexual reproduction of the co-cultures of the two parental strains on RW and SH

The total number of *P. multistriata* cells (parental cells, sexual stages and large F1 generation), i.e. the total biomass that developed in the flasks, showed a different growth dynamics between the two experimental setups (Fig. 5.4). In both setups, a lag-phase was observed that, in the case of the SH, corresponded to a considerable decrease in cell concentration. On RW the exponential phase lasted till day 10 ($1.27 \text{ div}\cdot\text{day}^{-1}$), while on SH it was much longer, till day 14 ($0.57 \text{ div}\cdot\text{day}^{-1}$). The total maximum cell density reached was $558\cdot 10^3$ and $330\cdot 10^3 \text{ cells}\cdot\text{ml}^{-1}$, on RW and SH, respectively. At the end of the exponential phase, cell concentration started to decrease on RW, but this decline was lasting only a few days, after which cell concentration increased, with a growth rate of $1.02 \text{ div}\cdot\text{day}^{-1}$ (Fig. 5.4a).

Also in the crosses, nitrate concentration declined over the exponential growth phase but its concentration remained very high. Nutrient concentration (nitrate, silicate and orthophosphates) decreased considerably on the first sampling day (two days after the inoculum) but resumed the concentration from the 2nd day on RW, so the 3rd day the nutrient concentrations were like the beginning (Fig. 5.4a). Silicate concentration did not vary a lot until day 6 on RW and till day 11 on SH, but then rapidly decreased and, within about 5 days, reached almost undetectable values; on RW an increase in concentration was observed during the last 2 days. The orthophosphates followed a similar trend, reaching undetectable values on day 10 on RW and on day 16 on SH.

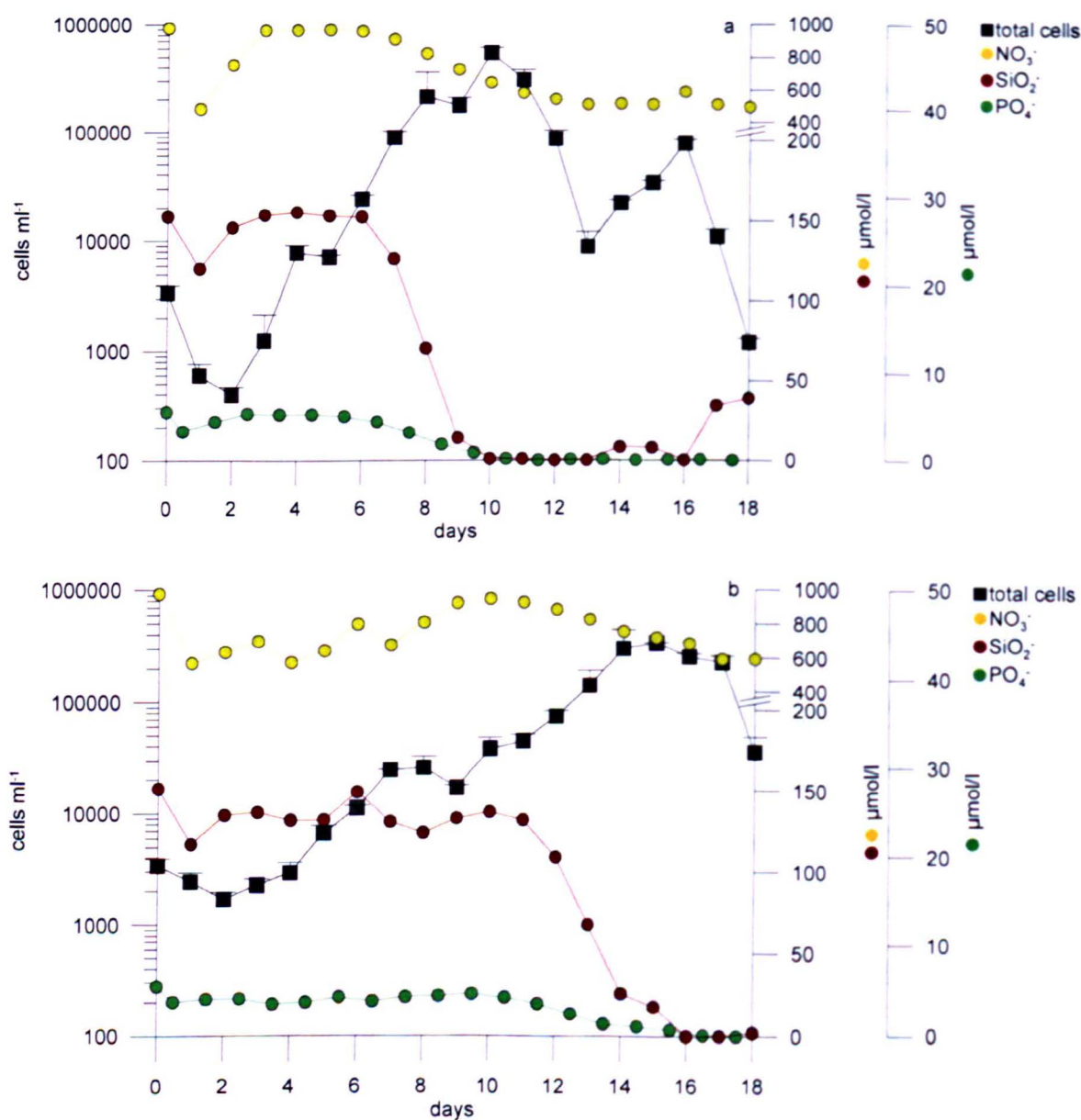


Figure 5.4. Cell concentration of the two parental strains in co-culture and concentration of nutrients on the rotating wheel (RW, panel a) and shelf (SH, panel b). On the left axis, concentration ($\text{cells} \cdot \text{ml}^{-1}$, grey squares) of the total number of cells: parental strains + sexual stages + large F1 Cells generation, where each point represents the average value of triplicates counts and st.dev. is represented with vertical bars. On the two right axis, nutrient concentration with different scales ($\mu\text{mol} \cdot \text{l}^{-1}$; yellow circles nitrate, brown circles silicates, green circles orthophosphates).

Sexual reproduction successfully occurred on both the RW and the SH. In Figure 5.5, the total amount of cells represented in Fig. 5.4 was split into '+' and '-' parental cells, total sexual stages and large F1 generation cells, to properly visualize and distinguish the dynamics of the vegetative cells from that of the sexual stages. In both RW and SH sexual

stages were recorded from the 2nd day after the inoculum. The decrease of the total cell biomass observed in the first days (mentioned above when illustrating Fig. 5.4) indeed corresponded to the time at which sexual reproduction started.

On RW, the general trend of the two parental strains reflected the dynamics of the total biomass, with an initial decrease in cell numbers, an exponential growth phase that lasted for 10 days (max. growth rate of 1.34 div·day⁻¹) for the '-' strain and 8 days (max. growth rate of 0.93 div·day⁻¹) for the '+' one followed with a decrease in abundance till day 12, a subsequent second increase until day 16, and a final decrease (Fig. 5.5a). The '+' strain had the same abundance as the '-' strain until day 4, but then it always showed considerably lower cell concentration values. Large F1 vegetative cells were recorded after a few days from the appearance of gametes and their abundance trend paralleled that of parental strains. Their maximum growth rate was 1.44 div·day⁻¹ (Fig. 5.5a). Gametes and auxospores were found from the 2nd day, while initial cells were observed on day 4 and 5 (Fig. 5.6a). Sexual stages were very rare in the flasks incubated on the RW: the maximum sexual stage concentration was 21 cells·ml⁻¹.

Also on the SH, the trends of cell concentration of the two mating types reflected that of the total biomass: a lag-phase during the first days and a slightly undulating exponential phase that lasted until day 12 – 14. Due to the presence of 'ups and downs', it was not easy to localize the exponential portion of the growth curve. If we consider it as lasting between day 2 and day 14 for the '-' strain, a maximum growth rate of 0.57 div·day⁻¹ was reached. The '+' strain showed instead a marked decrease in abundance between day 6 and day 12, and it is difficult to select the interval for interpolating the data. Also on the SH large F1 cells were recorded on day 3 and they started growing exponentially until day 7, with a maximum growth rate of 1.81 div·day⁻¹ (Fig. 5.5b). On the SH, gametes and auxospores were found starting from the 2nd day while initial cells were observed from day 3 until day 6 (Fig. 5.6b). The maximum number of sexual stages was much higher as

compared to RW and their concentration reached $450 \text{ cells}\cdot\text{ml}^{-1}$, with a percentage of about 16 % over the total cell number.

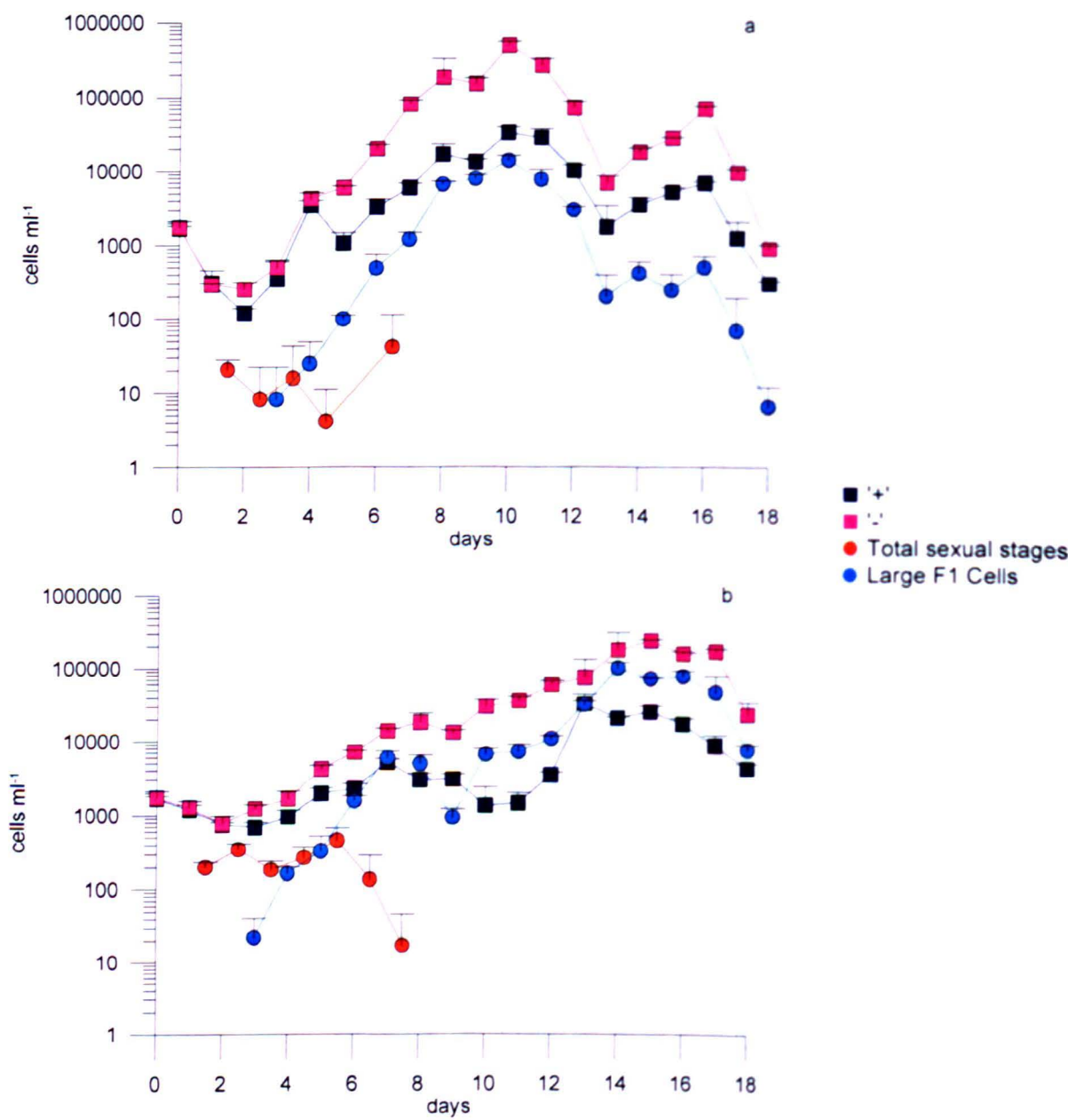


Figure 5.5. Cell concentration ($\text{cell}\cdot\text{ml}^{-1}$) of the two parental strains (blue square for '+' and pink square for '-'), sexual stages (orange circles for zygotes+auxospores+initial cells) and large F1 Cells generation (light blue circles) cells in co-cultures on the rotating wheel (RW, panel a) and shelf (SH, panel b). Each point represents the average value of triplicates counts; st.dev. is represented with vertical bars.

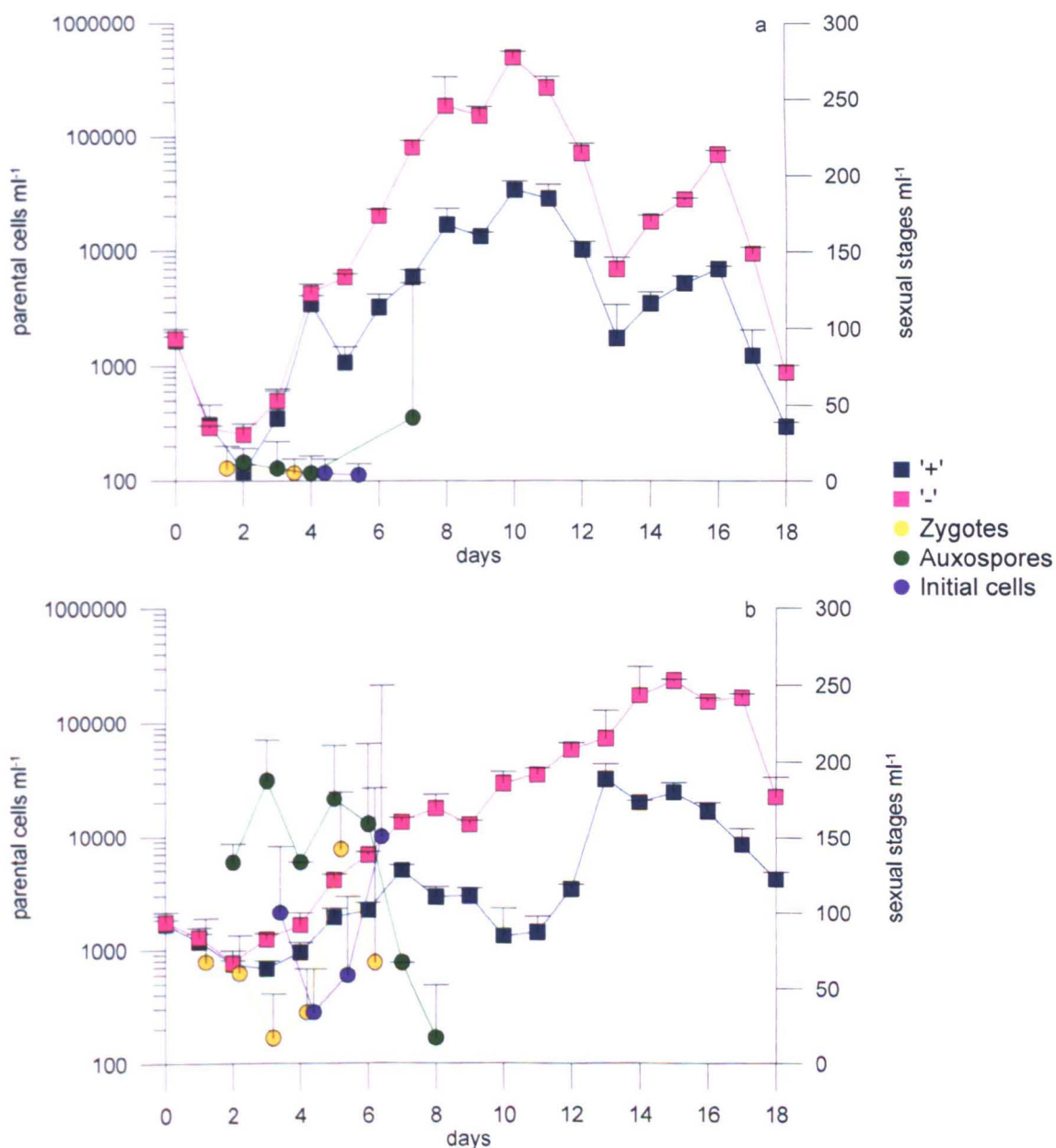


Figure 5.6. Cell concentration (cell·ml⁻¹) of the two parental strains (blue square for '+' and pink square for '-'), sexual stages (light yellow circles: gametes; green circles: auxospores and violet circles: initial cells) in co-cultures on the rotating wheel (RW, panel a) and shelf (SH, panel b). Each point represents the average value of triplicates counts; st.dev. is represented with vertical bars.

5.3.3 The dead cells

In this experiment, the empty frustules (= dead cells) were also enumerated. A considerable number of dead cells were recorded and their concentration generally followed the trend of living cells both on RW and SH, in both monoclonal cultures and crosses (Figs 5.7 and 5.8). The same trend was also observed in the large F1 generation; also in this case cells started to die even during the exponential growth phase (Fig. 5.9).

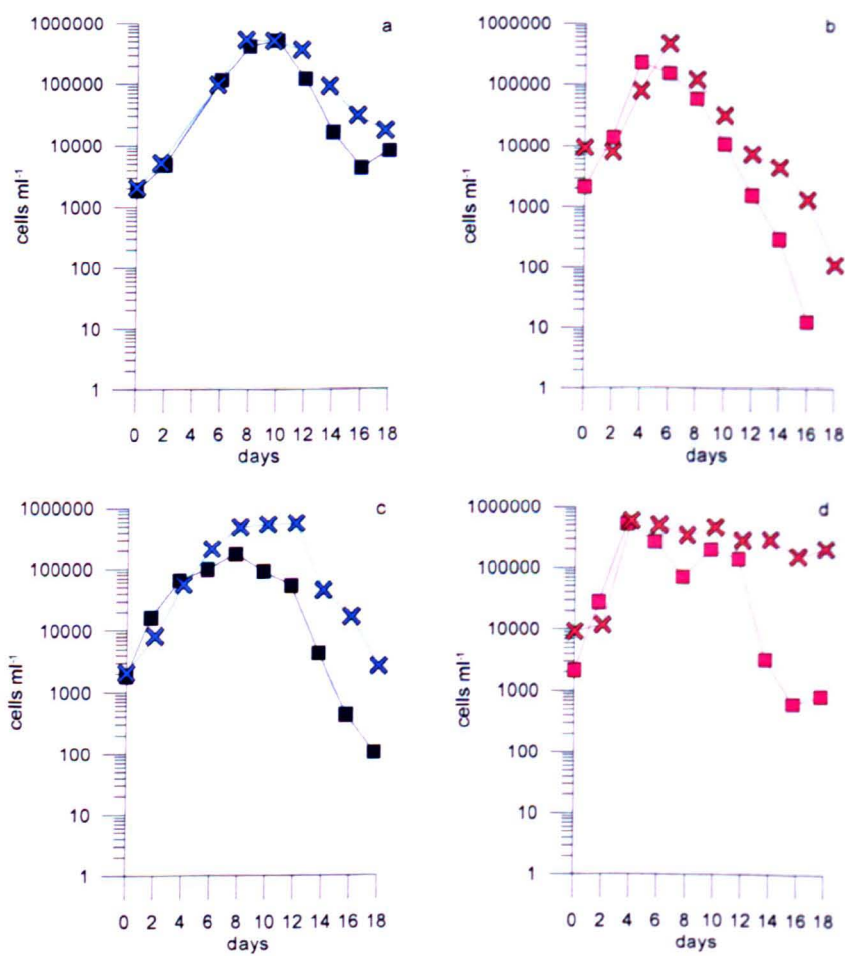


Figure 5.7. Cell concentration (cells·ml⁻¹) of live (square) and dead (cross) cells of parental strains in monoclonal cultures on the rotating wheel (RW; in panel a '+' and in panel b '-') and shelf (SH, in panel c '+' and in panel d '-').

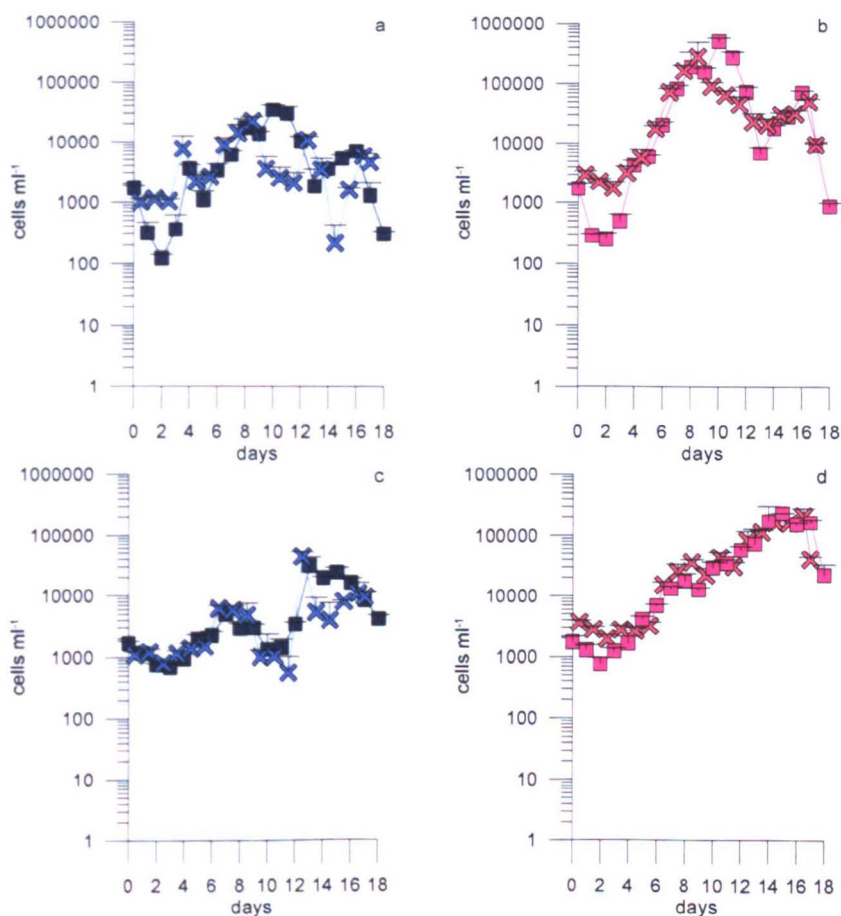


Figure 5.8. Cell concentration ($\text{cells}\cdot\text{ml}^{-1}$) of live (square) and dead (cross) cells of parental strains in co-cultures on the rotating wheel (RW; in panel a '+' and in panel b '-') and shelf (SH, in panel c '+' and in panel d '-'). Each point represents the average value of triplicates counts; st.dev. are represented with vertical bars.

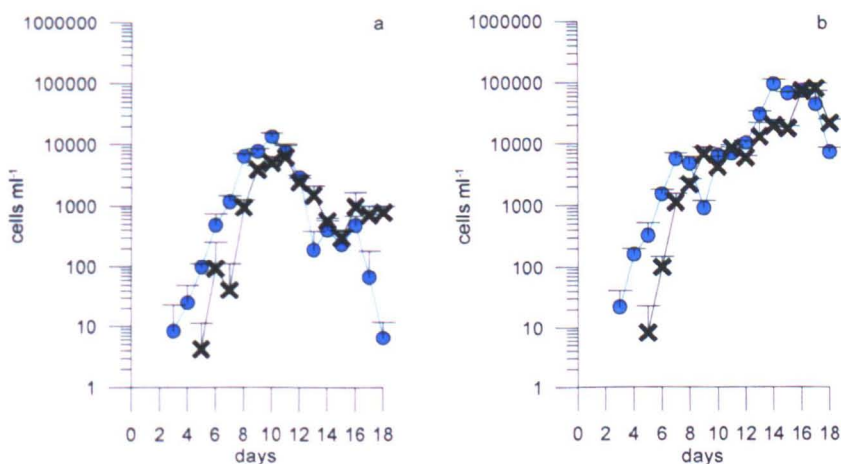


Figure 5.9. Cell concentration ($\text{cells}\cdot\text{ml}^{-1}$) of live (square) and dead (cross) cells of large F1 generation cells in co-cultures on the rotating wheel (RW, panel a) and shelf (SH, panel b). Each point represents the average value of triplicates counts; st.dev. are represented with vertical bars.

5.4 Discussion

The experimental results in this chapter show that a constant mixing of the co-cultures of two parental strains notably reduced the success of sexual reproduction of *P. multistriata*. In fact, the percentage of sexual stages recorded in the bottles incubated on the rotating wheel was much smaller compared to that recorded in the bottles incubated on the shelf under still conditions. In this latter condition, cells can accumulate at the bottom and reach concentrations suitable for the onset of the sexual phase. The concentration process is inhibited under continuous mixing. These results support the hypothesis that sexual reproduction in the natural environment might occur in thin layers and/or in other conditions where cells can aggregate.

5.4.1 *The dynamics in the cultures as related to nutrient concentration*

The growth curves of the two parental strains were different, showing a similar dynamics between the mixed (RW) and the still (SH) conditions. While the transition between the exponential and the post-exponential phase in the '-' strains might be explained by the limitation caused by P and/or Si, the '+' strains started the declining phase when nutrients were still available (Fig. 5.2). This is a puzzling result for which explanations are not easy to find. One can assume that some micro-nutrient was limiting the growth or that some internal regulation related to cell concentration might have determined the arrest of growth. For '+' strains, the maximum growth rate on the RW was higher than on SH: this seems reasonable due to fact that mixing should facilitate the uptake of new medium between cells. However, the opposite was found in '-' strains.

In the crosses, cell dynamics on RW and on SH was different: in the first condition, growth rates were higher and nutrient depletion was faster. The end of the exponential growth rate seemed to be related to nutrient exhaustion. It is however difficult to explain the second increase in cell concentration, occurring when both Si and P were almost

undetectable. A possible explanation is that cell death was accompanied by a rapid remineralization and subsequent uptake of the nutrients. Evidence for that comes from the slight increase in the concentration of Si towards the end of the experiment. On the SH, growth was much slower and nutrients were consumed later in time and nutrient exhaustion might explain the declining growth phase of the cultures in the last two days. Another interesting aspect is the rapid decrease in Si concentration that occurred after day 8 on RW and day 11 on SH. One can hypothesize that this rapid decrease might be due to the growth of large F1 cells that require more Si than the smaller parental strains.

Auxosporulation was observed after 2 days after the inoculum and until day 7 and 8 on RW and SH, respectively, where nutrient concentration was high. In the field the bloom of *P. australis* and *P. pungens* was observed after an up-welling event that increased the level of nutrients in the area; however, auxospores of both species were recorded at the end of the bloom when the silicate:nitrate ratio was near zero (Holtermann *et al.* 2010). At the end of *Pseudo-nitzschia* bloom, the area was interested by another up-welling event that restored nutrient concentration, and might have allowed the development of the sexual stages. In fact, in Chapter 3 it has been shown that gametes were not able to develop further into auxospores and initial cells when crosses were carried out with parental strains mixed at the end of the exponential phase, where nutrients were almost finished.

When the parental strains were grown in mono-culture, they immediately started the exponential growth phase on RW and on SH (see Figs 5.2 and 5.3). However, when the two strains were inoculated in the same flask, an arrest of growth (on SH) and even a decrease in cell concentration (in RW) was observed during the first days, in coincidence with the onset of the sexual phase. This is another example of a phenomenon that has been described for the experiments illustrated in Chapter 3 and 4, i.e. more evidence for the interaction between the sexual event and the growth of the vegetative cells, or maybe a sort of ‘allelopathic’ interaction between the two parental strains. This latter seems the case of

the RW, where too few sexual stages were produced to assume that they have negatively impacted vegetative cell division.

5.4.2 Sexual reproduction in mixed and still conditions

Water turbulence is known to influence the growth of phytoplankton species, although different species showed a considerable diversity in their growth response to mixing (Thomas and Gibson 1990, Peters *et al.* 2006). Small scale turbulence can favour the transport of nutrients in the vicinity of the cell surface, thus favouring their assimilation and growth. Turbulence also influences the interactions between particles of different size in the water column and several studies have been carried out on the effect of turbulent versus still regimes on predatory behaviours of zooplankton (Browman 1996). At a smaller scale, turbulence affects the interactions between phytoplankton cells and might favour particle aggregation, formation of aggregates and sinking of organic matter on the sea floor (Kiorboe and Hansen 1993). Turbulence also affects the detection of chemical signals produced by various organisms, e.g. the perception of preys or of mating signals of copepods (Jakobsen 2001). Water motion has strong effects on macroalgal reproduction and propagule release. In fact high mixing dilutes gametes and decreases fertilization success; some macroalgal species have evolved the capability to perceive the water motion and modulate some aspects of their life cycle accordingly. In the brown alga *Alaria esculenta*, gamete release was inhibited by water motion while zoospores (the life stage produced after fertilization) were released in high quantity in turbulent conditions, probably to favour dispersal. In the green alga *Ulva lactuca* water motion increased both gamete and zoospore release as compared to the calm conditions (Gordon 2001).

Pseudo-nitzschia multistriata was able to undergo sexual reproduction with the same timing in both treatments (RW and SH). A much higher density and percentage of sexual stages (gametes, zygotes, auxospores and initial cells) was, however, observed

under calm conditions. As previously hypothesized, the mixing movement from the rotating wheel, impaired the efficiency of sexual reproduction. This end-effect might be due to the fact that cell mixing limited the detection of the chemical signal that induces gametogenesis, or limited the contact between gametangia to allow fertilization. It has been shown that the first event is mediated by a diffusible chemical signal (Chapter 3 and 4), but it is not known how the gametangia/gametes of the opposite mating type attract each other. If this process is also mediated by a chemical signal, it will be probably impaired by water mixing. We can assume that in calm conditions on the shelf allowed sinking on the bottom of the culture flask and the ‘clumping’ of cells with an increased probability of gametogenesis/conjugation. The aggregation of cells on the bottom of culture vessels during sexual reproduction has been reported by various authors (e.g. Fryxell *et al.* 1991, Gordon 2001, Hiltz *et al.* 2000).

The fact that cells need to aggregate in a thin layer on the bottom of the culture plates to produce a good number of sexual stages, is also confirmed by some personal observations during several years of work on *Pseudo-nitzschia* species at the Department of Ecology and Evolution of Plankton at the Stazione Zoologica Anton Dohrn. When growing large volumes of co-cultures to obtain sexual stages, it is important to use bottles with a large surface area, a small amount of medium, and it is important not to move the culture bottles till the time in which sexual stages have to be harvested (Alberto Amato, personal communication; my own observations). These practical procedures can be interpreted in the light of these experiments; cells of opposite mating type need to aggregate, in this case on the bottom of the culture flask, and the larger the surface, the better it is. Any movement of the bottle disrupts aggregation and thus impairs the success of sexual reproduction. Where does aggregation take place in the natural environment? One possibility are the thin plankton layers in which high concentrations of *Pseudo-nitzschia* species have been reported (Rines *et al.* 2002, Velo Suárez *et al.* 2008). Another

possibility is that *Pseudo-nitzschia* species can use other organisms as substrate. Holterman *et al.* (2010) observed a massive sexual pairing between parental cells of *P. australis* and *P. pungens* on dense colonies of surf-zone diatoms during a sexual reproduction event. Another possibility is that sexual reproduction occurs on the sea bottom, at least in shallow coastal areas, and then new large initial cells can float up to the sea surface.

5.4.3 Dead cells

The abundance of dead cells was generally similar to the abundance of living cells; this was also true for the large F1 generation. A number of points should be considered when evaluating these results. i) Dead cells, i.e. empty frustules, are very difficult to recognize in light microscopy and their number might have been overestimated because it was not possible to distinguish between empty cells and single frustules. At times empty full cells are visible, but most times the thecae detach, and the two thecae might have been often counted as two distinct cells. ii) It has to be considered that, in successive counts, the number of dead cells includes the newly dead ones and the ones recorded in the previous counts. iii) In the monoclonal cultures and in the crosses, a more or less steep decrease in the numbers of live cells was detected (see Figs 5.2, 5.3, 5.5), which was not paralleled by the increase of dead cells. This mismatch can be explained by the rapid dissolution of the thin silica frustules. Evidence for that is provided by the considerable increase in silicates in the culture medium that has been detected towards the end of the experiment in both the monoclonal cultures and in the crosses. Cultures of *P. multistriata* were not axenic; it is known that bacterial activity can rapidly dissolve diatom silica frustules (Bidle and Azam 1999). Natural assemblages of marine bacteria in fact dramatically increased silica dissolution; between 4 to 17 % of the silica particulate was dissolved in 2 days in two species of marine diatoms. Cell death is a poorly explored factor in the dynamics of phytoplankton populations, both in lab experiments and in field studies. In laboratory

experiments, dead cells can only be recognized in those species with a mineral frustule, as diatoms, or a robust theca as thecate dinoflagellates, or by the use of specific dyes that only penetrate cells with a damaged membrane. Cell lysis has been documented in natural phytoplankton populations, where estimates exceeding 50% of phytoplankton growth have been reported (Bidle and Falkowski 2004). In some cases, cell lysis can be due to external factors such as viral attack but in some cases it can be due to programmed cell death (PCD), which is an endogenous factor.

The quantitative data obtained in this experiment should be considered with caution, for the reasons explained above and because in laboratory experiments not all the natural conditions are fulfilled and certain conditions can be stressed. However, these preliminary results are very interesting in showing that cell death can occur in the exponential growth phase of cultures, when nutrients are not limiting, and it seems a 'normal' factor in the *P. multistriata* life cycle. The mortality of vegetative cells should be investigated in more detail to be able to understand why it occurs.

Chapter 6

General conclusions and future perspectives

In my study, I have provided new information about the different phases of the life cycle of the marine pennate diatom *Pseudo-nitzschia multistriata* and I have gained an understanding of the factors that regulate the occurrence of sexual reproduction in this species.

General conclusion:

In Chapter 2, I have presented the results of an investigation on the life cycle of *P. multistriata* carried out in confocal and time-lapse microscopy. I have described the process of gametogenesis and gamete conjugation and the formation of auxospores, gaining insights into the process in the nucleus in the different life phases and on the timing and duration of these processes. The species is heterothallic, i.e. strains of opposite mating type have to be mixed together to allow sex to occur. The attribution of mating type to 233 strains collected over three different years in the Gulf of Naples provided the surprising result that only in two of the years the mating type ratio was about 50:50, whereas in the population of the first year about 90% of the strains belonged to the '+' type (Chapter 2). These results open new questions on the distribution of mating types in natural populations of unicellular organisms.

I have provided quantitative evidence that a successful sexual reproduction, i.e. the formation of a good number of gametes that can develop into initial cells, in *P. multistriata* requires the parental strains to be in the exponential phase of growth (Chapter 3). Sexual reproduction in diatoms is linked to conditions promoting active growth of the population and does not represent a response to stress or adverse conditions, as in the case of some other protists (e.g. *Chlamydomonas*, *Volvox*, dinoflagellates). Sexual reproduction also requires a threshold on the cell concentration to occur and this suggests that a chemical mediator should be involved in the process. In Chapter 4, I have presented the results of

experiments aimed at testing for the presence of a water soluble compound that can induce gametogenesis.

These experiments, involved the use of culture media conditioned by the growth of strains of the opposite mating type, by cultures in which sexual reproduction was taking place and, also by the growth of strains in the same medium but physically separated by a permeable membrane. Gametangia involved in the process of producing gametes, as well as fully formed gametes, were recorded proving the presence of a chemical mediator that induces gametogenesis in the opposite mating type. Another interesting result of the experiments illustrated in Chapter 3 and 4 was the finding that the growth dynamics of vegetative cells, when grown alone or in the presence of a strain of the opposite mating type, was different from the growth dynamics of co-cultures of strains in which sexual reproduction was induced. In fact, an apparent arrest of vegetative growth was observed in the co-cultures suggesting either, an inhibitory effect of the compound inducing gametogenesis on the cell cycle of vegetative cells or, a sort of 'allelochemical' interaction between strains of opposite mating type.

A final experiment was conducted to test the effect of a gentle and constant mixing of the cultures on the success of sexual reproduction, by comparing crosses performed on a rotating wheel and those incubated under still conditions (Chapter 5). Sexual reproduction was more abundant in the latter crosses demonstrating that mixing negatively affects sexual reproduction either by diluting the chemical mediator and/or by constraining gamete pairing. Moreover in this case, differences in the growth dynamics of the parental strains grown in mono-cultures and in crosses were detected.

The relevance of the results of my thesis:

Biology of diatoms. Diatoms are responsible for about 20% of the primary production of our planet, but very little is known about their biology. Diatoms have a very peculiar life cycle in which the persistence of a population is closely related with the sexual reproduction. I have showed evidence that sexual reproduction is a density-dependent process, mediated by diffusible chemical cues. I have also provided preliminary evidence for a possible ‘cross-talking’ mechanism between the two mating types. These results set the base for further investigations that might shed light on the complex chemical interactions in the diatom life cycle.

Ecology and phytoplankton population dynamics. Knowing the conditions under which sexual reproduction occurs in the marine environment is very important to understand the success, timing and persistence of diatom species. If a diatom species does not undergo sexual phase, it risks extinction. I have shown that cell aggregation is required to allow sex to occur, that mixing interferes with the success of sexual reproduction and that sexual reproduction occurs in the active growth phase of the population.

Biotechnological applications. Diatoms have a considerable biotechnological potential, which requires mass cultivation of the target species. For this purpose, a deep knowledge on their life cycle is necessary, since the sexual reproduction is a requirement to keep them alive for a long time, to control the sexual phase and so, take advantage for the selection of a specific progeny with certain chemical characteristics. The information provided on the life cycle features of *P. multistriata* will be useful for biotechnological applications with this species and other heterothallic diatoms. Moreover, a detailed information on the life cycle of this species will be very useful for its future use as a model organism for genetic studies.

Future perspectives:

The results produced within my thesis open new possibilities for future research.

Evidence has been produced on the presence of a chemical mediator that induces gametogenesis in *P. multistriata*. These compounds are present in the culture medium and thus should be water soluble compounds. The analysis of exometabolomes present in the culture medium at different steps of the sexual phase can be carried out to further verify and characterize these compounds (e.g. Barofsky *et al.* 2009). The same approach can be developed comparing parental strains, at different phases of their growth, as well as co-cultures of parental strains to test the presence of distinct metabolites that might mediate interactions between the strains.

The experiments that compare the timing and success of sexual reproduction in mixed and calm conditions, can be carried out with instruments especially designed to quantify the turbulence in order to gain information that can be extrapolated to the natural environment in a more precise way.

In the life cycle of *Pseudo-nitzschia multistriata* there are phases that are related to density thresholds. This is the case of the production of gametes, that requires a certain cell density, and the apparent arrest or decrease in growth that has been observed when co-culturing strains of opposite mating type. These phenomena are reminiscent of 'quorum sensing' mechanisms, i.e. the activation of certain processes activated as a response to the perception of a specific cell density. Research in this direction coupling experimental approaches, with e.g. searching for genes similar to those that regulate quorum sensing in other organisms, can be designed.

The genome of one *Pseudo-nitzschia* species is already available and the genome of *P. multistriata* will be becoming soon. Thanks to that, molecular markers could be designed to identify: different life cycle stages, such as meiosis, genes that regulate the mating type and/or mechanisms that regulate mating barriers. In this way, a mechanistic comprehension of the biology of sexual reproduction will be gained, as well as markers could be designed that allow the detection of these stages in the natural environment.

Appendix I

The life cycle of the raphid pennate diatom

Fragilariopsis kerguelensis

In this Appendix some preliminary results are presented on the life cycle of the pennate diatom *Fragilariopsis kerguelensis*. This study was carried out in the first six months of my PhD project in the frame of a collaboration between the Stazione Zoologica Anton Dohrn and the Alfred Wegener Institut for Polar and Marine Research.

Introduction

The marine pennate raphid diatom *Fragilariopsis kerguelensis* (O'Meara) Hustedt is a common species in the Southern Ocean plankton community; it is found among the dominant species in the ice-free water column in the offshore Antarctic Circumpolar Current (ACC) (Smetacek *et al.* 2004). This species constitutes up to 90% of the diatom ooze deposited in the sediments around Antarctica (Zielinski and Gersonde 1997) and, therefore, it is the most important diatom in the global silicon cycle. *Fragilariopsis kerguelensis* can be recorded in the plankton both as single cells and as long ribbon-shaped chains in which cells are joined together valve to valve. This species is characterized by a strong silicification; this feature, together with a coarse pattern of striae on the valvar face make it easy to distinguish from congeneric species in light microscopy (Hasle and Syvertsen 1990).

Differences in the valve size of *F. kerguelensis* collected in sediment samples of different sites of the Southern Ocean from the Holocene to the last glacial maximum suggested the possible use of this species as a proxy for paleo-productivity (Cortese and Gersonde 2007). Larger cells have been, in fact, recorded in the Antarctic Polar front area, characterized by high productivity, while smaller ones have been recorded in the less productive north and south sediments. Cell size frequency distribution in diatoms is strongly determined by the species life cycle. The peculiar morphology of diatom cells surrounded by two rigid siliceous thecae, slightly different in size, and its unique mitotic

division modality that causes a progressive decrease of the average of the cell size population. This progressive reduction in cell size can be limited by sexual reproduction with the formation of large-sized cells (Chepurnov *et al.* 2004, Round *et al.* 1990). Auxospores of *F. kerguelensis* have been recently recorded in field samples from the Southern Ocean, that demonstrate that the presence of sexual reproduction in this species (Assmy *et al.* 2006).

Due to the important ecological and biogeochemical role of *F. kerguelensis*, and its potential role as paleoproxy, it is important to gain further information on its life cycle. In this chapter, some preliminary results obtained with laboratory observation carried out with clonal strains are presented.

Materials and Methods

The cultures of *Fragilariopsis kerguelensis* were established by Marina Montresor (SZN) during the cruise ANT-XXV/3 (LOHAFEX) carried out in Atlantic sectors of the Southern Ocean from January, 27th to March, 17th 2009. Short chains were isolated with a micropipette from surface water samples collected with a 20 μm -mesh-size phytoplankton hand net. Strains were maintained at a temperature of 5 °C, an irradiance of 50 $\mu\text{mol photons m}^{-2} \text{ s}^{-1}$, a photocycle of 12L:12D h light:dark in standard f/2 culture medium prepared with oligotrophic Mediterranean seawater adjusted to a salinity of 35 p.s.u.

Strain L2-d6 (average apical length: 13.2 μm) and L9-c3 (average apical length: 15.5 μm) were used in this work. These strains belong to opposite mating types, as proven by the results of a matrix of crosses, including all the pairwise combinations of different strains. A stock culture was prepared with 150 ml of f/2 culture medium in which the exponentially growing strains were inoculated to reach a final concentration of about 4,000 cells·ml⁻¹. Aliquots of 4 ml were dispensed in two 6-well tissue culture plates (Corning Glass Works, New York) and incubated at 5 °C, 50 $\mu\text{mol photons m}^{-2} \text{ s}^{-1}$ and 12L:12D photocycle. Every day, culture plates were observed at the light microscope and the content of two culture wells was pooled together in a plastic vial and fixed with formaldehyde solution at a final concentration of 1.6%. The number of single cells and of cells in chain was estimated in each parental culture. The fixed samples were stained with DAPI at a final concentration of 0.5 $\mu\text{g} \cdot \text{ml}^{-1}$. The material was examined and photographed with a Zeiss Axiovert epifluorescence microscope and photographed with an Zeiss Axiocam photcamera (Carl Zeiss, Oberkochen, Germany).

For the observations of auxospores at the Scanning Electron Microscopy (SEM), the fixed samples were filtered slowly within a sweenex-holder (3 μm pore size) connected to a syringe. The material was dehydrated with an increasing concentration of ethanol (30, 50, 70, 90, 100 %) after that the sample was critical point dried, sputter-coated with

palladium and gold and observed at a Cambridge 250 MARK 3 scanning electron microscope (Cambridge, Cambridge United Kingdom).

Results

Sexual stages of this species have never been observed in monoclonal cultures but only when mixing together two compatible strains. When strains of the complementary mating type were inoculated in the same culture vessel, the detachment of cells from the chain was observed after a few days. A quantitative estimation was obtained for the cross L2-d6 x L9-c3, where about 90% of the cells were arranged in chains in the parental strains (Figs A1 and A2a). On day 10 after the inoculum, when the first sexual stages were observed in the crosses, only 30% of the cells were arranged into chains. Single cells were often in contact with each other, but the contact point was variable: in some cases they seemed in contact valve to valve, in other cases one cell seemed in valvar view and the other in cingular view. Several cells, either paired or single, had a considerably enlarged nucleus, that can be interpreted as a meiotic profase nucleus (Fig. A2b), in which the chloroplasts were appressed to the cell wall. These cells with expanded nucleus started with their enlargement along the perivalvar axis. In these expanded cells – the gametangia – the two-steps meiotic division took place (Fig. A2c-f). Meiosis I was followed by cytokinesis and subsequently Meiosis II occurred with the formation of two bi-nucleate gametes (Fig. A2g,h). The gametes separated and each of them remained attached to one gametangial theca. In most cases, meiosis was observed occurring in two appressed gametangia. I could not follow gamete conjugation in real time, so I could not assess whether the gametes produced by one mating type were both moving towards the gametes of the opposite mating type or whether one gametangium produced one ‘motile’ and one sessile gamete. Four-nucleate stages (zygotes) were observed, attached to the valve of one gametangium (Fig. A2i,j) and an empty valve – most probably the valve of the gamete of the opposite mating type – was often observed in the vicinity.

The degeneration of the two extranumerary nuclei occurred in the zygote, because

early stage auxospores, i.e. auxospores at the beginning of their elongation, were binucleate (Fig. A2*k,l*). When auxospore expansion was completed, karyogamy occurred and the nucleus was visible inside the stage at which the formation of the initial cell was taking place (Fig. A2*m,n*). The vast majority of the auxospores remained attached to the valve of the sessile gamete until their complete development, The auxospores presented two caps at their extremity, which correspond to the two primary zygote halves of the wall, that gets broken when auxospore expansion starts (Fig. A3*a*, for the cap ultrastructure see below). The transversal perizonium was constituted by a series of slightly silicified perizonial bands, the primary bands were broader and gave the auxospore a slightly enlarged shape in its central portion. in SEM preparations, the fully developed auxospore appeared surrounded by 35-42 transversal perizonial bands (Fig. A3*a*). Both tips of the auxospore were surrounded by a cap constituted by thin, tightly appressed and partially overlapping rounded scales (Fig. A3*b,c*).

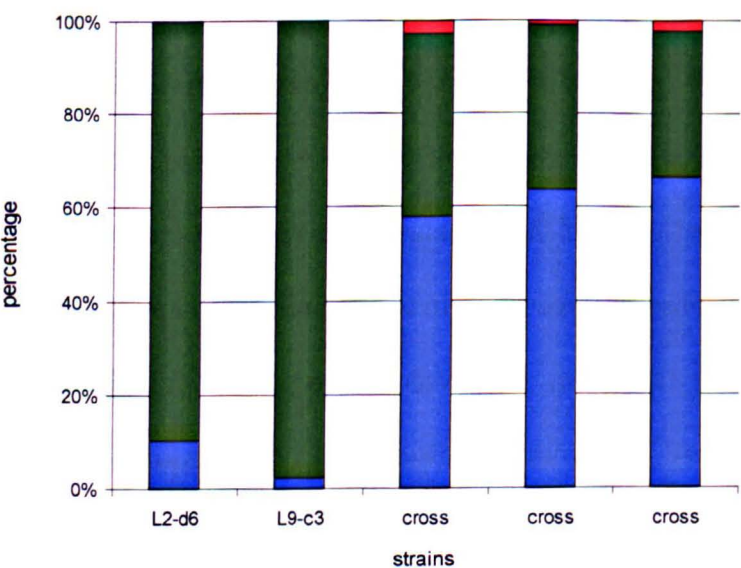


Figure A1. Percentage distribution of single cells (blue), cells in chains (green) and sexual stages (gametes + zygotes; red) in the monoclonal parental strains (L2-d6 and L9-c3) and in the cross between them (cross).

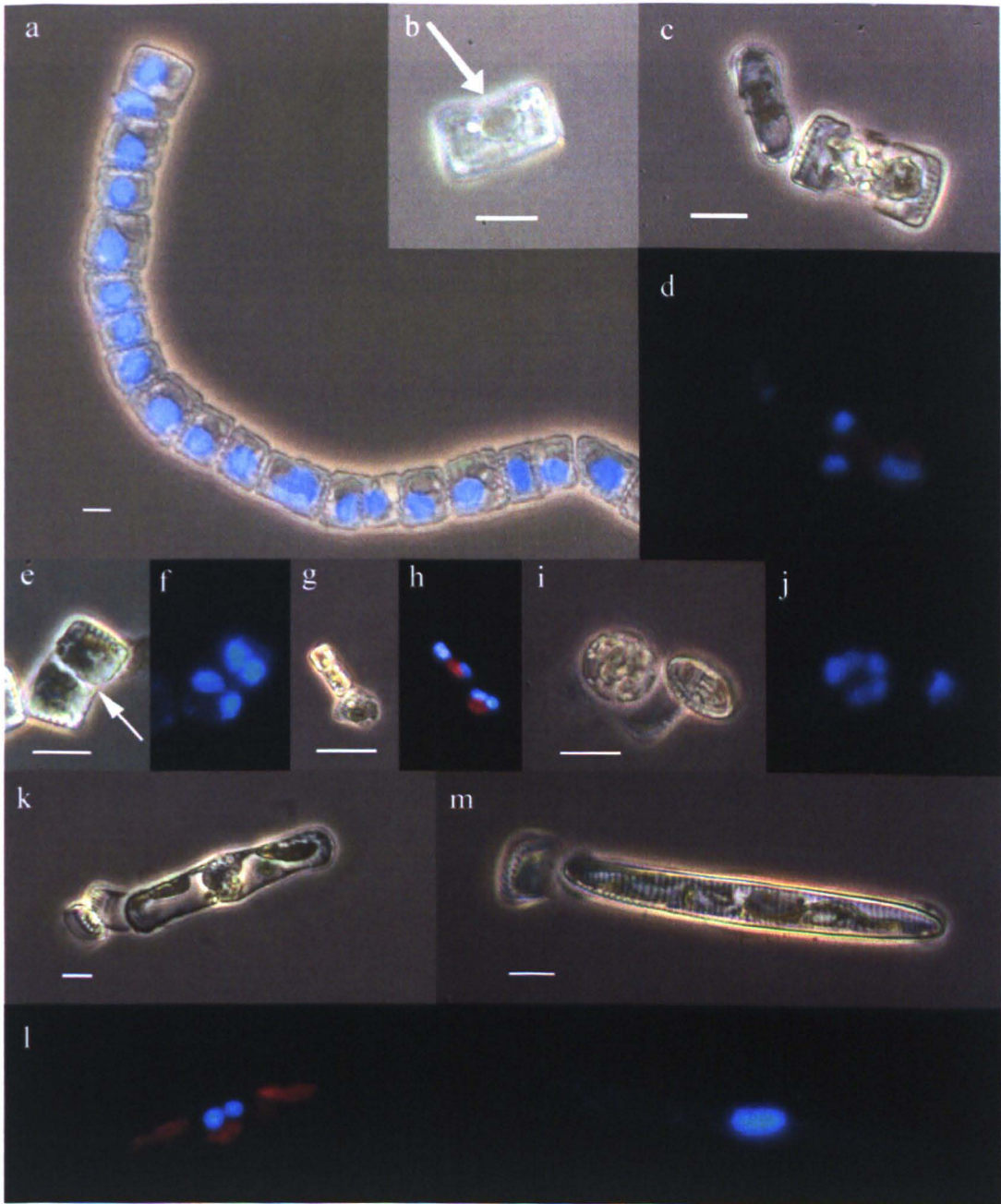


Figure A2. Phase contrast (*b-c,e,g,i,k,m*) and epifluorescence (*a,d,f,h,l,n*) micrographs of *Fragilariopsis kerguelensis* life stages. Vegetative cells in chain; DAPI-stained nuclei in blue (*a*); gametangium is approaching Meiosis I, the enlarged nucleus is arrowed (*b*). Meiosis I has taken place, meiosis II is completed in the left protoplasm and is in progress in the right protoplasm (the same subject *c* phase contrast, *d* epifluorescence). Gametangium after completion of meiosis II, the separation of the protoplasm is arrowed (the same subject *e* phase contrast *f* epifluorescence). A bi-nucleated rounded gamete inside a valve (the same subject: *g* phase contrast, *h* epifluorescence). Zygote with 4 nuclei (the same subject: *i* phase contrast, *j* epifluorescence). Auxospore with two nuclei (the same subject: *k* phase contrast, *l* epifluorescence). Formation of the initial cell, only one nucleus is visible, the first valve has been deposited (same subject: *m* phase contrast, *n* epifluorescence). Scale bars = 10 μm .

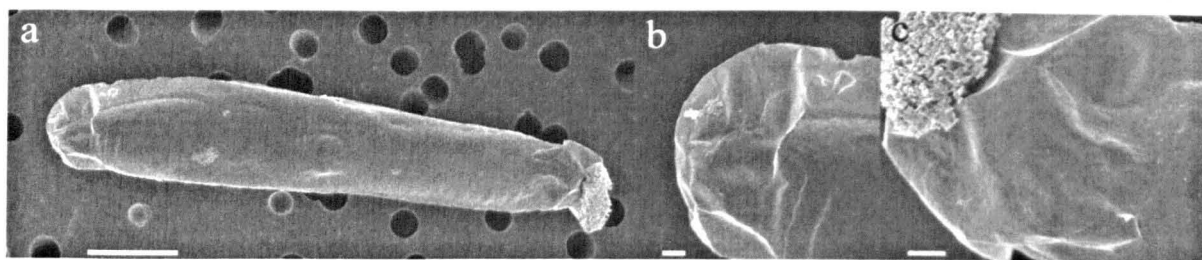


Figure A3. Scanning Electron Microscopy (SEM) micrographs of *F. kerguelensis* auxospore. Fully expanded auxospore (a); detail of the auxospore cap, note the rounded thin scales (b,c). Scale bars: a, 10 μm ; b,c, 1 μm .

Appendix II

Glossary of the terminology used in studies on diatom
life cycles

Acytokinetic division: derives from 'a' (= Greek prefix meaning 'without') and 'cytokinesis' (= the division of the cytoplasm of a cell following the division of the nucleus). A mitotic division that is not followed by the division of the cytoplasm.

Allogamous: characterized by allogamy.

Allogamy: the process of cross-fertilization, i.e. fertilization of a gamete with a gamete of the opposite mating type.

Anisogamete: a gamete differing in size or morphology from the one with which it conjugates.

Anisogamy: sexual reproduction involving the fusion of two dissimilar gametes (anisogametes).

Apomixis: the formation of auxospore-like structures without the conjugation of two gametes (asexual auxosporulation without fertilization).

Autogamy: the process of self-fertilization, i.e. fertilization of a gamete with a gamete of the same mating type.

Automixis: auxospore formation resulting from sexual processes occurring within a single cell. There are two different possibilities: i) meiosis occurs in an unpaired mother cell, 2 haploid gametes are produced, they conjugate producing the diploid zygote (paedogamy); ii) meiosis occurs in an unpaired mother cell, 4 haploid nuclei are produced, two degenerate, cytokinesis is suppressed and two nuclei fuse (autogamy).

Auxospore: specialized life cycle stage produced by the expansion of the zygote that is the product of fertilization. The auxospore can expand, being surrounded by modular elements, and within it the formation of the large initial cell takes place.

Auxosporulation: production of auxospores by sexual reproduction.

Cytokinesis: The division of the cytoplasm following the division of the nucleus.

Dioecious: in plants; having male and female reproductive organs in different individuals. In diatoms: strains belonging to two different mating types (heterothallic).

Gametangium: a cell in which gametes are produced.

Gamete: in eukaryotic diploid organisms, a mature germ cell possessing a haploid chromosome set. The gamete is capable of producing a new diploid individual by fusion with a gamete of the opposite mating type (in heterothallic species).

Heterothallic: Producing male and female gametangia in different structures or plants (as in some algae and fungi) or in different strains (as in diatoms).

Homothallic: Producing male and female gametangia in the same structure or plant (as in some algae and fungi) or in the same strains (as in diatoms).

Initial cell: vegetative cell of the maximum species-specific cell size that is produced within the auxospore.

Interphase: the interval between the end of one mitotic or meiotic division and the beginning of another.

Isogamete: a gamete with the same size and morphology of the one with which it conjugate.

Karyogamy: is the fusion of haploid gametic nuclei.

Karyokinesis: the division of the cell nucleus during mitosis or meiosis.

Monoecious: in plants; having male and female reproductive organs in the same individual. In diatoms: strains belonging to two the same mating type (homothallic).

Oogamy: the fertilization of large, non-motile egg by small and motile sperms.

Oogonium: female gametangium.

Perizonium: the covering that surrounds the auxospore. It consists of a series of transversal and/or longitudinal slightly silicified bands.

Plasmogamy: fusion of the cytoplasm of two or more cells without the fusion of nuclei.

Plastokinesis: chloroplast division.

Polar body: certain diploid cells undergo cytokinesis after meiosis and produce a relatively small cytoplasmic matrix with or without DNA that usually degenerates.

Pronucleus: the nucleus of a sperm or an egg cell during the process of fertilization, after the sperm enters the ovum, but before they fuse.

Protoplasm: the living content of a cell that is surrounded by a plasma membrane.

Pyknosis: (also karyopyknosis) the irreversible condensation of chromatin in the nucleus of a cell undergoing programmed cell death, necrosis or apoptosis.

Resting spores: cell morphologically differentiated from the vegetative cells and produced following mitotic divisions; can undergo quiescence and/or withstand a broader range of environmental conditions as compared to vegetative cells.

Syngamy: The fusion of gametes resulting in the formation of a zygote, which develops into a new organism.

Zygote: the result of the fusion of two gametes.

References

- AMATO, A., ORSINI, L., D'ALELIO, D. & MONTRESOR, M. 2005. Life cycle, size reduction patterns, and ultrastructure of the pennate planktonic diatom *Pseudo-nitzschia delicatissima* (Bacillariophyceae). *Journal of Phycology* 41: 542-556.
- AMATO, A., KOOISTRA, W.H.C.F., LEVIALDI GHIRON, J.H., MANN, D.G., PRÖSCHOLD, T. & MONTRESOR, M. 2007. Reproductive isolation among sympatric cryptic species in marine diatoms. *Protist* 158: 193-207.
- AMATO, A. & MONTRESOR, M. 2008. Morphology, phylogeny, and sexual cycle of *Pseudo-nitzschia mannii* sp. nov. (Bacillariophyceae): a pseudo-cryptic species within the *P. pseudodelicatissima* complex. *Phycologia* 47: 487-497.
- AMATO, A. 2010. Diatom reproductive biology: living in a crystal cage. *The International Journal of Plant Reproductive Biology* 2: 1-10.
- ARMBRUST, E.V., CHISHOLM, S.W. & OLSON, R.J. 1990. Role of light and the cell cycle on the induction of spermatogenesis in a centric diatom. *Journal of Phycology* 26: 470-478.
- ARMBRUST, E.V. & CHISHOLM, S.W. 1992. Patterns of cell size change in a marine centric diatom: variability evolving from clonal isolates. *Journal of Phycology* 28: 146-156.
- ASSMY, P., HENJES, J., SMETACEK, V. & MONTRESOR, M. 2006. Auxospore formation in the silica-sinking oceanic diatom *Fragilariopsis kerguelensis* (Bacillariophyceae). *Journal of Phycology* 42: 1002-1006.
- BAROFSKY, A., VIDOUDEZ, C. & POHNERT, G. 2009. Metabolic profiling reveals growth stage variability in diatom exudates. *Limnology and Oceanography-Methods* 7: 382-390.
- BATES, B.B., GARRISON, D.L. & HORNER, R.A. 1998. Bloom dynamics and physiology of domoic-acid-producing *Pseudo-nitzschia* species. In *Physiological Ecology of Harmful Algal Blooms*. (Ed. by D.M. Anderson, A.D. Cembella & G.M. Hallegraeff), pp. 267-292. Springer-Verlag, Berlin.
- BATES, S.S. & DAVIDOVICH, N.A. 2002. Factors affecting the sexual reproduction of diatoms, with emphasis on *Pseudo-nitzschia* spp. In *LIFEHAB: Life histories of microalgal species causing harmful algal blooms*. (Ed. by E. Garcés, A. Zingone, M. Montresor, B. Reguera, B. Dale & E. Lipiatou), pp. 31-36. European Commission, Brussels.
- BIDLE, K.D. & AZAM, F. 1999. Accelerated dissolution of diatom silica by marine bacterial assemblages. *Nature* 397: 508-512.
- BIDLE, K.D. & FALKOWSKI, P.G. 2004. Cell death in planktonic, photosynthetic microorganisms. *Nature Reviews Microbiology* 2: 643-655.
- BROWMAN, H.I. 1996. Predator-prey interactions in the sea: commentaries on the role of turbulence. *Marine Ecology Progress Series* 139: 301-312.
- CASTELEYN, G., CHEPURNOV, V.A., LELIAERT, F., MANN, D.G., BATES, S.S., LUNDHOLM, N., RHODES, L., SABBE, K. & VYVERMAN, W. 2008. *Pseudo-nitzschia pungens* (Bacillariophyceae): A cosmopolitan diatom species? *Harmful Algae* 7: 241-257.

- CERINO, F., ORSINI, L., SARNO, D., DELL'AVERSANO, C., TARTAGLIONE, L. & ZINGONE, A. 2005. The alternation of different morphotypes in the seasonal cycle of the toxic diatom *Pseudo-nitzschia galaxiae*. *Harmful Algae* 4: 33-48.
- CHEPURNOV, V.A., MANN, D.G., VYVERMAN, W., SABBEM, K. & DANIELIDIS, D.B. 2002. Sexual reproduction, mating system, and protoplast dynamics of *Seminavis* (Bacillariophyceae). *Journal of Phycology* 38: 1004-1019.
- CHEPURNOV, V.A., MANN, D.G., SABBE, K. & VYVERMAN, W. 2004. Experimental studies on sexual reproduction in diatoms. *International Review of Cytology* 237: 91-154.
- CHEPURNOV, V.A., MANN, D.G., SABBE, K., VANNERUM, K., CASTELEYN, G., VERLEYEN, E., PEPPERZAK, L. & VYVERMAN, W. 2005. Sexual reproduction, mating system, chloroplast dynamics and abrupt cell size reduction in *Pseudo-nitzschia pungens* from the North Sea (Bacillariophyta). *European Journal of Phycology* 40: 379-395.
- CHEPURNOV, V.A., MANN, D.G., VON DASSOW, P., ARMBRUST, E.V., SABBE, K., DASSEVILLE, R. & VYVERMAN, W. 2006. Oogamous reproduction, with two-step auxosporulation, in the centric diatom *Thalassiosira punctigera* (Bacillariophyta). *Journal of Phycology* 42: 845-858.
- CORTESE, G. & GERSONDE, R. 2007. Morphometric variability in the diatom *Fragilariopsis kerguelensis*: Implications for Southern Ocean paleoceanography. *Earth and Planetary Science Letters* 257: 526-544.
- CRAWFORD, R.M. 1995. The role of sex in the sedimentation of a marine diatom bloom. *Limnology and Oceanography* 40: 200-204.
- CRAWFORD, S.A., HIGGINS, M.J., MULVANEY, P. & WETHEEBEE, R. 2001. Nanostructure of the diatom frustule as revealed by atomic force and scanning electron microscopy. *Journal of Phycology* 37: 543-554.
- D'ALELIO, D., AMATO, A., LUEDEKING, A. & MONTRESOR, M. 2009a. Sexual and vegetative phases in the planktonic diatom *Pseudo-nitzschia multistriata*. *Harmful Algae* 8: 225-232.
- D'ALELIO, D., AMATO, A., KOOISTRA, W.H.C.F., PROCACCINI, G., CASOTTI, R. & MONTRESOR, M. 2009b. Internal Transcribed Spacer polymorphism in *Pseudo-nitzschia multistriata* (Bacillariophyceae) in the Gulf of Naples: recent divergence or intraspecific hybridization? *Protist* 160: 9-20.
- D'ALELIO, D., RIBERA D'ALCALÀ, M., DUBROCA, L., SARNO, D., ZINGONE, A. & MONTRESOR, M. 2010. The time for sex: a biennial life cycle in a marine planktonic diatom. *Limnology and Oceanography* 55: 106-114.
- D'IPPOLITO, G., LAMARI, N., MONTRESOR, M., ROMANO, G., CUTIGNANO, A., GERECHT, A., CIMINO, G. & FONTANA, A. 2009. 15S-Lipoxygenase metabolism in the marine diatom *Pseudo-nitzschia delicatissima*. *New Phytologist* 183: 1064-1071.
- DAVIDOVICH, N.A. 1994. Factors controlling the size of initial cells in diatoms. *Russian Journal of Plant Physiology* 41: 220-224.
- DAVIDOVICH, N.A. 1998. Transition to sexual reproduction and control of initial cell size in *Nitzschia lanceolata*. *Diatom Research* 13: 29-38.
- DAVIDOVICH, N.A. & BATES, S.S. 1998. Sexual reproduction in the pennate diatoms *Pseudo-nitzschia multiseriata* and *P. pseudodelicatissima* (Bacillariophyceae). *Journal of Phycology* 34: 126-137.
- DAVIS, C.O., HARRISON, P.J. & DUGDALE, R.C. 1973. Continuous culture of marine diatoms under silicate limitation. I. Synchronized life cycle of *Skeletonema costatum*. *Journal of Phycology* 9: 175-180.

- DAVIS, C.O., HOLLIBAUGH, J.T., SEIBERT, D.L.R., THOMAS, W.H. & HARRISON, P.J. 1980. Formation of resting spores by *Leptocylindrus danicus* (Bacillariophyceae) in a controlled experimental ecosystem. *Journal of Phycology* 16: 296-302.
- DE MARTINO, A., MEICHENIN, A., SHI, J., PAN, K. & BOWLER, C. 2007. Genetic and phenotypic characterization of *Phaeodactylum tricornutum* (Bacillariophyceae) accessions. *Journal of Phycology* 43: 992-1009.
- DE MARTINO, A., AMATO, A. & BOWLER, C. 2009. Mitosis in diatoms: rediscovering an old model for cell division. *BioEssays* 31: 874-84.
- DERENBACH, J.B. & PESANDO, D. 1986. Investigations into a small fraction of volatile hydrocarbons .3. 2 Diatom cultures produce ectocarpene, a pheromone of brown-algae. *Marine Chemistry* 19: 337-341.
- DREBES, G. 1966. On the life history of the marine plankton diatom *Stephanopyxis palmeriana*. *Helgoländer wissenschaftliche Meeresuntersuchungen* 13: 104-114.
- DREBES, G. 1977. Sexuality. In *The biology of diatoms*. (Ed. by D. Werner), pp. 250-283. Blackwell Scientific Publications, Oxford.
- DURHAM, W.M. & STOCKER, R. 2012. Thin phytoplankton layers: characteristics, mechanisms, and consequences. *Annual Review of Marine Science* 4: 177-207.
- EDLUND, M.B. & STOERMER, E.F. 1997. Ecological, evolutionary, and systematic significance of diatom life histories. *Journal of Phycology* 33: 897-918.
- EDLUND, M.B. & BIXBY, R.J. 2001. Intra- and inter-specific differences in gametangial and initial cell size in diatoms. In *Proceedings of the 16th International Diatom Symposium 2000*. (Ed. by A. Economou-Amilli), pp. 169-190. University of Athens, Athens.
- EILERTSEN, H.C.H.R., SANDBERG, S. & TOLLEFSEN, H. 1995. Photoperiodic control of diatom spore growth: a theory to explain the onset of phytoplankton blooms. *Marine Ecology Progress Series* 116: 303-307.
- FALCIATORE, A. & BOWLER, C. 2002. Revealing the molecular secrets of marine diatoms. *Annual Review of Plant Biology* 53: 109-130.
- FIGUEROA, R.I., BRAVO, I. & GARCÉS, E. 2006. Multiple routes of sexuality in *Alexandrium taylori* (Dinophyceae) in culture. *Journal of Phycology* 42: 1028-1039.
- FINK, P. 2007. Ecological functions of volatile organic compounds in aquatic systems. *Marine and Freshwater Behaviour and Physiology* 40: 155-168.
- FLORIO, D. 2011. Genetica di popolazione della diatomea planctonica *Pseudo-nitzschia multistriata* nel Golfo di Napoli. Università degli Studi Federico II, Napoli.
- FRENCH, F. & HARGRAVES, P.E. 1980. Physiological characteristics of plankton diatom resting spores. *Marine Biology Letters* 1: 185-195.
- FRENCH III, F.W. & HARGRAVES, P.E. 1985. Spore formation in the life cycles of the diatoms *Chaetoceros diadema* and *Leptocylindrus danicus*. *Journal of Phycology* 21: 477-483.
- FRENCH III, F.W. & HARGRAVES, P.E. 1986. Population dynamics of the spore-forming diatom *Leptocylindrus danicus* in Narragansett Bay, Rhode Island. *Journal of Phycology* 22: 411-420.
- FRYXELL, G.A., GARZA, S.A. & ROELKE, D.L. 1991. Auxospore formation in an Antarctic clone of *Nitzschia subcurvata* Hasle. *Diatom Research* 6: 235-245.

- FURNAS, M.J. 1985. Diel synchronization of sperm formation in the diatom *Chaetoceros curvisetus* Cleve. *Journal of Phycology* 21: 667-671.
- GALLAGHER, J.C. 1983. Cell enlargement in *Skeletonema costatum* (Bacillariophyceae). *Journal of Phycology* 19: 539-542.
- GEITLER, L. 1932. Der formwechsel der pennaten diatomeen (Kieselalgen). *Archiv für Protistenkunde* 78: 1-226.
- GEITLER, L. 1973. Auxosporenbildung und systematik bei penaten diatomeen und die zytologie von *Cocconeis*-sippen. *Österreichische Botanische Zeitschrift* 122: 299-321.
- GORDON, R. 2001. The role of water motion in algal reproduction. pp. chapter 4, 61-84. University of Maine, Maine.
- GREGOR, T., FUJIMOTO, K., MASAKI, N. & SAWAI, S. 2010. The onset of collective behavior in social amoebae. *Science* 328: 1021-1022.
- GROSS, F. 1937. The life history of some marine planktonic diatoms. *Scianeces* 228: 1-48.
- GUILLARD, R.R.L. 1975. Culture of phytoplankton for feeding marine invertebrates. In *Culture of Marine Invertebrate Animals*. (Ed. by W.L. Smith & M.H. Chanley), pp. 29-60. Plenum Press, New York.
- GUILLARD, R.R.L. 1980. Division rates. In *Handbook of Phycological Methods*. (Ed. by J.E. Stein), pp. 300-311. Cambridge University Press, Cambridge.
- HANSEN, H.P. & GRASSHOFF, K. 1983. Automated chemical analysis. In *Methods of seawater analysis*. (Ed. by K. Grasshoff, M. Ehrhardt & K. Kremling), pp. 347-379. Verlag Chemie, Weinheim.
- HARGRAVES, P.E. 1976. Studies on marine plankton diatoms. II. Resting spores morphology. *Journal of Phycology* 12: 118-128.
- HASLE, G.H. & SYVERTSEN, E.E. 1990. Marine diatoms. In *Identifying marine phytoplankton*. (Ed. by C.R. Tomas), pp. 5-385. Academic press, San Diego.
- HICKEL, B. 1988. Sexual reproduction and life cycle of *Ceratium furcoides* (Dinophyceae) *in situ* in the lake Plussee (F.R.G.). *Hydrobiologia* 161: 41-48.
- HILTZ, M., BATES, S.S. & KACZMARSKA, I. 2000. Effect of light:dark cycles and cell apical length on the sexual reproduction of the pennate diatom *Pseudo-nitzschia multiseries* (Bacillariophyceae) in culture. *Phycologia* 39: 59-66.
- HOLMES, R.W. 1966. Short-term temperature and light conditions associated with auxospore formation in the marine centric diatom *Coscinodiscus concinnus* W. Smith. *Nature* 209: 217-218.
- HOLTERMANN, K.E., BATES, S.S., TRAINER, V.L., ODELL, A. & ARMBRUST, E.V. 2010. Mass sexual reproduction in the toxigenic diatoms *Pseudo-nitzschia australis* and *P. pungens* (Bacillariophyceae) on the Washington coast. *Journal of Phycology* 46: 41-52.
- HUANG, K.Y. & BECK, C.F. 2003. Phototropin is the blue-light receptor that controls multiple steps in the sexual life cycle of the green alga *Chlamydomonas reinhardtii*. *Proceedings of the National Academy of Sciences of the United States of America* 100: 6269-6274.
- IANORA, A., MIRALTO, A., POULET, S.A., CAROTENUTO, Y., BUTTINO, I., ROMANO, G., CASOTTI, R., POHNERT, G., WICHARD, T., COLUCCI-D'AMATO, L., TERRAZZANO, G. & SMETACEK, V. 2004. Aldehyde suppression of copepod recruitment in blooms of a ubiquitous planktonic diatom. *Nature* 429: 403-407.

- IANORA, A., BOERSMA, M., CASOTTI, R., FONTANA, A., HARDER, J., HOFFMANN, F., PAVIA, H., POTIN, P., POULET, S.A. & TOTH, G. 2006. New trends in marine chemical ecology. *Estuaries and Coasts* 29: 531-551.
- JAKOBSEN, H.H. 2001. Escape response of planktonic protists to fluid mechanical signals. *Marine Ecology Progress Series* 214: 67-78.
- JEWSON, D.H. 1992a. Size reduction, reproductive strategy and the life strategy of a centric diatom. *Philosophical Transactions of the Royal Society of London. Serie B* 336: 191-213.
- JEWSON, D.H. 1992b. Life cycle of a *Stephanodiscus* sp. (Bacillariophyta). *Journal of Phycology* 28: 856-866.
- JONES, H.M., SIMPSON, G.E., STICKLE, A.J. & MANN, D.G. 2005. Life history and systematics of *Petroneis* (Bacillariophyta), with special reference to British waters. *European Journal of Phycology* 40: 61-87.
- KACZMARSKA, I., BATES, S.S., EHRLMAN, J.M. & LÉGER, C. 2000. Fine structure of the gamete, auxospore and initial cell in the pennate diatom *Pseudo-nitzschia multiseries* (Bacillariophyta). *Nova Hedwigia* 71: 337-357.
- KAWAI, H., BOLAND, W. & MÜLLER, D.G. 1994. Sexual reproduction and sexual pheromones in *Myelophycus Simplex* (Harvey) Papenfuss (Phaeophyceae). *Japanese Journal of Phycology* 42: 227-231.
- KELLER, L. & SURETTE, M.G. 2006. Communication in bacteria: an ecological and evolutionary perspective. *Nature Reviews Microbiology* 4: 249-258.
- KIORBOE, T. & HANSEN, J.L.S. 1993. Phytoplankton aggregate formation: observations of patterns and mechanisms of cell sticking and the significance of exopolymeric material. *Journal of Plankton Research* 15: 993-1018.
- KOESTER, J.A., BRAWLEY, S.H., KARP-BOSS, L. & MANN, D.G. 2007. Sexual reproduction in the marine centric diatom *Ditylum brightwellii* (Bacillariophyta). *European Journal of Phycology* 42: 351-366.
- KOOISTRA, W.H.C.F., GERSONDE, R., MEDLIN, L.K. & MANN, D.G. 2007. The origin and evolution of the diatoms: their adaptation to a planktonic existence. In *Evolution of Primary Producers in the Sea* (Ed. by P.G. Falkowski & A.H. Knoll), pp. 207-250. Elsevier Academic Press, Burlington.
- LELONG, A., HÉGARET, H., SOUDANT, P. & BATES, S.S. 2012. *Pseudo-nitzschia* (Bacillariophyceae) species, domoic acid and amnesic shellfish poisoning: revisiting previous paradigms. *Phycologia* 51: 168-216.
- LEVIALDI GHIRON, J.H., AMATO, A., MONTRESOR, M. & KOOISTRA, W.C.H.F. 2008. Plastid inheritance in the planktonic raphid pennate diatom *Pseudo-nitzschia delicatissima* (Bacillariophyceae). *Protist* 159: 91-98.
- LEWIS, W.M.J. 1983. Interruption of synthesis as a cost of sex in small organisms. *American Naturalist* 121: 825-833.
- LUNDHOLM, N., HASLE, G.R., FRYXELL, G.A. & HARGRAVES, P.E. 2002. Morphology, phylogeny and taxonomy of species within the *Pseudo-nitzschia americana* complex (Bacillariophyceae) with descriptions of the two new species *P. brasiliensis* and *P. lineata*. *Phycologia* 41: 480-497.
- LUNDHOLM, N., MOESTRUP, Ø., HASLE, G.R. & HOEF-EMDEN, K. 2003. A study of the *Pseudo-nitzschia pseudodelicatissima/cuspidata* complex (Bacillariophyceae): what is *P. pseudodelicatissima*? *Journal of Phycology* 39: 797-813.

- LUNDHOLM, N., MOESTRUP, Ø., KOTAKI, Y., HOEF-EMDEN, K., SCHOLIN, C. & MILLER, P. 2006. Inter- and intraspecific variation of the *Pseudo-nitzschia delicatissima* complex (Bacillariophyceae) illustrated by rRNA probes, morphological data and phylogenetic analyses. *Journal of Phycology* 42: 464-481.
- LUNDHOLM, N., BATES, S.S., BAUGH, K.A., BILL, B.D., CONNELL, L.B., LÉGER, C. & TRAINER, V.L. 2012. Cryptic and pseudo-cryptic diversity in diatoms—with descriptions of *Pseudo-nitzschia hasleana* sp. nov. and *P. fryxelliana* sp. nov. *Journal of Phycology* 48: 436-454.
- MACDONALD, J.D. 1869. On the structure of the diatomaceous frustule, and its genetic cycle. *The Annals and Magazine of Natural History* 3: 1-8.
- MANN, D.G. 1986. Methods of sexual reproduction in *Nitzschia*: systematic and evolutionary implications. *Diatom Research* 1: 193-203.
- MANN, D.G. 1988. Why didn't Lund see sex in *Asterionella*? A discussion of the diatom life cycle in nature. In *Algae and the Aquatic Environment*. (Ed. by F.E. Round), pp. 385-412. Biopress, Bristol.
- MANN, D.G. & MARCHANT, H.J. 1989. The origins of the diatom and its life cycle. In *The Chromophyte Algae: Problems and Perspectives*. (Ed. by J.C. Green, B.S.C. Leadbeater & W.L. Diver), pp. 307-323. Clarendon Press, Oxford.
- MANN, D.G. & STICKLE, A.J. 1989. Meiosis, nuclear cyclosis, and auxospore formation in *Navicula sensu stricto* (Bacillariophyceae). *British Phycological Journal* 24: 167-181.
- MANN, D.G. 1993a. Sexual reproduction in a marine member of the Bacillariophyceae. *Diatom Research* 8: 109-116.
- MANN, D.G. 1993b. Patterns of sexual reproduction in diatoms. *Hydrobiologia* 269-270: 11-20.
- MANN, D.G. 1999. The species concept in diatoms. *Phycologia* 38: 437-495.
- MANN, D.G., CHEPURNOV, V.A. & DROOP, S.J.M. 1999. Sexuality, incompatibility, size variation, and preferential polyandry in natural populations and clones of *Sellaphora pupula* (Bacillariophyceae). *Journal of Phycology* 35: 152-170.
- MANN, D.G., CHEPURNOV, V.A. & IDEI, M. 2003. Mating system, sexual reproduction, and auxosporulation in the anomalous raphid diatom *Eunotia* (Bacillariophyta). *Journal of Phycology* 39: 1067-1084.
- MANN, D.G., POULÍČKOVÁ, A., SATO, S. & EVANS, K.M. 2011. Scaly incunabula, auxospore development, and girdle polymorphism in *Sellphora marvanii* sp. nov. (Bacillariophyceae). *Journal of Phycology* 47: 1368-1378.
- MCDONALD, S.M., SARNO, D. & ZINGONE, A. 2007. Identifying *Pseudo-nitzschia* species in natural samples using genus-specific PCR primers and clone libraries. *Harmful Algae* 6: 849-860.
- MCMANUS, M.A., KUDELA, R.M., SILVER, M.W., STEWARD, G.F., DONAGHAY, P.L. & SULLIVAN, J.M. 2008. Cryptic blooms: Are thin layers the missing connection? *Estuaries and Coasts* 31: 396-401.
- MCQUOID, M.R. & HOBSON, L.A. 1996. Diatom resting stages. *Journal of Phycology* 32: 889-902.
- MIZUNO, M. & OKUDA, K. 1985. Seasonal change in the distribution of cell size of *Cocconeis scutellum* var. *ornata* (Bacillariophyceae) in relation to growth and sexual reproduction. *Journal of Phycology* 21: 547-553.

- MONTRESOR, M. & LEWIS, J. 2006. Phases, stages, and shifts in the life cycles of marine phytoplankton. In *Algal cultures, analogues of blooms and applications*. (Ed. by D.V. Subba Rao), pp. 91-129. Science Publishers, Enfield.
- MOUGET, J.L., GASTINEAU, R., DAVIDOVICH, O., GAUDIN, P. & DAVIDOVICH, N.A. 2009. Light is a key factor in triggering sexual reproduction in the pennate diatom *Haslea ostrearia*. *Fems Microbiology Ecology* 69: 194-201.
- NAGAI, S., HORI, Y., MANABE, T. & IMAI, I. 1995. Restoration of cell size by vegetative cell enlargement in *Coscinodiscus wailesii* (Bacillariophyceae). *Phycologia* 34: 533-535.
- NAGAI, S., IMAI, I., YAMAUCHI, K. & MANABE, T. 1996. Induction of sexuality in the diatom *Coscinodiscus wailesii* Gran by a marine bacterium *Alcaligenes* sp. in culture. In *14th Diatom Symposium*. (Ed. by I. Mayama & I. Koizumi), pp. 198-212. Koeltz Scientific Books, Koenigstein.
- NAGAI, S. & IMAI, I. 1997. The effect of irradiance and irradiation time on the size of initial cells in vegetative cell enlargement of *Coscinodiscus wailesii* (Centrales, Bacillariophyceae) in culture. *Phycological Research* 45: 117-121.
- NAGAI, S. & IMAI, I. 1998. Enumeration of bacteria in seawater and sediment from the Seto Island Sea of Japan that promote sperm formation in *Coscinodiscus wailesii* (Bacillariophyceae). *Phycologia* 37: 363-368.
- NAGAI, S. & IMAI, I. 1999. The effect of salinity on the size of initial cells during vegetative cell enlargement of *Coscinodiscus wailesii* (Bacillariophyceae) in culture. *Diatom Research* 14: 337-342.
- NAGAI, S. & IMAI, I. 2001. Relationships between *Coscinodiscus wailesii* and bacteria promoting its sperm formation in the coastal area, Japan. In *Proceedings of the 16th International Diatom Symposium 2000*. (Ed. by A. Economou-Amilli), pp. 213-223. University of Athens, Faculty of Biology, Athens.
- NEDELCO, A.M. & MICHOD, R.E. 2003. Sex as a response to oxidative stress: the effect of antioxidants on sexual induction in a facultatively sexual lineage. *Proceedings of the Royal Society of London Series B-Biological Sciences* 270: S136-S139.
- NEDELCO, A.M., MARCU, O. & MICHOD, R.E. 2004. Sex as a response to oxidative stress: a twofold increase in cellular reactive oxygen species activates sex genes. *Proceedings of the Royal Society of London Series B-Biological Sciences* 271: 1591-1596.
- OLSON, R.J., WATRAS, C. & CHISHOLM, S.W. 1986. Patterns of individual cell growth in marine centric diatoms. *Journal of General Microbiology* 132: 1197-1204.
- ORSINI, L., SARNO, D., PROCACCINI, G., POLETTI, R., DAHLMANN, J. & MONTRESOR, M. 2002. Toxic *Pseudo-nitzschia multistriata* (Bacillariophyceae) from the Gulf of Naples: morphology, toxin analysis and phylogenetic relationships with other *Pseudo-nitzschia* species. *European Journal of Phycology* 37: 247-257.
- PAUL, C., BAROFSKY, A., VIDOUDEZ, C. & POHNERT, G. 2009. Diatom exudates influence metabolism and cell growth of co-cultured diatom species. *Marine Ecology-Progress Series* 389: 61-70.
- PETERS, F., ARIN, L., MARRASÉ, C., BERDALET, E. & SALA, M.M. 2006. Effects of small-scale turbulence on the growth of two diatoms of different size in a phosphorus-limited medium. *Journal of Marine Systems* 61: 134-148.
- PFITZER, E. 1869. Über den bau und zellteilung der diatomeen. *Botanische Zeitung* 27: 774-776.

- POHNERT, G. & BOLAND, W. 2002. The oxylipin chemistry of attraction and defense in brown algae and diatoms. *Natural Products Reports* 19: 108-122.
- POULÍČKOVÁ, A. & MANN, D.G. 2006. Sexual reproduction in *Navicula cryptocephala* (Bacillariophyceae). *Journal of Phycology* 42: 872-886.
- POULÍČKOVÁ, A., MAYAMA, S., CHEPURNOV, V.A. & MANN, D.G. 2007. Heterothallic auxosporulation, incunabula and perizonium in *Pinnularia* (Bacillariophyceae). *European Journal of Phycology* 42: 367-390.
- POULÍČKOVÁ, A. & MANN, D.G. 2008. Autogamous auxosporulation in *Pinnularia nodosa* (Bacillariophyceae). *Journal of Phycology* 44: 350-363.
- QUARMBY, L.M. 1994. Signal-transduction in the sexual life of *Chlamydomonas*. *Plant Molecular Biology* 26: 1271-1287.
- QUIJANO-SCHEGGIA, S., GARCÉS, E., ANDREE, K., FORTUÑO, J.M. & CAMP, J. 2009a. Homothallic auxosporulation in *Pseudo-nitzschia brasiliiana* (Bacillariophyta). *Journal of Phycology* 45: 100-107.
- QUIJANO-SCHEGGIA, S.I., GARCÉS, E., LUNDHOLM, N., MOESTRUP, O., ANDREE, K. & CAMP, J. 2009b. Morphology, physiology, molecular phylogeny and sexual compatibility of the cryptic *Pseudo-nitzschia delicatissima* complex (Bacillariophyta), including the description of *P. arenysensis* sp. nov. *Phycologia* 48: 492-509.
- REED, D.C., NEUSHUL, M. & EBELING, A.W. 1991. Role of settlement density on gametophyte growth and reproduction in the kelps *Pterygophora-californica* and *Macrocystis-pyrifera* (Phaeophyceae). *Journal of Phycology* 27: 361-366.
- RENGEFORS, K. & LEGRAND, C. 2007. Broad allelopathic activity in *Peridinium aciculiferum* (Dinophyceae). *European Journal of Phycology* 42: 341-349.
- RIBERA D'ALCALÀ, M., CONVERSANO, F., CORATO, F., LICANDRO, P., MANGONI, O., MARINO, D., MAZZOCCHI, M.G., MODIGH, M., MONTRESOR, M., NARDELLA, M., SAGGIOMO, V., SARNO, D. & ZINGONE, A. 2004. Seasonal patterns in plankton communities in a pluriannual time series at a coastal Mediterranean site (Gulf of Naples): an attempt to discern recurrences and trends. *Scientia Marina* 68: 65-83.
- RINES, J.E.B., DONAGHAY, P.L., DEKSHENIEKS, M.M., SULLIVAN, J.M. & TWARDOWSKI, M.S. 2002. Thin layers and camouflage: hidden *Pseudo-nitzschia* spp. (Bacillariophyceae) populations in a fjord in the San Juan Islands, Washington, USA. *Marine Ecology Progress Series* 225: 123-137.
- ROSOWSKI, J.R., JOHNSON, L.M. & MANN, D.G. 1992. On the report of gametogenesis, oogamy, and uniflagellated sperm in the pennate diatom *Nitzschia pungens*. *Journal of Phycology* 28: 570-574.
- ROUND, F.E. 1972. The problem of reduction of cell size during diatom cell division. *Nova Hedwigia* 23: 291-303.
- ROUND, F.E. 1982. Auxospore structure, initial valves and the development of populations of *Stephanodiscus* in farmoor reservoir. *Annals of Botany* 49: 447-459.
- ROUND, F.E., CRAWFORD, R.M. & MANN, D.G. 1990. *The diatoms. Biology and morphology of the genera*. Cambridge University Press, Cambridge.
- RYAN, J.P., CHAVEZ, F.P. & BELLINGHAM, J.G. 2005. Physical-biological coupling in Monterey Bay, California: topographic influences on phytoplankton ecology. *Marine Ecology Progress Series* 287: 23-32.

- SABBE, K., CHEPURNOV, V.A., VYVERMAN, W. & MANN, D.G. 2004a. Apomixis in *Achnanthes* (Bacillariophyceae); development of a model system for diatom reproductive biology. *European Journal of Phycology* 39: 327-341.
- SABBE, K., CHEPURNOV, V.A., MANN, D.G. & VYVERMAN, W. 2004b. Sexual behaviour, auxosporulation and chloroplast dynamics in a marine *Amphora* (Bacillariophyceae) studied in culture. *Botanica Marina* 47: 53-63.
- SAHRAOUI, I., BATES, S.S., BOUCHOUICHA, D., MABROUK, H.H. & HLAILI, A.S. 2011. Toxicity of *Pseudo-nitzschia* populations from Bizerte Lagoon, Tunisia, southwest Mediterranean, and first report of domoic acid production by *P. brasiliana*. *Diatom Research* 26: 293-303.
- SANDGREN, C.D. & FLANAGIN, J. 1986. Heterothallic sexuality and density dependent encystment in the crysophycean alga *Synura petersenii* Korsh. *Journal of Phycology* 22: 206-216.
- SARNO, D., ZINGONE, A. & MONTRESOR, M. 2010. A massive and simultaneous sex event of two *Pseudo-nitzschia* species. *Deep Sea Research Part II: Topical Studies in Oceanography* 57: 248-255.
- SATO, M.S., SUZUKI, M. & HAYASHI, H. 1998. The density of a homogeneous population of cells controls resetting of the program for swarmer formation in the unicellular marine microorganism *Noctiluca scintillans*. *Experimental Cell Research* 245: 290-293.
- SATO, S., BEAKES, G., IDEI, M., NAGUMO, T. & MANN, D.G. 2011. Novel sex cells and evidence for sex pheromones in diatoms. *PLoS ONE* 6: e26923.
- SCHMID, A.M.M. 1995. Sexual reproduction in *Coscinodiscus granii* Gough in culture: a preliminary report. In *Proceedings of the 13th international diatom symposium 1994*. (Ed. by D. Marino & M. Montresor), pp. 139-159. Biopress, Bristol.
- SCHOLIN, C.A., GULLAND, F., DOUCETTE, G.J., BENSON, S., BUSMAN, M., CHAVEZ, F.P., CORDARO, J., DELONG, R., VOGETAERE, A.D., HARVEY, J., HAULENA, M., LEFEBVRE, K., LIPSCOMB, T., LOSCUTOFF, S., LOWENSTINE, L.J., MARIN III, R., MILLER, P.E., MCLELLAN, W.A., MOELLER, P.D.R., POWELL, C.L., ROWLES, T., SILVAGNI, P., SILVER, M., SPRAKER, T., TRAINER, V. & VAN DOLAH, F.M. 2000. Mortality of sea lions along the central California coast linked to a toxic diatom bloom. *Nature* 403: 80-84.
- SCHULTZ, M.E. & TRAINOR, F.R. 1968. Production of male gametes and auxospores in the centric diatoms *Cyclotella meneghiniana* and *C. cryptica*. *Journal of Phycology* 4: 85-88.
- SILVER, M.W., BARGU, S., COALE, S.L., BENITEZ-NELSON, C.R., GARCIA, A.C., ROBERTS, K.J., SEKULA-WOOD, E., BRULAND, K.W. & COALE, K.H. 2010. Toxic diatoms and domoic acid in natural and iron enriched waters of the oceanic Pacific. *Proceedings of the National Academy of Sciences* 107: 20762-20767.
- SMETACEK, V. 1999. Diatoms and the ocean carbon cycle. *Protist* 150: 25-32.
- SMETACEK, V., ASSMY, P. & HENJES, J. 2004. The role of grazing in structuring Southern Ocean pelagic ecosystems and biogeochemical cycles. *Antarctic Science* 16: 541-558.
- STEELE, R. 1965. Induction of sexuality in two centric diatoms. *BioScience* 15: 298.
- SUBBA RAO, D.V., PARTENSKY, F., WOHLGESCHAFFEN, G. & LI, W.K.W. 1991. Flow cytometry and microscopy of gametogenesis in *Nitzschia pungens*, a toxic, bloom-forming, marine diatom. *Journal of Phycology* 27: 21-26.

- SULLIVAN, J.M., TWARDOWSKI, M.S., DONAGHAY, P.L. & FREEMAN, S.A. 2005. Use of optical scattering to discriminate particle types in coastal waters. *Applied optics* 44: 1667-1680.
- TAKANO, H. 1993. Marine diatom *Nitzschia multistriata* sp. nov. common at inlets of southern Japan. *Diatom* 8: 39-41.
- TAKANO, H. 1995. *Pseudo-nitzschia multistriata* (Takano) Takano, a new combination for the pennate diatom *Nitzschia multistriata* Takano. *Diatom* 10: 73-74.
- TESSON, S.V.M. 2010. Population genetic structure of a planktonic diatom in the Gulf of Naples: *Pseudo-nitzschia multistriata*. PhD Thesis Stazione Zoologica Anton Dohrn, Open University of London.
- THOMAS, W.H. & GIBSON, C.H. 1990. Effects of small-scale turbulence on microalgae. *Journal of Applied Phycology* 2: 71-77.
- TRAINER, V.L., BATES, S.S., LUNDHOLM, N., THESSSEN, A.E., COCHLAN, W.P., ADAMS, N.G. & TRICK, C.G. 2012. *Pseudo-nitzschia* physiological ecology, phylogeny, toxicity, monitoring and impacts on ecosystem health. *Harmful Algae* 14: 271-300.
- VARDI, A., FORMIGGINI, F., CASOTTI, R., DE MARTINO, A., RIBALET, F., MIRALTO, A. & BOWLER, C. 2006. A stress surveillance system based on calcium and nitric oxide in marine diatoms. *Plos Biology* 4: 419-411.
- VELO SUÁREZ, L., GONZÁLEZ-GIL, S., GENTEN, P., LUNVEN, M., BECHEMIN, C., FERNAND, L., RAINE, R. & REGUERA, B. 2008. Thin layers of *Pseudo-nitzschia* spp. and the fate of *Dinophysis acuminata* during an upwelling-downwelling cycle in a Galician Ría. *Limnology and Oceanography* 53: 1816-1834.
- VON DASSOW, P., CHEPURNOV, V.A. & ARMBRUST, E.V. 2006. Relationships between growth rate, cell size, and induction of spermatogenesis in the centric diatom *Thalassiosira weissflogii* (Bacillariophyta). *Journal of Phycology* 42: 887-899.
- VON STOSCH, H.A. 1965. Manipulierung der zellgrösse von diatomeen in experiment. *Phycologia* 5: 21-44.
- VRIELING, E.G., GIESKES, W.W.C. & BEELEN, T.P.M. 1999. Silicon deposition in diatoms: Control by the pH inside the silicon deposition vesicle. *Journal of Phycology* 35: 548-559.
- WIESE, L. 1969. Algae. In *Fertilization*. (Ed. by C.B. Metz & A. Monroy), pp. 135-188. Academic Press, New York.
- YAMASAKI, Y., NAGASOE, S., MATSUBARA, T., SHIKATA, T., SHIMASAKI, Y., OSHIMA, Y. & HONJO, T. 2007. Allelopathic interactions between the bacillariophyte *Skeletonema costatum* and the raphidophyte *Heterosigma akashiwo*. *Marine Ecology-Progress Series* 339: 83-92.
- ZIELINSKI, U. & GERSONDE, R. 1997. Diatom distribution in Southern Ocean surface sediments (Atlantic sector): implications for paleoenvironmental reconstructions. *Palaeogeography, Palaeoclimatology, Palaeoecology* 129: 213-250.
- ZINGONE, A., LICANDRO, P. & SARNO, D. 2003. Revising paradigms and myths of phytoplankton ecology using biological time series. In *Mediterranean Biological Time Series*. (Ed. by F. Briand), pp. 109-114. CIESM Workshop Monographs n° 22, Monaco.